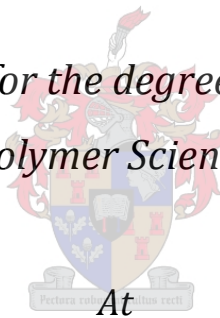# The effect of controlled degradation with an organic peroxide on the molecular characteristics and properties of heterophasic propylene-ethylene copolymers (HECO)

By

Morné Swart

Dissertation presented for the degree of Doctor of Philosophy
(Polymer Science)

At

Stellenbosch University

Promoter: Prof. A.J. van Reenen

! š®œe

Declaration

By submitting this dissertation, I declare that the entirety of the work contained herein is my own, original work, that I am the owner of the copyright thereof (unless to the extent explicitly otherwise stated) and that I have not previously in its entirety or in part submitted it for obtaining any qualification.

Signature: ....   Date: 7 December 2012

Abstract

Heterophasic copolymers (also known as HECO polymers) or often referred to only as impact copolymers or block copolymers comprise a polymer matrix with a dispersed rubbery copolymer phase. The polymer under investigation in this study consists of a polypropylene homopolymer matrix and ethylene-propylene copolymers (EPCs). Due to its diverse range of applications and unique properties, polypropylene is the choice of polymer for a vast array of applications. This has led to the development of an entire class of polypropylene materials known as visbroken or controlled rheology polypropylene. By adding a suitable peroxide to the polymer in the presence of heat, radicals are formed which will attack the polymer chains in a random fashion. The resultant polymers generally have a higher melt flow rate (MFR), a narrower molecular weight distribution than the parent polymer, and good impact-stiffness balance.

The main focus of this investigation was to determine if there exist any differences in the molecular structure and physical properties of controlled rheology HECO polymers and if differences do exist, how they influence the physical characteristics of the polymer. Eight HECO polymers with equal ethylene contents were visbroken to varying degrees by making use of two different types of organic peroxide. The effects of the amount of visbreaking on the molecular characteristics and physical properties were subsequently studied by making use various types of fractionation techniques, including preparative temperature rising elution fractionation (P-TREF) and crystallisation analysis fractionation (CRYSTAF). Subsequent offline analysis was then done on the fractionated samples that included nuclear magnetic resonance spectroscopy (NMR), differential scanning calorimetry (DSC), high temperature size exclusion chromatography (HT-SEC), Fourier transform infrared spectroscopy (FTIR) and deposition of the SEC fractions via the LC Transform Interface (SEC-FTIR) as well as high temperature high performance liquid chromatography (HT-HPLC), a novel technique for the characterization of olefins according to their chemical composition.

Opsomming

Heterofase kopolimere, ook bekend as HECO polimere, of dikwels na verwys net as impak kopolimere of blok kopolimere bestaan uit 'n polimeer matriks met 'n verspreide rubberagtige kopolimeer fase. Die polimeer wat in hierdie studie ondersoek was het bestaan uit 'n polipropileen homopolimeer matriks en etileen-propileen kopolimere (EPCs). As gevolg van sy veelseidigheid van toepassings en unieke eienskappe is polipropileen die keuse van polimeer vir 'n wye verskeidenheid van toepassings. Hierdie veelseidigheid het gelei tot die ontwikkeling van 'n hele klas van polipropileen materiaal bekend as gevisbreekte of beheerde reologie polipropileen. Deur die byvoeging van 'n geskikte peroksied tot die polimeer in die teenwoordigheid van hitte, word radikale gevorm wat die polimeerkettings in 'n ewekansige wyse sal aanval. Die gevolglike polimere in die algemeen het 'n hoë smelt vloeitempo (MFR), 'n smaller molekulêre gewig verspreiding as die moeder polimeer, en 'n goeie impak/styfheid balans.

Agt HEKO polimere met gelyke etileen inhoude was gevisbreek in wisselende hoeveelhede deur gebruik te maak van twee verskillende tipes organiese peroksiedes. Die gevolge van die hoeveelheid van visbreeking op die molekulêre eienskappe en fisiese eienskappe was vervolgens gebestudeer deur gebruik te maak van verskillende fraksionasie tegnieke, insluitend preparatiewe TREF (P-TREF) en CRYSTAF. Daaropvolgende analiese is gedoen op die gefraktioneerde monsters en sluit in kernmagnetiese resonansie spektroskopie (KMR), differensiële skandeer kalorimetrie (DSC), 'n hoë temperatuur grootte uitsluitings chromatografie (HT-SEC), Fourier transform infrarooi spektroskopie (FTIR) met deponeering van die SEC fraksies via die LC transform koppelvlak (SEC-FTIR) sowel as 'n hoë temperatuur hoë werkverrigting vloeistof chromatografie (HT-HPLC), 'n nuwe tegniek vir die karakterisering van olefiene volgens hul chemise samestelling

This thesis is dedicated to my family

Chanél, Caitlyn and Benjamin

Without your unwavering and loving support this would not have been possible

Acknowledgements

The author would like to convey his sincere thanks to the following:

A special thanks to Prof Albert van Reenen for his interest, enthusiasm, assistance and his willingness to take on a part time student.

To Dr John Mellor for giving me the opportunity and financial support to further my studies whilst in the employment of Sasol Polymers.

To Dr Gareth Harding for all his help, ideas and endless patience to all my questions. And especially for his help with the TREF and characterization aspects of this study. Gareth, I cannot thank you enough!

The staff at Sasol Polymers' Polymer Technology Services Centre, especially Robert Kwinda and Bhekani Mdabe, your help with various aspects of this study is much appreciated.

To Dr Volker Joerres and Dr Anita Dimeska from Novolen Technologies for their assistance with analytical TREF.

To Monja Smith, Arrie Kruger, Dr Brian Sole and Jenny Green, the best managers a fresh graduate could have hoped for. Your guidance and leadership is world class and will always be appreciated, your friendship will always be treasured!

To Linda Botha, words simply cannot express my gratitude for all your help. From analysing samples to endless discussions around the intricacies of balancing part time studies with ever increasing pressure at work. Thank you!

To Sadiqali Cheruthazhekatt for all his help with the HT-HPLC and SEC analysis.

A special thanks to my friend Liesl Keulder, your assistance with various parts of this study is much appreciated. Without your help in the lab this would not have been possible!

To Nadine and Ashwell thanks for every cup of coffee (there were a lot) and every glass of wine, you guys made everything much easier.

On a more personal note, I would like to thank my parents. Mom, Dad, your trust, support, love, guidance and encouragement will always be my cornerstone. Also to my brother and sister, thank you for your support throughout.

Lastly and most importantly to my wife, Chanel, my daughter Caitlyn and my son, Benjamin, without your support and love none of this would have been possible. Thank you for being there every step of the way. You kept me focused and motivated on what is important. For this I can never thank you enough!

Table of Contents

List of Figures

List of Tables

List of Abbreviations

ΔT	Difference in temperature
^{13}C	Carbon 13
AFM	Atomic force microscopy
A-TREF	Analytical temperature rising elution fractionation
CCD	Chemical composition distribution
CEF	Crystallisation elution fractionation
CR	Controlled rheology
CRYSTAF	Crystallisation analysis fractionation
DEAC	Diethylaluminium chloride
DMA	Dynamic mechanical analysis
DSC	Differential scanning calorimetry
EGMBE	Ethylene glycol monobutyl ether
ELSD	Evaporative light scattering detector
EPC	Ethylene-propylene copolymers
EPR	Ethylene propylene rubber
GC	Gas chromatography
GPC	Gel permeation chromatography
HDPE	High density polyethylene
HECO	Heterophasic copolymers
HPLC	High performance liquid chromatography
HT-HPLC	High temperature high performance liquid chromatography
HT-SEC	High temperature size exclusion liquid chromatography
iPP	Isotactic polypropylene
IR	infra-red
LCCC	Liquid chromatography at critical conditions
LDPE	Low density polyethylene
LLDPE	Linear low density polyethylene
MFR	Melt flow rate
MMD	Molar mass distribution
M_n	Number average molecular weight
M_w	Weight average molecular weight
MWD	Molecular weight distribution
NMR	Nuclear magnetic resonance
PD	Polydispersity

PMMA	Polymethyl methacrylate
PP	Polypropylene
PS	Polystyrene
P-TREF	Preparative temperature rising elution fractionation
RI	Refractive index
rTPO	Reactor-made thermoplastic olefin copolymers
SCALLS	Solution crystallisation analysis by laser light scattering
SEC	Size exclusion chromatography
SEC-FTIR	Size exclusion chromatography Fourier transform infrared spectroscopy
SEM	Scanning electron microscopy
Tan	Tangent
T_c	Crystallisation temperature
TCB	Trichlorobenzene
TCE	Tetrachloroethylene
T_e	Elution temperature
TEA	Triethylaluminium
TEM	Transmission electron microscopy
TFA	Turbidity fractionation analysis
T_g	Glass transition temperature
TGA	Thermal gravimetric analysis
TIBA	Tri-isobutylaluminium
T_m	Melting temperature
TREF	Temperature rising elution fractionation
TWIM	Thin wall injection moulding
USA	United States of America
WAXD	Wide angle x-ray diffraction
W_i	Weight fraction
$W_i\%$	Weight fraction percentage
XS	Xylene solubles
ZN	Ziegler-Natta
ΔH_f	Enthalpy of fusion
ΔH_{fc}	Enthalpy of fusion of ideal 100% crystalline polypropylene

Chapter 1

Introduction and Objectives

This chapter will give a general introduction to heterophasic copolymers, how they are produced, what their general characteristics are and for what applications they are used. The chapter will further provide the objectives of this study and will also explain the layout of the dissertation

1.1   Introduction

In 2010 global polypropylene (PP) production stood at approximately 48.8 million metric tons. Polypropylene resins constitute one of the fastest growing commodity resins in the world. The estimated value of production in 2010 stood in the range of $115.6 billion and represented an average annual growth rate of 7.0% per annum since 1990. World consumption in 2010 grew to an all-time high of 48.5 million metric tons [1]. There is a continuing need for PP heterophasic copolymers with improved properties, notably materials with good flow and impact characteristics, especially for moulding, injection moulding, thin wall packaging and engineering applications.

Heterophasic copolymers (HECO polymers) also often referred to as impact copolymers or block copolymers comprise a polymer matrix with a dispersed rubbery copolymer phase. The polymers tested in this study consist of a polypropylene homopolymer matrix and ethylene-propylene copolymers (EPCs). Together with these types and as a result of the nature of the process used to produce them, there are also small fractions of ethylene homopolymer and amorphous polypropylene present. The method used to prepare the samples used in this study is an *in situ* double reactor polymerization of ethylene and propylene. The polypropylene matrix homopolymer was produced by standard polymerization with a heterogeneous transition metal catalyst system in a gas phase reactor. In the second stage, the polymer produced in the first reactor is transferred to a second reactor and polymerization is continued and the rubbery copolymer phase is produced by adding ethylene and propylene in a certain ratio in the second reactor. This happens in the presence of matrix polymer produced in the first reactor. Polymerization also takes place with a heterogeneous transition metal catalyst in the second reactor [2].

Due to its diverse range of applications and unique properties, polypropylene is the choice of polymer for a vast array of applications. Propylene monomer cannot be polymerized using free radical polymerization. In fact, the presence of free radicals leads to random degradation of the polymer chains. As a result of this significant research has been conducted to study the influence of free radicals on the degradation of polypropylene. This has led to the development of an entire class of polypropylene materials known as visbroken or controlled rheology polypropylene. By adding a suitable peroxide to the polymer in the presence of heat, radicals are formed which will attack the polymer chains in a random fashion. Statistically the longest molecules are most susceptible to attack. The resultant polymers generally have a higher melt

flow rate (MFR), a narrower molecular weight distribution than the parent polymer, and good impact-stiffness balance. Typical applications for these controlled rheology grade polypropylenes include film, fibre, non-wovens and injection moulding (housewares, pails, automotive, packaging, thin walled injection moulding or TWIM). Propylene-ethylene heterophasic copolymers generally have good impact/stiffness performance properties, good aesthetic characteristics and good creep resistance.

Controlled Rheology grades show several processing advantages over conventional grades. The most significant of these are [3]:

i.   The decreased viscosity means less injection pressure is required for mould filling.
ii.   Lower melt temperatures are required to achieve the same viscosity i.e. approximately 30 °C lower mass temperature.
iii.   Cycle times can generally be reduced by 10-15%.
iv.   Lower temperatures mean that warpage on de-moulding is reduced.
v.   Pigment/colour mixing may be improved due to decreased viscosity and better flow at a given temperature.
vi.   The narrower MWD should show minimal differences parallel to and across the flow direction.
vii.   The decreased injection pressure may allow a machine with a lower clamping force to be used.

1.2   Objectives

As described in Section 1.1 of this chapter visbreaking or controlled rheology (CR) is a process used during the manufacturing of polypropylene to decrease the average molecular weight of the polymer. By decreasing the average molecular weight of the polymer a higher melt flow rate (MFR) as well as a decrease in the molecular weight distribution (MWD) is achieved. All factors being equal, this will result in a polymer that will show reduced warpage, more uniform shrinkage and drawdown, higher extrusion rates for fibres and films and significantly increased elongation at break. The effect of visbreaking on the molecular characteristics of HECO polymers is still relatively unknown[4].

The **main** objective of this study is to determine firstly if there are any differences in the molecular structure and physical properties of controlled rheology grades of propylene-

ethylene heterophasic copolymers and secondly, if differences exist, what they are and how do they influence the overall properties of these polymers. A **secondary** objective was also to determine if there are any differences in the molecular structure of HECO polymers based on the type of organic peroxide used to facilitate the controlled rheology process.

In the present study, eight HECO polymers with equal ethylene contents were visbroken to varying degrees by making use of two different types of organic peroxide. The effects of the amount of visbreaking on the molecular characteristics and physical properties were subsequently studied by making use of various types of fractionation techniques, including preparative temperature rising elution fractionation (P-TREF) and CRYSTAF. Subsequent offline analysis was then done on the fractionated samples that included nuclear magnetic resonance (NMR), differential scanning calorimetry (DSC), high temperature size exclusion chromatography (HT-SEC), Fourier transform infrared spectroscopy (FTIR) and deposition of the SEC fractions via the LC Transform Interface (SEC-FTIR) as well as high temperature high performance liquid chromatography (HT-HPLC), a novel technique for the characterization of olefins according to their chemical composition.

1.3   Dissertation layout

The dissertation is divided into the following five chapters:

Chapter 1

A general introduction is provided in the first section and the objectives of the study are laid out and formulated.

Chapter 2

This chapter provides a more detailed history of heterophasic copolymers, how they are produced, their main characteristics, their market value and landscape as well as their main applications. Chapter 2 further discusses the various means of polymer degradation with emphasis on the method of controlled rheology with organic peroxides. This chapter also outlines the history of various techniques traditionally used to characterize these polymers and in particular an overview of a new novel technique for the characterization of polyolefins

according to their chemical composition is discussed, namely high temperature high performance liquid chromatography or HT-HPLC.

Chapter 3

This chapter details the procedures and methods used to produce and analyse the various HECO polymer samples. The experimental conditions for all the analytical instrumentation is supplied, together with a brief discussion on the principles of temperature rising elution fractionation (TREF), size exclusion chromatography coupled to Fourier transform infrared spectroscopy via the LC transform interface (SEC-FTIR) and high temperature high performance liquid chromatography (HT-HPLC)

Chapter 4

In Chapter 4 the results obtained through the various characterization techniques outlined in Chapter 3 are given and discussed. Data obtained through this investigation is also presented in the subsequent addendums following Chapter 5.

Chapter 5

The results and conclusions drawn in Chapter 4 are briefly summarized and recommendations for future work in this field of study is proposed

1.4   References

1.   Borruso, A., *CEH Marketing Research Report: Polypropylene Resins*. 2011.

2.   Malm, B., P. Jaaskelainen, and T. Vestberg, *Heterophasic Copolymers*, U.S. Patent, Editor. 2004, Borealis Technology: United States of America.

3.   Kent, R.J. and V.E. Kent, *PP - Controlled rheology grades* 2005, Tangram Technology Ltd.

4.   Silvestre, C., S. Cimmino, and R. Triolo, *Structure, morphology and crystallisation of a random ethylene-propylene copolymer.* Journal of Applied Polymer Science: Part B: Polymer Physics, 2002. **41**: p. 493-500.

Chapter 2

Historical and Literature Review

This chapter gives an introduction and overview to the field of heterophasic copolymers with regards to their synthesis, characterization, application and market influence. It further reviews the different means of degradation of polymers in general. Focus is also placed on gradient high temperature high performance liquid chromatography as a novel technique in characterizing heterophasic copolymers.

2.1   Heterophasic copolymers

2.1.1   Introduction

There is a continuing need for PP heterophasic copolymers with improved properties, notably materials with good flow and impact characteristics, especially for moulding, injection moulding, thin wall packaging and engineering applications.

Heterophasic copolymers, also referred to as block copolymers or impact copolymers, comprise a crystalline polymer matrix with a dispersed rubbery copolymer phase. The matrix is a homopolymer or random copolymer matrix, usually consisting of a polypropylene homopolymer or polypropylene-ethylene random copolymer. The rubbery copolymer phase is a reactor blend of an amorphous rubber, a rubber-like polymer which is normally an ethylene-propylene copolymer (rubber), and semi-crystalline propylene-ethylene copolymers [1]. Figure 2.1 (a) shows an AFM image of a propylene-ethylene heterophasic copolymer. The difference between the polypropylene matrix and the ethylene-propylene rubber phase can clearly be seen. Figure 2.1b shows a simplified graphic representation of the copolymer [2].
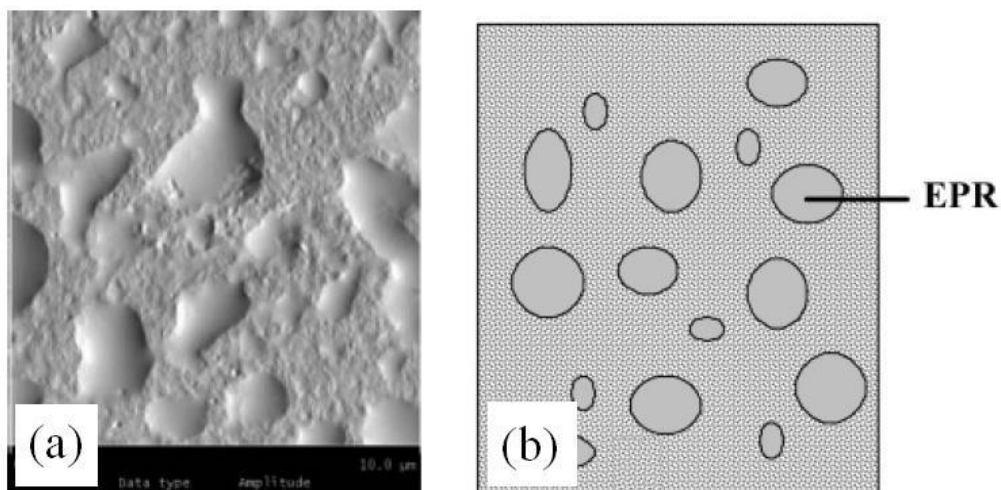
Figure 2.1   *(a) AFM image of a PP-EPR heterophasic copolymer and (b) simplified representation of the same copolymer [2].*

2.1.2   Synthesis of heterophasic copolymers

2.1.2.1   General mechanism of a Ziegler-Natta catalysed polymerization

Ziegler-Natta catalysts are widely used in industry to produce polyolefins. Typically a Ziegler-Natta catalyst consists of a metal compound incorporating a metal-carbon bond which is able to achieve repeated insertions of an olefin unit [3]. The typical make-up of a Ziegler-Natta catalytic system thus generally consists of an $MgCl_2$ support, $TiCl_3$ or $TiCl_4$ and an internal electron donor. These components are used in conjunction with an aluminium alkyl co-catalyst (AlR_3). The most common co-catalysts used in industry today are triethyl aluminium (TEA), diethylaluminium chloride (DEAC) or tri-isobutylaluminium (TIBA). External electron donors (Lewis bases) are typically added to produce highly isotactic polypropylene, whereas internal donors like monoesters, diesters or diethers are incorporated in the catalyst to control the distribution of $TiCl_4$ on the support surface [4]. The polymerization of α-olefins with solid Ti-based catalysts occur at specific active centres that are created by the exchange of an halogen atom from the transition metal compound and the co-catalyst [5]. This is illustrated by the equation below:

$$[TiCl_3] + [AlEt_3] \rightarrow [Cl_2TiEt] + AlEt_2Cl \qquad\qquad\qquad (2.1)$$

A crucial element with regards to the bond between the transition metal and the carbon atom is to be able to react with the double bond of the α-olefins [5, 6]. It is well known from literature that a multitude of models have been proposed for the polymerization of α-olefin using a Ziegler-Natta catalysed system [7-10]. By far the most accepted model to date is the one proposed by Cossee [11, 12] and Arlman [13]. The model is divided into two steps. The first step involves the coordination of the monomer parallel to the metal-carbon bond (step (i) in Figure 2.2 below). The second step then involves the chain migratory insertion of the monomer unit between the metal atom of the catalyst and the last carbon atom of the growing polymer chain (step (ii) in Figure 2.2 below). Step two is enabled via a four-member transition state consisting of the metal atom, the two carbons of the monomer and the last carbon of the polymer chain.
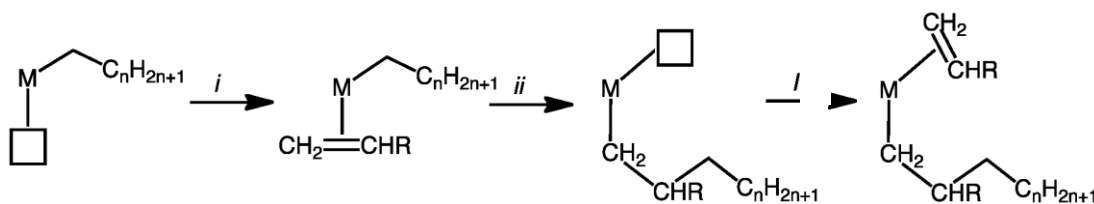
Figure 2.2   *Illustration of the Ziegler-Natta catalysed mechanism for the polymerization of polyolefins proposed by Cossee and Arlman.*

2.1.2.2   In situ synthesis of heterophasic ethylene-propylene copolymers

Heterophasic copolymers are usually produced in two or more reactors. The matrix homopolymer or random copolymer may be produced by standard polymerization with a Ziegler-Natta catalyst system in one or more slurry or bulk (loop) reactors or gas phase reactors or combinations of both. In a second stage, the polymerization is continued and the rubbery copolymer phase is produced in the matrix polymer using one or more gas phase reactors [14]. Figure 2.3 shows an illustration of a typical process used to produce heterophasic copolymers, in this case the Novolen® process.
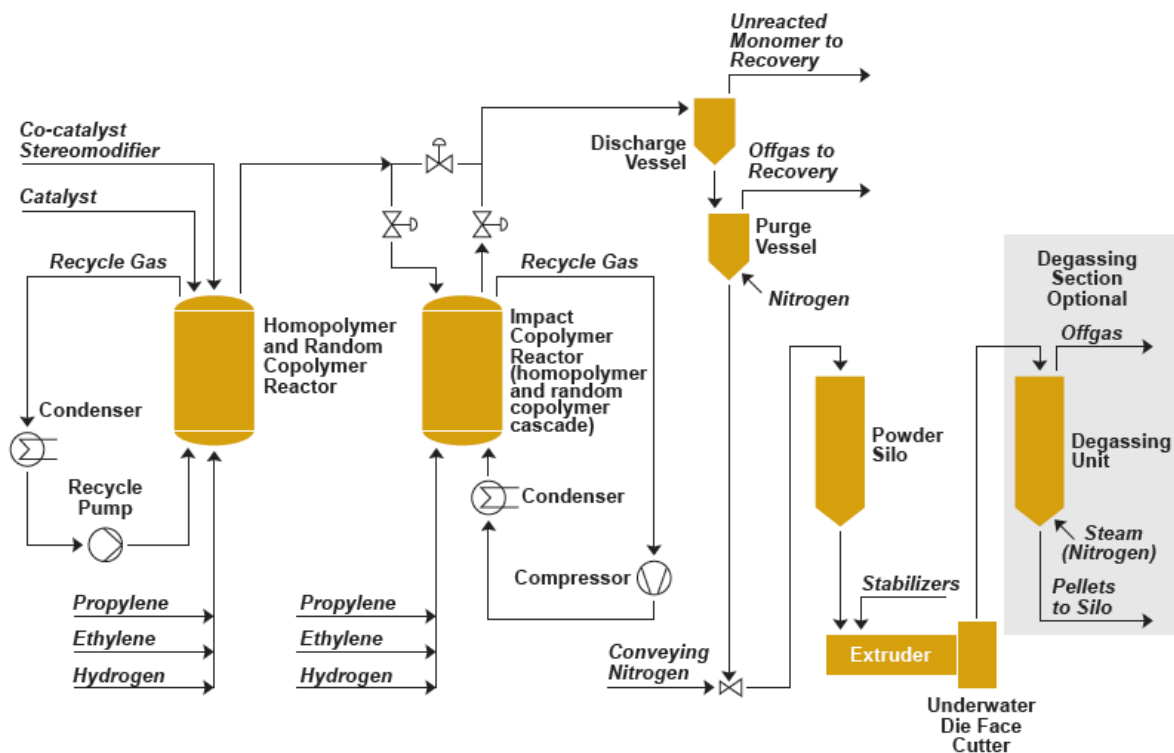
Figure 2.3   *Illustration of the Novolen® process to produce heterophasic copolymers [15]*

The composition of the rubbery phase is controlled in the second stage by the ethylene/propylene ratio and the amount of hydrogen. The co-monomer ratio ethylene/propylene in mol/mol, which is otherwise expressed as

Co-monomer ratio = C2 /C3   **(2.2)**

determines the rubbery copolymer composition. When the co-monomer ratio is equal to or higher than 9, essentially ethylene copolymers are produced, and when co-monomer ratio is lower than around 0.1, essentially PP random copolymers are produced. Generally, the lower the co-monomer ratio, the fewer ethylene copolymers are present in the rubbery phase [14].

2.1.3   *Typical morphology of gas phase produced heterophasic copolymers*

The mechanism of polymer growth for propylene/ethylene heterophasic copolymers is described by Debling et al. [16, 17] . According to this model the polypropylene particles are formed by mesoparticles of relatively small sizes (less than 1 μm). Each mesoparticle is formed by primary polymer particles containing catalyst crystallites. The polymer particle therefore contains mesoparticles separated by macropores and microparticles separated by micropores. This can be seen when looking at Figure 2.4. The EPR formed in the second reactor encapsulated in the polypropylene microparticles progressively expands into the small micropores and then into the larger macropores. McKenna et al. [18] and Cecchin et al. [19] proposed that the EPR formed on the active catalyst sites underneath the polypropylene homopolymer will create stresses in the viscoelastic polypropylene homopolymer and will therefore lead to the formation of cracks. The EPR will then flow through these cracks into the pores and onto the surface of the polymer particle. The polymer particle usually consists of a few mesoparticles with catalyst fragments located on the surface of the fragmented mesoparticles. The EPR formed in the second stage is at the surface of these mesoparticles ensuring a polymer particle containing a continuous network of EPR.
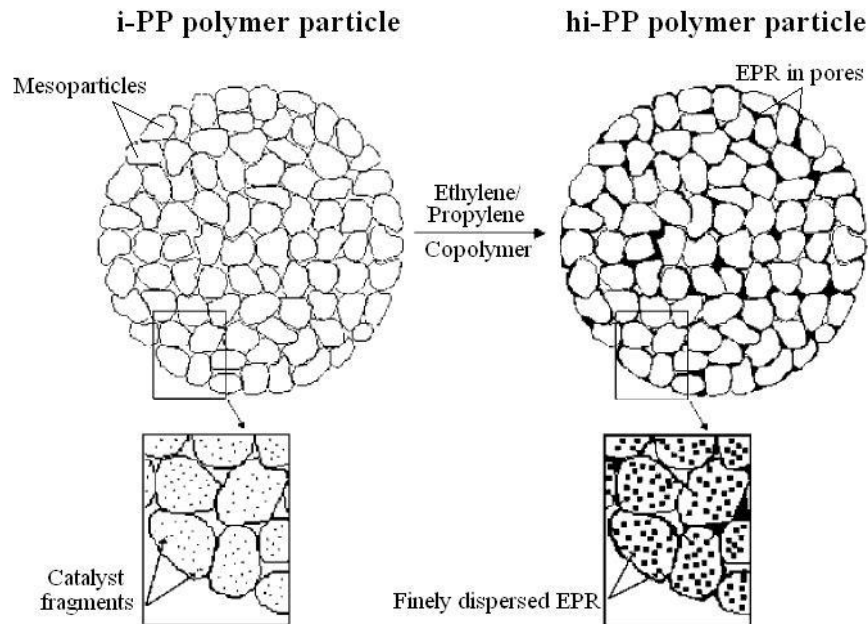
Figure 2.4   *Graphic representation of how a PP/EPR heterophasic copolymer is formed [2]*

Urdampiletta et al. [2] used scanning electron microscopy (SEM) to illustrate the difference between isotactic homo-polypropylene particles produced in the first reactor (or first stage) and high impact polypropylene particles produced after the second reactor. These images, as seen in Figures 2.5 (a-e), clearly show the difference between a polypropylene homopolymer particle and a heterophasic copolymer. Figure 2.5 (a) and (b) shows a rough surface area whereas Figure 2.5 (c) and (d) shows a much smoother surface area. This is due to the fact that the EPR fills in the cracks. Figure 2.5 (e) shows the result when the EPR phase is extracted with n-hexane and the polymer particle again takes on a similar appearance than in Figure 2.5 (a) and (b).
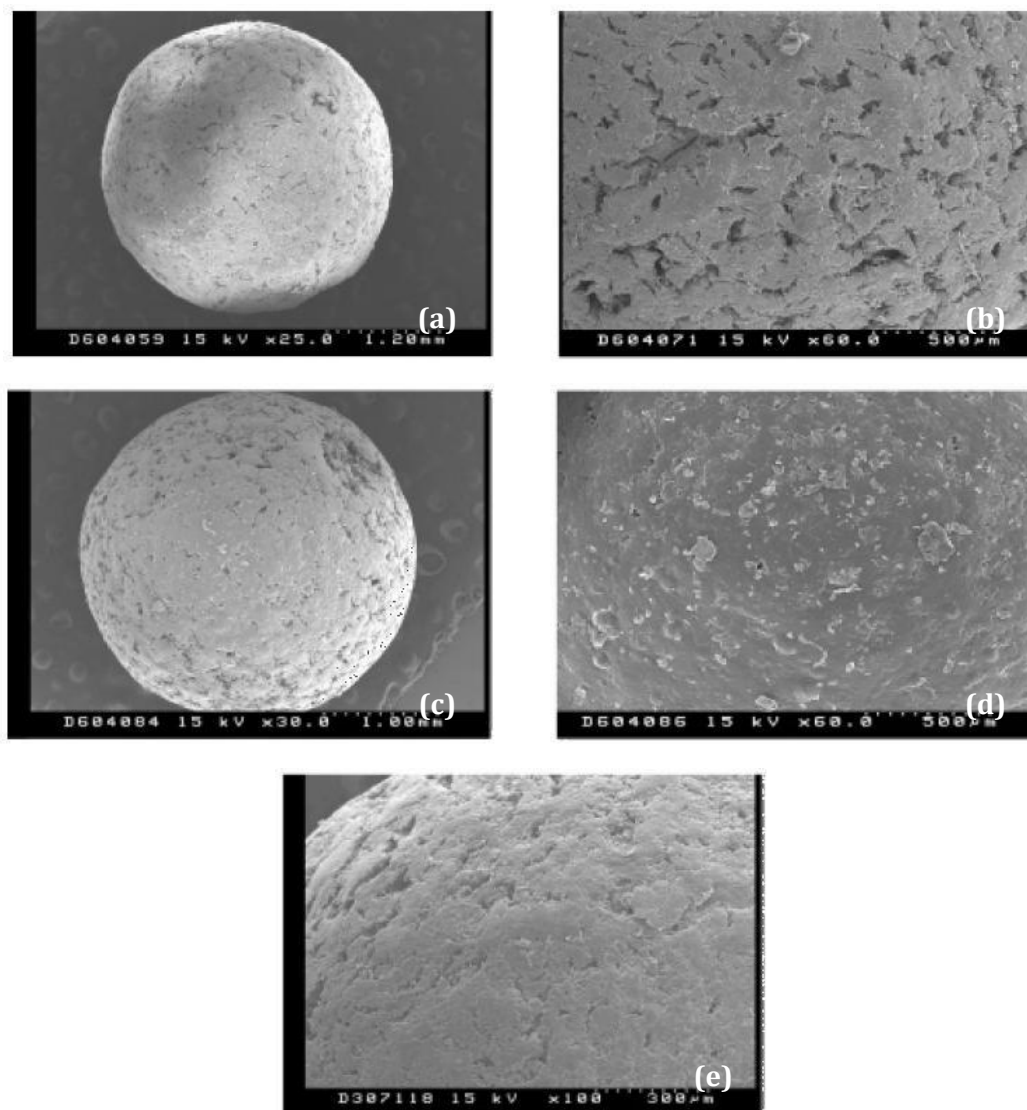
Figure 2.5   *SEM images showing the difference between polypropylene homopolymer and a heterophasic PP/EPR copolymer [2]*

The cross sectional SEM images in Figure 2.6 (a-d) further illustrates that the pores and the subsequent filling thereof is not limited to the surface of the copolymer particle, but actually extends throughout the particle.
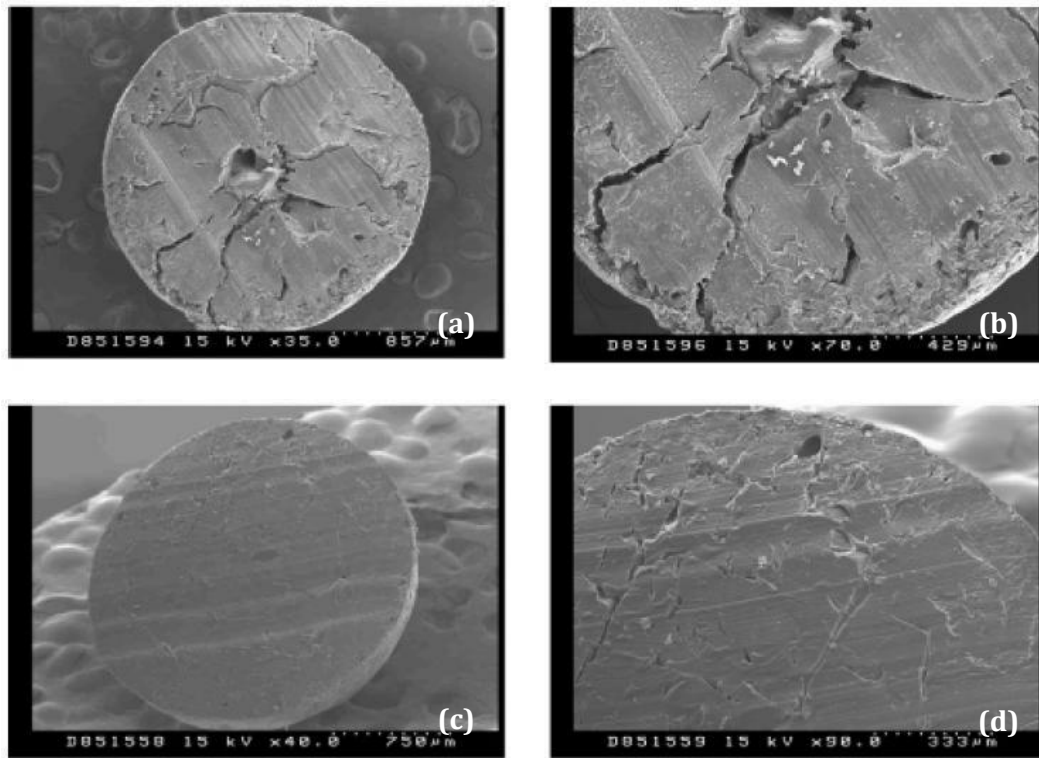
Figure 2.6   *Cross sectional SEM images of (a) and (b) polypropylene homopolymer particle and (c) and (d) high impact heterophasic polypropylene-ethylene copolymer [2]*

The types and properties of heterophasic copolymers vary, ranging from low MFR to very high MFR polymers. Heterophasic copolymers mostly consist of a polypropylene matrix and an ethylene-propylene or EPR phase, where the EPR phase varies in ethylene/propylene ratio, size and distribution within the polypropylene matrix. Polypropylene heterophasic copolymers with a high melt flow rate, e.g. MFR > 40 g/10 min and with medium or high impact strength are difficult to produce directly by polymerization with a Ziegler-Natta catalyst system. The difficulty arises because the matrix polymer of a heterophasic copolymer needs to have an MFR which is 50 to 100% higher than the MFR of the final copolymer. In turn this requirement means that very high hydrogen concentrations have to be used in the polymerization of the matrix polymer. In many cases that is not possible. In addition a matrix with a very high MFR is very brittle. This in turn affects the whole copolymer [2].

Heterophasic copolymers with very high amounts of rubber (Xylene Solubles > 20 wt-%), so called super high impact copolymers or reactor-made thermoplastic olefin copolymers (rTPOs), are even more difficult to produce with high MFR.

Another known route to a high MFR product involves chemical treatment, i.e., visbreaking (or also known as controlled rheology) of a molten polypropylene heterophasic copolymer. The

visbroken copolymer, also called a controlled rheology polymer, generally has higher impact properties than the parent polymer [20].

By visbreaking polypropylene with heat, or in more controlled conditions, with organic peroxides, the resultant molar mass distribution (MWD) will be narrower because the long molecular chains are more easily broken down. The molar mass (M_w) will also decrease, which of course corresponds to an increased melt flow rate (MFR). The MFR will increase with an increase in the amount of peroxide used during the visbreaking process [14].

As the molar mass distribution and the molar mass is decreased by visbreaking, the flowability of the resultant polymer will be improved (thus the term controlled rheology). The changes in M_w and MWD also affect the mechanical properties of a polymer. For example, visbroken PP homopolymers and random copolymers have lower stiffness (tensile and flexural modulus) and slightly better impact properties than a non visbroken PP homopolymer or random copolymer with the same MFR [14].

During visbreaking, ethylene polymers and copolymers are cross-linked by the peroxide. That means that the molar mass of the ethylene polymer will increase corresponding to a great drop in MFR. This is seen as gel formation and lack of flowability [14].

Visbreaking of a propylene/ethylene heterophasic copolymer is more complicated because of the complex composition comprising homopolymer or random copolymer matrix, amorphous rubber and semi-crystalline ethylene-propylene copolymers. Both the matrix polymer and the rubber should decrease in molar mass, giving higher MFR, but the ethylene copolymers may be cross-linked. This may cause problems, like flow problems or gel formation. This causes the mechanical properties, both stiffness and impact resistance, to decrease. The visbreaking of a heterophasic copolymer to a given MFR consumes more organic peroxide than visbreaking of a corresponding homopolymer to the same MFR, because of the negative (crosslinking) reactions that occur with the ethylene copolymer. The consumption of these expensive peroxides increases the higher the content of the rubbery copolymer there is in the heterophasic copolymer. The same applies regarding the more ethylene-rich the (crystalline) copolymers present in the heterophasic copolymer are [14].

The amorphous rubber content is generally assessed by dissolving the polymer in xylene. The amount of xylene solubles (XS-weight-%) at room temperature (RT), is generally regarded as corresponding to the amount of rubber present in the HECO.

2.1.4   Market overview of polypropylene (2011)

Polypropylene resins constitute one of the fastest growing commodity resins in the world. In 2010 PP production stood at approximately 48.8 million metric tons. The estimated value of production stood in the range of $115.6 billion and represented an average annual growth rate of 7.0% per annum since 1990. World consumption in 2010 grew to an all-time high of 48.5 million metric tons [21].

The United States and China now represent more than 12.1% and 26.6%, respectively, of world consumption for polypropylene, nearly three times the consumption of the next largest consumers, Japan and Germany. Table 2.1 below presents the world consumption of polypropylene resins by end 2010 [21].

Table 2.1   World consumption of polypropylene resins by end use - 2010

	North America	Western Europe	Central and Eastern Europe	Middle East	China	Japan	Other Asia	Other Regions	Total
Total Consumption (1000's MT)	7,200	7,908	2,195	3,096	12,932	2,644	8,434	4,146	48,554
End Uses (%)									
Fibers and Filaments	17.8	23.2	13.6	33.9	52.9	6.2	40.1	12.2	31.5
Injection Moulding	32.4	46.2	30.0	36.9	15.7	53.8	23.9	37.4	31.2
Film and Sheet	9.7	18.8	12.1	16.2	19.8	21.4	21.5	28.6	18.3
Blow Moulding	1.6	2.2	0.2	2.0	5.9	1.0	5.6	1.8	3.5
Other	38.6	9.6	44.0	10.9	5.7	17.6	8.8	20.0	15.5
Total	100.0	100.0	100.0	100.0	100.0	100.0	100.0	100.0	100.0

From Table 2.1 it can be seen that injection moulding and fibre and filament are the largest world uses at 31.2% and 31.5% respectively. By 2015, world consumption of PP is expected to reach approximately 62.9 million metric tons, representing an average annual growth of 5.3% from 2010 – 2015. Table 2.2 below shows the world per capita consumption by region in 2010 and 2015 [21].

Table 2.2 World per capita consumption of PP (kilograms)*[21]*

	2010	2015
North America*	17.9	23.5
Central and South America	5.4	6.9
Western Europe	19.2	22.3
Central and Eastern Europe	4.5	5.8
Africa	1.3	1.6
Middle East	14.5	18.5
China	9.3	11.7
Japan	20.8	22.0
Other Asia	3.8	5.1
Oceania	15.8	18.6
World	7.1	8.7

* Includes the United States, Canada and Mexico

It can be seen that Western Europe and Japan are the highest per capita consumers of PP, followed by North America. What is also noticeable is the significant lower per capita consumption of other regions, which indicates the tremendous growth potential in the short and medium term [21].

2.2   Degradation of polymers

Polymer degradation can be classified as a result of chemical, physical or biological reactions taking place in the polymer material that will lead to bond scissions and subsequent chemical transformation of the polymer material. Therefore, degradation will reflect a change in the material's properties such as mechanical, optical or electrical characteristics caused by crazing, cracking, erosion, discoloration and phase separation. Polymer degradation has therefore been classified under the following sub categories:

- Photo-oxidative degradation
- Thermal degradation
- Ozone-induced degradation
- Mechano-chemical degradation
- Catalytic degradation
- Biodegradation
- Non-oxidative degradation
- Controlled rheology with the use of organo-peroxides

These sub categories of degradation as well as the mechanisms and means of studying them will be discussed in the sections below.

2.2.1   *Photo-oxidative degradation*

When a material undergoes a process whereby it is decomposed by the action of light in the presence of oxygen, it is known as photo-oxidative degradation. Photo-oxidative degradation is known as one of the primary causes of degradation in polymeric materials. Most polymers (especially those without stabilizers) are susceptible to degradation. Light in the visible and UV regions can cause or accelerate this degradation process. In many cases this is due to the presence of hydroperoxides that are formed during processing, when heat and oxygen initiate autoxidation. UV radiation has sufficient energy to cleave C – C bonds. The wavelength at which most damage takes place depends on the type of bonds present in the material. For example, the wavelength at which the most degradation will take place due to photo-oxidative degradation in polyethylene (PE) is approximately 300 nm and for polypropylene (PP) it is 370 nm. UV degradation mostly affects the optical properties (yellowing effect), loss of mechanical properties, molecular weight and molecular weight distribution. Polyethylene and polypropylene readily lose their extensibility, mechanical integrity and strength and generally there will be a decrease in molecular weight, although initially PE may actually increase in molecular weight due to crosslinking reactions [22, 23]. Furthermore, at any given temperature and moisture content, the rate of degradation will increase with an increase in UV flux.

Oxidative degradation reactions are determined by the extraneous groups and/or impurities in the polymer material. These groups and/or impurities will absorb light (or quanta) and will lead to the formation of long lived triplet states from shorter lived singlet states. Out of these triplet states two types of reactions can take place, they are (1) Norrish Type 1 reactions [24], where the excited triplet state will lead to the cleaving of a polymer chain to form radical pairs, or (2) Norrish Type 2 reactions [25] where the triplet state will lead to the formation of saturated or unsaturated chain ends by means of hydrogen transfer. If radicals are formed (be it through Norrish Type 1, chain scission or the decomposition of hydroperoxides), the formed alkyl radical will react with molecular oxygen to form peroxy radicals, which can abstract hydrogen from a suitable carbon on the polymer chain to form hydroperoxide groups, which in turn can absorb UV light and become excited by energy transfer. The weak O – O bonds will break and pairs of alkoxy and hydroxyl radicals are formed which may react in various ways

that will lead to chain scission or rearrangement. The simplified mechanism is set out in Scheme 2.1. It can be seen that there are three main steps involved in photo-oxidative degradation. They are initiation, propagation and termination.

Initiation involves the process where the initial alkyl radical is formed. This can be due to UV light with sufficient energy to cleave a polymer chain, thermal chain scission or, mechanical chain scission. This radical can then undergo various reactions that lead to the propagation step. Initiation in the presence of light can take place in various ways, for example via direct UV initiated photolysis of C – C and C – H bonds with the formation of a C● and H● radical species, or via photosensitized cleavage where photosensitizers get excited on the exposure to light which in turn leads to effective homolysis of the polymeric chain. Other means of initiation include the addition of catalysts like certain salts to generate radicals, or the incorporation of carbonyl groups during synthesis or processing which can act as chromophores. Another way of initiation is the deliberate introduction of peroxides.

During the propagating step certain reactions take place that leads to the formation of hydroperoxide species. Hydroperoxide species are not directly related to chain scission but form key intermediates to further reactions that are. During propagation the O – O bonds of the hydroperoxide species are cleaved and this could be subsequently followed by β-scission of the polymer chain.

$$Initiator \rightarrow R_i^\bullet$$
$$R_i^\bullet + O_2 \rightarrow R_iOO^\bullet$$
$$R_iOO^\bullet + R - H \rightarrow R_iOOH + R^\bullet$$

Initiation

$$R^\bullet + O_2 \rightarrow ROO^\bullet$$
$$ROO^\bullet + R - H \rightarrow ROOH + R^\bullet$$

Propagation

$$R^\bullet + R^\bullet \rightarrow R - R$$
$$R^\bullet + ROO^\bullet \rightarrow ROOR$$
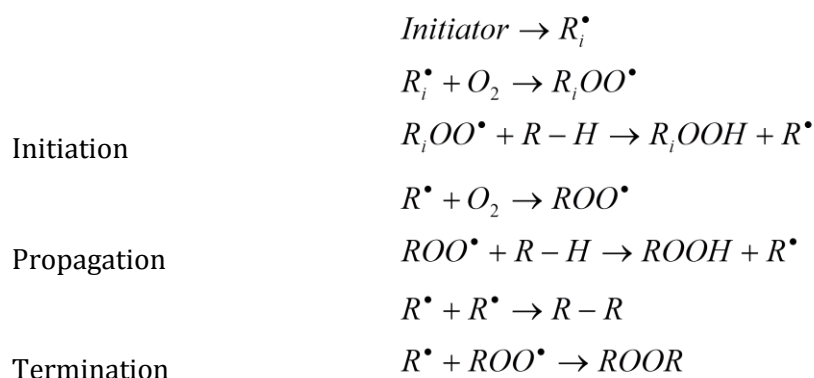
Termination

Scheme 2.1 *Simplified mechanism of oxidative degradation*

The termination of the process takes place when the free radicals combine. Macroalkyl radicals may combine to form cross-linked, branched or disproportionate structures and peroxy radicals will eventually combine with other radicals to give dialkyl peroxides, carbonyl species or alcohols [22].

Photo-oxidative degradation mechanisms can be reduced by the addition or introduction of small amounts of stabilizers that can inhibit the initiation, propagation or termination reactions in various ways. Figure 2.7 shows the auto-oxidation cycle and various points where stabilizers can be added to inhibit the degradation of the polymer material.

The inhibition of auto-oxidation by the use of stabilizers is well documented in literature. According to the mode of action the stabilizers can be classified as antioxidants, which forms the rate determining step in the cycle and can act by either donating hydrogen to the peroxy radical and forming a stable oxy radical, and also decomposing the hydroperoxide species into a non-radical, non-reactive thermally stable species or via effective alkyl radical scavenging. Stabilizers can further be classified into metal deactivators, which form stable complexes with reactive radicals, or light stabilizers, i.e. UV-absorbers or quenchers.
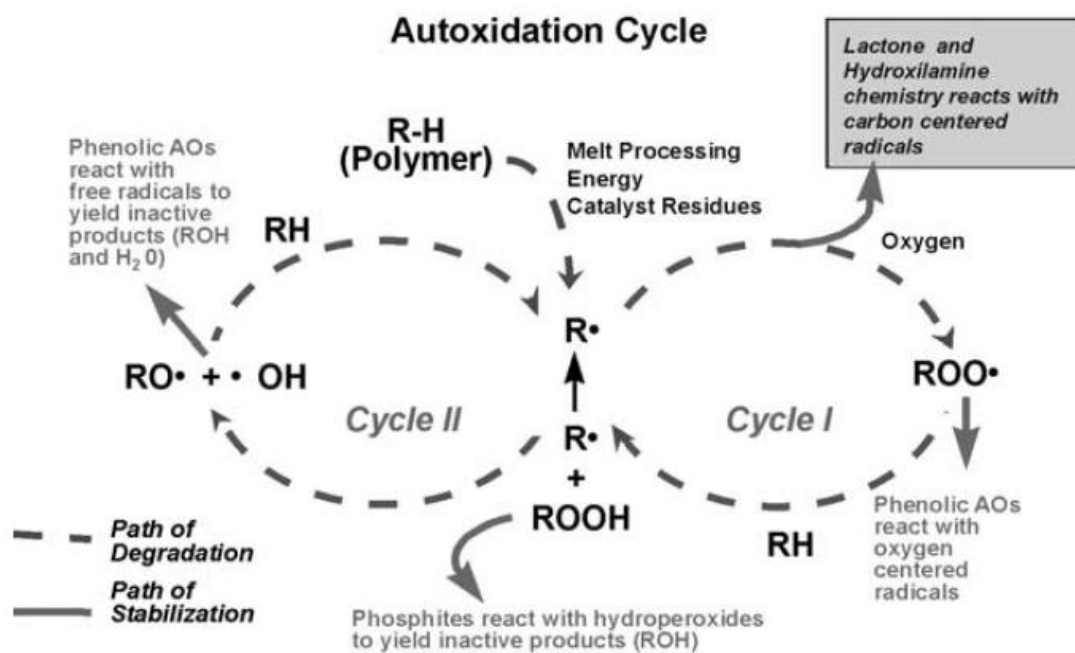
Figure 2.7   *The auto-oxidation cycle and the means to inhibit degradation at various stages through the addition of stabilizers [26]*

2.2.2   Thermal degradation

Under normal conditions there are no differences between photochemical and thermal degradation, however, under certain conditions there are certain differences. The main difference between the two is the sequence of initiation steps leading to auto-oxidation. Another difference is that thermal degradation takes place throughout the bulk of the polymer whereas photochemical degradation takes place at the surface of the polymer.

Thermal degradation occurs through chain degradation or depolymerization reactions initiated by thermal and UV light. A large number of addition polymers may undergo depolymerization reactions. For example, PMMA (polymethyl methacrylate) has been converted almost quantitatively back to monomer [22] and polyethylene has been decomposed into longer olefinic fragments and actually producing small amounts of monomer. Above 200 °C thermal degradation leads to chain scission and depends largely on the presence of impurities like unsaturated bonds and head-to-head units etc.

Hace et al. [27] studied thermally stimulated oxidative degradation of high impact polystyrene (PS) with nitric acid. The mechanism of oxidation and nitration depends on the temperature and leads to molecular and chemical heterogeneity and also lowering in mechanical properties of the polymer. Complex reactions that occur during thermal degradation will depend on various factors such as heating rate, pressure, reaction medium and reactor geometry. Polymers also have high viscosities which will impede on heat and mass transfer [28]. Thermal degradation of polymers can be divided into two main reactions which occur simultaneously. The first reaction is the random scission of links. This will lead to a reduction in the molecular weight. The second reaction consists of the scission of chain-end C – C bonds. This scission will lead to the formation of volatile products. This type of thermal degradation will usually take place at the gas-liquid interface [29]. The type and composition of these volatiles can give useful information about the mechanism of degradation. The thermal degradation of polymers follows either chain end degradation, shown in equation 2.3 and 2.4, or random degradation shown in equation 2.5.

$$M_n^* \rightarrow M_{n-1}^* + M$$
(Eq. 2.3)

$$M_{n-1}^* \rightarrow M_{n-2}^* + M$$
(Eq. 2.4)

$$M_n \rightarrow M_x + M_y$$
(Eq. 2.5)

Chain-end degradation starts from the end of the chain and successively releases the monomer units. This is also known as depolymerization and is essentially the opposite of propagation. In general chain-end degradation occurs when the backbone bonds are weaker than the bonds of the side-chains and only with polymers with active chain ends i.e. free radical, anion and cation. α-Substituted vinyl polymers (like PMMA, poly α-methylstyrene and PP) degrade mostly via this route.

Random degradation will take place anywhere along the polymer chain and no monomer units are released. There is also not the necessity for an active site to be present, as is the case for chain-end degradation. For example, PE undergoes random degradation through migration of the hydrogen atom from one carbon to another and will thus lead to the formation of two fragments [30]. Redryguez-Vazquez et al. [31] observed that during thermal degradation of LDPE at 400 °C intra-molecular hydrogen is abstracted and this is followed by β-scission. The thermal oxidation of PP at between 120 - 280 °C on the other hand will result in multiple oxidative chain scissions, resulting in approximately 40 possible volatile compounds [32].

2.2.3   *Ozone-induced degradation*

Ozone in air, even in small concentrations, will lead to accelerated ageing of polymer materials. This process will also lead to the generation of oxygen-containing compounds, a reduction in molecular weight and impairment of electrical and mechanical properties. Reaction of ozone occurs with polymers with C = C bonds, aromatic rings or saturated hydrogen links. When polymers are exposed to ozone a variety of carbonyl products based on aliphatic esters, ketones and lactones are formed. This will be followed by the formation of other hydroxyl and terminated vinyl end-groups [33].

The reactions proceed through unstable intermediates such as bipolar ions or peroxy radicals, which in turn can isomerize or degrade and that in turn, will lead to degradation of the polymer material.

Ozone degradation usually starts at the unsaturation in unsaturated polymers and will occur in 3 general steps. Step 1 (as seen in Scheme 2.2) involves the cyclo-addition of ozone to the olefinic double bond to form an ozone-olefinic adduct (primary ozonide). This specie, due to the O – O bonds, is very unstable and will react further, leading to the second step in the mechanism.
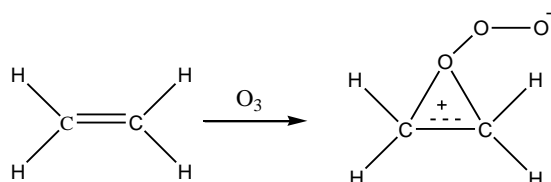
Scheme 2.2   *Step 1 of the ozone-induced degradation mechanism: Cyclo-addition and ozonide formation*

During the second step (as seen in Scheme 2.3 below) the ozonide is decomposed to carbonyl and carbonyl-oxide compounds.
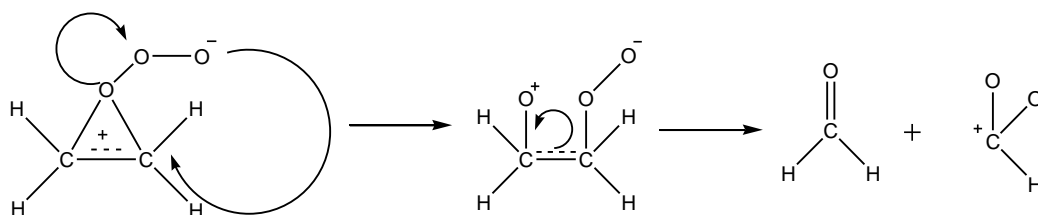
Scheme 2.3   *Step 2 of the ozone-induced degradation mechanism: Decomposition of the ozonide and the formation of carbonyl and carbonyl-oxide compounds.*

Finally in step 3 the carbonyl-oxide flips over with the nucleophilic oxy-anion attacking the carbon atom of the carbonyl group. This is shown in Scheme 2.4 below.
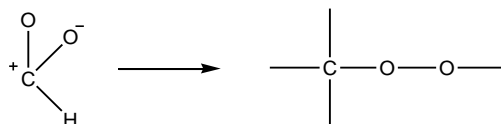
Scheme 2.4   *Step 3 of the ozone-induced degradation mechanism: The formation of a ROOR compound.*

2.2.4   *Mechano-chemical degradation*

According to J Li et al. [34] mechano-chemical degradation of polymers will involve the degradation of the material under mechanical stress as well as by strong ultrasonic irradiations. When polymers are subjected to mechanical stresses that result in the breakdown of molecular chains it is often accompanied by a chemical reaction. A good example of mechanical shear followed by chemical reaction is the mastication of rubber. Here chain breakage will take place as well as the development of plasticity. However, when in a nitrogen atmosphere at normal temperature mastication does not change the plasticity and molecular weight remarkably. In an oxygen atmosphere however, the degradation will occur rapidly. This is due to the fact that the rubber material breaks into radicals and seeing that oxygen is a radical scavenger the radicals will react with the oxygen leading to permanent chain breakage. In a nitrogen atmosphere the nitrogen will not react with the radicals. The radicals will therefore re-combine and no permanent chain breakage will take place [35].

Mechano-chemical degradation in polymer melts also occurs due to free radical processes. These processes will lead to a narrower molecular weight distribution, a quantitative relation between ruptures and crosslinks, a change in the concentration of double bonds and an increase in long-chain branches. This is due to the reaction of chain side radicals [36-38]

GPC studies of LDPE and HDPE degradation under high shear have shown that most of the changes in molecular weight and long-chain branching are a result of thermal-oxidative degradation. However, the orientation of PP under shear conditions produces oxidation products directly as a result of the shear process.

2.2.5   Catalytic degradation

Polyolefins like PE and PP constitute an important part of commercial and domestic waste. Due to this there has been a surge of interest in recent years to come up with an effective means of recycling or disposing of these polymers. During catalytic degradation these materials are catalytically converted or degraded to gasses and oils, which in turn has more commercial value. Garforth et al. [39] investigated catalytic degradation of polyolefins using TGA and found that the presence of a catalyst greatly reduces the apparent activation energy. Different types of catalyst for polymer degradation are known in literature. They include Pt-Co and Pt-Mo catalysts supported on SiO_2, zeolites, non-zeolites and transition metal catalysts.

Sekine and Fukimoto [40] proposed a free radical mechanism for the catalytic degradation of PP using a Fe/activated carbon catalyst. The mechanism is shown in Scheme 2.6. During the initiation stage C – C bonds are broken with heat to produce radicals. In the propagation step the hydrocarbon radicals decompose to produce lower hydrocarbons such as propylene, followed by β-scission and abstraction of H radicals to produce new alkyl radicals. Termination takes place by disproportionation reactions or the re-combination of radicals. During catalytic degradation with Fe/activated charcoal (AC) in a hydrogen atmosphere, hydrogenation of hydrocarbon radical and the abstraction of the H radical from hydrocarbon or hydrocarbon radical generate radicals, enhancing degradation rate. In a reaction temperature lower than 400 °C or a reaction time shorter than 1.0 h, many macromolecular hydrocarbon radicals exist in the reactor, and recombination occurs readily because these radicals cannot move fast. However, with Fe/activated carbon in a hydrogen atmosphere, these radicals are hydrogenated and therefore recombination may be suppressed. Consequently, it seems as if the decomposition of

the solid product is promoted, including low polymers whose molecular diameter is larger than the pore size of the catalysts. Wall et al. [41] have studied the catalytic degradation of waste plastics and have found that when these polymers have been heated above 380 °C, they undergo depolymerization and degradation by a free radical chain reaction.
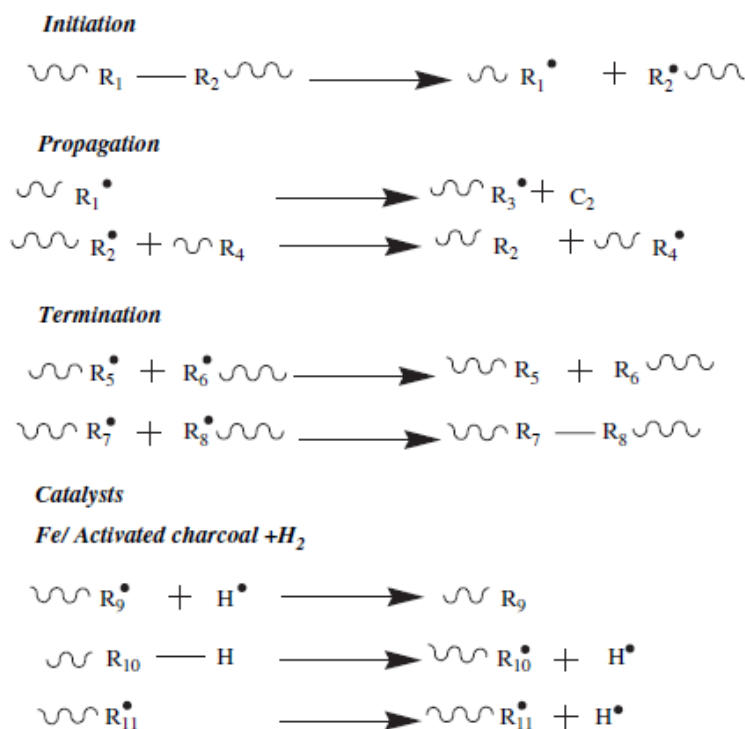
Scheme 2.5   *The catalytic degradation mechanism of polypropylene according to Sekine and Fujimoto[40].*

2.2.6   Biodegradation

According to Singh et al. [22] biodegradation is a biochemical transformation of compounds by microorganisms. Mineralization of organic compounds leads to the production of carbon dioxide and water under aerobic conditions and methane and carbon dioxide under anaerobic conditions. Abiotic hydrolysis, photo-oxidation and physical disintegration of polymers will all lead to enhancement of biodegradation due to the increase in surface area for microbial colonization or by simply reducing the molecular weight [42]. Biodegradation has been defined in multiple ways depending on the specific investigator. Lemm et al. [43] defined it as a change in the surface properties or a loss of mechanical strength, Potts et al. [44] defined it as assimilation by microorganisms, Swift [45] as the degradation by enzymes and Ratner et al. [46] and Hergenrother et al. [47] defined it as backbone chain breakage and subsequent reduction in

the average molecular weight. It is generally accepted that biodegradation can occur by any of the above definitions or by a combination of them. According to ASTM standard D-5488-94d, biodegradation can be defined as "process which is capable of decomposition of materials into carbon dioxide, methane, water, inorganic compounds, or biomass in which the predominant mechanism is the enzymatic action of microorganisms, that can be measured by standard tests, in a specified period of time, reflecting available disposal conditions".

Biodegradation can occur on a molecular, macromolecular, microscopic or macroscopic level depending on the specific mechanism involved [48]. There are four different mechanisms that govern biodegradation: solubilization, charge formation followed by dissolution, hydrolysis and enzyme-catalysed degradation [49, 50].

For solubilization, the hydration of polymers depends on their hydrophilicity and that will result from the disruption of secondary and tertiary structure stabilized by Van Der Waals forces and hydrogen bonds. During and after hydration the polymer will become water soluble or the backbone may be cleaved by chemical or enzyme-catalysed hydrolysis and will thereby result in the loss of polymer strength [51].

Most often polymers are water-insoluble, but may become solubilized after ionization or protonation of a pendent group. At high pH polyacids become soluble and hydrophilic [52]. Cellulose acetate phthalate becomes water soluble at a pH > 6, while poly(vinyl acetate phthalate) and hydroxyl propyl methyl cellulose phthalate are ionized at a lower pH [53].

Water insoluble polymers containing pendent anhydride or ester groups can become solubilized if any of the anhydride or ester groups hydrolyse to form ionized acids. For example, poly(methacrylate) and poly(methyl methacrylate) are esters derived from poly(acrylic acid) and poly(methacrylic acid) respectively. Both these polymers are not water soluble but will become water soluble upon hydrolysis of the pendent esters and subsequent ionization of the carboxylic group [54]. For hydrolysis to occur, the polymer has to contain hydrolytically unstable bonds, which should be reasonably hydrophilic for the access of water [22].

Enzyme-catalysed hydrolysis occurs when enzymes function as catalysts for a specific reaction of series of reactions, i.e. oxidation, reduction, hydrolysis, esterification, synthesis and molecular inter-conversions [55].

Microbial degradation will result from the action of naturally occurring microorganisms like bacteria, fungi or algae. The production of biodegradable polymers that are able to get decomposed completely in nature have recently become very popular. They are considered to be totally eco-friendly and are considered extremely useful in waste landfill management. Addition of natural polymers to thermoplastics having long-term potential is one of the approaches to enhance biodegradability [56].

2.2.7   *Controlled rheology (Controlled Degradation)*

Due to its diverse range of applications and unique properties, polypropylene has become the polymer of choice for various market sectors. As propylene monomer cannot be polymerized by free radicals the result of the presence of any free radicals in the manufacturing process will be the random degradation of the polymer backbone by scission. This phenomenon has prompted a significant amount of research and has led to the development of an entire class of polypropylene materials known as visbroken or controlled rheology polypropylene.

Visbroken polypropylene is especially used in the fibre and automotive industry. Fibre requires a high flow and a well-controlled, narrow molecular-weight distribution. The current trend in the automotive industry is to reduce the weight and thickness of parts, which also requires a polymer with a high flow. Adding free radicals to the process will result in chain scission and a resultant narrower molecular weight distribution and higher MFR polymers will be produced. These polymers are ideal for this specific purpose [57]. Although research does exist into how to balance the need for high melt flow polymers with the necessary properties required, no real effort has been made to account for the exact effects of peroxides (which are generally used as a source for free radicals) on the molecular properties of polypropylene. Two main factors that will influence the effect of peroxides on polypropylene are the residence time and the half-life of the peroxide [57].

The residence time (how long the material remains in the polymer extruder or processing chamber) of the peroxide is mostly determined by the extruder's throughput and free volume. The half-life of the peroxide (the time required for consumption of 50% of the peroxide) is dependent on the specific temperature that the extruder/reactor is run at and, of course, the type of peroxide used. Longer half-lives and higher/lower decomposition temperatures will lead to better reaction control, but may influence product quality and safety. For this reason it is crucial to understand the effect of the specific peroxide used on the molecular properties of the

polymer as well as the ability to predict how much of the peroxide is required to achieve certain properties.

2.3   Fractionation techniques

Due to the complex nature of semi-crystalline polymers it is important to comprehensively characterize these polymers to understand the link between the molecular make-up of the polymer and its inherent properties. Suitable methods to comprehensively understand the properties such as the molecular weight and molar mass distribution (MMD), chemical composition and chemical composition distribution (CCD) and molecular topology or branching is therefore crucial in evaluating these complex systems. The most common means of characterizing a material is by means of fractionation. Fractionating a material is used to investigate the heterogeneity of molecular species that make up the polymer. There are three main areas in which polymers can be fractionated that include fractionating according to crystallisability, fractionating according to molecular mass and fractionating according to chemical composition distribution.

2.3.1   Fractionation by crystallinity

Several techniques have been developed over the years in order to analyse semi-crystalline polymers based on crystallinity. By far the most used and most established techniques are temperature rising elution fractionation (TREF), crystallisation analysis fractionation (CRYSTAF) and crystallisation elution fractionation (CEF). These three techniques differentiate by differences in crystallisability as a function of temperature. However, more recently developments in turbidity fractionation analysis (TFA) and solution crystallisation analysis by laser light scattering (SCALLS) have also been shown to be useful as a fractionation analyses tool.

The principle of polymer fractionation by crystallisability is based on the Flory-Huggens statistical thermodynamic treatment that will account for the melting point depression by the presence of a diluent [58, 59]. Equation 2.6 below represents this principle.

$$\frac{1}{T_m} - \frac{1}{T_m^o} = \frac{R}{\Delta H_u} \frac{V_u}{V_1} \left[-\frac{\ln v_2}{x} + \left(1 - \frac{1}{x}\right) v_1 - x_1 v_1^2 \right] \qquad \textbf{(Eq. 2.6)}$$

Where, T_m^o is the melting temperature of the pure polymer, T_m is the equilibrium melting temperature of the "diluted" polymer, ΔH_u is the heat of fusion per polymer repeating unit, x is the number of segments per molecule, and xV1/Vu is the number of units per molecule. Crystallisation temperature will decrease with an increase in diluent [60].

2.3.1.1   Temperature rising elution fractionation (TREF)

Desreux and Spiegels [61] first realized that semi-crystalline polymers could be fractionated according to solubility at a given temperature and that this was based on the ability of the polymer to crystalize. Their work involved the elution of fractions of polyethylene at increasing temperatures. Thereafter Shirayama et al. [62] developed a method for fractionating low density polyethylene according to the degree of short chain branching and it was this work that gave rise to the name of temperature rising elution fractionation or TREF as it is more commonly known.

The principle upon which TREF fractionates semi-crystalline polymers is based on separation according to crystallisability [63-65]. Therefore, the actual molecular structure and composition of the polymer will affect the way in which, or the ability, of the chains to crystallize [65]. TREF can be divided into two main steps, namely crystallisation and elution. In the crystallisation step the semi-crystalline polymer is first dissolved in a suitable solvent at high temperatures and then allowed to cool down slowly under a controlled temperature profile. Typically the fastest cooling rate is no more than 2 °C/hour [63]. The critical step in the TREF process is that of the crystallisation which is important to obtain good, reproducible separations. From literature it is well established that the crystallisation step can either be done in the presence of a support, or from solution [66-71]. In both cases the addition of an antioxidant is advised in order to act against polymer degradation. During the elution step the polymer that was crystallized is dissolved off the support or out of solution at successively higher temperatures. Due to this part of the experimental process the importance of a suitable medium to perform the fractionation in became important and it is well documented in literature that both glass and stainless steel columns provide a simple yet very effective medium [64, 66-68, 71]. The basic principle of separation according to crystallisability upon which the TREF process is based is graphically represented in Figure 2.8 and Figure 2.9. Here it is illustrated that the less crystalline "short" chains crystallize last, or at lower temperatures, whereas the more crystalline "longer" chains

crystallize at higher temperatures. Thus, during the elution step, which starts at room temperature, the fractions coming off first will be those of least crystallinity.
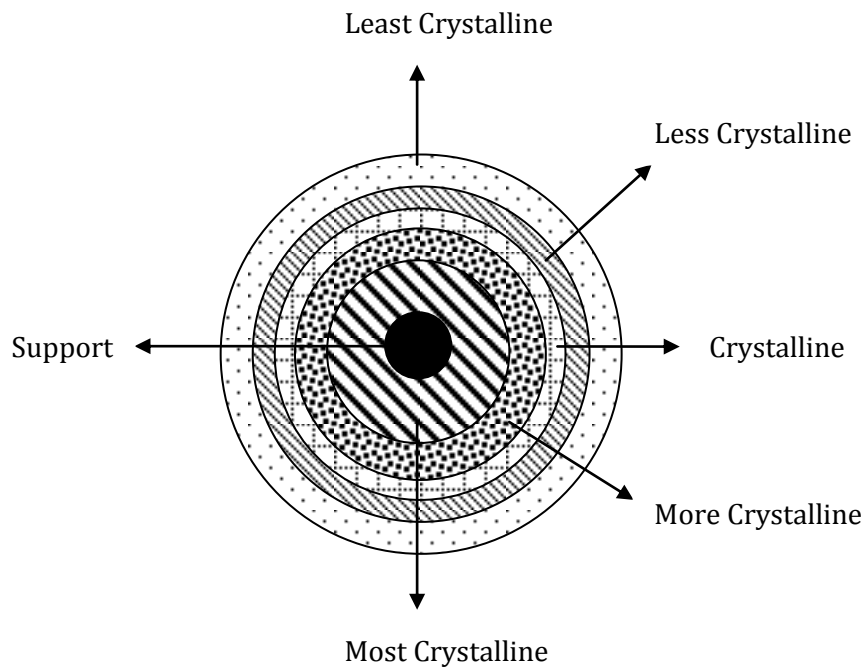
Figure 2.8   *Graphic illustration of sample after crystallisation on support*
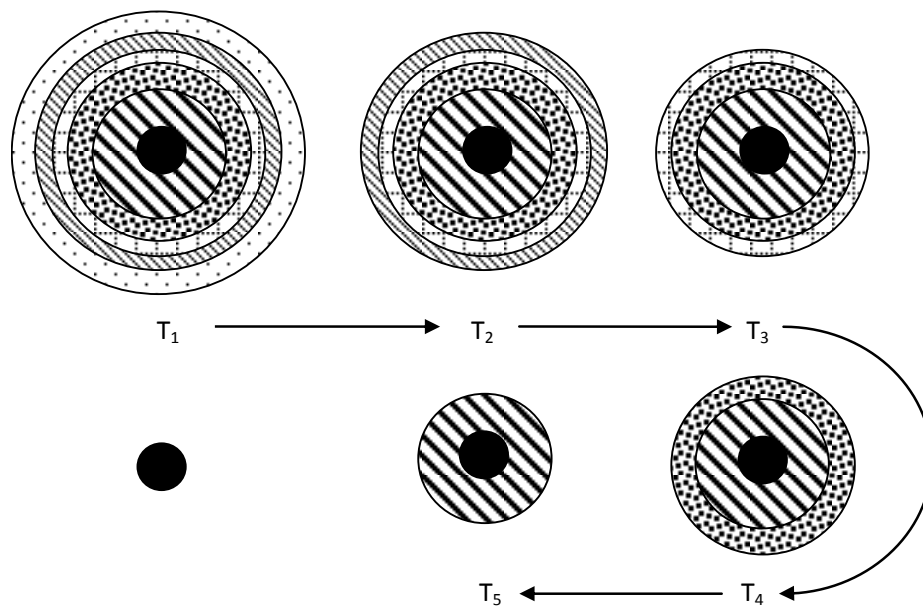
Figure 2.9   *Graphic illustration of the elution step with T1 - T5 indicating increasing temperatures*

Two types of TREF techniques have been developed which are now commonly used. The first involves continuous on-line signal detection known as analytical TREF (A-TREF). The second

involves the collection of much larger fractions that are subsequently used in off-line analysis and is known as preparative TREF (P-TREF).

In A-TREF the result is a weight fraction of eluted polymer vs. temperature profile that is obtained by continuously increasing the column temperature and measuring the polymer concentration in the eluent by means of an RI/IR on-line detector [5, 60]. Copolymer standards with narrow chemical composition distributions (CCD's) can be used to translate the temperature axis into a chemical composition distribution axis by making use of a calibration curve. These narrow CCD's are typically obtained from P-TREF fractionation or direct synthesis from single site catalysts [60].

P-TREF involves the stepwise elution and isolation of fractions from the eluent. These fractions are then collected and sent for offline analysis to characterize the specific fractions. Typical offline characterization methods that are used include ^{13}C-NMR, DSC, wide-angle x-ray diffraction (WAXD), high temperature size exclusion chromatography and CRYSTAF. These techniques, together with a wide variety of others, then gives a complete molecular picture regarding the different fractions that make up the polymer sample [5].

2.3.1.2   Crystallisation analysis fractionation (CRYSTAF)

Benjamin Monrabal [72] developed crystallisation analysis fractionation (CRYSTAF). The technique is based on stepwise precipitation. By monitoring the polymer solution concentration during precipitation or crystallisation the cumulative short chain branching distribution can be obtained (if the polymer is branched, such as is the case with LLDPE), without the need to physically separate the fractions. As mentioned in the previous section TREF requires two steps, namely crystallisation and elution. CRYSTAF however only requires crystallisation and as such is much less time consuming than TREF. It further has the capability to simultaneously analyse various samples. With the help of a suitable IR detector, the concentration of the polymer in the solution can be measured as a function of the temperature. The resultant concentration profile of the polymer left in the solution can then be obtained as a function of temperature. The technique rests on the principle that with decreasing temperatures, more polymer crystallizes out of the solution and therefore the concentration of the polymer in the solution decreases. By then making use of a calibration curve with narrow CCD copolymers (similar to the method described in Section 2.3.1.1) the concentration of the polymer at a given temperature can be correlated to a chemical composition distribution. Each

calibration curve is obtained for specific experimental conditions like co-monomer content, cooling rate, solvent, etc. [60, 72]. The technique developed by Monrabal [72] also fractionates semi-crystalline material on the basis of crystallisability [73].

As described by Monrabal [73] and Soares [64] the analytical CRYSTAF technique is automated for ease of use and allows for the simultaneous analysis of up to five samples. Stainless steel reaction vessels not containing any support medium are used to facilitate the reactions. The polymer is dissolved in a suitable solvent for use with a IR detector, typically 1,2,4,-trichlorobenzene (TCB) and cooled under controlled conditions [5, 72, 74]. As in the case of TREF, the addition of 0.1% of an antioxidant is recommended to prevent polymer degradation [72]. By decreasing the solution temperature the chains are allowed to crystallize out of the solution and by doing so lower the concentration of the solution. While the precipitate is ignored, samples of the solution are taken through a filter and analysed with the IR detector [5, 75-77]. The chains with the least branching, highest tacticity or lowest co-monomer content, or in other words the chains that can crystallize the easiest, will precipitate out of solution first. As the temperature decreases more and more of the polymer will precipitate out of solution. Due to the freezing point of the solvents used, there is usually a lower limit at which the equipment can operate. Therefore, a certain amount of the polymer will always stay in solution. This fraction of the polymer that does not precipitate out is represented on the CRYSTAF profile by a rectangle that has a constant base but has a varying height. The area under the curve represents the amount of material that did not precipitate out of the solution [78]. The first derivative of the CRYSTAF profile gives a graph that is equivalent to the one obtained in A-TREF. However, before CRYSTAF samples that were run with different solvents can be compared it will be necessary to use a calibration curve that will convert the raw CRYSTAF data into the number of branches per 1000 carbon atoms [78].

2.3.1.3   Crystallisation elution fractionation (CEF)

Crystallisation elution fractionation or CEF combines the separation power of TREF and CRYSTAF into one fast single run. Monrabal et al. [79] demonstrated that by using only TREF or CRYSTAF for polyolefin analysis equivocal results will be obtained and the use of both techniques were needed for unequivocal results. CEF combines the processes of TREF and dynamic crystallisation [60]. Figure 2.10 below demonstrates the differences between TREF, dynamic crystallisation and CEF. The first step in all three cases is that of sample loading. For TREF that is typically followed by a crystallisation and elution step as explained in Section

2.3.1.1 of this chapter. The second step in dynamic crystallisation is performed with a small solvent flow through a column while slowly cooling the column. The fraction that reach crystallisation temperatures first will precipitate and anchor to the support while other components that are still in solution will move on until they reach their crystallisation temperature and segregate out. This therefore allows the physical separation of fractions according to crystallisability. Once the crystallisation cycle is completed the solvent flow is stopped and the column is heated to higher temperatures whilst the solvent flow with a suitable solvent is then started again to allow for elution of the fractions one at a time. For CEF the first step is the same as with TREF and dynamic crystallisation, namely sample loading. The second step is a combination of the crystallisation part of dynamic crystallisation and the elution step of TREF. This combination will enhance the resolution power. By replacing the third step of dynamic crystallisation with a typical TREF elution cycle enhanced resolution of fractions in shorter times with better results can be achieved.
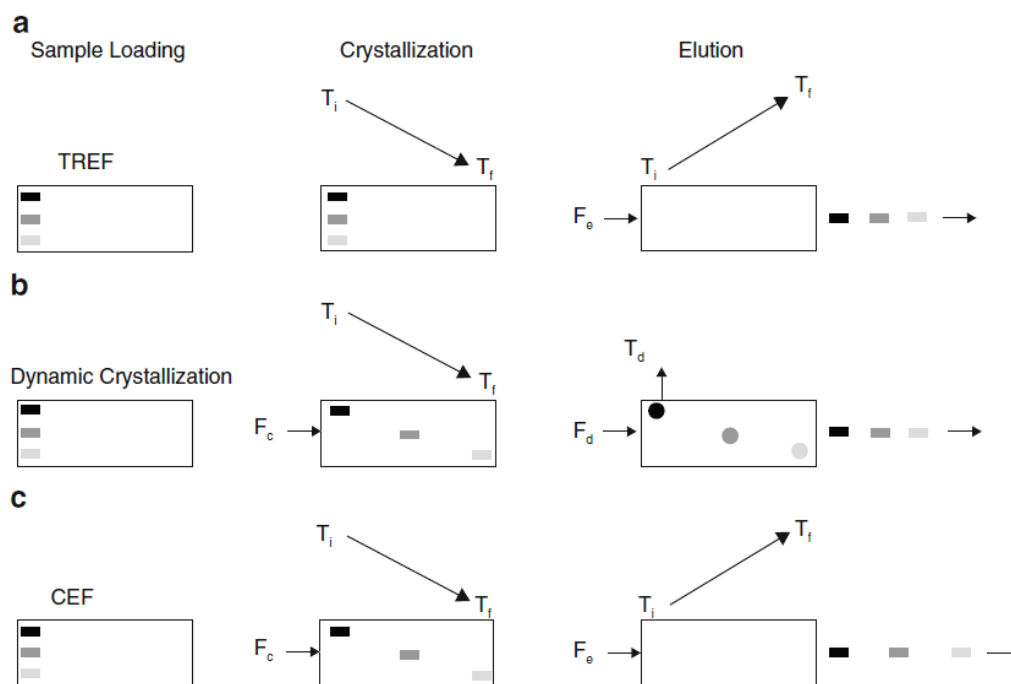
Figure 2.10   *Differences between TREF, dynamic crystallisation and CEF. (a)Typical TREF process, (b) dynamic crystallisation and (c) crystallisation elution fractionation [60]*

Monrabal et al. [80] developed this approach which combines the separation power of CRYSTAF and TREF and provides very fast analysis, unlike the very long analysis times associated with TREF and other crystallisation based techniques.

2.3.1.4   Turbidity fractionation analysis (TFA) and solution crystallisation analysis by laser light scattering (SCALLS)

Turbidity Fractionation Analysis or TFA as a technique to analyse semi-crystalline polymers was developed by Shan et al. [81]. The technique rests on the premise than the scattering of laser light can be observed when it passes through a polymer solution. The temperature of the polymer solution is closely controlled and as the temperature is decreased and the polymer starts crystallizing out of solution the turbidity of the solution increases. The laser light that passes through the sample can be used in conjunction with a suitable detector to measure the excitation voltage. As the turbidity increases as a result of the polymer precipitating out of solution the laser light that passes through the solution will decrease, resulting in the amount of scattering to increase [82]. In their article, Shan et al. [81] proved that the short chain branching distribution of semi-crystalline polymers can indeed be determined by making use of TFA and the data obtained was comparable with that of TREF and CRYSTAF.

Van Reenen et al. [83] used a similar experimental setup developed by Shan et al. [81] to study the crystallisation behaviour of commercial polyolefins. A schematic representation of the experimental setup is shown in Figure 2.11. It consists out of a diode laser, an aluminium block equipped with a heater coil and temperature controller mounted on a heater/stirrer, two photodiode detectors mounted perpendicular to each other and a diode laser. One photodiode detector measures the intensity in the forward direction due to scattering whereas a second photodiode detector measures the scattering caused by crystallisation of the polymer in solution due to changes in temperature.

In their work, Van Reenen et al. [83] observed that there is a molar mass dependence on the separation of polymer chains for polypropylene materials prepared with metallocene catalysts. As a result of their work done on the crystallisation behaviour of commercial polyolefins in solution the technique was rebranded to solution crystallisation analysis by laser light scattering (SCALLS). A major advantage SCALLS has over conventional fractionation techniques like TREF and CRYSTAF are the very fast analysis times [83].
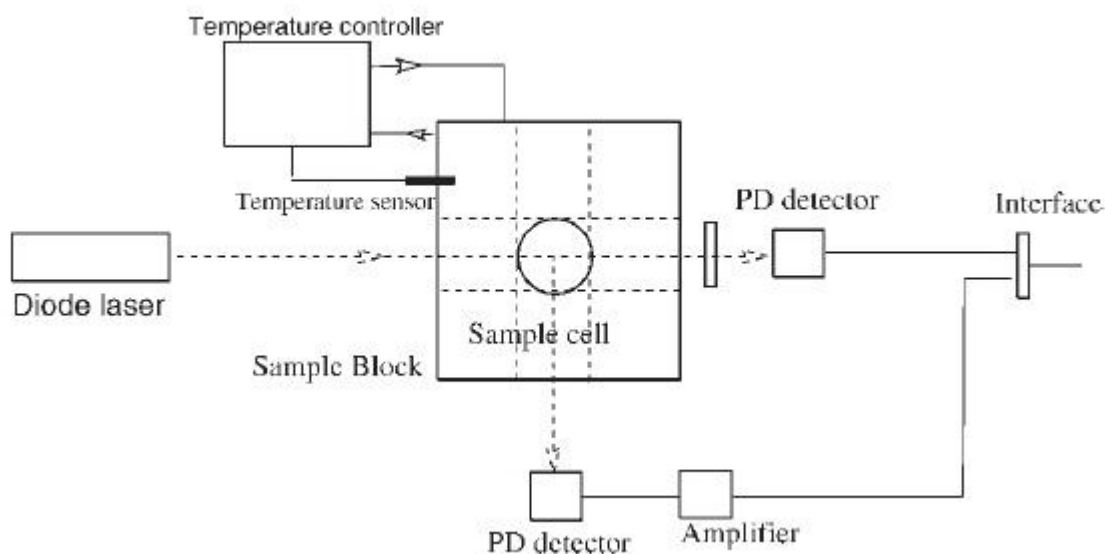
Figure 2.11   *Schematic representation of a turbidity fractionation analyzer*

2.3.2   Fractionation by molecular weight

2.3.2.1   Size exclusion chromatography (SEC)

Size exclusion chromatography (SEC) fractionates polymers according to their hydrodynamic volume, which in turn is coupled to the molar mass of the material [84, 85]. The separation of synthetic molecules is also more commonly known as gel permeation chromatography (GPC) and makes use of porous gels or rigid inorganic packing materials. Due to the solubility of polymers, especially polyolefins, high temperatures are often needed to ensure solubility of the polymer. Under those conditions this technique is therefore also referred to as high temperature GPC.

The basic principle that used is that a sample solution is introduced into the column of the instrument and by using a suitable solvent it is carried through the column. Separation will occur as the smaller molecules will enter the porous packing material more readily and deeper than the larger chains. This will result in the fact that the larger chains will exit the column first. Retention time therefore increases with decreasing chain sizes [86]. With the use of known standards, the GPC chromatogram can be converted to a molar mass distribution curve.

2.3.2.2   Size exclusion chromatography using the LC transform interface (SEC-FTIR)

Size exclusion chromatography coupled to FTIR supplies valuable information on the chemical composition as a function of molecular weight distribution of heterogeneous complex polymers, especially polyolefins [87]. SEC-FTIR can be used to study the chemical heterogeneity across a molar mass distribution by determining the ratio between two functional groups. It is further useful as a tool to study polymer degradation [88-93]. De Goede et al. [93] used SEC-FTIR analysis on abraded layers of degraded polypropylene. The results were that the Gram-Schmidt plot shifted towards lower molecular weights on the surface, compared to higher molecular weights at the core. The highest concentration of carbonyl functionalities were found in the low molecular weight species of each layer. This proved that heterogeneous degradation of polyolefins can be successfully studied with techniques such as TREF, CRYSTAF and SEC-FTIR. It has been shown by Cheruthazhekatt et al. [94] that SEC-FTIR is an effective tool to measure not only the propylene and ethylene content as a function of molecular weight of ethylene-propylene copolymers but also the crystallinity distributions of crystallisable propylene and ethylene sequences in these copolymers as a function of molecular weight. SEC-FTIR has also been applied by Provder et al. [95] to determine functional group content as a function of molar mass. Verdurmen-Noel et al. [96] also used this technique to determine backbone compositional heterogeneities of polyalkenes, whereas DesLauriers et al. [97] used it to determine the degree of short chain branching in polyalkenes. It will be the aim of this study to further demonstrate SEC-FTIR's ability to characterize the complex nature of heterophasic ethylene-propylene copolymers.

2.3.3   Fractionation by chemical composition

2.3.3.1   High temperature high performance liquid chromatography (HT-HPLC)

In 2004 a joint venture between Polymer Laboratories Ltd and the group of Pasch and Macko developed an instrument that combines both high temperature operation as well as gradient HPLC. The ability to combine isocratic and solvent gradient separations is crucial in order to separate complex polymers, especially those with high molecular weights [98]. The instrument is equipped with a high pressure gradient pump that can either run binary solvent gradients or single solvents for SEC or a mixture of two solvents at constant composition for HPLC. The instrument was further equipped with a high-temperature differential refractive index detector

for isocratic elution as well as an evaporative light scattering detector (ELSD) for gradient and isocratic elution modes.

A technique for the chromatographic characterization of polyethylene and polypropylene and separation of polyethylene copolymers according to their chemical composition, which has received a large amount of interest in recent times, is that of High Temperature High Performance Liquid Chromatography (HT-HPLC).

2.3.3.1.1 HT-HPLC at critical conditions

At critical conditions, polymers of identical chemical composition will elute at the same elution volume, irrespective of their molecular weight [60]. The analysis of polyethylene-polystyrene blends by liquid chromatography at critical conditions (LCCC) has been performed by Heinz et al. [99] and is illustrated in Figure 2.12 and Figure 2.13. It was shown that with Lichrosorb as the stationary phase and decalin-cyclohexane as the mobile phase at a column temperature of 140 °C, blend separations can be achieved. Figure 2.13 shows that the polyethylene in a separation of a polyethylene-polystyrene blend will elute in the SEC mode whereas polystyrene will elute regardless of its molar mass. Using LCCC for polystyrene, separation of polystyrene/polyethylene block copolymers has also been achieved.
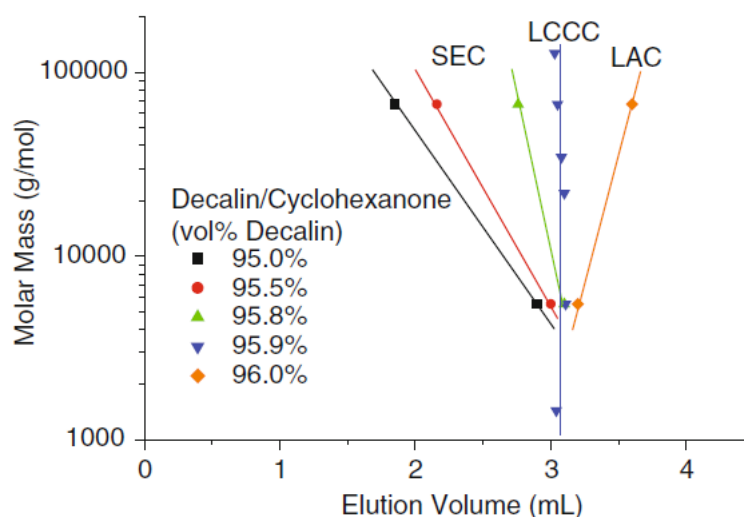
Figure 2.12   *Dependence of the elution volume of polystyrene standards on the composition of the mobile phase [60, 99]*
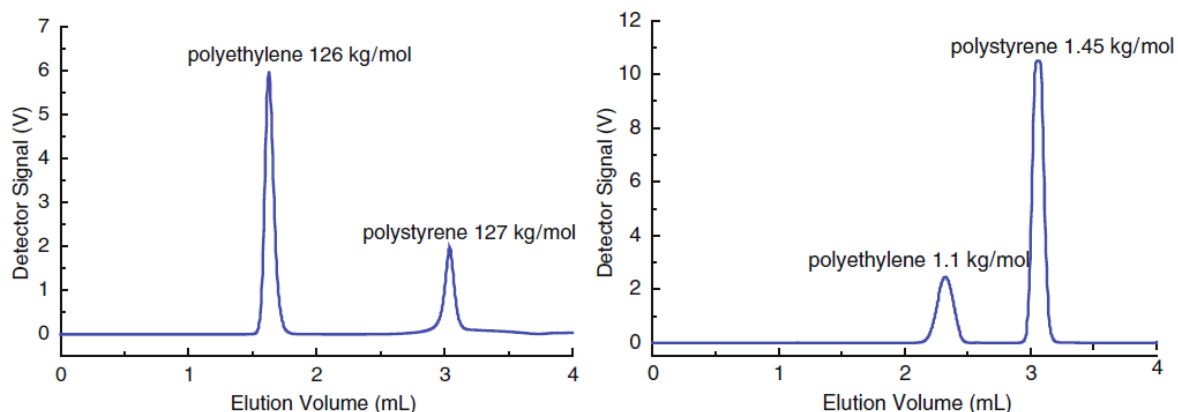
Figure 2.13   *Chromatograms of polyethylene and polystyrene blends with similar molecular weights obtained at LCCC conditions for polystyrene [60, 99].*

2.3.3.1.2   HT-HPLC on precipitation-redissolution

A multitude of combinations of solvents and non-solvents have been used for preparative separations of polyolefins according to molecular weight and/or chemical composition [60]. In their work Lehtinen et al. [100] used ethylene glycol monobutyl ether (EGMBE) based on the fact that EGMBE is a good solvent for polypropylene and a non-solvent for polyethylene. It has subsequently been shown that by using TCB as the injection solvent, EGMBE as the mobile phase and oligo(dimethyl)siloxane modified silica gel as the stationary phase enabled HPLC separations of PE and PP [101]. During this study, PP eluted in the SEC mode and PE eluted at limiting conditions. However, full recovering of the polyethylene and poor separation were severe limiting factors.

With the use of an HT-HPLC gradient system these limitations can be overcome. By using a solvent gradient with a good solvent for both PE and PP full recovery of the same can be achieved. By dissolving the sample in n-decanol and using EGMBE-TCB as the gradient with a silica-gel column a good baseline separation of PE and PP can be achieved, as is shown in Figure 2.14. Here, PE is completely precipitated on the column with the initial mobile phase, while PP elutes in the SEC mode. When the composition of the mobile phase is returned to TCB the precipitated PE elutes [102].

By using HT-HPLC Albrecht et al. [103] and Dolle et al. [104] showed that different polyolefin blends can be separated quantitatively over a range of concentrations by using liquid chromatography at 140 °C. Furthermore, ethylene-propylene copolymers were separated into a propylene-rich part and an ethylene-rich part.
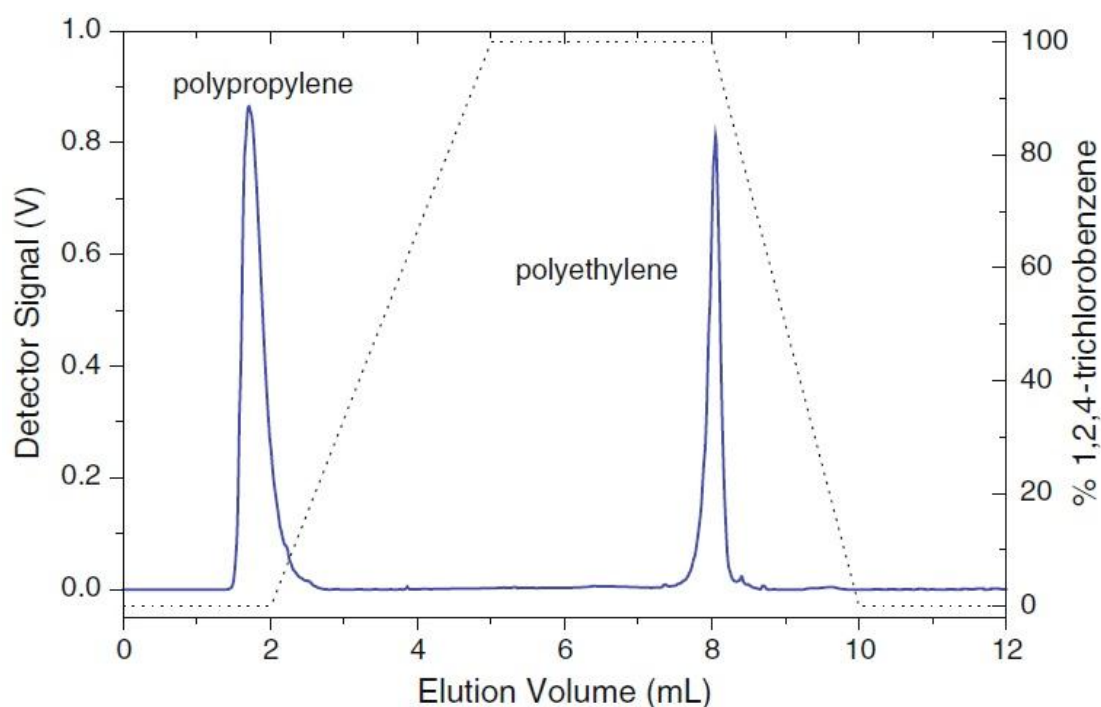
Figure 2.14   *Chromatogram of an isotactic PP and linear PE blend separated with HT-HPLC*
                   [103]

2.3.3.1.3   HT-HPLC on adsorption-desorption

Albrecht et al. [105] showed that by using gradient HT-HPLC it was possible to separate random ethylene/vinyl acetate copolymers. Using a silica gel stationary phase and decaline-cyclohexanone as eluent, full separation of copolymers with different compositions were achieved. In addition to this, the homopolymers of polyethylene and polyvinyl acetate were well separated from the copolymers. This was the first chromatographic technique that was able to separate polyolefin copolymers irrespective of crystallinity and solubility over the entire range of compositions.

Macko et al. [106] reported the first experimental observation of polyethylene adsorption from a solvent on a chromatographic stationary phase. Columns were packed with different zeolites (Silicalite, SH-300 and CBV-780) and 1,2,4-trichlorobenzene, cyclohexanone, 2-ethyl-hexanol, decalin and tetralin used as mobile phases. The elution behaviour of polyethylene and polystyrene standards are presented in Figure 2.15. From this it can be seen that decalin proved to be the solvent from which polyethylene was most readily adsorbed for each type of zeolite.

Polypropylene was not adsorbed at all. It would thus appear that this would be a good way of separating ethylene and propylene copolymers.

Column packing	Mobile phase	Polyethylene	Polypropylene
Silicalite	1,2,4-trichlorobenzene	Eluted	Eluted
Si−Al=400	Cyclohexanone	Eluted	Eluted
Pores 5−6 Å	2-ethyl-1-hexanol	Eluted*	Eluted
	Decalin	**Partially retained**	Eluted
	Tetralin	Eluted	Eluted
SH-300	1,2,4-trichlorobenzene	**Partially retained**	Eluted
Si−Al=150	Cyclohexanone	Eluted	Not measured
Pores 5−6 Å	2-ethyl-1-hexanol	Eluted*	Eluted
	Decalin	**Fully retained**	Eluted
	Tetralin	**Partially retained**	Eluted
CBV-780	1,2,4-trichloro-benzene	Eluted	Eluted
Si−Al=40	Cyclohexanone	Eluted	Eluted
Pores 7−12 Å	2-ethyl-1-hexanol	Eluted*	Eluted
Mesopores	Decalin	**Partially retained**	Eluted
40-400 Å	Tetralin	Eluted	Eluted

*PE injected after dissolution in cyclohexanone.

Figure 2.15 *Elution behaviors of polyethylene and polystyrene standards [106]*

Further work done by Macko et al. [107] showed the selective removal of polyethylene or polypropylene from their blends based on differences in their adsorption behaviour. Mixtures of polyethylene and polypropylene were first injected into a silica gel column flushed with decalin or diphenyl ether. The polymers eluted according to their size in solution. Following this, polymer mixtures eluted from the silica column were then injected into a series of two columns; one consisting of silica gel and the other packed with a zeolite (SH-300 or CBV-780). As can be seen from Figure 2.16, it allowed the selective removal of either ethylene or propylene from mixtures of both.

In general it was found that polyethylene is retained on the stationary phase when a zeolite SH-300/decalin system is used whereas polypropylene requires a zeolite 780/diphenyl ether system for its retention.
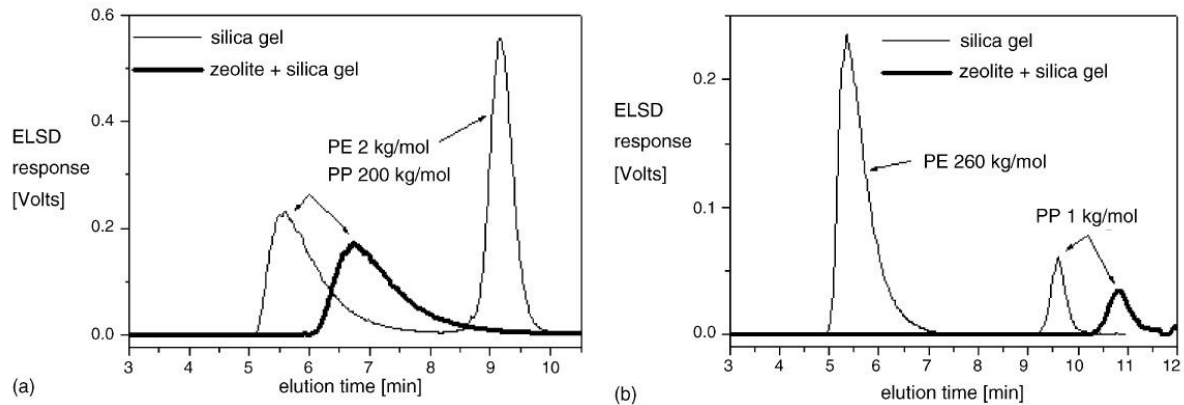
Figure 2.16   *Chromatograms of polyethylene and polypropylene blends eluted from a series of columns packed with silica and zeolites [107]*

Macko et al. [108] found that a specific carbon based stationary phase known as Hypercarb, enables highly selective separations of polyolefins. Originally developed by Knox et al. [109] Hypercarb was used for HPLC analysis of small molecules. It was never used for synthetic polymers however. Macko et al. [60, 108, 110] found that porous Hypercarb adsorbs linear polyethylene from 1-decanol as the mobile phase at 160 °C. The polymer that was retained was adsorbed from the column using a gradient from 1-decanol to TCB. This HPLC technique also separated isotactic, atactic and syndiotactic polypropylene fractions from each other, as is illustrated in Figure 2.17.
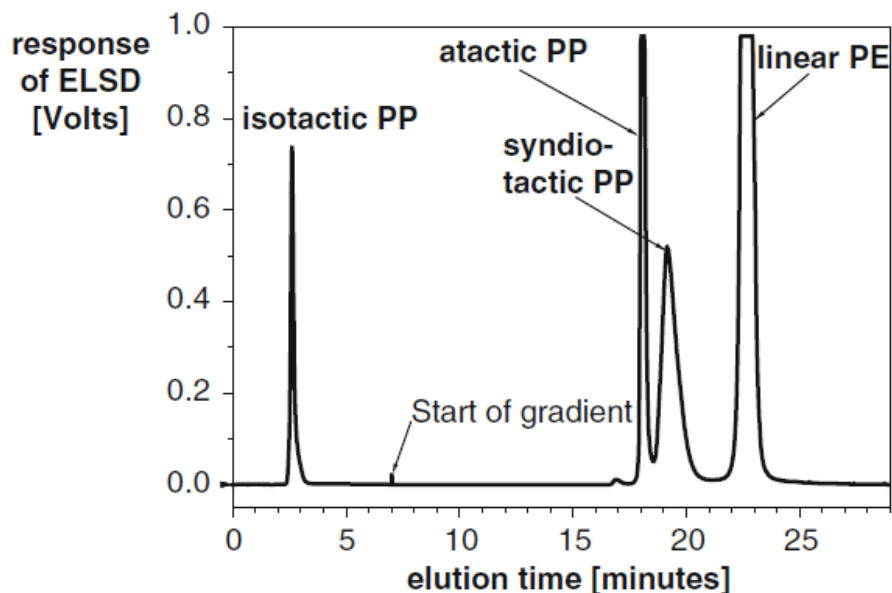
Figure 2.17   *Chromatogram showing the separation of a blend consisting out of isotactic PP, atactic PP, syndiotactic PP and linear PE [60]*

It was also shown that the system separates ethylene-hexene and propene/1-alkene copolymers according to their chemical compositions. The major advantage of this chromatographic system is that it can be used to analyse and characterize both semi-crystalline and amorphous polyolefinic samples.

2.4   Concluding remarks and methodology

To understand the complex nature of organically visbroken (or controlled rheology) propylene-ethylene heterophasic copolymers it is necessary to thoroughly investigate the various fractions that contribute to the specific and unique properties of the polymer. This will require thorough fractionation and analysis of various polymers with varying degrees of visbreaking under closely controlled conditions. It is further important to understand what contribution each individual fraction has to the polymer as a whole and how it is affected by the addition of an organic peroxide.

2.5   References

1.   Camurati I, Gioia G, Piemontesi F, Tartarini S, Bonazza A, Farotti A, Colonnesi M. NMR Characterization of Ethylene/Propylene Copolymers and Propylene Impact Copolymers from $MgCl_2/TiCl_4/ID+AlR_3/ED$ Catalytic Systems. Macromol Symp 2009:282(Polyolefin Characterization--ICPC 2008):101-110.

2.   Urdampilleta I, Gonzalez A, Iruin JJ, de la Cal JC, Asua JM. Morphology of High Impact Polypropylene Particles Macromolecules 2005:38(7):2795-2801.

3.   Soga K, Shiono T. Ziegler-Natta catalysts for olefin polymerizations. Progress in Polymer Science 1997:22(7):1503-1546.

4.   Andoni A. A flat model approach to Ziegler-Natta Olefin polymerization Catalysts. Eindhoven: University of Eindhoven, 2009.

5.   Harding G. The Structure-Property relationship of polyolefins. Stellenbosch: University of Stellenbosch, 2009.

6.   Krentsel BA, Kissin YV, Kleiner VJ, Stotskaya LL. Polymers and copolymers of higher alpha olefins. Munich, 1999.

7.   Patat F, Sinn H. Zum Ablauf der Niederdruckpolymerisation der α-Olefine. Komplexpolymerisation I. Angewandte Chemie 1958:70(16):496-500.

8.   Natta G, Mazzanti G. Organometallic complexes as catalysts in ionic polymerizations. Tetrahedron 1960:8(12):86-100.

9.   Rodriguez LAM, van Looy HM. Studies on Ziegler-Natta catalysts. Part V. Stereospecificity of the active center. Journal of Polymer Science Part A-1: Polymer Chemistry 1966:4(8):1971-1992.

10.   Ystenes M. The trigger mechanism for polymerization of α-olefins with Ziegler-Natta catalysts: A new model based on interaction of two monomers at the transition state and monomer activation of the catalytic centers. Journal of Catalysis 1991:129(2):383-401.

11.   Cossee P. Ziegler-Natta catalysis I. Mechanism of polymerization of alpha-olefins with Ziegler-Natta catalysts. Journal of Catalysis 1964:3(1):80-88.

12.   Cossee P. On the reaction mechanism of the ethylene polymerization with heterogeneous Ziegler-Natta catalysts. Tetrahedron Letters 1960:1(38):12-16.

13.   Arlman EJ. Ziegler-Natta catalysis II. Surface structure of layer-lattice transition metal chlorides. Journal of Catalysis 1964:3(1):89-98.

14.   Malm B, Jaaskelainen P, Vestberg T. Heterophasic Copolymers. In: Patent US, editor. United States of America: Borealis Technology, 2004.

15.   Lummus Novolen Technology GmbH (Novolen) - Polypropylene Overview. Chicago Bridge & Iron Company, 2012.

16.   Debling JA. Modeling particle growth and morphology of impact polypropylene produced in the gas phase. University of Wisconsin--Madison, 1997.

17.   Debling JA, Ray WH. Morphological development of impact polypropylene produced in gas phase with a $TiCl_4/MgCl_2$ catalyst. Journal of Applied Polymer Science 2001:81(13):3085-3106.

18.   McKenna T, Bouzid D, Matsunami S, Sugano T. Polymer Reaction Engineering 2003(11):177-197.

19. Cecchin G, Marchetti E, Baruzzi G. On the Mechanism of Polypropene Growth over MgCl2/TiCl4 Catalyst Systems. Macromolecular Chemistry and Physics 2001:202(10):1987-1994.

20. Lee CD. Structure Property Relations in Visbroken (Peroxide Treated) Impact Polypropylene Copolymers. 2005.

21. Borruso A. CEH Marketing Research Report: Polypropylene Resins. 2011.

22. Singh B, Sharma N. Mechanistic implications of plastic degradation. Polymer Degradation and Stability 2008:93(3):561-584.

23. Hamid SH, Amin MB, Maadhah AG. Handbook of polymer degradation. M. Dekker, 1992.

24. Turro NJ. Modern Molecular Photochemistry. University Science Books, 1991.

25. Otsu T, Tanaka H, Wasaki H. Photodegradation of chloromethyl vinyl ketone polymer and copolymers with styrene and α-methylstyrene. Polymer 1979:20(1):55-58.

26. Voigt W, Todesco R. New approaches to the melt stabilization of polyolefins. Polymer Degradation and Stability 2002:77(3):397-402.

27. Hace D, Kovacevic V, Pajc-Liplin D. Thermally stimulated oxidative degradation of high impact polystyrene with nitric acid. Polymer Engineering & Science 1996:36(8):1140-1151.

28. Bremner T, Rudin A, Cook DG. Melt flow index values and molecular weight distributions of commercial thermoplastics. Journal of Applied Polymer Science 1990:41(7-8):1617-1627.

29. Murata K, Hirano Y, Sakata Y, Uddin MA. Basic study on a continuous flow reactor for thermal degradation of polymers. Journal of Analytical and Applied Pyrolysis 2002:65(1):71-90.

30. Aguado J, Serrano DP, Miguel GS. European trends in the Feedstock Recycling of Plastic Wastes. Global NEST Journal 2007:9(1):12 - 19.

31. Rodryguez-Vazquez M, Liauw CM, Allen NS, Edge M, Fontan E. Degradation and stabilisation of poly(ethylene-stat-vinyl acetate): 1. Spectroscopic and rheological examination of thermal and thermo-oxidative degradation mechanisms. Polymer Degradation and Stability 2006:91(1):154-164.

32. Mark HF, Bikales NM, Overberger CG, Menges G. Encyclopedia of Polymer Science and Engineering. New York: Wiley Interscience Publication, 1986. p. 630 - 696.

33. Allen NS, Edge M, Mourelatou D, Wilkinson A, Liauw CM, Dolores Parellada M, Barrio JA, Ruiz Santa Quiteria V. Influence of ozone on styrene-ethylene-butylene-styrene (SEBS) copolymer. Polymer Degradation and Stability 2003:79(2):297-307.

34. Li J, Guo S, Li X. Degradation kinetics of polystyrene and EPDM melts under ultrasonic irradiation. Polymer Degradation and Stability 2005:89(1):6-14.

35. Ghosh P. Polymer science and technology of plastics and rubbers. New Delhi: Tata McGraw-Hill Publishing Company Ltd, 1990.

36. Li Y, Chen G, Guo S, Li H. Studies on Rheological Behavior and Structure Development of High• Density Polyethylene in the Presence of Ultrasonic Oscillations During Extrusion. Journal of Macromolecular Science, Part B 2006:45(1):39-52.

37.   Gol'dberg VM, Zaikov GE. Kinetics of mechanical degradation in melts under model conditions and during processing of polymers: A review. Polymer Degradation and Stability 1987:19(3):221-250.

38.   Striegel AM. Influence of chain architecture on the mechanochemical degradation of macromolecules. Journal of Biochemical and Biophysical Methods 2003:56(1):117-139.

39.   Garforth A, Fiddy S, Lin YH, Ghanbari-Siakhali A, Sharratt PN, Dwyer J. Catalytic degradation of high density polyethylene: An evaluation of mesoporous and microporous catalysts using thermal analysis. Thermochimica Acta 1997:294(1):65-69.

40.   Sekine Y, Fujimoto K. Catalytic degradation of PP with an Fe/activated carbon catalyst. Journal of Material Cycles and Waste Management 2003:5(2):107-112.

41.   Wall LA, Madorsky SL, Brown DW, Straus S, Simha R. The Depolymerization of Polymethylene and Polyethylene. Journal of the American Chemical Society 1954:76(13):3430-3437.

42.   Palmisano AC, Pettigrew CA. Biodegradability of plastics. Bioscience 1992:42(9):680 - 685.

43.   Lemm W, Krukenburg T, Regier G, Gerlach K, Bucherl ES. Biodegradation of some biomaterials after subcutaneous implantation. Proceedings of the European Society of Artificial Organisms 1981:8.

44.   Potts JE, Clendinning RA, Ackart WB, Neigisch WD. The biodegradability of synthetic polymers. In: Guillet J, editor. Polymers and ecological problems. New York: Plenum Press, 1973.

45.   Swift G. Biodegradable polymers in the environment: are they really biodegradable? Proceedings of the ACS Division for Polymeric Materials in Science and Engineering 1992:66.

46.   Ratner BD, Gladhill KW, Horbett TA. Analysis of in vitro enzymatic and oxidative degradation of polyurethanes. Journal of biomedical materials research 1988:22.

47.   R.W. Hergenrother, Wabers HD, Cooper SL. The effect of chain extenders and stabilizers on the in-vivo stability of polyurethanes. Journal of Applied Biomaterials 1992:3.

48.   Merchant RE, Anderson JM, Phua K, Hiltner A. In vivo biocompatibility studies. II. Biomer: preliminary cell adhesion and surface characterization studies. Journal of Biomedical Materials Research 1984:21.

49.   Gilding DK. Biodegradable polymers. In: Williams DF, editor. Biocompatibility of clinic implant materials. Boca Raton: CRC Press, 1981.

50.   Kronenthal RL. Biodegradable polymers in medicine and surgery. In: Kronenthal RL, Oser Z, Martin E, editors. New York, NY: Plennum Press, 1975.

51.   Ishigaki T, Y.Kawagoshi, Fujita MIM. Biodegradation of a polyvinyl alcoholestarch blend plastic film. Worl Journal of Microbiological Biotechnology 1999:15.

52.   Chambliss WG. The forgotten dosage form: enteric-coated tablets. Journal of Pharmaceutical Technology 1983:7.

53.   Gennaro AR. Pharmaceutical sciences. Easton, PA: Mack Publishers Co., 1985.

54.   Murphy KS, Enders NA, Mahjour M, Fawzi MB. A comparative evaluation of aqueous enteric polymers in capsule coatings. Pharmaceutical Technology 1986.

55. Kopecek J, Rejmanova P. Enzymatically degradable bonds in synthetic polymers. In: Bruck SD, editor. Controlled drug delivery. Basic concepts. Boca Raton, Fl: CRC Press, 1983.

56. Dave H, Rao PVC, Desai JD. Biodegradation of starch polyethylene films in soil and by microbial cultures. World Journal of Microbiological Biotechnology 1997:13.

57. Dutta S, Rai A. More efficient manufacture of controlled-rheology polypropylene. Plastic Research Online 2010.

58. Flory PJ. Principles of polymer chemistry. Ithaca: Cornell University Press, 1953.

59. Mandelkern L. Crystallisation of Polymers: Volume 1, Equilibrium Concepts. Cambridge University Press, 2002.

60. Pasch H, Malik MI, Macko T. Recent Advances in High-Temperature Fractionation of Polyolefins. 2012.

61. Desreux V, Spiegels MC. Fractionation of polyethylene by extraction. Bulletin des Societes Chimiques Belges 1950:59:476.

62. Shirayama K, Okada T, Kita S. Journal of Polymer Science Part A-3: 907916 1965.

63. Wild L. Temperature Rising Elution Fractionation. Advances in Polymer Science 1990:98(1):1.

64. Soares J, Hamielec A. Temperature Rising Elution Fractionation. John Wiley & Sons, 1999.

65. Fonseca CA, Harrison IR. Temperature Rising Elution Fractionation. Chichester: John Wiley & Sons, 1999.

66. Wild L, Ryle TR, Knobeloch DC, Peat IR. Determination of branching distributions in polyethylene and ethylene copolymers. Journal of Polymer Science: Polymer Physics Edition 1982:20:441.

67. Mirabella FMJ. Temperature Rising Elution Fractionation (TREF) charaterization of polypropylene copolymers. Journal of Liquid Chromatography 1994:17:3201.

68. Unami T, Gotoh Y, Takayama S. Generation mechanism of short-chain branching distribution in linear low-density polyethylenes. Macromolecules 1986:19(11):2722.

69. Zhang YD, Wu CJ, Zhu SN. Fractionation and characterization for a propylene-ethylene random copolymer. Polymer Journal 2002:34(9):700.

70. Mirabella FMJ, Ford EA. Characterization of linear low-density polyethylene: Cross-fractionation according to copolymer composition and molecular weight. Journal of Polymer Science Part B: Polymer Physics 1987:25:777.

71. Wild L, Blatz C. Development of high performance TREF for polyolefin analysis. Polymeric Materials: Science and Engineering 1992:67:153.

72. Monrabal B. Crystallisation analysis fractionation: A new technique for the analysis of branching distribution in polyolefins. Journal of Applied Polymer Science 1994:52(4):491-499.

73. Monrabal B. Temperature rising elution fractionation and crystallisation analysis fractionation. Chichester: John Wiley & Sons Ltd. 8074, 2000.

74. Monrabal B. Crystallisation Analysis Fractionation. United States of America, 1991.

75.   Monrabal B. CRYSTAF: Crystallisation analysis fractionation. A new approach to the composition analysis of semi-crystalline polymers. Macromolecular Symposium 1996:110:81.

76.   Britto LJD, Soares JBP, Penlidis A, Monrabal B. Polyolefin analysis by single-step crystallisation fractionation. Journal of Polymer Science Part B: Polymer Physics 1999:37:539.

77.   Sarzotti SM, Soares JBP, Penlidis A. Ethylene/1-hexene copolymers synthesized with a single-site catalyst: Crystallisation analysis fractionation, modelling and reactivity ratio estimation. Journal of Polymer Science Part B: Polymer Physics 2002:40:2595.

78.   Monrabal B, Blanco J, Nieto J, Soares JBP. Characterization of homogeneous ethylene/1-octene copolymers made with a single-site catalyst. CRYSTAF analysis calibration. Journal of Polymer Science Part A-1: Polymer Chemistry 1999:37:89.

79.   Monrabal B, del Hierro P. Characterization of polypropylene–polyethylene blends by temperature rising elution and crystallisation analysis fractionation. Analytical and Bioanalytical Chemistry:399(4):1557-1561.

80.   Monrabal B, Sancho-Tello J, Mayo N, Romero L. Crystallisation Elution Fractionation. A New Separation Process for Polyolefin Resins. Macromolecular Symposia 2007:257(1):71-79.

81.   Shan CLP, Groot WAd, Hazlitt LG, Gillespie D. A new turbidimetric approach to measuring polyethylene short chain branching distributions. Polymer 2005:46:11755 - 11767.

82.   Brand M. Investigation of molecular weight effects during the solution crystallisation of polyolefins. Stellenbosch: University of Stellenbosch, 2008.

83.   van Reenen AJ, Rohwer EG, Walters P, Lutz M, Brand M. Development and use of a turbidity analyzer for studying the solution crystallisation of polyolefins. Journal of Applied Polymer Science 2008:109(5):3238-3243.

84.   Kostanski LK, Keller DM, Hamielec AE. Size-exclusion chromatography: A review of calibration methodologies. Journal of Biochemical and Biophysical Methods 2004:58(2):159-186.

85.   Mark HF, Kroschwitz JI. Encyclopedia of Polymer Science and Engineering, Fibers, Optical to Hydrogenation. Wiley, 1987.

86.   Karger-Kocsis J, editor. Molecular structure of polypropylene homo- and copolymers. Chapman & Hall: London, 1995.

87.   Wheeler LM, Willis JN. Gel Permeation Chromatography/Fourier Transform Infrared Interface for Polymer Analysis. Appl Spectrosc 1993:47(8):1128-1130.

88.   Dekmezian AH, Morioka T. Interface to eliminate high-boiling gel permeation chromatographic solvents on-line for polymer composition drift studies. Analytical Chemistry 1989:61(5):458-461.

89.   Ver Strate G, Cozewith C, West RK, Davis WM, Capone GA. Block Copolymers of Polyethylene and Ethylene-Propylene-Diene Elastomer. Synthesis, Characterization, and Properties. Macromolecules 1999:32(12):3837-3850.

90.   Adrian J, Esser E, Hellmann G, Pasch H. Two-dimensional chromatography of complex polymers Part 1. Analysis of a graft copolymer by two-dimensional chromatography with on-line FTIR detection. Polymer 2000:41(7):2439-2449.

91.   Pasch H, Siewing A, Heinz L-C. Analysis of Crosslinked Styrene-Butadiene Rubbers by Liquid Chromatography and FT-IR Spectroscopy, 1. Macromolecular Materials and Engineering 2003:288(10):771-777.

92.   De Goede S. Novel Analytical Approaches for Studying PP and PP-1 Pentene Copolymers. Stellenbosch: University of Stellenbosch, 2006.

93.   de Goede S, Brüll R, Pasch H, Marshall N. Monitoring thermo-oxidative degradation of polypropylene by CRYSTAF and SEC-FTIR. Macromolecular Symposia 2003:193(1):35-44.

94.   Cheruthazhekatt S, Pijpers TFJ, Harding GW, Mathot VBF, Pasch H. Multidimensional Analysis of the Complex Composition of Impact Polypropylene Copolymers: Combination of TREF, SEC-FTIR-HPer DSC, and High Temperature 2D-LC. Macromolecules 2012.

95.   Provder T, Whited M, Huddleston D, Kuo C-Y. Characterization of compositional heterogeneity in copolymers and coatings systems by GPC/FTIR. Progress in Organic Coatings 1997:32(14):155-165.

96.   Verdurmen-Noël L, Baldo L, Bremmers S. SEC-FTIR characterization of semi-crystalline HDPE and PP. Polymer 2001:42(13):5523-5529.

97.   DesLauriers PJ, Rohlfing DC, Hsieh ET. Quantifying short chain branching microstructures in ethylene 1-olefin copolymers using size exclusion chromatography and Fourier transform infrared spectroscopy (SEC-FTIR). Polymer 2002:43(1):159-170.

98.   Heinz LC, Macko T, Williams A, O'Donohue S, Pasch H. A New System for High-Temperature Gradient HPLC Polymers. The Column (Electronic Journal) February 2006.

99.   Heinz L-C, Macko T, Pasch H, Weiser M-S, Malhaupt R. High-Temperature Liquid Chromatography at Critical Conditions: Separation of Polystyrene from Blends with Polyethylene and Ethylene-Styrene Block Copolymers. International Journal of Polymer Analysis and Characterization 2006:11(1):47-55.

100.   Lehtinen A, Paukkeri R. Fractionation of polypropylene according to molecular weight and tacticity. Macromolecular Chemistry and Physics 1994:195(5):1539-1556.

101.   Macko T, Pasch H, Kazakevich YV, Fadeev AY. Elution behaviour of polyethylene in polar mobile phases on a non-polar sorbent. Journal of Chromatography A 2003:988(1):69-76.

102.   Heinz L-C, Pasch H. High-temperature gradient HPLC for the separation of polyethylene-polypropylene blends. Polymer 2005:46(26):12040-12045.

103.   Albrecht A, Heinz L-C, Lilge D, Pasch H. Separation and Characterization of Ethylene-Propylene Copolymers by High-Temperature Gradient HPLC Coupled to FTIR Spectroscopy. Macromolecular Symposia 2007:257(1):46-55.

104.   Dolle V, Albrecht A, Brüll R, Macko T. Characterisation of the Chemical Composition Distribution of LLDPE Using Interactive Liquid Chromatography. Macromolecular Chemistry and Physics:212(9):959-970.

105.   Albrecht A, Brall R, Macko T, Pasch H. Separation of Ethylene Vinyl Acetate Copolymers by High-Temperature Gradient Liquid Chromatography. Macromolecules 2007:40(15):5545-5551.

106.   Macko T. Adsorption of polyethylene standards from decalin on liquid chromatography column packings. A Journal of Chromatography 2003:1002:55-62.

107.   Macko T, Pasch H, Brull R. Selective removal of polyethylene or polypropylene from their blends based on difference in their adsorption behaviour. A Journal of Chromatography 2006:1115:81-87.

108.   Macko T, Pasch H, Wang Y. Liquid Chromatographic Separation of Olefin Oligomers and its Relation to Separation of Polyolefins – an Overview. Macromolecular Symposia 2009:282(1):93-100.

109.   Gilbert MT, Knox JH, Kaur B. Porous Glassy Carbon, A new columns packing material for Gas Chromatography and High Performance Liquid Chromatography. Chromatographia 1982:16(1).

110.   Macko T, Pasch H. Separation of Linear Polyethylene from Isotactic, Atactic, and Syndiotactic Polypropylene by High-Temperature Adsorption Liquid Chromatography. Macromolecules 2009:42(16):6063-6067.

Chapter 3

Experimental

This chapter gives an overview of the materials and equipment used during the synthesis, compounding and characterization of the propylene-ethylene heterophasic copolymers. It also gives details on where the materials used were sourced from as well as the methods and settings used during the preparation and analysis of the samples.

3.1   Polymerization materials

3.1.1   The commercial process

The heterophasic copolymers used in this study were all prepared from a commercial reactor grade sample (denoted the base polymer) by making use of the Novolen® gas phase process. The base polymer sample was prepared via a continuous sequential polymerization batch process where the PP matrix is prepared in the first reactor in the gas phase. PP powder is then transferred to a second reactor with subsequent gas phase copolymerization of propylene and ethylene at a certain ratio to produce the elastomeric phase. This sequential process as well as the subsequent steps of polymer-gas separation and extrusion is illustrated in Figure 3.1 below. For the polymerization reaction a Ziegler-Natta based catalyst (BASF, Ludwigshafen, Germany) was used. Tri-ethyl Aluminium (Akzo Nobel Polymer Chemicals, Amersfoort, The Netherlands) was used as co-catalyst and acted as a poison scavenger and catalyst activator. Propylene and ethylene monomer (Sasol Synfuels, Secunda, South Africa) was used with purity higher than 99.2 and 99.9% respectively.
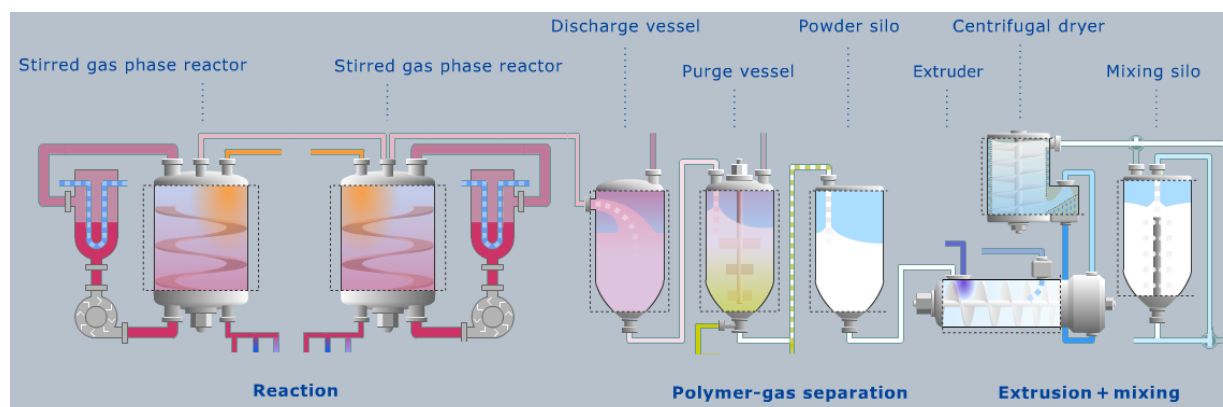
Figure 3.1   *The Novolen® gas phase polypropylene process used to prepare the base polymer sample[1]*

---

[1] Permission to use, copy and distribute the documentation published by Lummus Novolen Technology GmbH on this World Wide Web server is hereby granted on the condition that each copy contains this copyright notice in its entirety and that no part of the documentation is used for commercial purposes but restricted to use for information purposes within an organization. **© Copyright 2009 Lummus Novolen Technology GmbH. All rights reserved.**

3.1.2   Compounding equipment and methodology

After the synthesis of the base polymer powder the material was compounded with Irganox®
1010 and Irgafos® 168 (BASF, Ludwigshafen, Germany) in a twin screw ZSK 18 Coperion
extruder at 500rpm and barrel zone temperatures from 80 °C to 210 °C. Figure 3.2 gives a
graphic representation of the temperature profile used for compounding of the samples.
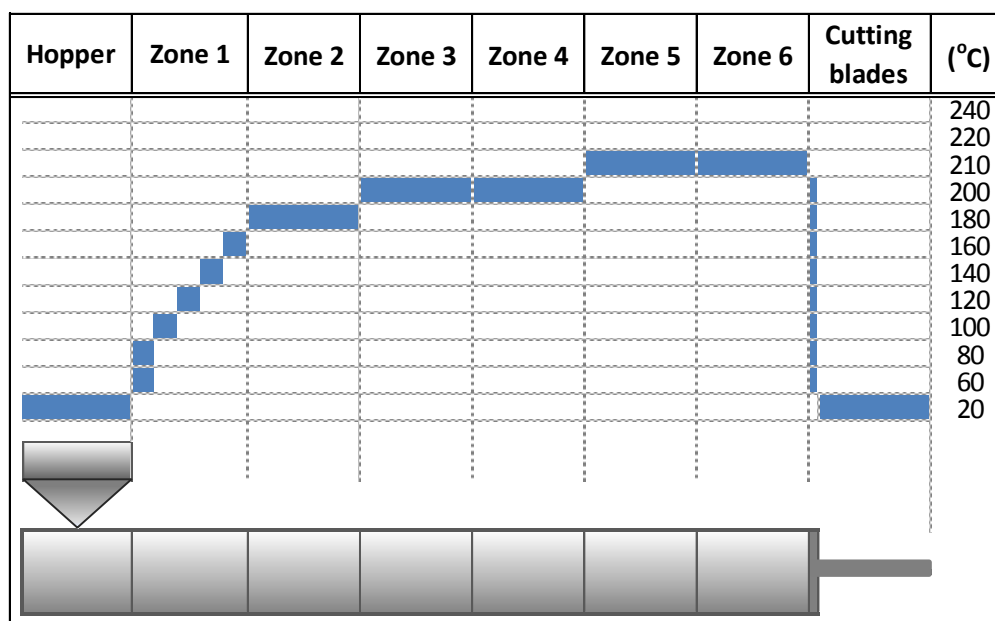
Figure 3.2   *Temperature profile per zone used for compounding*

Increasing amounts of Trigonox 301® (Akzo Nobel Polymer Chemicals, Amersfoort,
Netherlands) or Trigonox® 101 (Akzo Nobel Polymer Chemicals, Amersfoort, Netherlands) were
added in order to achieve varying degrees of visbreaking. The cyclic structure of Trigonox® 301
or 3,6,9-Triethyl-3,6,9-trimethyl-1,4,7-triperoxonane is illustrated in Figure 3.3 (a) below. It has
a molecular weight of 264.3 g.mol^{-1} and a total active oxygen content of 7.3 – 7.6%. The
molecular structure of Trigonox® 101 is illustrated in Figure 3.3 (b). Trigonox® 101 has a
molecular weight of 290.4 g.mol^{-1} and a total active oxygen content of 11.02%.
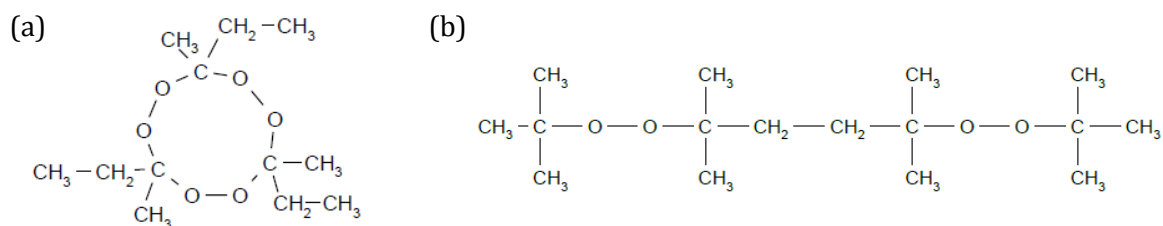
Figure 3.3   *Molecular structures of (a) Trigonox® 301 and (b) Trigonox® 101*

The reactivity of an organic peroxide is usually given in terms of its half-life ($t_{1/2}$) at various temperatures. The following equation can be used to determine the half-life for Trigonox® 301:

$$k_d = Ae^{-\frac{E_a}{RT}}$$
(Eq 3.1)

$$t_{1/2} = \frac{(\ln)}{k_d}$$
(Eq 3.2)

Where,

E_a = 150.23 kJ.mol^{-1}
A = 1.02 x 10^{15} per second
R = 8.3124 J.(mol.K)$^{-1}$
T = (273.15 + °C) K

3.2   Fractionation techniques

3.2.1   *Analytical and preparative temperature rising elution fractionation*

Analytical TREF was used as an initial test to see if any differences exist based on the crystallisability of the polymer chains of the various samples that were prepared using Trigonox® 301 and Trigonox® 101. The fractionation procedure for analytical TREF involved the slow crystallisation of the polymeric material in solution onto an inert support at a cooling rate of 2 °C.h^{-1}. The crystallisation step was then followed by an elution step where the temperature of the solvent used to dissolve the polymer samples was steadily increased at a rate of 50 °C.h^{-1}. During the elution process the concentration of the polymer solution was monitored by an on-line IR detector. The IR detector was set at a fixed wavelength to detect the C – H stretching frequencies of methylene groups and this absorbance band was used to measure the amount of polymer in the eluent from the column.

To allow for a more detailed study of the various fractions of the HECO polymers an in-house preparative TREF instrument was used. The method is divided into two parts i.e. crystallisation and elution. During the crystallisation step 3 g of the various samples prepared via the compounding step mentioned above are dissolved in 300 ml of xylene at 130 °C in a glass reactor. This setup is illustrated in Figure 3.4. After the material is completely dissolved, pre-heated sea sand (white quartz, Aldrich, South Africa) is added to the reactor as crystallisation support. The reactor was then transferred to a pre-heated oil bath where the mixture was then cooled down under controlled conditions at a rate of 1.0 °C.h^{-1} (also shown in Figure 3.4). After the mixture was cooled to room temperature the sand/polymer mixture was transferred to a stainless steel column and placed in a modified gas chromatography oven. The stainless steel

column is 1500 mm in length and has an internal diameter of 750 mm. It is equipped in such a way that a temperature probe can be fitted at the bottom of the column to measure its core temperature.   The way in which the column is packed with the quartz containing the crystallisable polymer is illustrated in Figure 3.5. Glass wool was placed at the bottom and top of the column as to prevent preferential solvent channelling. Pre heated xylene was then pumped through the column and the temperature of the oven and the xylene was steadily increased. Fractions were then collected at predetermined intervals, the xylene was evaporated and the precipitated polymer fractions were recovered by precipitating in acetone. All samples were then dried to consistent weight in a vacuum oven. The elution setup is shown in Figure 3.6 and consists of a solvent (xylene) reservoir with pump, a modified GC oven, a temperature controller, stainless steel column and a collection facility.
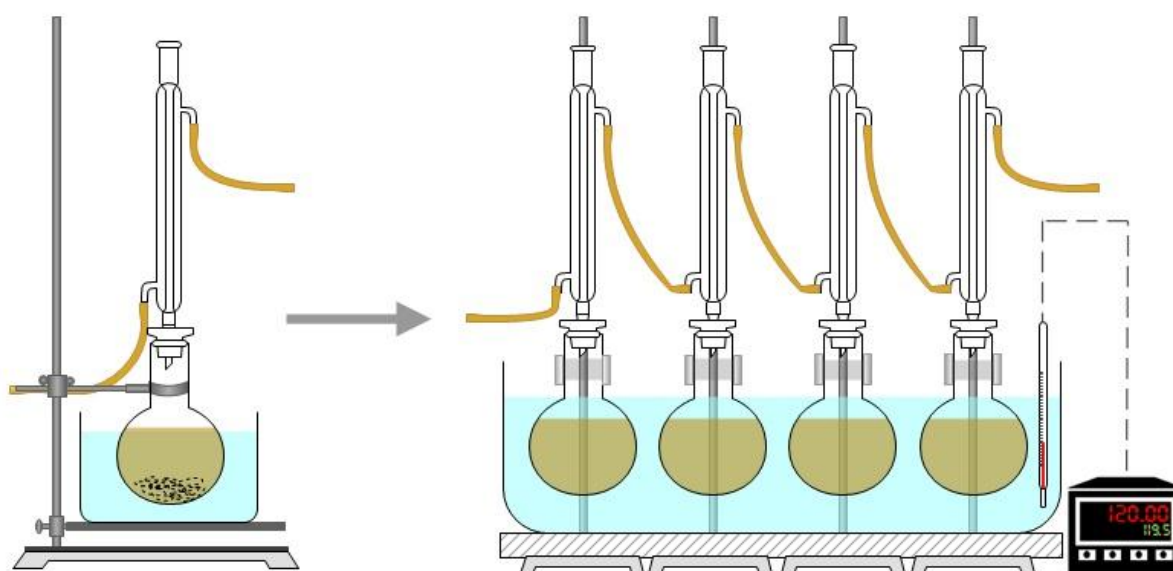
Figure 3.4   *Illustration of the TREF dissolving and crystallisation setups*
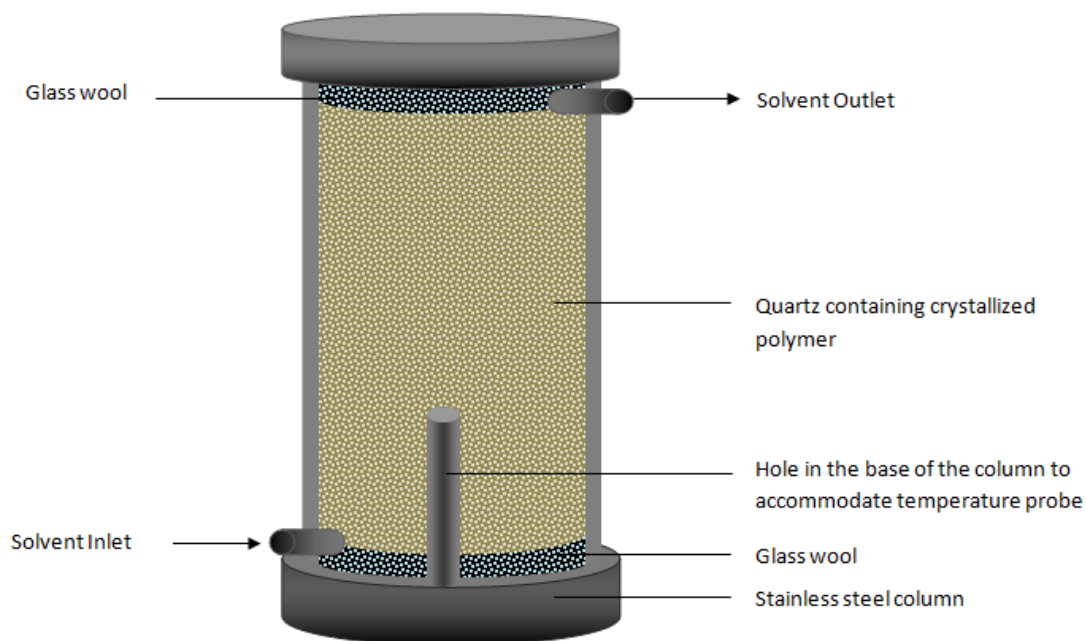
Figure 3.5   *Illustration of the column packing used during the elution phase*
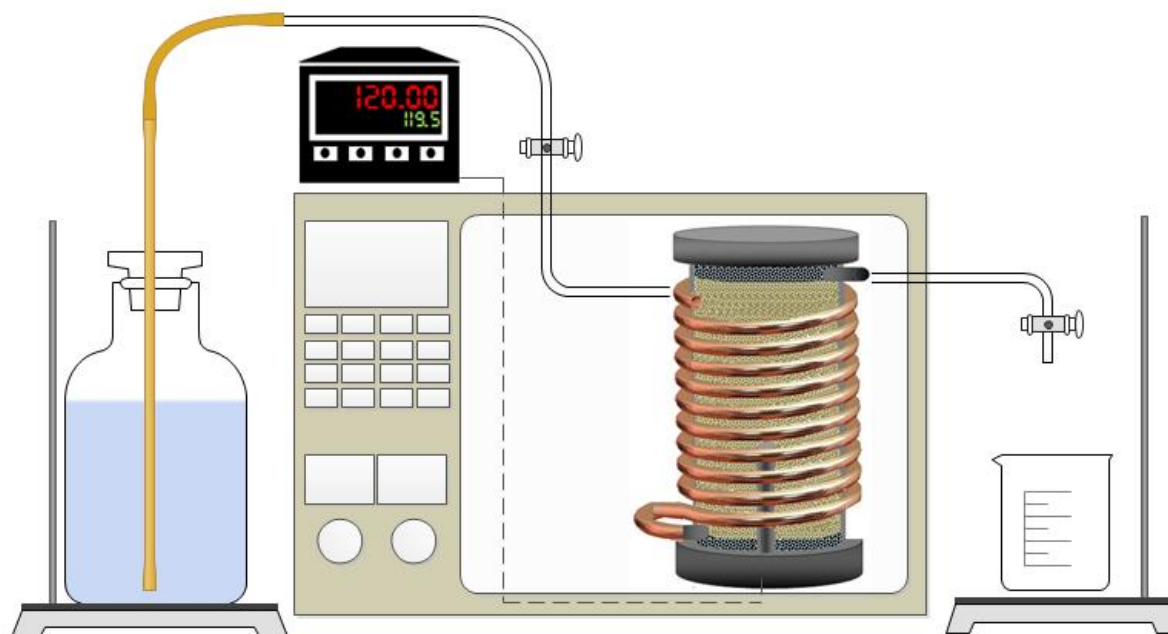
Figure 3.6   *Illustration of the elution step associated with preparative TREF*

3.2.2   CRYSTAF

A commercial CRYSTAF apparatus model 200 (Polymer Char S.A., Valencia, Spain) was used for crystallisation analysis fractionation of the bulk polymer samples. The crystallisation was

carried out in 60 mL stainless steel reactors where dissolution and filtration took place automatically. 10 mg of each sample prepared in the compounding step was dissolved in 30 mL 1,2,4 – trichlorobenzene. The temperature was then steadily decreased from 130 °C to 30 °C at a rate of 0.1 °C.min⁻¹. Fractions were taken automatically and the polymer concentration from the solution was determined by an infrared detector using 3.5 μm as the chosen wavelength.

3.3   Characterization techniques

3.3.1   Carbon 13 nuclear magnetic resonance spectroscopy (^{13}C NMR)

A 600 MHz Varian^{Unity} INOVA NMR Spectrometer was used to obtain high-resolution solution ^{13}C NMR spectra. Samples were prepared to a concentration of 6 wt.% in deuterated tetrachloroethane (d-TCE, Aldrich, South Africa). All spectra were obtained by making use of a 90° flip angle of ≈ 6 μs with continuous proton decoupling. An acquisition time of 1.8 s and a pulse delay of 15 s were also used. Provided that only carbon atoms with T_1 (relaxation delays) of less than 3 seconds are taken into account these conditions ensured spectra that were 99% quantitative[1]. The 600 MHz instrument was equipped with three channels, Z gradients, and the following probes:

    5mm 1H{15N-31P} indirect detection PFG
    5mm 15N-31P broadband
    5mm 1H{13C/15N} triple resonance PFG
    10mm 103Rh-15N broadband
    10mm 15N-31P broadband

3.3.2   Differential scanning calorimetry (DSC)

3.3.2.1   Crystallisation and melting behaviour

DSC scans were recorded using a TA Instruments 2920 modulated DSC. Approximately 6 mg of sample was used and each sample was heated from room temperature to 220 °C and held at that temperature for 1 minute to erase any thermal history. Samples were then cooled to 20 °C at a rate of 10 °C.min-1 and held at that temperature for 1 minute. Thereafter the sample was heated to 210 °C at a rate of 10 °C.min-1. DSC was used to determine the crystallisation and melting points, as well as the various crystallinities of the samples. Crystallinities were determined by

using the enthalpy of fusion (ΔH_f) of the samples and comparing that to the enthalpy of fusion of ideal 100% crystalline polypropylene (ΔH_{fc}) according to equation 3.3 below.

$$w_c = \frac{\Delta H_f}{\Delta H_{fc}} \times 100$$

(Eq. 3.3)

A value of 209 J/g [2] was used as the enthalpy of fusion for the ideal 100% crystalline polypropylene.

3.3.3 *Fourier transform infrared spectroscopy (FTIR)*

FTIR spectra were recorded on a Nicolet iS10 Spectrometer (Thermo Electron, Waltham, USA) at a resolution of 4 cm^{-1}. Samples were deposited on a germanium disc using the LC transform interface. The germanium disc was then transferred to the instrument for subsequent analysis.

3.3.4 *High temperature size exclusion chromatography (HT-SEC)*

Molar mass measurements for all samples were performed on a High Temperature Polymer Laboratories PL220 Chromatograph (Polymer Laboratories, Varian Inc., Church Stretton, Shropshire, England) operating at 150 °C and equipped with three 300 mm x 7.5 mm PLgel Olexis columns, a PLgel Olexis Guard and a refractive index detector was used. The eluent that was used was TCB with a flow rate of 1.0 ml.min-1. The TCB was stabilized with 0.0125% 2,6-ditert-butyl-4-methylphenol (BHT). Samples were dissolved at 160 °C for 2 hours in 0.025% BHT stabilized TCB at a concentration of 2 mg/ml. 200 μl of sample was injected into the column. Narrowly distributed polystyrene standards (Polymer laboratories, Church Stretton, England) were used to create a calibration curve.

3.3.5 *Size exclusion chromatography coupled to Fourier transform infrared spectroscopy via the LC transform interface (SEC-FTIR)*

A high temperature Polymer Laboratories PL220 chromatograph (Polymer Laboratories, Varian Inc., Church Stretton, Shropshire, England) operating at 150 °C and equipped with three 300 mm x 7.5 mm PLgel Olexis columns, a PLgel Olexis Guard and a refractive index detector was

used for the SEC part of the experiment. Samples were dissolved for 2 hours at 160 °C in TCB at a concentration of 2 mg.ml^{-1}. An automated sample injection system was used with TCB as the mobile phase at a flow rate of 1.0 ml.min^{-1}. 200 μl of each sample was injected. The column outlet was connected to a LC transform interface (Series 300, Lab Connections, Carrboro, USA) that acted as a solvent evaporation FTIR interface. The stage and nozzle temperatures were set at 165 °C and 150 °C respectively, with the line connecting the LC transform and the high temperature chromatograph kept constant at 150 °C. A constant flow of compressed air over the nebulizer kept it from overheating. The solutes were deposited on a heated germanium disc, which was subsequently transferred to a Nicolet iS10 Spectrometer (Thermo Electron, Waltham, USA) for FTIR analysis. This allows for the accumulation of individual spectra of each collected fraction (as can be seen in the so called waterfall plot in Figure 3.7). This data can then be used to draw up Gram Schmidt plots and chemigrams which provide valuable data concerning the chemical composition of each fraction. The SEC-FTIR data analysis was done by making use of an Omnic software package supplied by Thermo Electron.
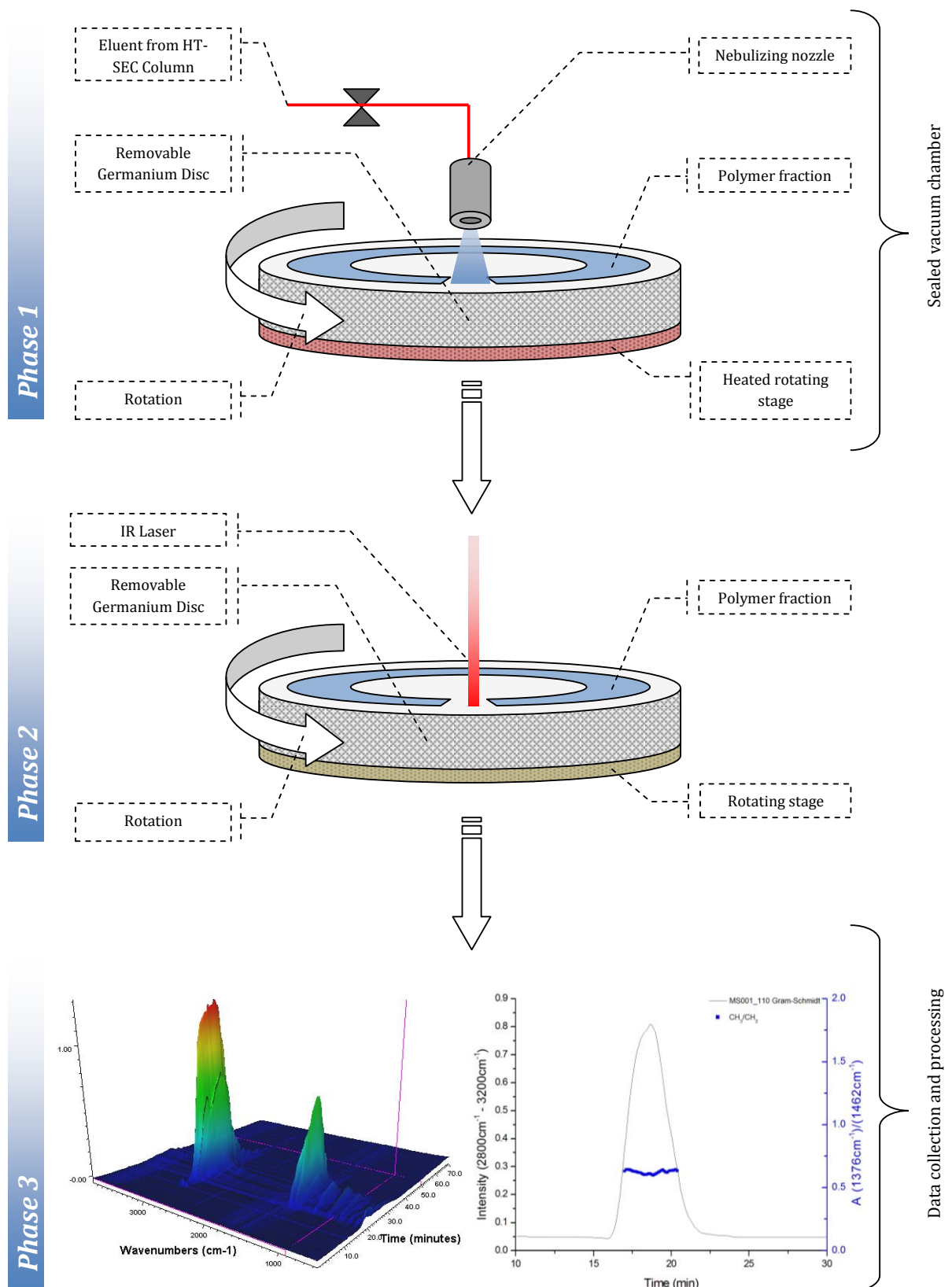
Figure 3.7   *Graphic illustration of the 3 phase SEC-FTIR process*

3.3.6 *Gradient high temperature high performance liquid chromatography (Gradient HT-HPLC)*

Gradient high temperature high performance liquid chromatography (HT-HPLC) was carried out with the use of a chromatographic system for HPLC manufactured by Polymer Char (Valencia, Spain) consisting of an auto sampler, two separate ovens and two pumps equipped vacuum degassers (Agilent, Waldbromm, Germany) and a evaporative light scattering detector or ELSD (model PL-ELS 1000, Polymer Laboratories, Church Stretton, England). The ELSD detector was used with a gas flow rate of 1.5 L.min^{-1}, a nebulizer temperature of 160 °C and an evaporative temperature of 270 °C. A Hypercarb column (Hypercarb, Thermo Scientific, Dreieich, Germany) was used for the HPLC phase. The column had the following specifications: 100 × 4.6 mm internal diameter, packed with porous graphite particles with diameters of 5 μm, a surface area of 120 m^2/g and a pore size of 250 Å. The column was placed in a column oven maintained at 160 °C. Separations were accomplished by applying a linear gradient from 1-decanol to TCB at a mobile phase flow rate of 0.5 mL.min^{-1}[3]. As illustrated in Figure 3.8 the volume fraction of TCB was increased to a 100% in 10 minutes after the sample was injected, kept constant at a 100% for 20 minutes where after the original chromatographic conditions were re-established with 100% 1-decanol. The HECO samples were injected at a concentration of 1.0 -1.2 mg.mL^{-1}, with 20 μL of each sample being injected.
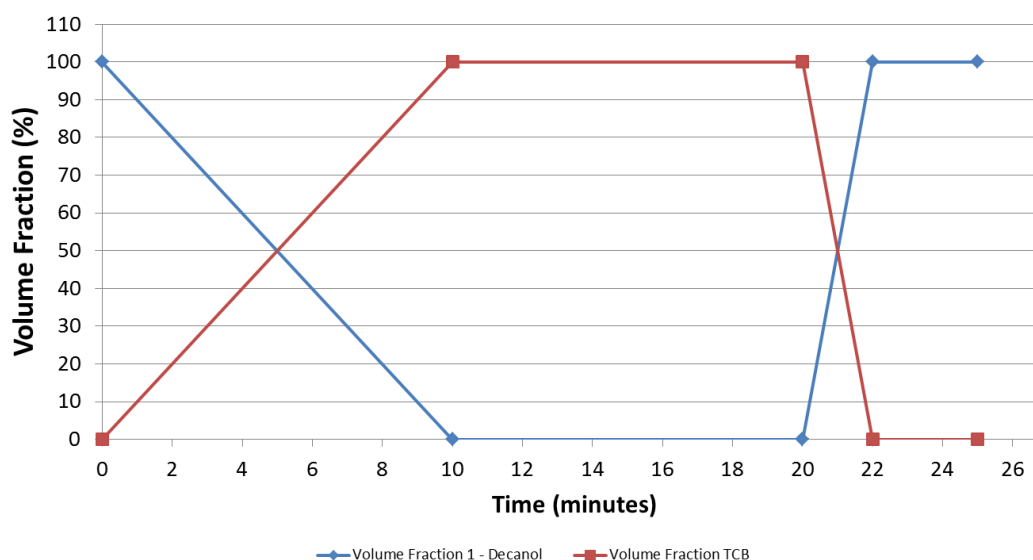
Figure 3.8   *HT-HPLC Gradient Profiles*

3.4   Mechanical testing

Test pieces for tensile testing, impact testing and DMA were prepared by using an ENGEL Victory 500 injection moulding machine (ENGEL, Schwartzberg, Austria). Table 3.1 shows the conditions used during the injection moulding process. It should be noted that heat sensitive polypropylenes may undergo molecular breakdown during moulding; therefore an increase in the MFR to >1.5 times the original value was avoided by lowering the melt temperature by 10 °C at a time until the increase in MFR was less than 1.5 times the original value. The uniformity of the moulded test pieces were checked by weighing and did not differ in mass by more than 1% [4].

Table 3.1   Conditions for injection moulding of test specimens

Material	Melt Temperature	Mould Temperature	Average Injection Velocity	Hold Pressure Time	Total Cycle Time
	(°C)	(°C)	(mm.sec^{-1})	(seconds)	(seconds)
MFR < 1.5g.10min^{-1}	255	40	200 ± 20	40	60
1.5g.10min^{-1} ≤ MFR ≥ 7g.10min^{-1}	230	40	200 ± 20	40	60
MFR > 7g.10min^{-1}	200	40	200 ± 20	40	60

3.4.1   Dynamic mechanical analysis (DMA)

A Q800 Dynamic Mechanical Analyser (TA Instruments Ltd, Herts, United Kingdom) was used for DMA measurements. DMA provides information regarding the viscoelastic behaviour of polymers by applying a sinusoidal stress and measuring the subsequent strain. This allows for the determination of the complex modulus. Varying the temperature will lead to variations in the complex modulus which in turn enables the determination of the glass transition temperature (T_g) as well as other transitions corresponding to other molecular motions[5]. Samples were cooled down from 25 °C to -100 °C at a rate of 10 °C per minute and kept isothermal at -100 °C for 5 minutes. Temperatures were then increased at a rate of 3 °C per minute to 80 °C.

3.4.2   Rheology measurements

3.4.2.1   Capillary rheometry measurements

A Rosand RH-7 capillary rheometer (Malvern Instruments Ltd, Worcestershire, United Kingdom) was used. Capillary rheometry gives information with regards to the processing properties of polymers by using different shear rates. This gives information regarding the processability of the samples during extrusion, injection molding, etc. depending on the specific application. Samples were tested at constant shear rates with both 0.5 and 1.0 mm dies (depending on the specific MFR of the samples being loaded) at 210-230 °C.

3.4.2.2   Parallel plate measurements

A TA Instruments ARES Parallel plate rheometer from AMS Laboratory Technology (Cape Town, South Africa) was used for parallel plate measurements. Parallel plate rheometry gives information with regards to the molecular properties of the polymer, i.e. molecular weight distribution and zero shear viscosity. Samples were subjected to an initial frequency of 490 rads.s^{-1} and a final frequency of 0.03 rads.s^{-1} at a constant strain of 5% and at a temperature of 230 °C. A 25 mm diameter plate was used with a gap size of 1.00 mm.

3.4.3   Tensile modulus measurements

Tensile modulus (also known as Young's modulus) measurements were carried out on an Instron 3365 (Instron, High Wycombe, United Kingdom) in order to determine the stiffness properties of the HECO samples prepared as described in Sections 3.1.1 and 3.1.2. All samples were conditioned for 48 hours at 23 °C and 50% humidity after moulding. The tensile modulus can be defined as the ratio of the uniaxial stress over the uniaxial strain in the range in which Hooke's Law holds[6]. The tensile modulus was calculated according to the following equation:

$$E = \frac{tensile\ stress}{tensile\ strain} = \frac{\sigma}{\varepsilon} = \frac{\frac{F}{A_0}}{\frac{\Delta L}{L_0}} = \frac{FL_0}{A_0 \Delta L} \qquad \textbf{(Eq. 3.5)}$$

Where,

E is the modulus of elasticity (tensile modulus)

F is the force exerted on an object under tension

A_0 is the original cross-sectional area through which the force is applied

ΔL is the amount by which the length of the object changes

L_0 is the original length of the object.

3.4.4   *Charpy notched impact strength measurements*

Impact strength measurements were performed using an automatic CEAST® Resil Impactor (Instron, High Wycombe, United Kingdom). The Charpy impact test is a high strain test which looks at the amount of energy absorbed during the fracture of a material. The absorbed energy is a measure of the specific material's toughness and acts as a means of determining temperature dependent ductile-brittle transitions. All samples were conditioned for 48 hours at 23 °C and 50% humidity after moulding. Tests were carried out at temperatures of 23 °C, 0 °C and -20 °C.

3.5   Microscopy techniques

3.5.1   *Scanning electron microscopy (SEM)*

SEM was used to establish the morphology of the EPR phase in the heterophasic copolymer. SEM analysis was performed on a Leo 1430VP SEM fitted with backscatter, cathodoluminescence, variable-pressure and energy-dispersive detectors, as well as a link EDS system and software for microanalysis and qualitative work. The SEM system was designed to perform high-resolution imaging and quantitative analysis. Injection moulded test bars were cryo-fractured using liquid nitrogen. The fractured samples were then placed in xylene for 17 hours in order to extract the EPR phase. Statistical imagery software was then used to randomly select 100 "holes" left by the extracted EPR particles. The diameter of these "holes" were then determined automatically. Three micrograms per sample was analysed using this technique and the average particle sizes were subsequently calculated.

3.6   References

1.   De Goede E, Mallon P, Pasch H. Fractionation and Analysis of an Impact Poly(propylene) Copolymer by TREF and SEC-FTIR. Macromol Mater Eng 2010:295(4):366-373.

2.   Quirk RP, Alsamarraie MAA. Physical properties of poly(propylene). Polymer Handbook. New York: John Wiley & Sons, 1989.

3.   Cheruthazhekatt S, Pijpers TFJ, Harding GW, Mathot VBF, Pasch H. Multidimensional Analysis of the Complex Composition of Impact Polypropylene Copolymers: Combination of TREF, SEC-FTIR-HPer DSC, and High Temperature 2D-LC. Macromolecules 2012.

4.   Bezuidenhout P. Operating Procedure for the ENGEL Injection Moulder. Polymer Technology Services Centre: Sasol Polymers, 2009. p. 16.

5.   Menard KP. Dynamic Mechanical Analysis: A Practical Introduction. CRC Press, 2008.

6.   McNaught AD, Wilkinson A. IUPAC. Compendium of Chemical Terminology. Oxford: Wilkinson. Blackwell Scientific Publications, 1997.

Chapter 4

Results and Discussion

This chapter details the analysis and characterization of the various visbroken propylene-ethylene heterophasic copolymers using established characterization techniques, multi-component analysis methods, as well as a new method to determine the chemical composition of heterophasic copolymers as a function of their molecular weight, namely, High Temperature gradient High Performance Liquid Chromatography. The results observed for each technique are also discussed in detail.

4.1   Introduction

Heterophasic propylene-ethylene copolymers (HECO), also known as impact copolymers (ICP), are widely known to have superior low temperature impact resistance properties over conventional polypropylene (PP) [1-3]. As a result of these superior properties, coupled with the good mechanical performance, heat resistance and versatility of conventional polypropylene, HECO polymers have seen a growing demand in the market in recent times. The most common commercial method to produce these polymers is the two stage copolymerization of propylene and ethylene. This multistage polymerization process consists of polymerization of propylene in the first reactor, resulting in a polypropylene homopolymer matrix, followed by copolymerization of propylene and ethylene in a second reactor. The result of this two stage polymerization process is a highly complex mixture of amorphous, random and blocky ethylene-propylene copolymers with different chemical composition distributions as well as different molar mass distributions, together with highly isotactic polypropylene and polyethylene homopolymer [3-5]. It has been proposed that this complex mixture of morphologies, especially the ethylene-propylene segmented or blocky copolymers can act as compatibilizers whereby they enhance the interfacial adhesion between the random copolymers and the polypropylene homopolymer. This interaction can be attributed to the enhancement of impact strength at low temperatures[6, 7].

Visbreaking or controlled rheology (CR) is a process used during the manufacturing of polypropylene to decrease the average molecular weight of the polymer. By decreasing the average molecular weight of the polymer a higher melt flow rate (MFR) as well as a decrease in the molecular weight distribution (MWD) is achieved. All factors being equal, this will result in a polymer that will show reduced warpage, more uniform shrinkage and drawdown, higher extrusion rates for fibres and films and significantly increased elongation at break. The effect of visbreaking on the molecular characteristics of HECO polymers is still relatively unknown[8].

In the present study, various HECO polymers with equal ethylene content were visbroken to varying degrees by making use of organic peroxides. The effects of the amount of visbreaking on the molecular characteristics and physical properties were subsequently studied by making use of preparative temperature rising elution fractionation (P-TREF), nuclear magnetic resonance spectroscopy (NMR), differential scanning calorimetry (DSC), high temperature size exclusion chromatography (HT-SEC), Fourier transform infrared spectroscopy (FTIR) and deposition of

the SEC fractions via the LC transform interface (SEC-FTIR) as well as gradient high temperature high performance liquid chromatography (HT-HPLC).

4.2   Experimental

The general experimental procedures and techniques used to characterize and analyse the various polymeric materials produced during this investigation are all described in detail in Chapter 3. Below is a brief summary of the main sections that will be covered in the following chapter.

4.2.1   Polymeric materials

The heterophasic copolymers used in this study were all prepared from a commercial reactor grade sample (denoted the base polymer). The base polymer sample was prepared via a continuous sequential polymerization process where the PP matrix is prepared in the first reactor in the gas phase. PP powder is then transferred to a second reactor with subsequent gas phase copolymerization of propylene and ethylene at a certain ratio to produce the elastomeric phase. After the synthesis of the base polymer powder the material was compounded with Irganox® 1010 and Irgafos® 168 (BASF, Ludwigshafen, Germany) in a twin screw ZSK 18 Coperion extruder at 500 rpm and barrel zone temperatures from 80 °C to 210 °C. Increasing amounts of Trigonox® 301 and Trigonox® 101 (Akzo Nobel Polymer Chemicals, Amersfoort, Netherlands) were added in order to achieve different vis-breaking steps using different types of organic peroxide. Table 4.1 (page 69) shows a summary of the main characteristics of the various samples.

4.2.3   Mechanical properties

Dynamic mechanical analysis (DMA) data was obtained for all samples by making use of the procedure described in Chapter 3 (Section 3.4.1). Further information regarding the flow characteristics of the bulk polymer samples were obtained by making use of capillary rheometry as well as parallel plate rheometry as described in Chapter 3 (Section 3.4.2.1 and

3.4.2.2). Tensile modulus and Charpy notched impact data were collected via the procedures described in Chapter 3 (Section 3.4.3 and 3.4.4).

4.2.3   Fractionation

The polymeric materials described above were first all fractionated by making use of analytical TREF. This initial fractionation was used as a guideline to see the affect (if any) varying amounts of organic peroxide will have on the molecular structure of the heterophasic copolymer. With sufficient evidence it was then decided to make use of preparative TREF in order to be able to do further off-line analysis on the various fractions. Therefore, the samples prepared as described in Chapter 3 (Section 3.1.1 and 3.1.2) were fractionated according to the general TREF procedure described in Chapter 3 (Section 3.2.1). As a control to the TREF analysis, CRYSTAF was also used to fractionate the bulk polymer samples according to the crystallisability.

4.2.4   Polymer characterization

^{13}C Nuclear magnetic resonance spectroscopy (NMR), differential scanning calorimetry (DSC), high temperature – size exclusion chromatography (HT-SEC), size exclusion chromatography coupled to FTIR via the LC transform interface (SEC-FTIR) and gradient high temperature high performance liquid chromatography (HT-HPLC) were all performed by making use of the equipment and techniques detailed in Chapter 3.

4.3   Results and discussion

4.3.1   Bulk polymer analysis

4.3.1.1   Dynamic mechanical analysis (DMA)

DMA measures a material's stiffness and damping, these properties are reported as the modulus and tan δ. Due to the fact that a sinusoidal force is applied during the testing the modulus can be expressed as an in-phase component or storage modulus and an out-phase component or loss modulus. The storage modulus is a measure of the sample's elastic behaviour. The ratio of the

loss modulus to the storage modulus is known as tan δ and is often referred to as damping. Tan δ is a measure of the energy that is dissipated in the material for every stress or strain cycle. This can thus give an indication of the impact strength of the material. Modulus values will change with temperature and changes in materials can therefore be seen in the storage modulus or tan δ curves. This includes glass transition temperatures. The glass transition temperature is seen as a drop in the storage modulus when viewed on a log scale against a linear temperature scale. The T_g can also be related to the tan δ peak. The area under this tan δ peak as well as the area under the loss modulus curve gives an indication of the impact strength of the material.

When looking at the data in Table 4.1 several interesting observations can be made. Firstly, the tensile modulus (or stiffness) of all samples, except for sample MS004 at -25 °C and at 0 °C, tend to show a gradual decrease with increasing visbreaking. This corresponds well with what is observed in industry. What is interesting to note however is that the decrease in stiffness seems to be more pronounced for samples prepared with Trigonox® 101 than for those prepared by Trigonox® 301. This immediately indicates that the Trigonox® 101 interacts more with the crystalline part of the polymer than the Trigonox® 301. This is illustrated in Figures 4.1 to 4.4 which show the change in stiffness at various temperatures as a function of the visbreaking step, comparing samples with similar MFR's.

Table 4.1   Summary of mechanical characteristics of the bulk polymer samples

Sample	Peroxide added	Melt Flow Rate	Tensile Modulus (MPa)			Stress at Yield	Charpy Notched Impact		
	(%)	*(g/10 min)*	*25 ℃*	*0 ℃*	*-25 ℃*	*(MPa)*	*23 ℃*	*0 ℃*	*-20 ℃*
MS001	0.000	1.5	1439	2098	2475	26.8	81.0	12.	7.3
MS002	0.125	3.7	1397	2026	2395	26.4	17.1	8.0	5.5
MS003	0.250	8.7	1399	1981	2401	26.1	14.1	6.8	5.3
MS004	0.500	13.8	1354	2084	2481	25.7	11.0	6.7	4.5
MS005	1.000	42.1	1269	1926	2323	26.2	14.7	7.6	5.6
MS006	0.250	7.8	1385	2013	2369	24.9	8.7	6.3	4.3
MS007	0.500	17.8	1365	1957	2310	25.2	10.5	6.4	4.7
MS008	1.000	40.6	1134	1710	2071	26.1	8.5	6.3	4.1
MS009	2.000	120.0	1103	1625	1981	25.1	7.8	6.3	3.5

Note: MS002-005 were prepared with Trigonox® 301, while MS006-009 were prepared with Triganox® 101
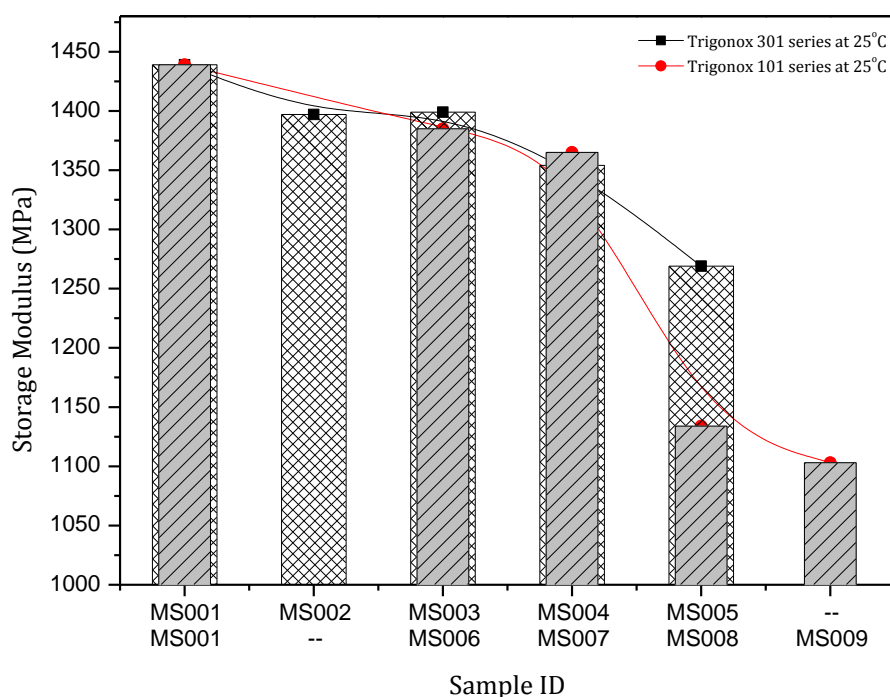

Figure 4.1   *DMA data indicating the differences in stiffness with an increase in visbreaking at 25 ℃*
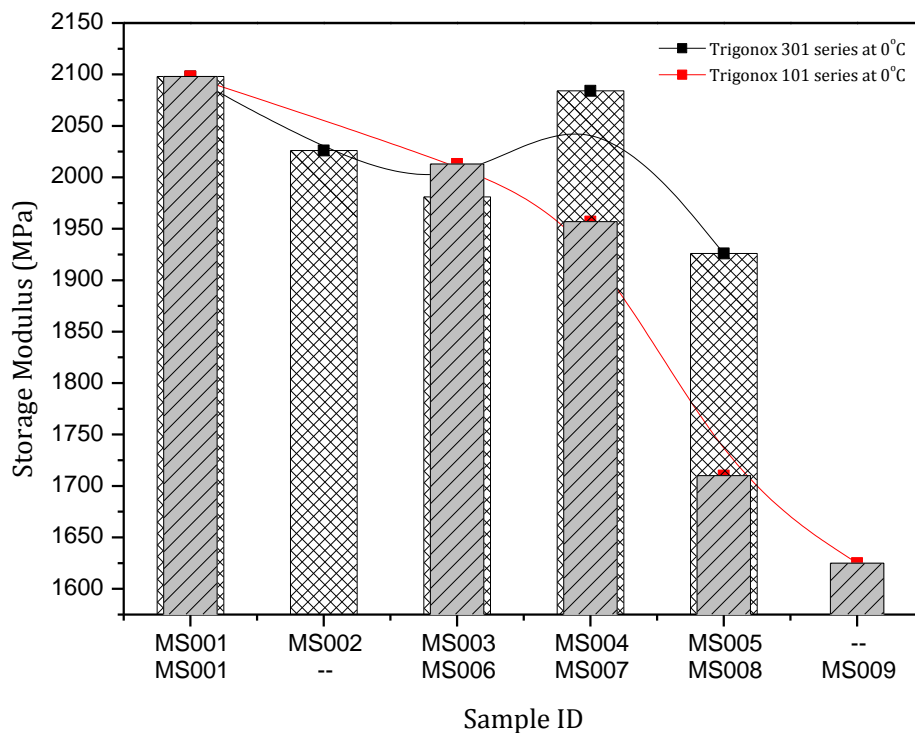
Figure 4.2 *DMA data indicating the differences in stiffness with an increase in visbreaking at 0 °C*
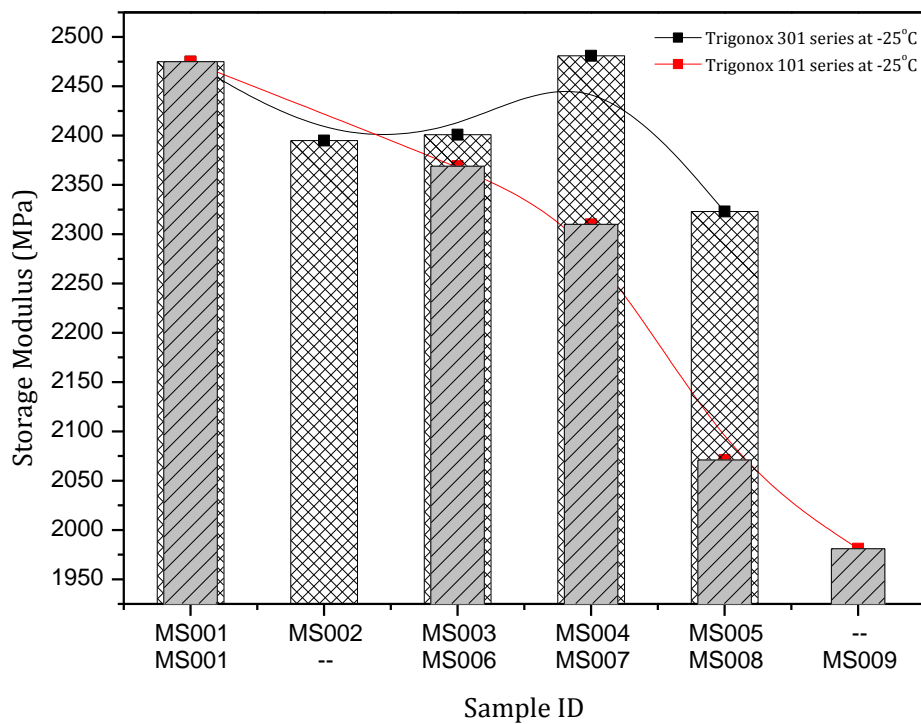
Figure 4.3 *DMA data indicating the differences in stiffness with an increase in visbreaking at -25 °C*

Figure 4.4 shows the data collected that reflects the impact strength of the HECO samples as a function of the amount of visbreaking, again comparing samples with similar MFR's. It can be seen that as expected there is a steep decrease in the impact strength when comparing the non-visbroken sample (MS001) to the visbroken samples. Samples prepared with Trigonox® 101 again show slightly lower impact resistance when compared to the Trigonox® 301 series.
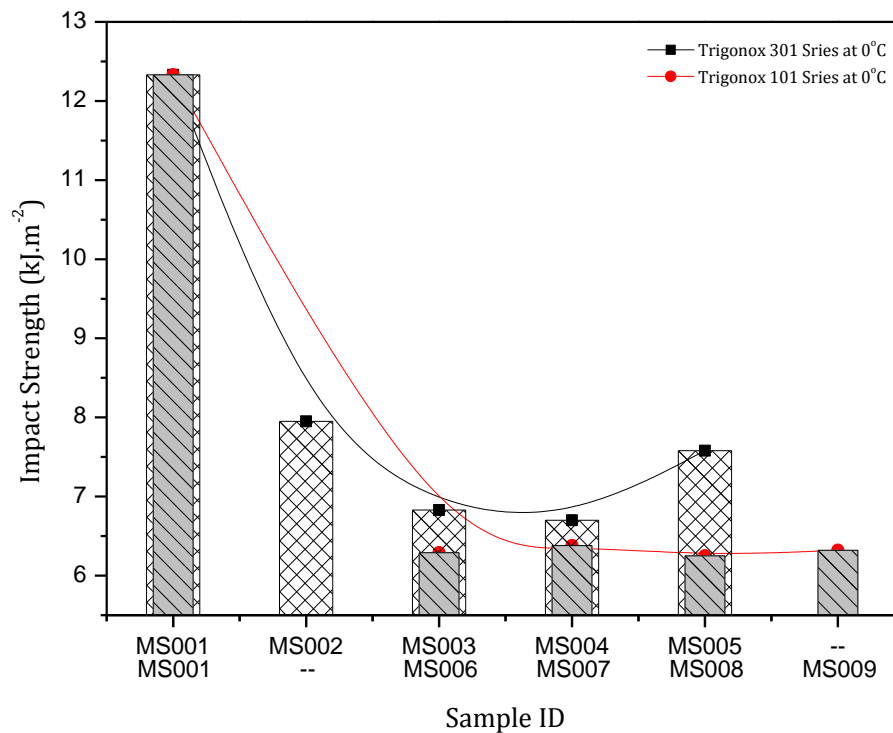
Figure 4.4   *Impact strength differences with an increase in visbreaking at 0 °C*

4.3.1.2   Rheology

For semi-crystalline polymers melt flow behaviour and solidification out of the molten state mainly due to cooling is of utmost importance. Solidification out of the molten state leads to the formation of ordered structures, or crystallites. During this process the rheological response of the material changes from fluid-like behaviour towards that of solid-like behaviour. Knowledge of the material rheology during this solidification process is important for process control and process modelling [9].

Using parallel plate rheometry, frequency sweep measurements were conducted on all samples and the complex viscosity data was determined. Using the Cross equation (Eq 4.1) and extrapolating, the zero shear viscosity for each sample was determined.

$$\eta^* = \eta_0 / (1 + (\tau\omega)^n) \qquad \textbf{(Eq 4.1)}$$

Where,

η^* = Complex Viscosity

η_0 = Zero Shear Viscosity

τ = Dynamic Stress

ω = Frequency

n   = a dimensionless constant

Dynamic data results are shown in Table 4.2 and an overlay of the complex viscosity curves is shown in Figure 4.5.

Table 4.2   Dynamic data collected via parallel plate rheometry

| Samples	Crossover Modulus (Pa)	Crossover Frequency (rad.s^{-1})	Polydispersity (PD)	Zero shear viscosity	MFR (g.10min^{-1})
MS001	No crossover	No crossover	No crossover	17718	1.5
MS002	3.8×10^4	25.2	2.6	10148	3.7
MS003	4.1×10^4	46.9	2.4	5560	8.7
MS004	4.4×10^4	87.7	2.2	3258	13.8
MS005	4.9×10^4	231.4	2.0	1266	42.0
MS006	4.4×10^4	80.3	2.3	3496	7.8
MS007	4.6×10^4	180.1	2.1	1697	17.8
MS008	5.2×10^4	420.5	1.9	889	40.6
MS009	No crossover	No crossover	No crossover	616	120.0
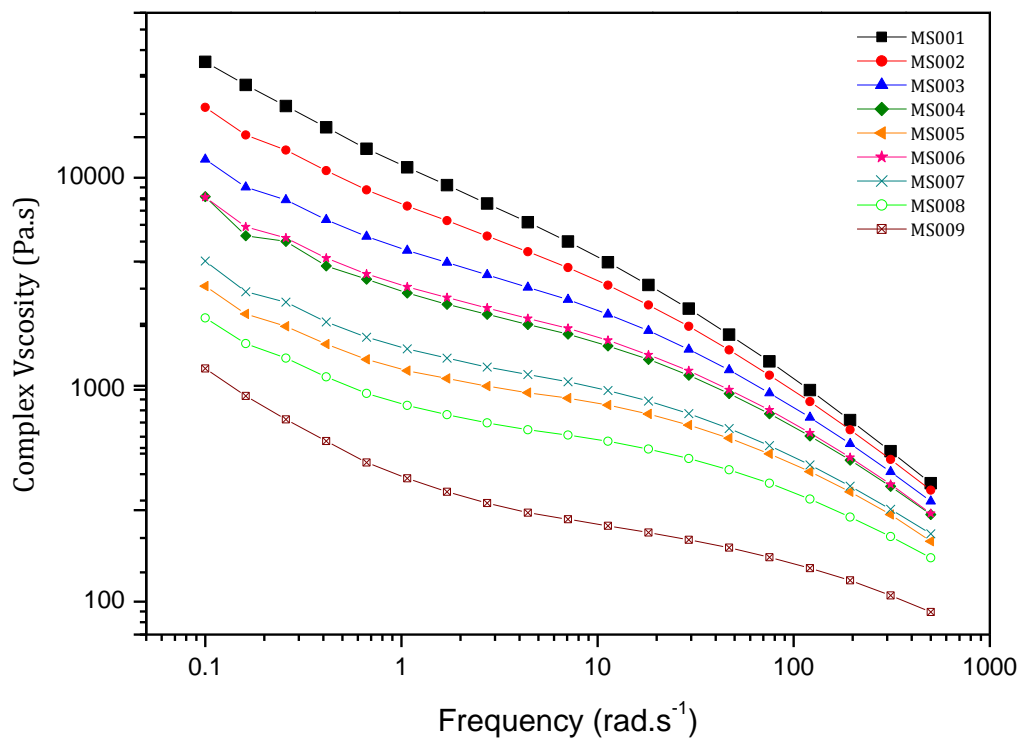
Figure 4.5   *Parallel plate rheometry results showing the complex viscosities.   For details regarding the sample ID refer to Table 4.1*

From this data it can clearly be seen that samples prepared with Trigonox® 101 tend to show lower zero shear viscosity than those prepared with Trigonox® 301 with similar melt flow rates (i.e. when comparing MS003 to MS006, MS004 to MS007 and MS005 to MS008). As expected samples MS001 and MS009 show the highest and lowest complex viscosities respectively. They also have the correspondingly lowest and highest melt flow rates. MS001 and MS009 have no crossover frequency meaning there is no point where elastic and viscous properties are similar. The crossover moduli for samples MS002 to MS008 range between 3.8 – 5.2 x 10^4 Pa.

Capillary rheometry was done to assess the constant viscosity of the polymer. Figure 4.6 shows that MS001 has the highest viscosity whilst MS009 has the lowest viscosity – this trend is expected because the higher the MFR the lower the viscosity. MS003 and MS006 have similar viscosities, MS004 and MS007 have similar viscosity and MS005 and MS008 have similar viscosities. This result is in contrast with the calculated zero shear viscosity seen from the parallel plate rheology results where the samples prepared with Trigonox® 101 tend to show lower viscosities than their Trigonox® 301 counterparts.
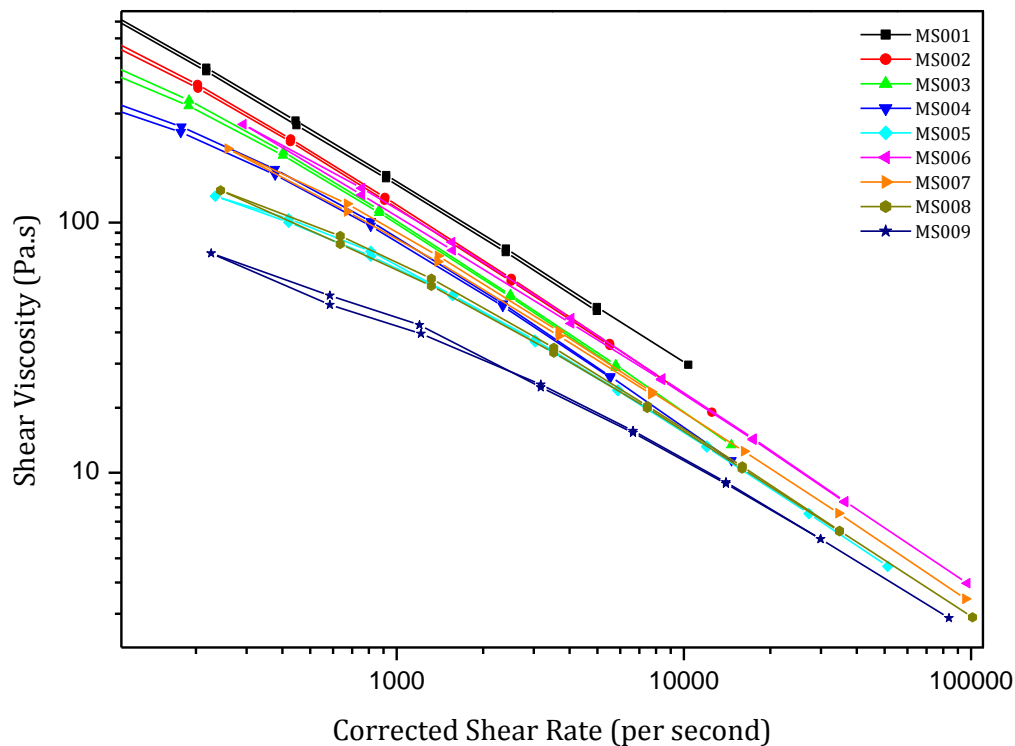
Figure 4.6   *Capillary rheometry results showing the constant viscosity curves*

From the data collected thus far it is evident that the type of peroxide used may determine which phase of the heterophasic polymer is affected. Due to the decrease in stiffness seen with samples prepared with Trigonox® 101 it is evident that this specific type of organic peroxide interacts more with the crystalline part of the heterophasic polymer than corresponding samples prepared with Trigonox® 301.

4.3.1.3   Scanning electron microscopy

By taking moulded test specimens obtained by injection moulding the bulk polymer samples and extracting the EPC fraction/phase with xylene followed by subsequent SEM analysis one can obtain an idea of the relative particle size distribution of the EPC or "rubbery" phase of the HECO polymer. Injection moulded test bars were cryofractured using liquid nitrogen. The fractured pieces were then sealed in chromatographic grade xylene for 18 hours to facilitate the extraction of the EPC particles from the fractured surfaces. The resultant SEM images as well as the particle size distribution (PSD) graphs are illustrated in Figure 4.7 – Figure 4.15.

Several observations can be made when looking at the results obtained from the cryo-fractured extraction process. Firstly, it can be noted that the bulk of the EPC particles are smaller than 1200nm. The non-visbroken sample (MS001) shows a good distribution of particle sizes with the bulk of the particles (42%) showing sizes of between 400 – 800nm. MS001 does however show that approximately 20% of particles have sizes above 1200nm. The slightly visbroken MS002 shows a similar PSD as that of MS001. It can however already be seen that there is a shift towards smaller particles sizes. As the visbreaking step increases it can be seen that there is a notable shift towards smaller particle sizes, with MS003 having 25% of the particles smaller than 400 nm, MS004 with 35% smaller than 400 nm and MS005 with 50% of particles that are smaller than 400 nm. With an increase in the percentage of these smaller particles with increasing visbreaking there is a subsequent decrease in the amount of bigger particles, with MS005 showing no particles larger than 1600 nm. It has been shown in literature [3, 4] that for multiphase polymer systems the toughening effect (better impact properties) is governed by mainly two factors. The first factor (and to a lesser extent) is the particle size and distribution. The smaller the particle size and the narrower the particle size distribution, the better the toughening effect is thought to be. This is in contradiction to what is seen in this specific case, where the impact strengths are seen to decrease with a decrease in the average particle size. A possible explanation for this is that the smaller particles are less likely to absorb energy and will in fact provide an easier path for failure propagation to occur along. The second governing factor is that the stronger the adhesion between the particles and the matrix, the better the impact properties. This can also be a possible explanation for the decrease in impact strength with an increase in visbreaking, i.e. that the smaller particles have less adhesion to the polymer matrix.

Samples prepared with Trigonox® 101 show a similar trend than those prepared with Trigonox® 301. What is noticeable is that samples MS006 – MS009 show even fewer larger sized particles than MS001 – MS005. MS008 and MS009 (the highly visbroken samples) show that more than 90% of the particles are smaller than 800 nm. Again this corresponds well with what is seen from DMA analysis with the samples being prepared with Trigonox® 101 having impact strengths that are slightly lower than those prepared with Trigonox® 301.

This is also the first indication that the visbreaking process to a large extent affects the ethylene-propylene copolymer phase dramatically. Further investigation is thus needed to try and establish why this is, and what the effect this has on the molecular structure of the HECO polymer. More information regarding the SEM analysis can be found in Addendum A.1.

Figure 4.7   *SEM image of sample MS001 after "rubber" extraction together with the particle size distribution (in nanometer) of the extracted "rubber" particles*

Figure 4.8   *SEM image of sample MS002 after "rubber" extraction together with the particle size distribution (in nanometer) of the extracted "rubber" particles*

Figure 4.9   *SEM image of sample MS003 after "rubber" extraction together with the particle size distribution (in nanometer) of the extracted "rubber" particles*
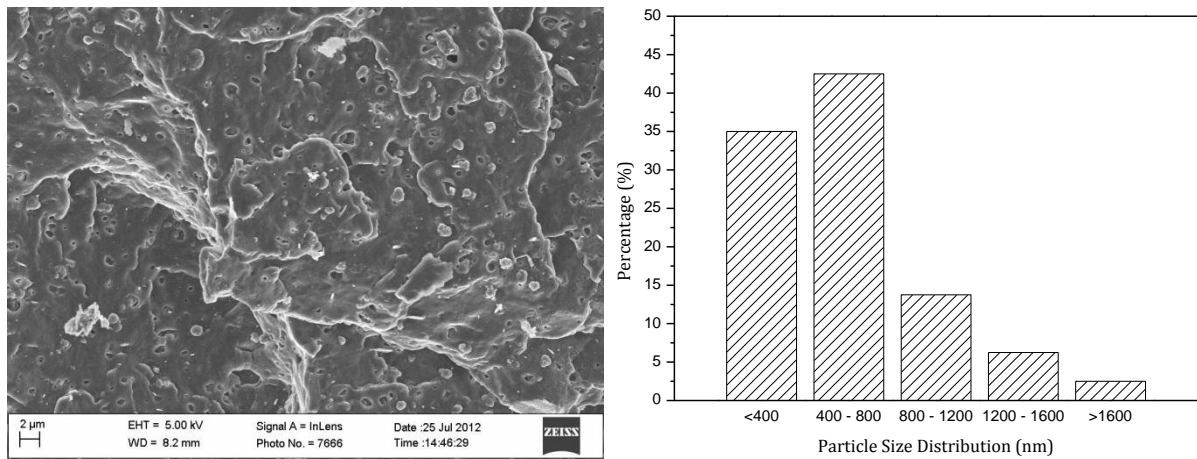
Figure 4.10   *SEM image of sample MS004 after "rubber" extraction together with the particle size distribution (in nanometer) of the extracted "rubber" particles*
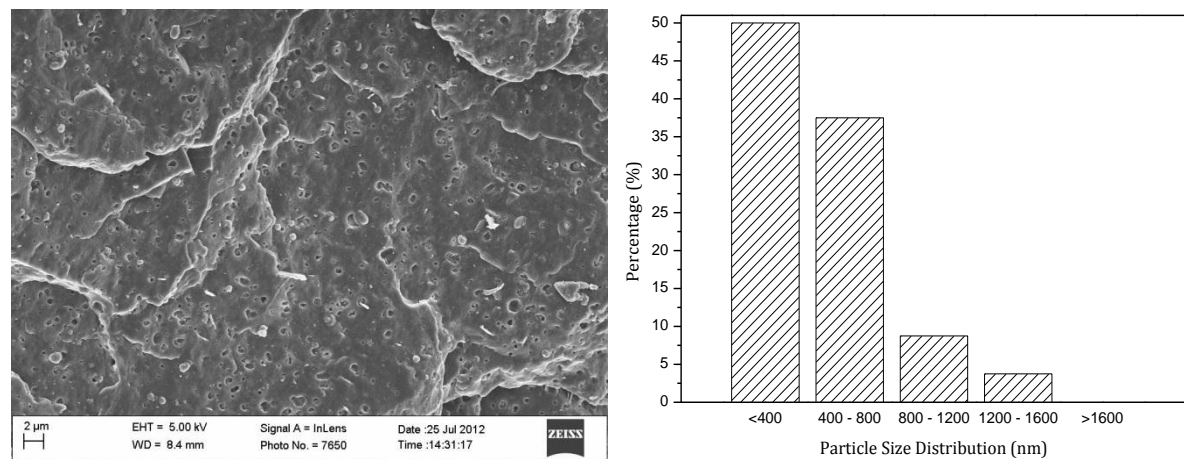
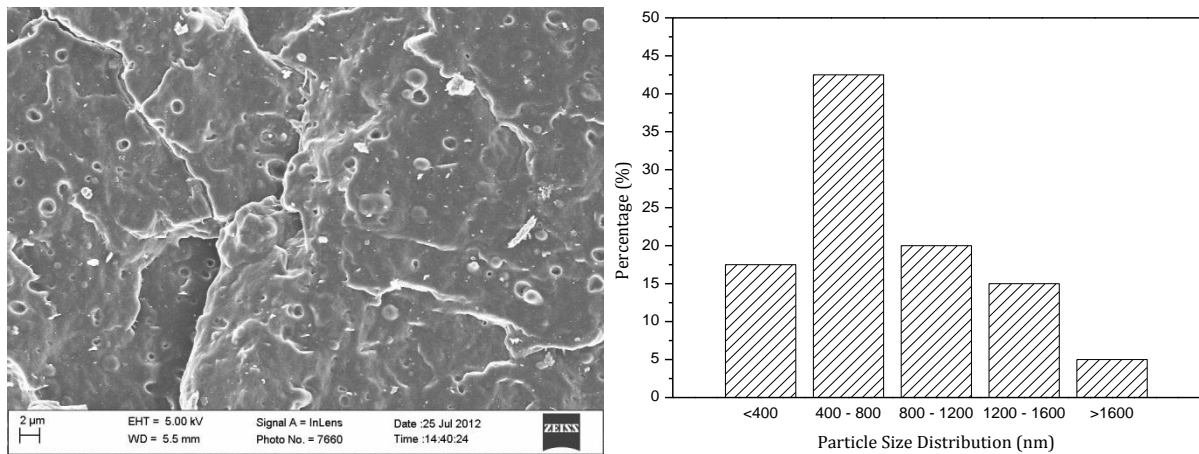
Figure 4.11   *SEM image of sample MS005 after "rubber" extraction together with the particle size distribution (in nanometer) of the extracted "rubber" particles*
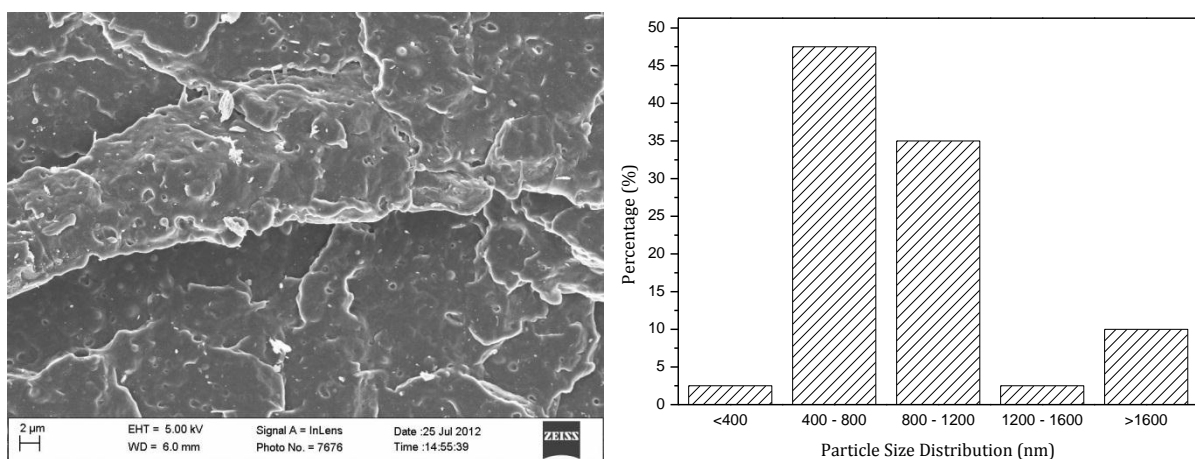
Figure 4.12   *SEM image of sample MS006 after "rubber" extraction together with the particle size distribution (in nanometer) of the extracted "rubber" particles*
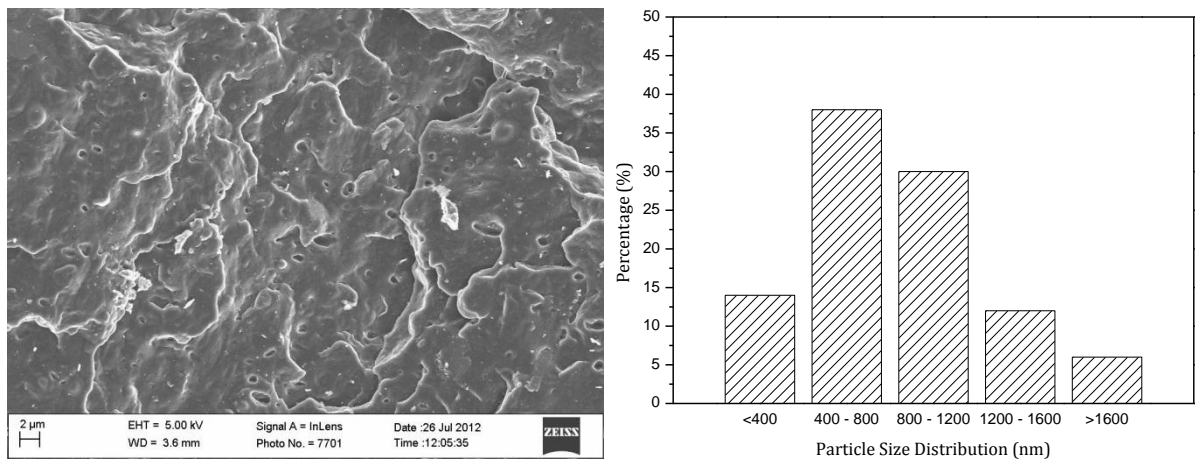
Figure 4.13   *SEM image of sample MS007 after "rubber" extraction together with the particle size distribution (in nanometer) of the extracted "rubber" particles*

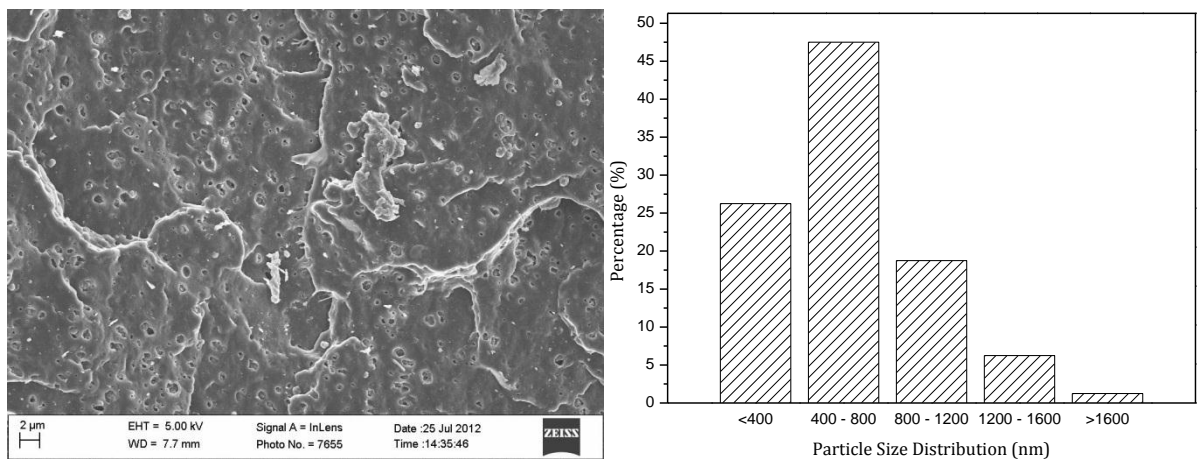
Figure 4.14   *SEM image of sample MS008 after "rubber" extraction together with the particle size distribution (in nanometer) of the extracted "rubber" particles*

Figure 4.15   *SEM image of sample MS009 after "rubber" extraction together with the particle size distribution (in nanometer) of the extracted "rubber" particles*

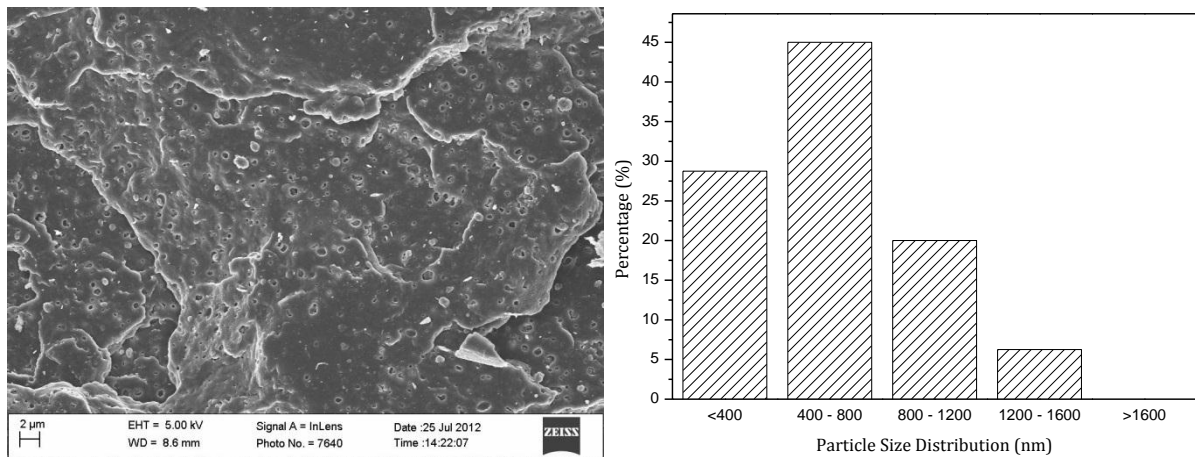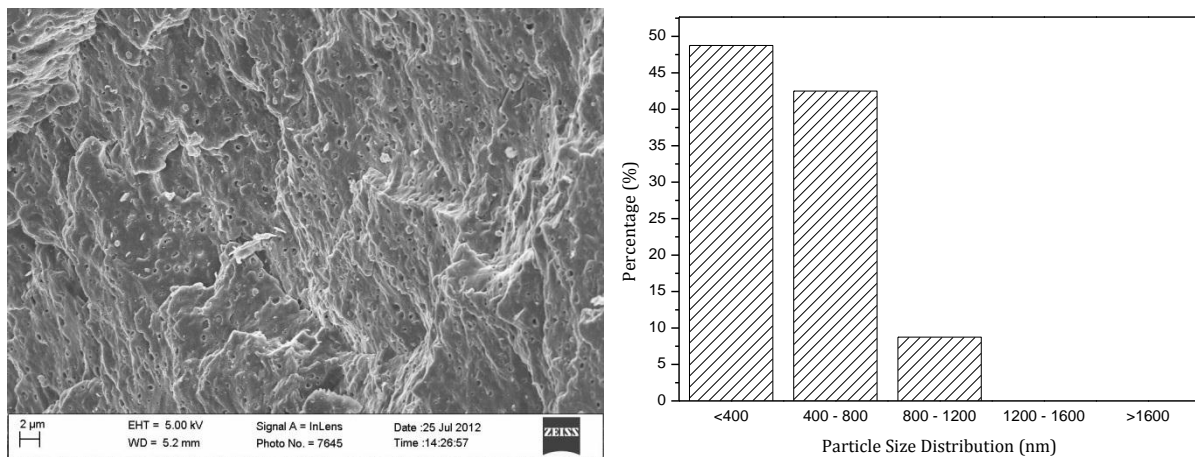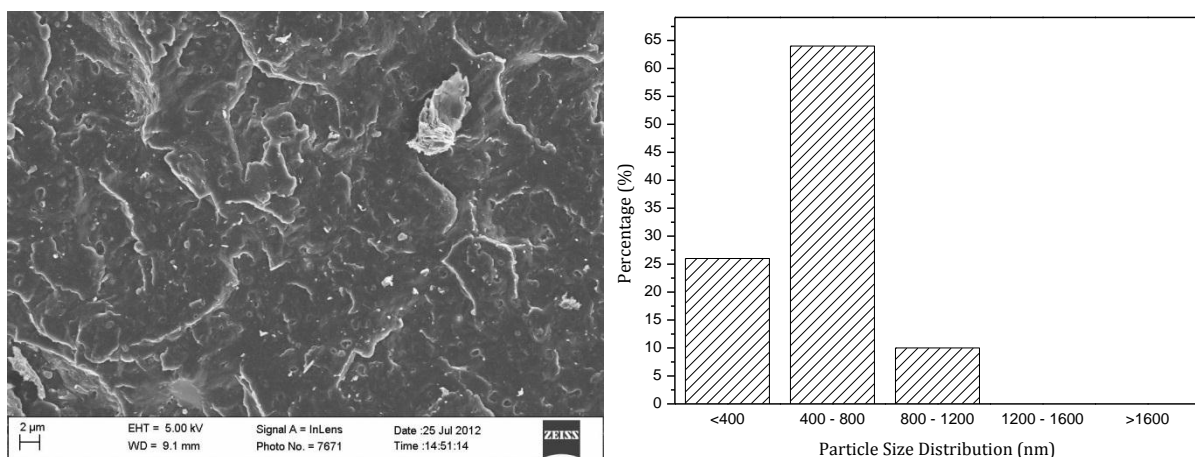### *4.3.2   Fractionation of bulk polymer samples*

4.3.2.1   Analytical TREF

Analytical TREF was used as an initial check to see if the amount of visbreaking has any effect on the chemical composition distribution of the HECO polymers as a function of its crystallinity. Samples are put into vessels and the instrument performs the dissolution, column loading, and temperature cycles combined with pump flow control. The concentration of the samples were then measured by an infrared detector.

Figure 4.16 – Figure 4.19 below shows the data recovered from analytical TREF for samples produced with both types of peroxide with Figure 4.16 (a) showing the un-expanded view of the base polymer sample MS001. Figure 4.16 (b) – Figure 4.19 give an expanded view of the weight percentage index for each sample across a temperature range from 25 °C to 140 °C. It can be seen that the bulk of the material elutes at approximately 26 °C – 30 °C and 116 °C – 122 °C. The fractions that are detected at lower temperatures are mainly amorphous polypropylene and small amounts of ethylene-propylene copolymer. The bulk of the material that is detected at approximately 120 °C is isotactic polypropylene. What is noticeable when looking at Figure 4.16 and Figure 4.18, which represents the higher temperature fractions, it can be observed that with an increase in visbreaking there is a corresponding decrease in the peak elution temperature. This is seen for both peroxide series but this phenomenon is more pronounced for the Trigonox® 101 series. It can also be seen that the low temperature fractions (amorphous part) increase in weight percentage with increasing visbreaking.

From this initial study it is therefore evident that the visbreaking process plays a significant role in the molecular structure of the HECO polymer and that the size of the visbreaking step also leads to molecular restructuring of the polymer. To further investigate what was seen with analytical TREF it was therefore decided to use preparative TREF. This would allow for the offline analysis of the various fractions collected at predetermined temperatures. By doing this, more insight could be gained as to which fractions are affected and how they are affected by the visbreaking process. More information on the results obtained from the analytical TREF can be found in Addendum B.1.
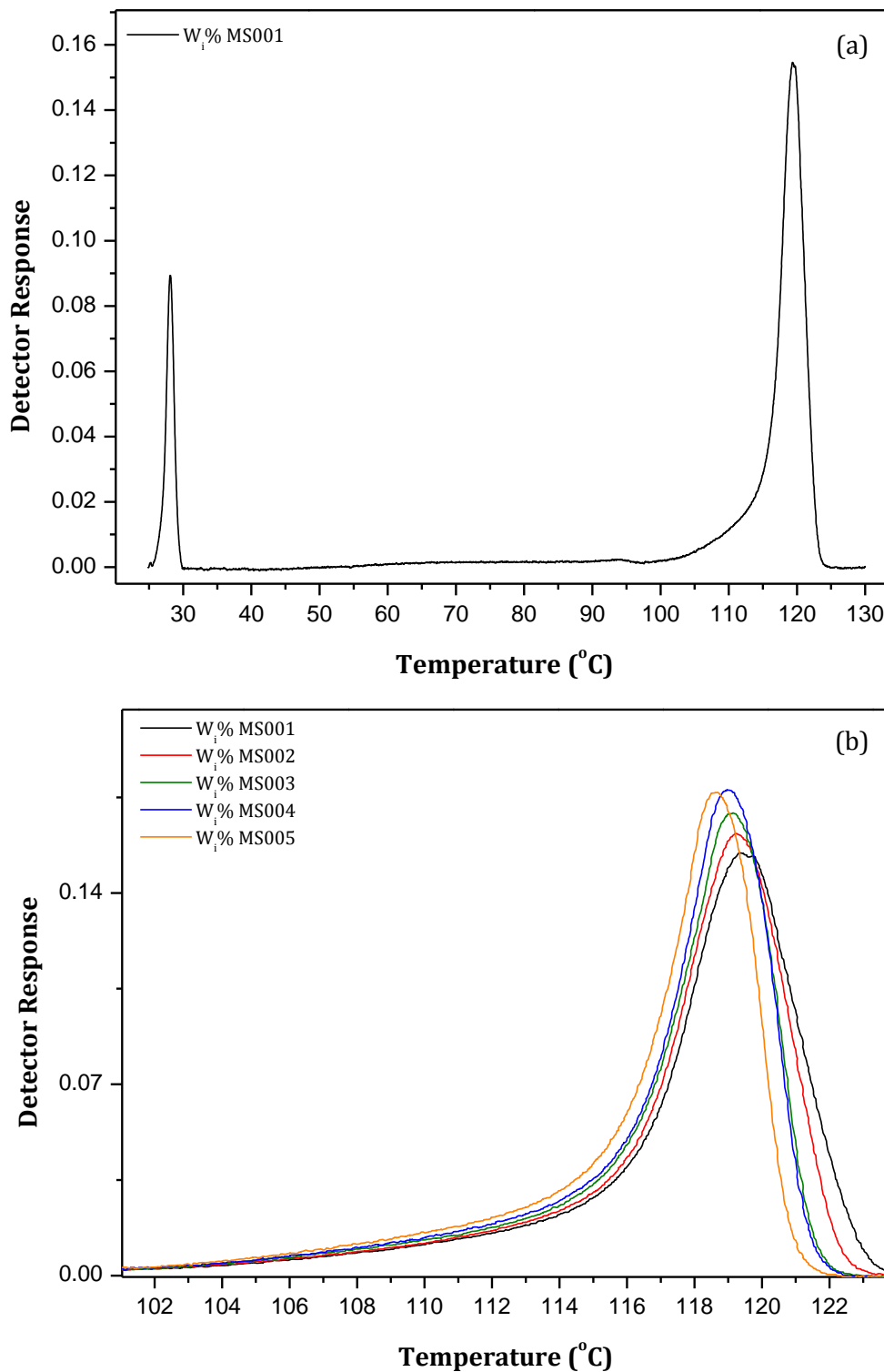
Figure 4.16   *Analytical TREF graphs of heterophasic copolymers prepared with Trigonox ® 301. Figure 4.16 (a) showing the full temperature range and (b) the 100 – 125 °C expanded region*

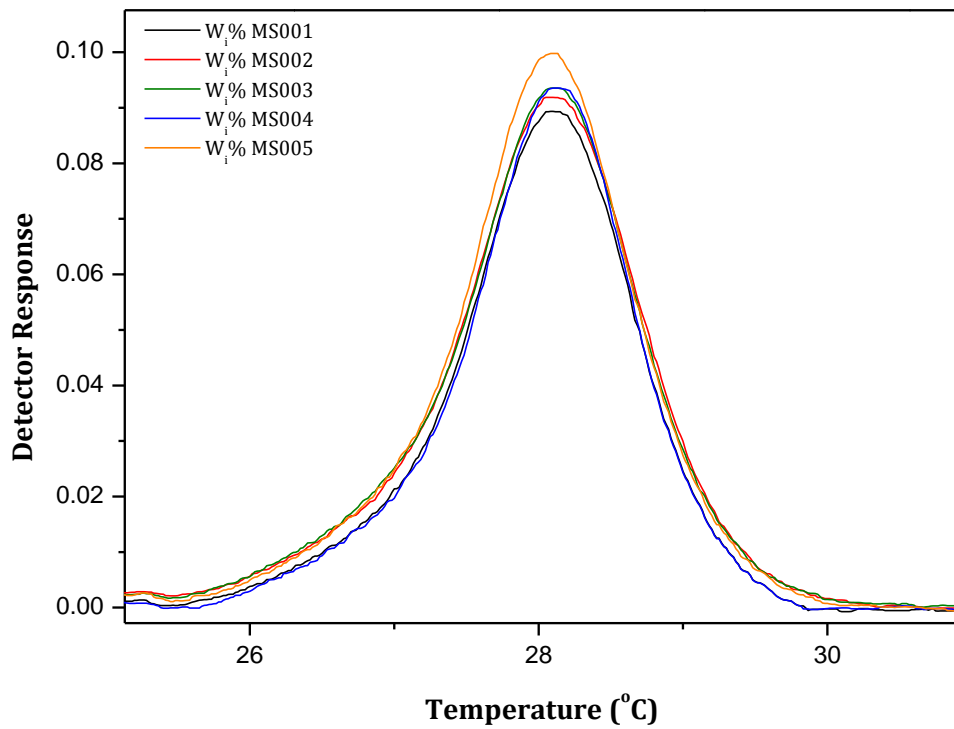**Figure 4.17**   *Analytical TREF graphs of heterophasic copolymers prepared with Trigonox ® 301 in the room temperature region*
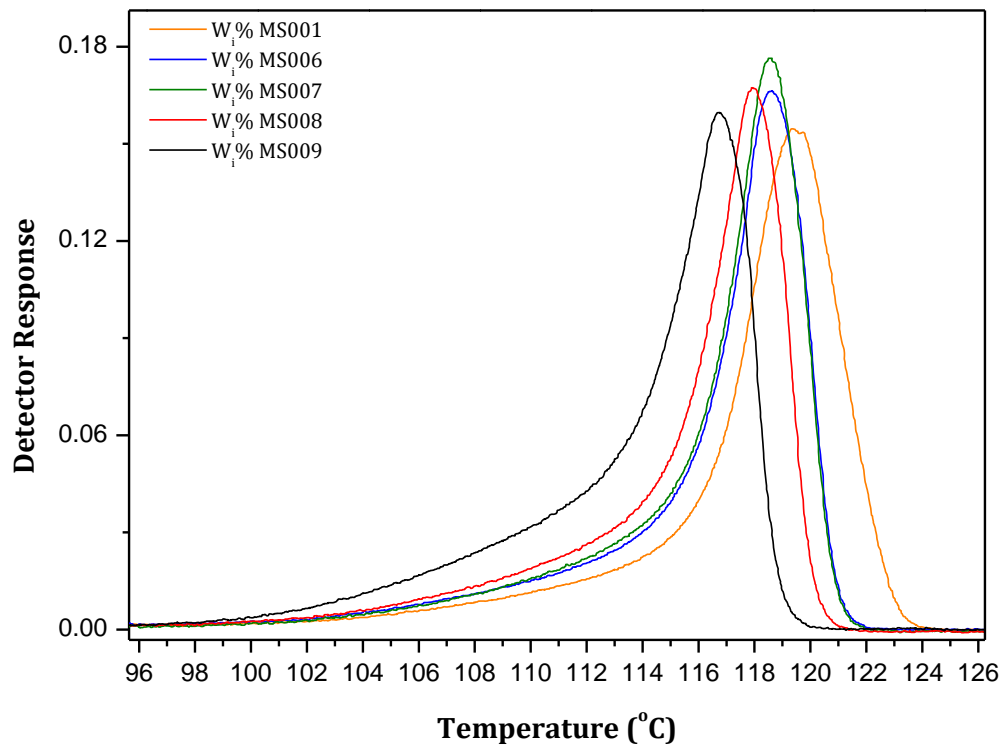
Figure 4.18   *Analytical TREF graphs of heterophasic copolymers prepared with Trigonox ® 101 in the 100 – 130 °C region*
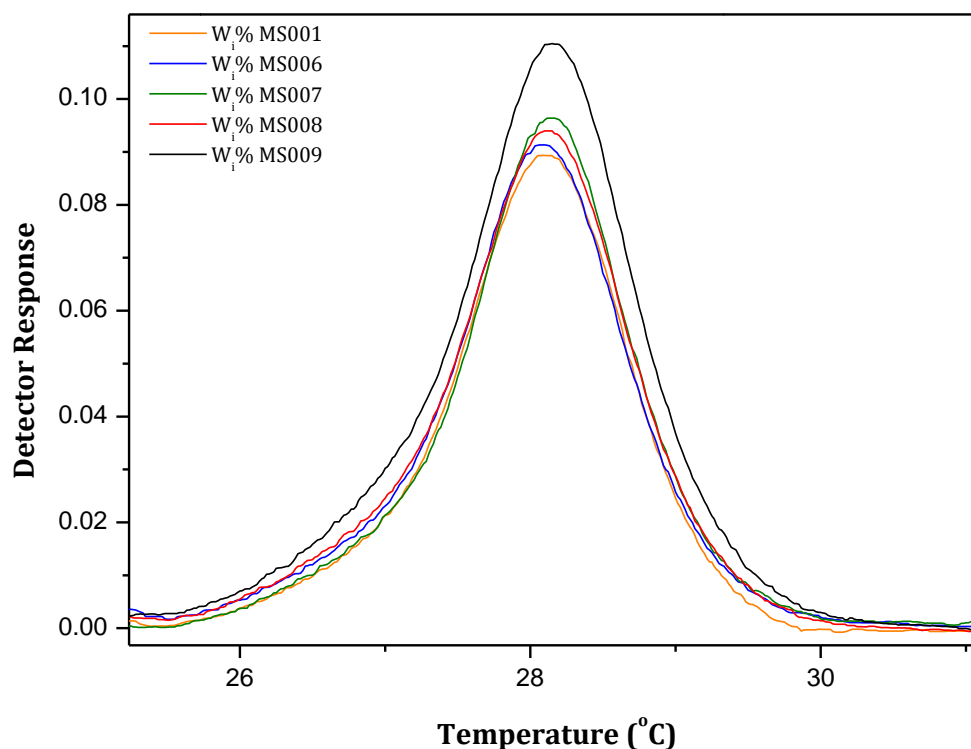
Figure 4.19   *Analytical TREF graphs of heterophasic copolymers prepared with Trigonox ® 101 room temperature region*

4.3.2.2   CRYSTAF

Figure 4.20 shows the changes in crystallisation behaviour for the selected heterophasic copolymer samples as a function of the amount of visbreaking as well as the type of peroxide used to facilitate the controlled rheology. The curves show a typical crystallisation behaviour associated with semi-crystalline materials with a relatively sharp peak centred on the 80 °C - 83 °C region and a small soluble fraction. For both types of peroxide it can be seen that a considerably narrower crystallisation peak commencing at a significantly lower temperature results as the extent of visbreaking increases. The changes seen in the main crystallisable fraction are accompanied with subtle changes in the soluble fraction, as seen when looking at Figure 4.21. The main crystallisable peak is seen to shift towards lower crystallisation temperatures with increasing amount of visbreaking. This shift is accompanied by an increase in the peak intensity indicating that there is also an increase in the amount of material crystallizing out at the maximum crystallisation temperature. A decrease in the soluble fraction is also seen with increasing visbreaking.

Figure 4.20   *CRYSTAF data showing the changes in results as a function of the amount and type of visbreaking*

Figure 4.21   *CRYSTAF data showing the changes in the soluble fraction as a function of the amount and type of visbreaking*

Table 4.3   Peak crystallisation temperatures and soluble fraction percentages

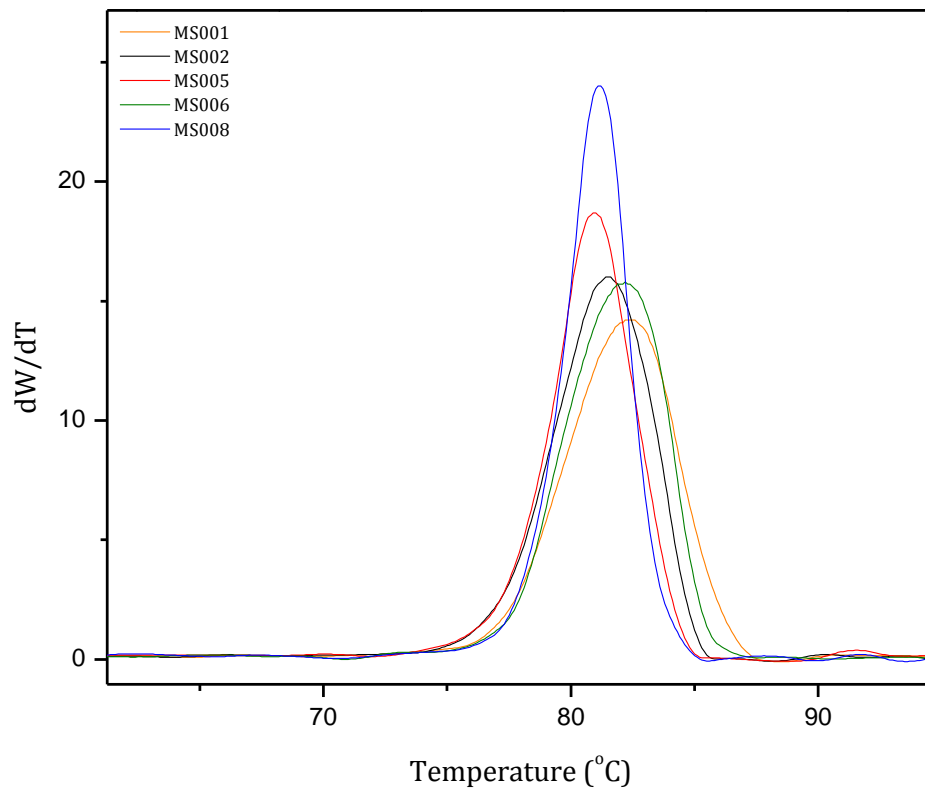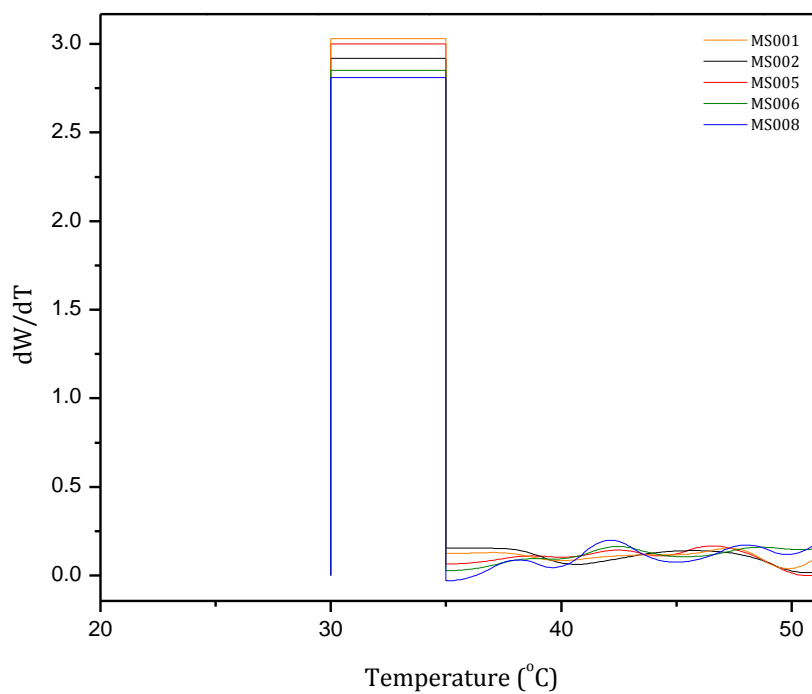| Sample	Crystallisation Temperature (°C)	Soluble fraction (wt%)
MS001	82.3	14.9
MS002	81.4	14.3
MS005	80.9	12.5
MS006	82.2	13.9
MS008	81.2	13.5

Table 4.3 above clearly indicates the shift in the crystallisation temperature seen with increased visbreaking. As is inherent to the visbreaking process these materials will tend to show higher melt flow rates (MFR's), lower molecular weights and narrower molecular weight distributions. Consequently this will also lead to easier and more consistent flow when in the molten state [9]. It is known from literature that as the degree of ethylene inclusion increases, the peak crystallisation temperature will decrease. Ethylene units (or segments) will act as defects in the chain structure and impede crystallisation of the chains[10, 11]. Due to the complex nature of heterophasic copolymers, further investigation is needed to try and determine which part of the polymer is affected by the organic peroxide and results in the shift observed in the crystallisation temperature. More information can be found in Addendum B.2.

Due to the fact that it has now been shown that the type of peroxide affects the molecular structure of the HECO polymer, it was decided to concentrate on only those samples that either had a small visbreaking step or a large visbreaking step.

4.3.2.3   Preparative TREF

Fractions were collected at predetermined temperatures of 30, 60, 80, 90, 100, 110, 120 and 130 °C. Figures 4.22 and 4.23 show the weight fraction per temperature increment ($W_i\%/\Delta T$) and weight percentage plots ($W_i\%$). The weight fraction per temperature increment curves are an approximation of the differential curve of the accumulative weight data. It can be seen in both Figures that the impact copolymer elutes over a broad range of temperatures indicating heterogeneity in both isotacticity and chemical composition. The fractionation data is also presented in Tables 4.4 – 4.8.
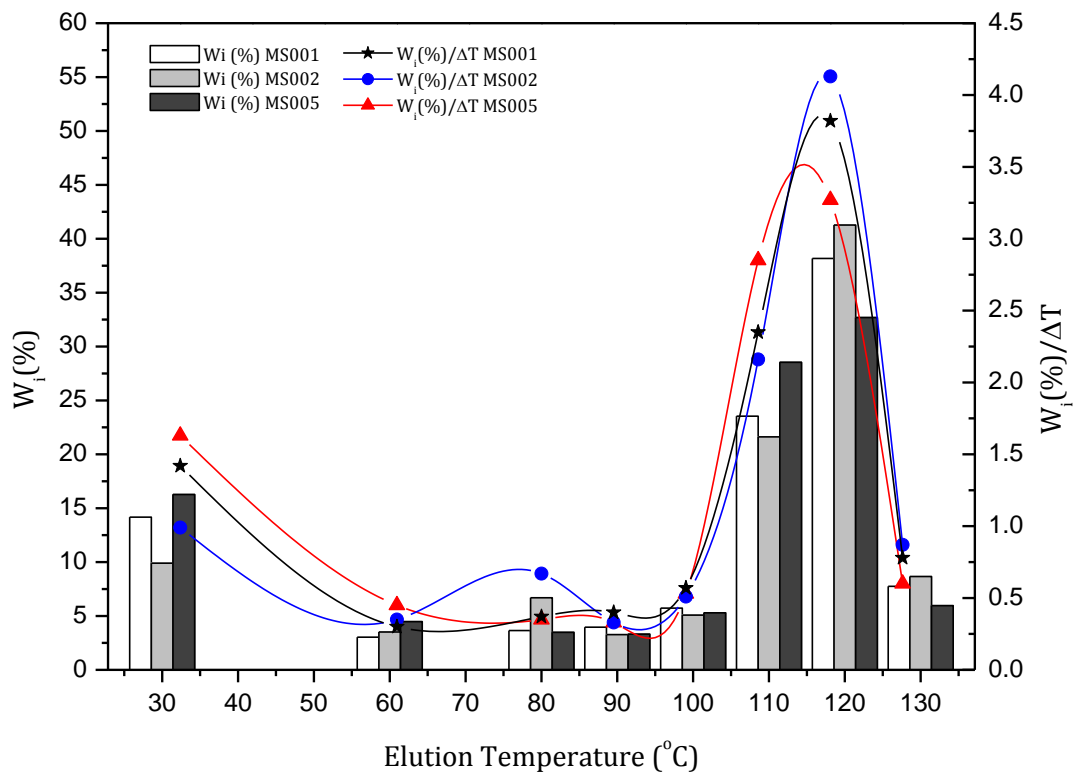
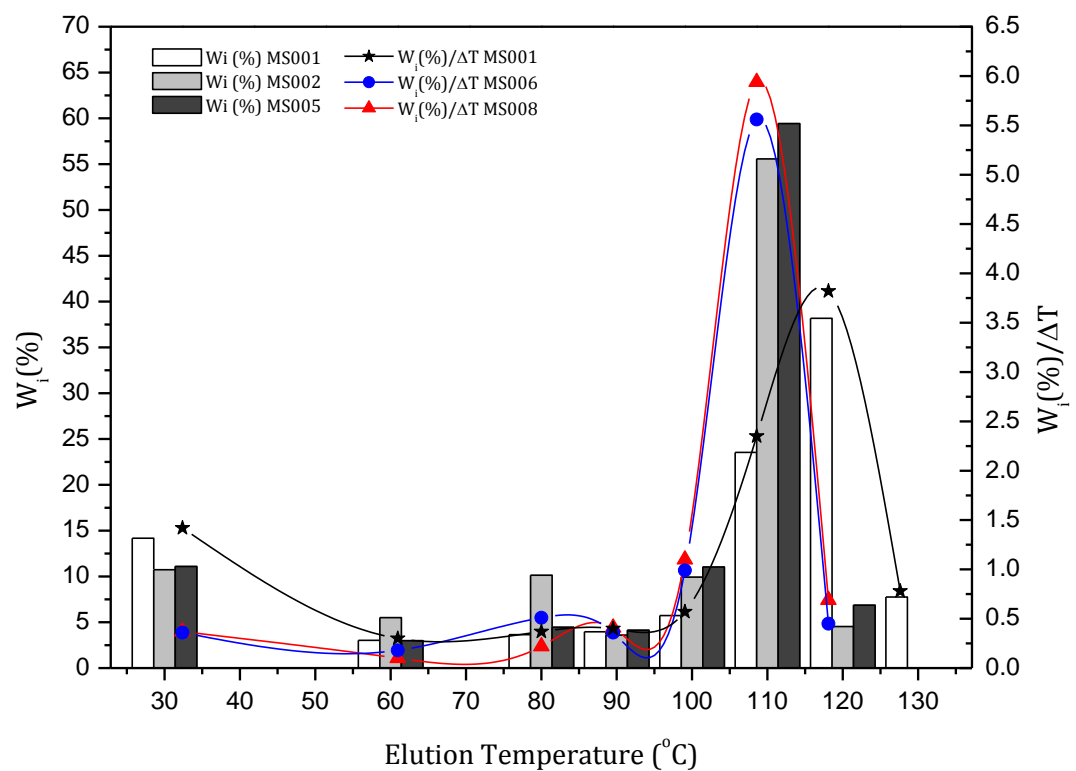**Figure 4.22**   *TREF elution curve comparison for MS001, MS002 and MS005*

Figure 4.23   *TREF elution curve comparison for MS001, MS006 and MS008*

From the fractionation data several observations can be made. First, samples MS001, MS002 and MS005 show similar elution trends and three main fractions can be identified, namely those eluting at 30, 110 and 120 °C. These fractions constitute approximately two thirds of the total sample weight. These fractions will therefore influence the bulk of the polymer to a large extent. Second, samples MS006 and MS008, prepared with a different organic peroxide, also show three main fractions, but eluting at different temperature intervals i.e. 30, 80-100 and 110 °C. This indicates that the molecular structure of the samples prepared with this specific organic peroxide differs from that of the other. The MS005 polymer has a broadening of the "crystalline peak" and a shift to a lower temperature. For the Trigonox® 101 samples this shift results in a narrower fraction, thus indicating a significant attack on the more crystalline areas of the polymer

More information on the preparative TREF results can be found in Addendum B.3

The individual fractions obtained by P-TREF were subsequently analysed by DSC and ^{13}C-NMR to try and establish exactly what these differences are and to try and explain why they are seen.

Table 4.4   *TREF Elution Data for Sample MS001*

Sample	T_e (°C)	W_i (g)	W_i (%)	ΣW_i (%)	W_i (%)/ΔT
MS001-30	30	0.495	14.17	14.17	1.42
MS001-60	60	0.106	3.03	17.20	0.30
MS001-80	80	0.128	3.65	20.85	0.37
MS001-90	90	0.138	3.96	24.81	0.40
MS001-100	100	0.200	5.73	30.54	0.57
MS001-110	110	0.823	23.54	54.08	2.35
MS001-120	120	1.334	38.17	92.25	3.82
MS001-130	130	0.271	7.75	100.00	0.78

Table 4.5 *TREF Elution Data for Sample MS002*

Sample	T_e (°C)	W_i (g)	W_i (%)	ΣW_i (%)	W_i (%)/ΔT
MS002-30	30	0.280	9.90	9.90	0.99
MS002-60	60	0.099	3.51	13.41	0.35
MS002-80	80	0.189	6.69	20.10	0.67
MS002-90	90	0.092	3.27	23.37	0.33
MS002-100	100	0.143	5.08	28.45	0.51
MS002-110	110	0.611	21.62	50.07	2.16
MS002-120	120	1.166	41.27	91.34	4.13
MS002-130	130	0.245	8.66	100.00	0.87

Table 4.6 *TREF Elution Data for Sample MS005*

Sample	T_e (°C)	W_i (g)	W_i (%)	ΣW_i (%)	W_i (%)/ΔT
MS005-30	30	0.496	16.27	16.27	1.63
MS005-60	60	0.136	4.47	20.74	0.45
MS005-80	80	0.106	3.48	24.22	0.35
MS005-90	90	0.101	3.31	27.53	0.33
MS005-100	100	0.161	5.29	32.82	0.53
MS005-110	110	0.870	28.53	61.35	2.85
MS005-120	120	0.997	32.69	94.04	3.27
MS005-130	130	0.182	5.96	100.00	0.60

Table 4.7 *TREF Elution Data for Sample MS006*

Sample	T_e (°C)	W_i (g)	W_i (%)	ΣW_i (%)	W_i (%)/ΔT
MS006-30	30	0.322	10.73	10.73	0.36
MS006-60	60	0.165	5.50	16.23	0.18
MS006-80	80	0.304	10.13	26.37	0.51
MS006-90	90	0.108	3.60	29.97	0.36
MS006-100	100	0.298	9.93	39.90	0.99
MS006-110	110	1.667	55.57	95.47	5.56
MS006-120	120	0.136	4.53	100.00	0.45
MS006-130	130	-	-	-	-

Table 4.8   *TREF Elution Data for Sample MS008*

Sample	T_e (°C)	W_i (g)	W_i (%)	ΣW_i (%)	W_i (%)/ΔT
MS008-30	30	0.349	11.09	11.09	0.37
MS008-60	60	0.094	2.99	14.08	0.10
MS008-80	80	0.140	4.45	18.53	0.22
MS008-90	90	0.130	4.13	22.66	0.41
MS008-100	100	0.347	11.03	33.68	1.10
MS008-110	110	1.870	59.42	93.10	5.94
MS008-120	120	0.216	6.86	99.97	0.69
MS008-130	130	-	-	-	-

4.3.3   *Nuclear magnetic resonance spectroscopy (NMR)*

Detailed analysis using NMR was performed to determine the co-monomer content and monomer sequence distributions on all TREF fractions in order to determine the effect of visbreaking with an organic peroxide on the molecular characteristics if the polymer. The ^{13}C-NMR method for determining the co-monomer content, monomer sequence distributions and stereoregularity of ethylene-propylene copolymers and impact copolymers is well established and co-monomer content and monomer sequence distributions were calculated according to relationships determined by Ray et al. [12] and Randall [13]. Results from the sequence analysis together with isotacticity data determined using the method described by Viville et al. [14] is shown in Tables 4.9 – 4.13. Figure 4.24 and Figure 4.25 shows a typical ^{13}C-NMR spectrum for an ethylene-propylene copolymer with low ethylene content and an illustration of the nomenclature associated with methylene carbons in ethylene-propylene copolymers without monomer inversion respectively. Chemical shifts were referred to isolated methylene groups at 30 ppm and assignment of the resonances followed the terminology described by Carmen and Wilkes where the letters S, P and T indicate secondary (methylene), primary (methyl) and tertiary (methane) carbon atoms respectively. The two Greek subscripts seen in Figure 4.24 and Figure 4.25 refer to the distance, in both directions, of any given carbon to the nearest neighbouring tertiary carbon bearing a methyl side group. Therefore, a carbon labelled $S_{\alpha\alpha}$ is a secondary carbon with two tertiary carbons on either sides, whereas a $S_{\alpha\beta}$ carbon is a secondary carbon with one tertiary carbon on one side and another tertiary carbon found one carbon away, until a $S_{\delta\delta}$ carbon is reached which indicates a secondary carbon with tertiary carbons

bearing methyl groups, being four carbons away on both sides. When the distance to the nearest tertiary carbon exceeds four, the δ^+ notation is used.
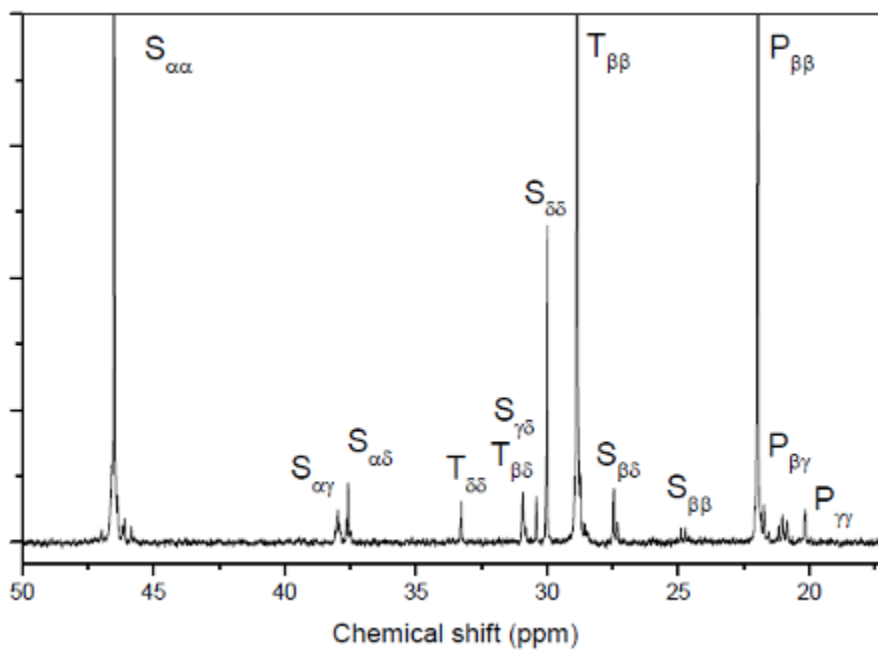

Figure 4.24   *^{13}C-NMR peak assignments for an ethylene-propylene impact copolymer with low ethylene content*
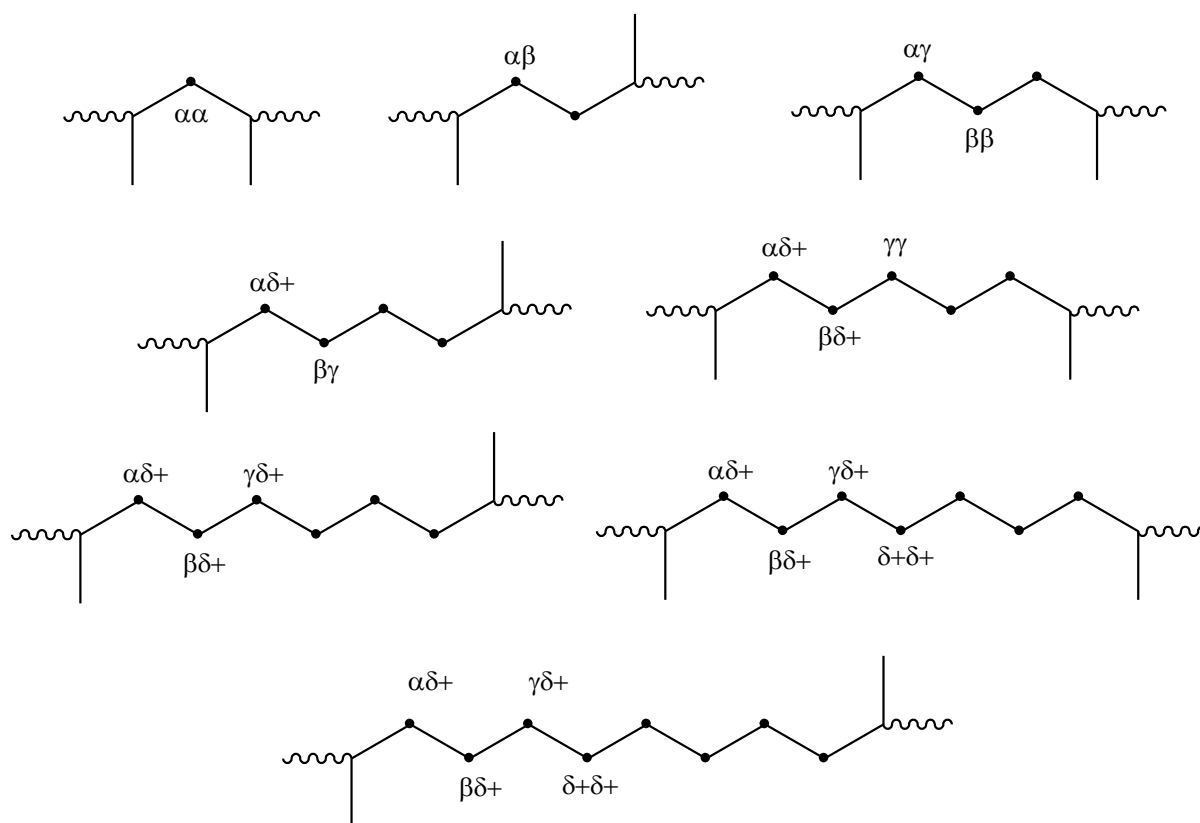
Figure 4.25   *Illustration of the nomenclature used for the methylene carbons in ethylene-propylene copolymers without monomer inversion*

Figure 4.26 below shows the ^{13}C-NMR stack plots for the base polymer sample (MS001). The chemical shift is represented on the x-axis, TREF elution fractions on the y-axis and the intensity on the z-axis.
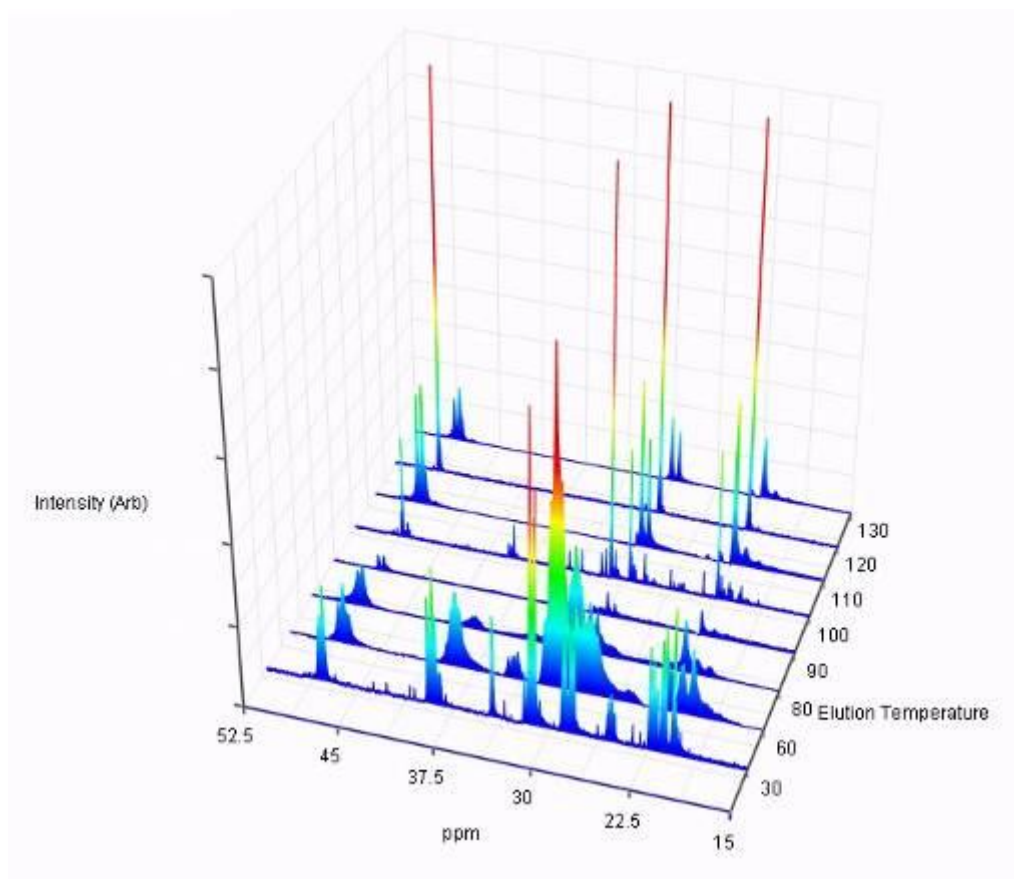
Figure 4.26   *¹³C-NMR stack plot of MS001 TREF fractions collected at various temperature intervals*

From the sequence analysis data in all of the samples it can be seen that, with increasing elution temperature, there is an initial increase in ethylene content followed by a decrease. For samples prepared with Trigonox® 301 as well as the base polymer sample (MS001, MS002, MS005) the decrease in ethylene content is seen as early as from 60 °C onwards, whereas with the samples prepared with Trigonox® 101 (MS006 and MS008) the ethylene content only starts decreasing after about 80 °C. Samples prepared with Trigonox® 301, as well as the base polymer sample, also show some long ethylene sequences (EEE) sequences at high temperatures (120 °C and 130 °C) whereas the samples prepared with Trigonox® 101 show none of these sequences at higher temperatures. Together with the above observation it is also noted that the propylene content and isotacticity is seen to increase with increasing elution temperatures. This indicates that the fractionation is governed mainly by decreasing co-monomer content and increasing isotacticity. Long propylene sequences (PPP) are seen to increase as the temperatures increase up to approximately 99.5%. PPP triad sequences for samples produced with Trigonox® 301 as well as the base polymer sample reached a maximum at 120 °C, whereas for samples produced with Trigonox 101 the PPP triad maximum is seen at 110 °C. The amount of EP junctions is seen

to decrease with increase temperature. The high amount of (PE+EP) diads in the first fractions indicates that ethylene and propylene segments are linked to some degree. This value becomes virtually zero in higher temperature fractions. These fractions are therefore seen to consist of mainly long propylene homopolymer sequences. What should be noted is that the (PE + EP) junction segments for samples produced with Trigonox® 301 is seen in fractions up to 100 ℃, whereas samples prepared with Trigonox® 101 only show these junction segments up to 80 ℃. $S_{\alpha\alpha}$ (CH$_2$), $T_{\beta\beta}$ (CH) and $P_{\beta\beta}$ (CH$_3$) corresponds to the three distinct carbon atoms in the constitutional base unit of polypropylene, whereas $S_{\delta\delta}$ peaks represent the CH$_2$'s associated with polyethylene. Minor peaks ($S_{\alpha\gamma}$, $S_{\alpha\delta}$, $S_{\beta\delta}$, $S_{\gamma\delta}$, $T_{\delta\delta}$, $S_{\beta\delta}$, $P_{\beta\gamma}$ and $P_{\gamma\gamma}$) are also present in the spectrums and indicates various transition segments such as PEP, EPE, PPE and PEE. Co-monomer content and monomer sequence distributions were calculated based on the relationship established by Ray et al. [12] and Randall [15] and is represented in Tables 4.9 – 4.13 below.

Table 4.9 *^{13}C-NMR sequence analysis and tacticity of MS001 and its TREF fractions*

Sample	P'	E'	P	E	PP	PE EP	EE	PPP	EPP PPE	EPE	EEE	EEP PEE	PEP
MS001-30	16.96	25.10	40.32	59.68	22.44	35.76	27.92	21.10	5.54	13.68	17.99	22.28	6.74
MS001-60	14.38	61.27	19.01	80.99	11.73	14.56	60.18	9.07	2.38	7.56	49.05	10.34	2.11
MS001-80	13.00	18.23	41.62	58.38	33.50	16.24	45.93	31.06	5.69	4.87	40.48	8.17	4.04
MS001-90	16.94	25.13	40.26	59.74	33.62	13.29	50.26	33.57	0.00	6.69	45.40	6.21	3.54
MS001-100	12.08	15.88	43.21	56.79	35.05	16.33	42.12	33.03	6.57	3.60	37.45	11.34	2.50
MS001-110	34.28	7.58	81.90	18.10	81.90	0.00	17.70	81.90	0.00	0.00	17.70	0.00	0.00
MS001-120	33.33	0.00	100.00	0.00	100.00	0.00	0.00	100.00	0.00	0.00	0.00	0.00	0.00
MS001-130	38.72	7.66	83.49	16.51	83.49	0.00	16.51	83.49	0.00	0.00	16.51	0.00	0.00

Table 4.10 *^{13}C-NMR sequence analysis and tacticity of MS002 and its TREF fractions*

Sample	P'	E'	P	E	PP	PE EP	EE	PPP	EPP PPE	EPE	EEE	EEP PEE	PEP
MS001-30	14.98	23.45	38.99	61.01	23.35	31.26	28.06	28.34	1.67	8.97	11.95	21.84	4.71
MS001-60	13.19	26.60	33.15	66.85	18.37	29.55	39.42	11.45	13.50	8.19	30.65	21.10	4.22
MS001-80	14.86	25.18	37.11	62.89	23.44	27.35	38.83	17.18	12.73	7.20	30.93	17.96	4.69
MS001-90	15.17	19.35	43.95	56.05	37.65	12.61	46.35	20.23	21.30	2.42	37.16	0.00	6.30
MS001-100	18.46	14.82	55.47	44.53	48.03	14.88	27.98	39.88	8.97	6.62	18.34	7.83	3.53
MS001-110	33.36	0.45	98.68	1.32	98.68	0.00	1.32	98.68	0.00	0.00	1.32	0.00	0.00
MS001-120	34.02	0.33	99.04	0.96	99.04	0.00	0.96	99.04	0.00	0.00	0.96	0.00	0.00
MS001-130	27.33	1.46	94.94	5.06	94.94	0.00	5.06	94.94	0.00	0.00	5.06	0.00	0.00

Table 4.11 *¹³C-NMR sequence analysis and tacticity of MS005 and its TREF fractions*

Sample	P'	E'	P	E	PP	PE EP	EE	PPP	EPP PPE	EPE	EEE	EEP PEE	PEP
MS001-30	15.16	23.51	39.20	60.80	23.46	31.48	28.60	25.07	3.29	10.83	15.64	21.77	4.86
MS001-60	13.37	22.70	37.06	62.94	23.08	27.95	37.44	19.31	10.01	7.74	29.06	19.20	4.37
MS001-80	11.98	23.39	33.88	66.12	24.96	17.85	48.63	22.02	5.85	6.02	41.36	11.55	3.15
MS001-90	13.55	25.22	34.95	65.05	26.30	17.30	49.48	30.98	0.00	3.96	41.69	10.38	3.46
MS001-100	23.26	36.35	39.02	60.98	34.34	9.36	34.38	32.26	2.76	4.00	7.20	4.85	2.26
MS001-110	32.56	0.58	98.26	1.74	98.26	0.00	1.74	98.26	0.00	0.00	1.74	0.00	0.00
MS001-120	40.97	8.99	82.01	17.99	82.01	0.00	17.17	78.92	3.09	0.00	17.17	0.00	0.00
MS001-130	37.33	9.52	79.68	20.32	78.35	2.66	17.76	77.12	2.56	0.00	17.76	1.86	0.40

Table 4.12 *¹³C-NMR sequence analysis and tacticity of MS006 and its TREF fractions*

Sample	P'	E'	P	E	PP	PE EP	EE	PPP	EPP PPE	EPE	EEE	EEP PEE	PEP
MS001-30	22.71	24.40	48.20	51.80	28.57	39.27	25.39	20.48	21.53	6.20	15.78	19.19	10.04
MS001-60	27.45	32.93	45.45	54.55	31.40	28.11	34.36	26.32	13.33	5.81	27.22	14.77	6.67
MS001-80	28.63	20.63	58.12	41.88	56.58	3.09	38.43	55.47	1.63	1.02	37.38	2.21	0.44
MS001-90	45.83	0.44	99.06	0.94	99.06	0.00	0.94	99.06	0.00	0.00	0.94	0.00	0.00
MS001-100	44.84	1.66	96.44	3.56	96.44	0.00	3.56	96.44	0.00	0.00	3.56	0.00	0.00
MS001-110	47.18	0.21	99.56	0.44	99.56	0.00	0.44	99.56	0.00	0.00	0.44	0.00	0.00
MS001-120	51.65	3.15	94.25	5.75	94.25	0.00	5.75	94.25	0.00	0.00	5.75	0.00	0.00
MS001-130	0.00	0.00	0.00	0.00	0.00	0.00	0.00	0.00	0.00	0.00	0.00	0.00	0.00

Table 4.13 *¹³C-NMR sequence analysis and tacticity of MS008 and its TREF fractions*

Sample	P'	E'	P	E	PP	PE EP	EE	PPP	EPP PPE	EPE	EEE	EEP PEE	PEP
MS001-30	24.27	27.21	47.14	52.86	29.20	35.90	23.69	22.86	20.54	3.75	14.72	22.86	6.52
MS001-60	23.21	29.19	44.29	55.71	33.59	21.40	38.77	31.79	8.22	4.29	32.26	12.00	4.70
MS001-80	21.16	26.42	44.47	55.53	39.93	9.08	45.98	39.02	3.67	1.79	42.19	6.26	1.41
MS001-90	37.91	5.10	88.14	11.86	87.43	1.42	9.53	88.14	0.00	0.00	8.38	0.53	0.44
MS001-100	46.38	0.43	99.08	0.92	99.08	0.00	0.87	98.27	0.81	0.00	0.80	0.00	0.00
MS001-110	48.38	0.00	100.00	0.00	100.00	0.00	0.00	97.50	2.50	0.00	0.00	0.00	0.00
MS001-120	68.72	0.00	100.00	0.00	100.00	0.00	0.00	100.00	0.00	0.00	0.00	0.00	0.00
MS001-130	0.00	0.00	0.00	0.00	0.00	0.00	0.00	0.00	0.00	0.00	0.00	0.00	0.00

From literature we know that TREF not only fractionates impact copolymers according to isotacticity of the polypropylene phase, but also according to the ethylene and propylene sequence lengths, or isotacticity sequence lengths [16]. Using the following relationships to determine the average number sequence lengths of the propylene and ethylene segments this can be confirmed. Table 4.14 gives a comparison of all samples.

$$\overline{n}_P = \frac{(PP) + \frac{1}{2}(PE)}{\frac{1}{2}(PE)} \qquad \textbf{(Eq 4.2)}$$

$$\overline{n}_E = \frac{(EE) + \frac{1}{2}(PE)}{\frac{1}{2}(PE)} \qquad \textbf{(Eq 4.3)}$$

Average sequences were not determined for certain fractions, since the amount of long ethylene (EEE) sequences is 0. The concentration of propylene and long propylene sequences (PPP) in these fractions are close to or actually become 100%, therefore it can be accepted that these fractions consists mainly of polypropylene homopolymer, in which case the average length of polypropylene sequences is expected to be infinite.

Table 4.14   *Number average sequence lengths of polypropylene and polyethylene*

Sample	MS001		MS002		MS005		MS006		MS008	
	n_E	n_P	n_E	n_P	n_E	n_P	n_E	n_P	n_E	n_P
30	2.56	2.26	2.79	2.49	2.82	2.49	2.29	2.46	2.32	2.63
60	9.27	2.61	3.67	2.24	3.68	2.65	3.45	3.23	4.62	4.14
80	6.66	5.13	3.84	2.71	6.45	3.80	25.91	37.67	11.13	9.80
90	8.56	6.06	8.35	6.97	6.72	4.04	n.d	n.d	14.44	124.28
100	6.16	5.29	4.76	7.45	8.34	8.33	n.d	n.d	n.d	n.d
110	n.d	n.d	n.d	n.d	n.d	n.d	n.d	n.d	n.d	n.d
120	n.d	n.d	n.d	n.d	n.d	n.d	n.d	n.d	n.d	n.d
130	n.d	n.d	n.d	n.d	14.38	60.01	n.d	n.d	n.d	n.d

n.d - not determined

n_E - Number average sequence length for polyethylene segments

n_P - Number average sequence length for polypropylene segments

In all samples the length of both ethylene and propylene increases with increasing elution temperature. However, for the samples prepared with Trigonox® 101 the sequence lengths of polypropylene approach infinity earlier than the corresponding samples produced with Trigonox® 301. The ethylene sequence lengths also approach zero at lower elution temperatures. These sections are indicative of the long ethylene and propylene sections that are linked and due to the nature of the in-situ gas phase polymerization process are classified as "blocky" copolymers. The long ethylene and propylene sequences with fair amounts of PE and EP junctions are crucial for good impact properties. Figure 4.27 below illustrates the difference between samples produced with Trigonox® 301 and Trigonox® 101 based on these EP and PE junction sequences. This clearly indicates that the molecular structure, and thus the physical properties, of the polymers differ when using different organic peroxides.
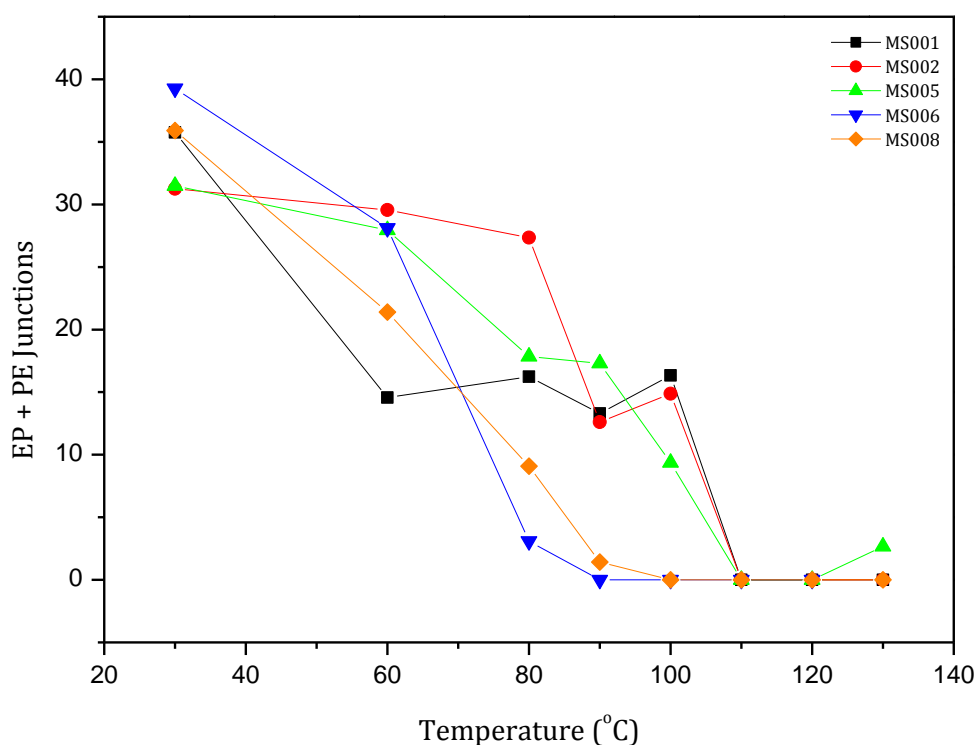
Figure 4.27   *Illustration of the PE and EP junctions for samples prepared with Trigonox® 101 and Trigonox® 301*

Figure 4.28 below also shows the difference in the long sequence propylene segments (PPP). Samples prepared with Trigonox® 301 show a much more gradual increase with increasing elution temperature, whereas those samples prepared with Trigonox® 101 shows a steep increase with increasing elution temperature.

More information on the NMR analysis of the TREF fractions can be found in Addendum C.1
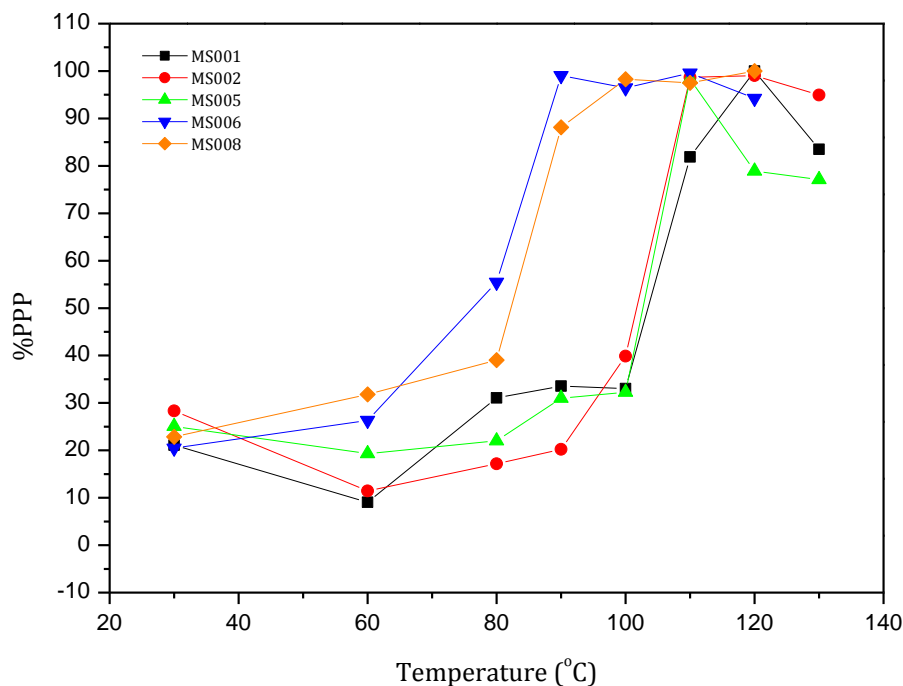
Figure 4.28   *Illustration of the %PPP segments for samples prepared with Trigonox® 101 and Trigonox® 301*

4.3.4   *Differential scanning calorimetry*

The DSC curves of the TREF fractions for all 5 samples are shown in Figure 4.29 and Figure 4.30. No melt endotherm is present in any of the 30 °C fractions. This, combined with the results obtained from ^{13}C NMR and FTIR, further proves that the 30 °C fraction of propylene-ethylene heterophasic copolymers consists out of atactic material and ethylene-propylene random copolymers. Multiple melting peaks can be observed for the mid-temperature fractions (60, 80, 90 and 100 °C). This indicates that there are both PE and PP crystallisable segments present in these fractions. The high-temperature fractions (> 110 °C) show one single melting endotherm peak in the region of 160 °C, which can be therefore be ascribed that these fractions consist predominantly out of isotactic PP. It is also seen that there is a steady increase in the peak temperatures for both components with increasing TREF elution temperature. This indicates an increase in lamellae thickness of both components. Peak areas are also seen to increase and we can therefore conclude that there is an increase in crystallinity with increasing TREF elution temperatures.

When looking at the data presented in Figure 4.29 - Figure 4.30 (exothermal is in the upwards direction and endothermal in the downwards direction) and listed in Table 4.15 it can be seen that both the visbroken samples exhibit crystallisation temperatures as well as melt temperatures that are lower than those observed in the non-visbroken sample. An increase in peak temperatures associated with increasing TREF temperature-elutions indicates an increase in lamellar thickness. The difference in the crystallisation temperatures between the visbroken and non-visbroken samples can therefore be ascribed to the fact that the visbroken samples have slightly lower overall lamellar thicknesses.

Results also show multiple melting DSC endotherms. This presence of multiple melting endotherms has been well documented and debated in literature [17-22]. According to various literature sources the multiple melting endotherms may be the result of different polymeric forms, melting or re-crystallisation behaviour, segregation by tacticity or molecular weight, melting of different regions in the crystal structure (i.e. radial or transverse lamellae) or simply the orientation effects of the polymer chains [17-19, 22].
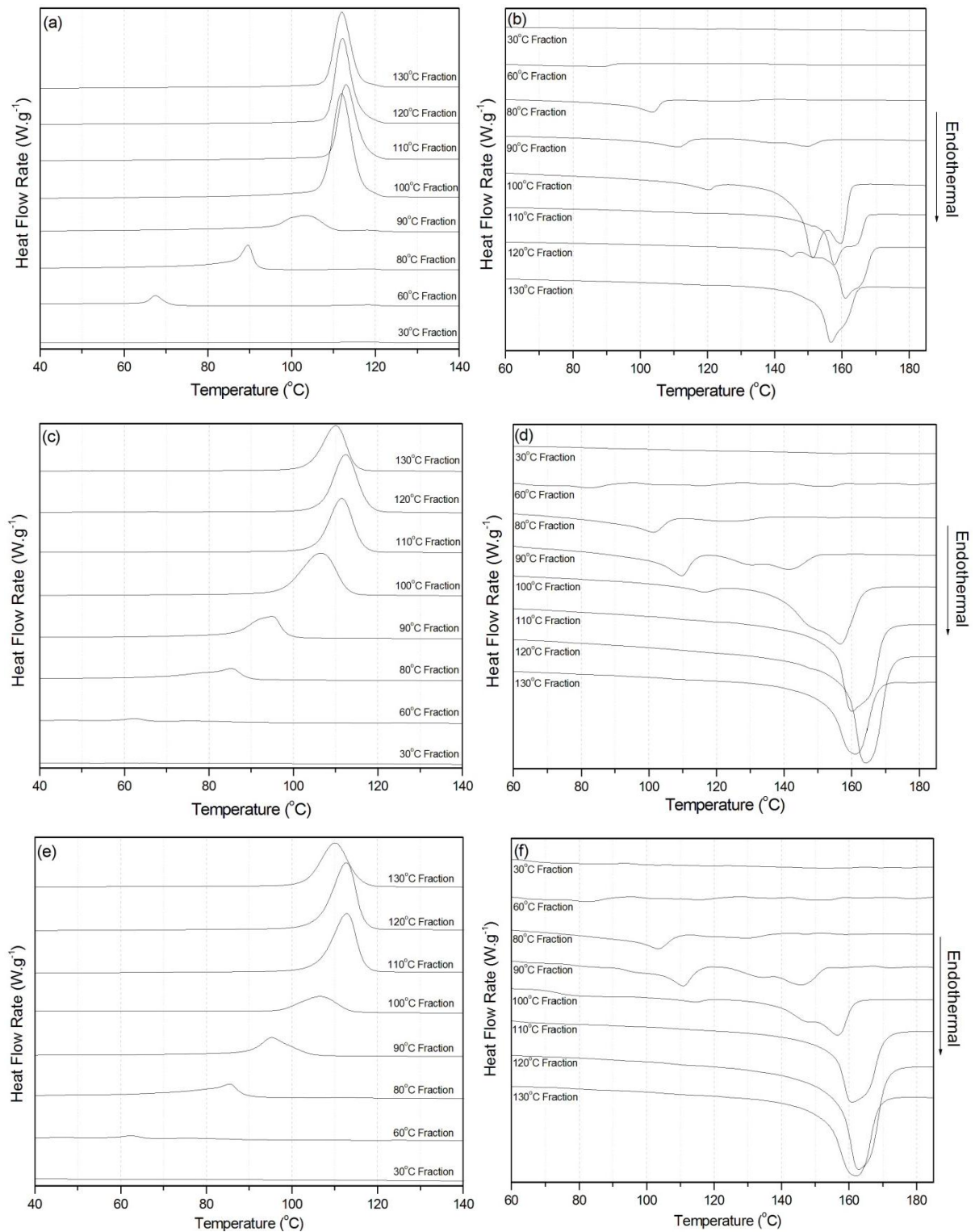
Figure 4.29   *DSC curves for MS001 (a and b), MS002 (c and d) and MS005 (e and f)*
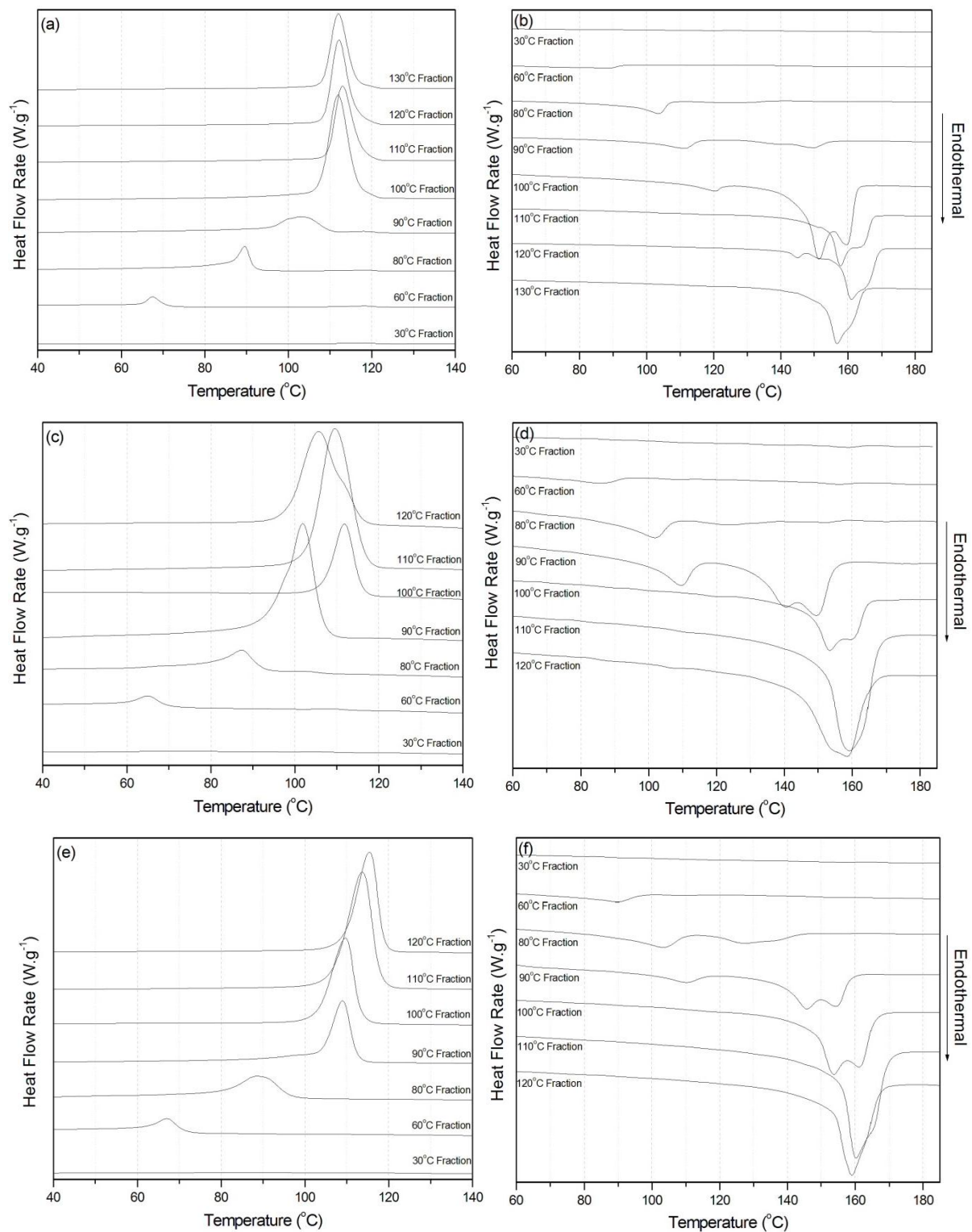
Figure 4.30   *DSC curves for MS001 (a and b), MS006 (c and d) and MS008 (e and f)*

Table 4.15 *DSC data of the bulk samples and their TREF fractions*

Sample	Fraction (°C)	T_c (°C)	T_m (°C)
MS001 Bulk Sample		122.03	115.13 / 167.00
MS001	30	-	-
	60	67.45	87.88
	80	89.43	103.49
	90	103.14	111.10 / 149.61
	100	111.82	120.44. / 151.46 / 159.46
	110	113.05	157.76 / 163.69
	120	112.10	144.88 / 161.32
	130	112.10	156.91
MS002 Bulk Sample		121.99	115.07 / 166.53
MS002	30	-	-
	60	62.02	81.79
	80	85.36	101.29 / 123.99
	90	95.13	109.57 / 130.10 / 141.12
	100	106.39	116.19 / 148.77 / 156.77
	110	111.41	160.28
	120	112.51	164.34
	130	10.05	160.79
MS001 Bulk Sample		121.75	113.74 / 165.60
MS005	30	-	-
	60	62.15	83.30
	80	85.51	103.31 / 129.78
	90	95.13	110.95 / 133.83 / 145.70
	100	106.39	114.34 / 147.56 / 156.73
	110	112.77	161.14
	120	112.77	163.00
	130	109.92	162.16
MS006 Bulk Sample		122.43	115.21/ 166.18
MS006	30	-	-
	60	64.48	85.95
	80	87.21	101.99
	90	101.99	149.38/ 140.07/ 109.35
	100	111.57	159.63/ 153.54
	110	109.67	159.64
	120	105.82	159.32
MS008 Bulk Sample		122.55	114.05/ 164.90
MS008	30	-	-
	60	66.75	89.79
	80	88.84	127.29/ 102.94
	90	109.35	154.49/ 145.54/ 109.98
	100	109.67	161.22/ 153.86
	110	113.51	160.27
	120	115.41	159.00

At this stage it has now been well established that not only does the amount of organic peroxide used during the visbreaking step influence the polymer's physical and molecular characteristics, but also the specific type of peroxide plays a key role in establishing these characteristics. To

maintain the focus of this investigation i.e. to study the effect of an organic peroxide on the molecular characteristics of heterophasic propylene-ethylene copolymers, it was decided to continue with a more detailed multi-component (or hyphenated) characterization approach while only investigating one organic peroxide and by so doing eliminate the variable that the type of peroxide has on the molecular characteristics of the copolymers. It should however be noted that this investigation should in future be expanded to include the influence of different organic peroxides.

4.3.5   *Fourier transform infrared spectroscopy (FTIR)*

FTIR analyses were performed on all three bulk samples together with their respective TREF fractions. The results of the data obtained for the non-visbroken MS001 sample is shown in Figure 4.31. Both MS002 and MS005 show similar profiles. The 100 °C fraction of MS001 does however show a doublet peak at 720–740 cm^{-1}, indicative of the presence of a crystalline polyethylene sequence, which is not seen for samples MS002 and MS005. It is known from literature [23, 24] that the absorptions 998 cm^{-1} and 841 cm^{-1} are caused by methyl-rocking vibrations associated with isotactic polypropylene, whereas the peak at 973 cm^{-1} can be associated with the methyl rocking vibrations of amorphous polypropylene. The band at 720 cm^{-1} is indicative of rocking vibrations of CH_2 sequences of more than 5. Low polyethylene crystallinity will cause the doublet at 730 cm^{-1} to exhibit a shoulder at 720 cm^{-1} [24]. From this data it can therefore be concluded that the 30 °C fractions consist mainly of ethylene-propylene random copolymer (EPR) due to the single band at 720 cm^{-1} and the absence or very weak bands at 998 cm^{-1} and 841 cm^{-1}. When looking at the mid-temperature fractions (i.e. 60, 80 and 90 °C) it can be seen that there is a steady increase in the weak band at 998 cm^{-1} as well as the doublet at 730 cm^{-1} indicating that propylene sequences have begun crystallizing and that there is an increase in crystallisable ethylene segments. These fractions therefore consist mainly out of propylene-ethylene segmented copolymers, as confirmed by NMR analysis. For the high temperature fractions (i.e > 100 °C) the bands at 720 cm^{-1} and 730 cm^{-1} are completely invisible (except for MS001 as discussed above), indicating that these fractions are nearly pure polypropylene. NMR analyses however, does indicate that very small amounts of EEE sequences do exist in some of these fractions. They are however believed to be too small to form crystallisable polyethylene.
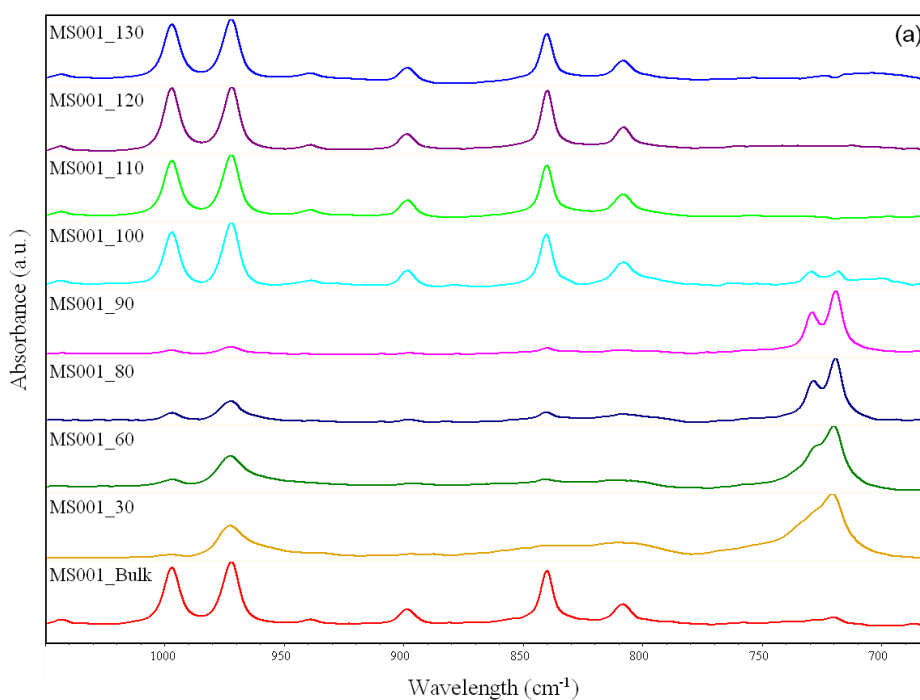
Figure 4.31   *FTIR spectra for the bulk MS001 sample and its TREF fractions*

Information gathered on MS002 and MS005 can be found in Addendum C.2

4.3.6   *Size exclusion chromatography (SEC)*

The molecular weight distributions of the TREF fractions for the three bulk samples are shown in Figure 4.32 (a-d) and Figure 4.33 (e-h). Similar to what was shown by De Goede et al. [25], the TREF fractions of all three samples exhibit the characteristic ethylene-propylene heterophasic copolymer molecular weight distributions. The high temperature fractions (100, 110, 120 and 130 °C) exhibit mono-modal molecular weight curves, whereas the mid temperature fractions (80 and 90 °C) have clear bi-modal distributions. The 30 °C and 60 °C fractions show a very slight shoulder at the higher molecular weight side. Bi-modal molecular weight distributions are indicative of compositional heterogeneity. This is due to the co-elution of non-identical products and is often seen in the mid-temperature elution fractions of heterophasic copolymers[26, 27].

Several interesting phenomena are observed when comparing the individual fractions of the three different samples. When looking at the 30 °C fraction it can be seen that the two visbroken samples not only have narrower molecular weight distributions, but that the molecular weight distribution has also shifted to lower molecular weights with increasing the visbreaking step.

This clearly indicates that the organic peroxide has a dramatic effect on the EPR and atactic components of the heterophasic copolymer. It can also be seen that the lower molecular weight portions of the 80 °C and 90 °C fractions are significantly altered. The low molecular weight component of the 80 °C fraction decreases with increasing the visbreaking step, whereas an increase with increasing the visbreaking step for the 90 °C fraction can be seen.

As it was established with NMR that these fractions contain ethylene and propylene sequences that are linked [25], more information is required before drawing a conclusion as to why these specific regions are influenced by the organic peroxide.
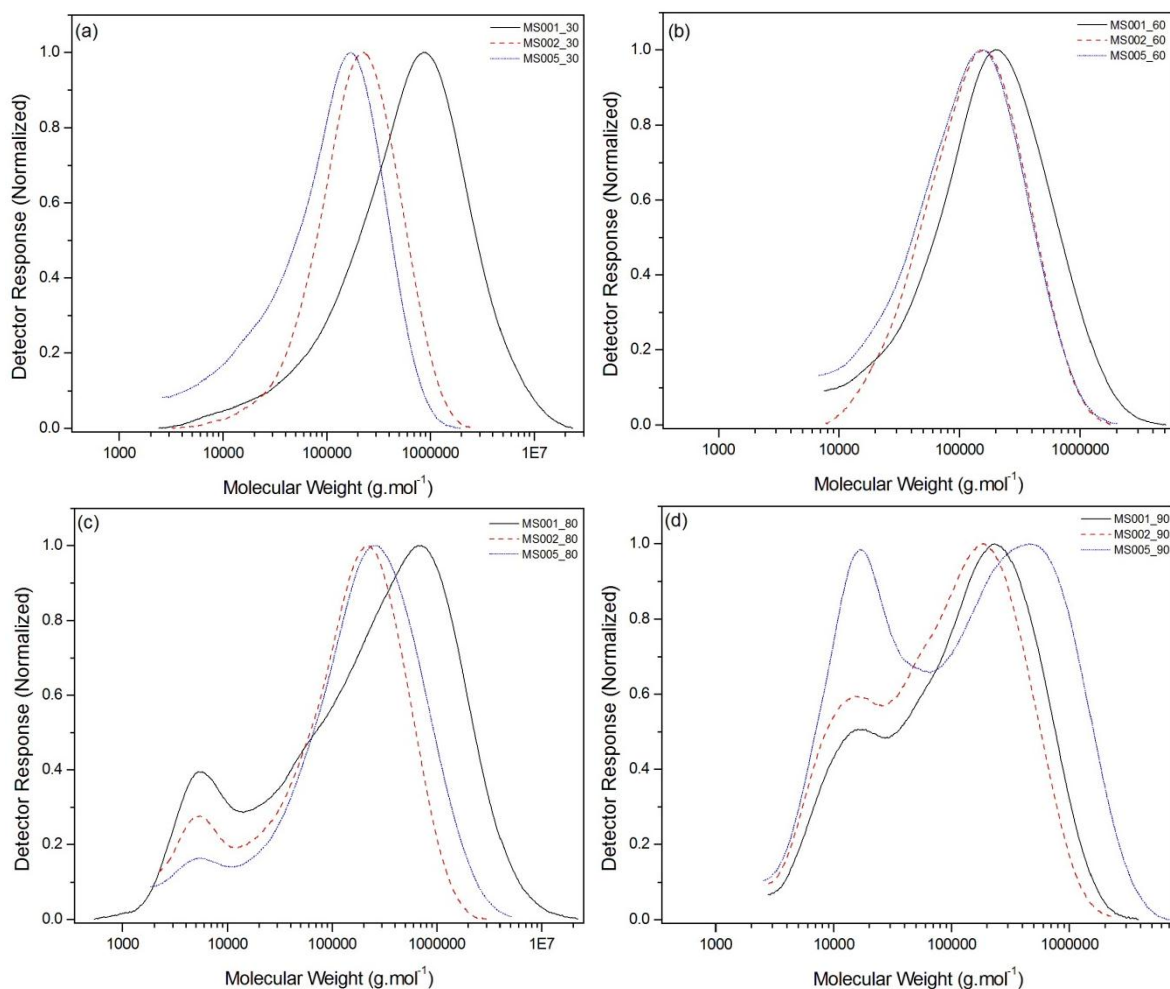
Figure 4.32   *SEC curves comparing the molecular weight distributions for the TREF fractions of the three bulk samples prepared with Trigonox ® 301.*
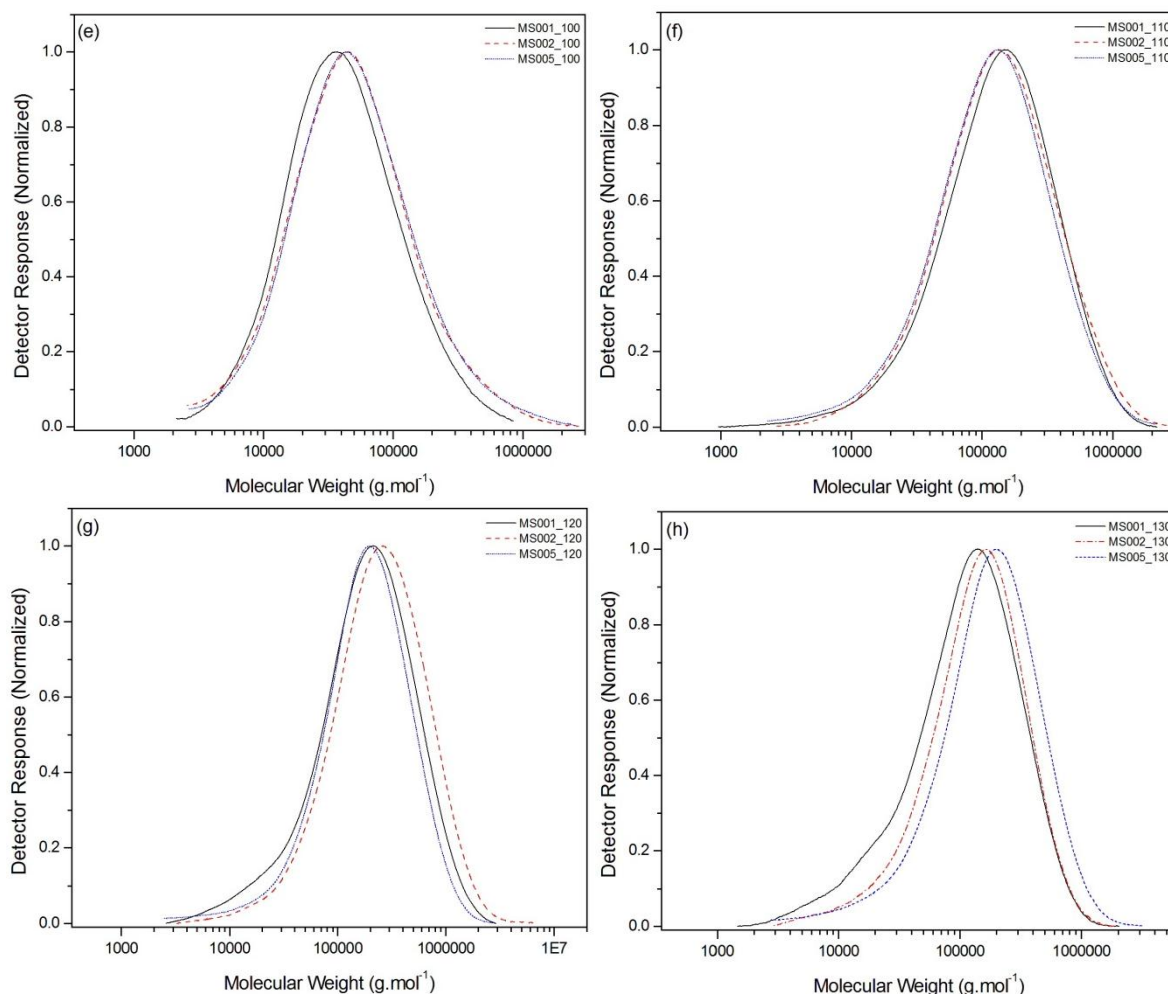
Figure 4.32   *SEC curves comparing the molecular weight distributions for the TREF fractions of the three bulk samples prepared with Trigonox ® 301.*

Similar results for all the TREF fractions for samples MS001, MS002 and MS005 can be found in Addendum C.3.

4.3.7 Size exclusion chromatography coupled to Fourier transform infrared spectroscopy via the LC transform interface (SEC-FTIR)

As TREF-SEC does not supply any information on the chemical heterogeneity of these TREF fractions, coupling the TREF-SEC via a LC transform interface to FTIR can be used to try and explain the anomalies observed with the results obtained from conventional TREF-SEC. The coupling of SEC to FTIR provides information on the propylene and ethylene content as well as their respective crystallinity distributions as a function of molecular weight. The 80 °C and 90 °C fractions were therefore analysed to investigate the differences seen as a result of visbreaking

in the HT-SEC data presented above. The SEC-FTIR analyses of these fractions are shown in Figures 4.33 – 4.35. Both 80 °C and 90 °C fractions for non-visbroken and visbroken samples show a steady increase in the CH_3/CH_2 ratio with increasing time and thus elution volumes (decreasing molecular weight). A slight decrease in the ratio is seen at approximately 23 min (23 mL). Correspondingly, it is found that at high molecular weights (low elution volumes) these fractions are rich in ethylene content, which steadily decreases to zero with decreasing molecular weight. It can therefore be concluded that the lower molecular weight component of the bi-modal distribution in these fraction consists mainly of propylene homopolymer, whereas the higher molecular weight component of these fractions consist of ethylene-propylene copolymer. According to Cheruthazhekatt et al. [28] crystalline polypropylene is found in the low molecular weight components of these heterophasic copolymers, while crystalline polyethylene or polyethylene segments of ethylene-propylene copolymers are found at high molecular weights.
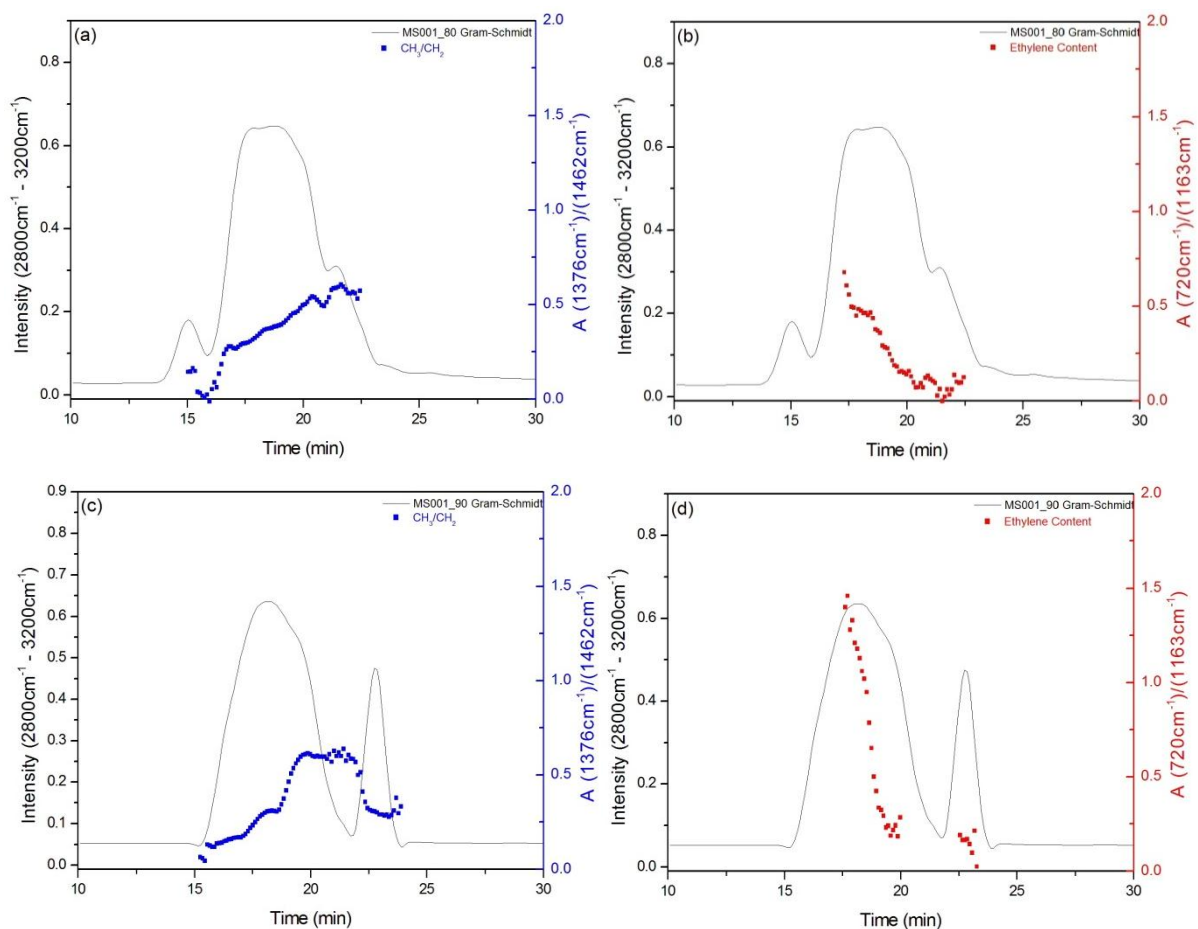
Figure 4.33   *SEC-FTIR analysis of MS001 illustrating the propylene content (a and c) and the ethylene content (b and d) as a function of molecular weight for the 80 °C and 90 °C fractions respectively.*
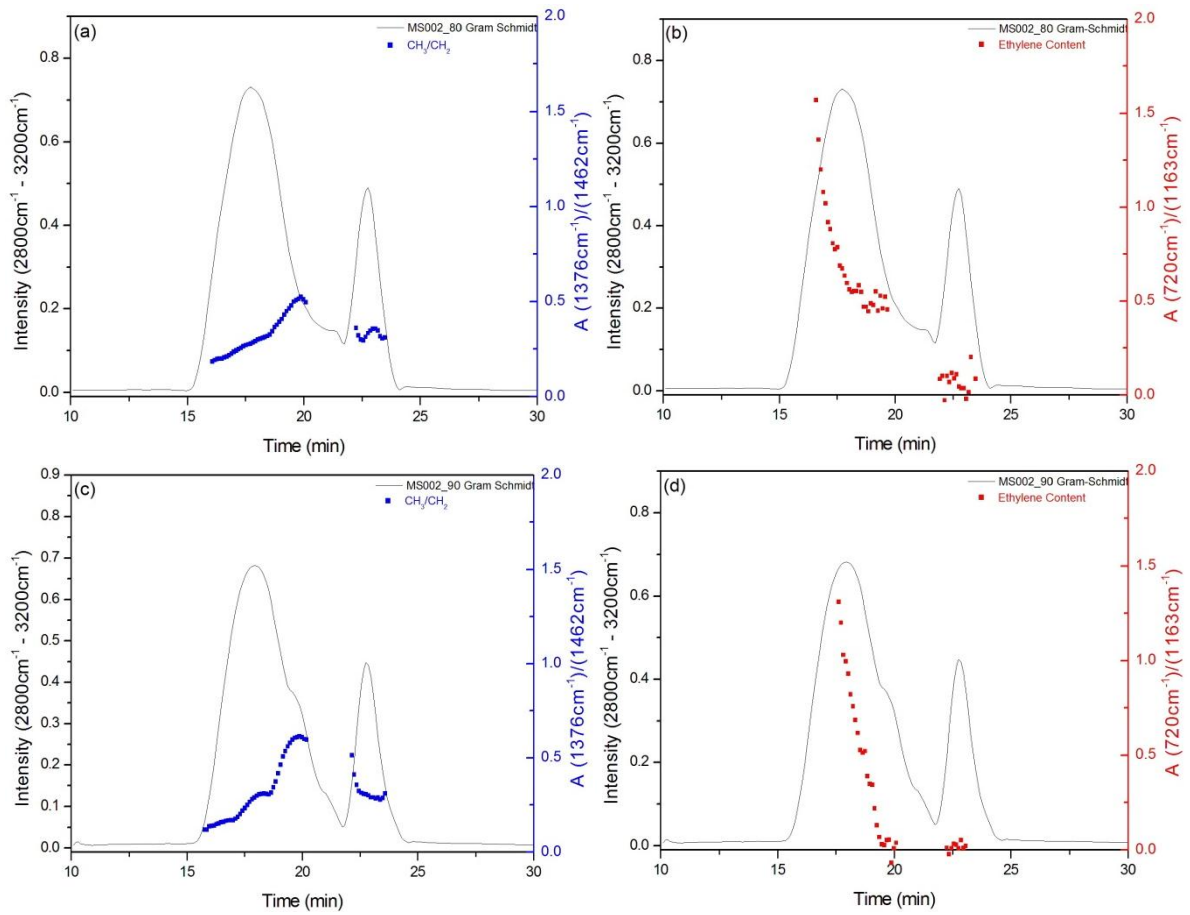
Figure 4.34   *SEC-FTIR analysis of MS002 illustrating the propylene content (a and c) and the ethylene content (b and d) as a function of molecular weight for the 80 °C and 90 °C fractions respectively.*
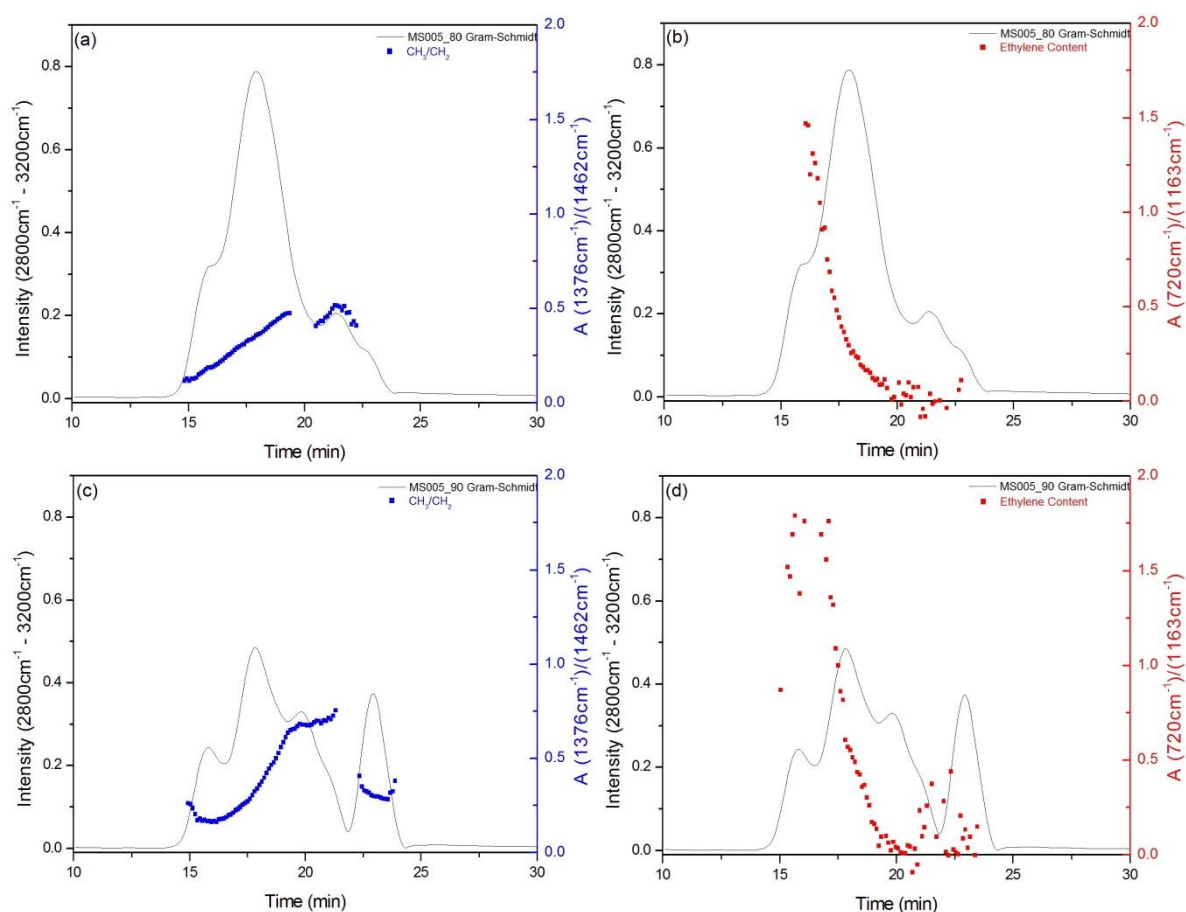
Figure 4.35   *SEC-FTIR analysis of MS005 illustrating the propylene content (a and c) and the ethylene content (b and d) as a function of molecular weight for the 80 °C and 90 °C fractions respectively.*

The full set of results for the three samples together with their corresponding TREF fractions can be found in Addendum C.4

4.3.8   *Gradient high temperature high performance liquid chromatography*

High temperature liquid chromatography has only recently been developed for the separation of polyolefins [29]. Initially zeolites were used to separate polyolefins according to their chemical composition, however, desorbing the various components from the column proved to be a problem [30, 31]. This work led to the development of a HT-HPLC method capable of separating polypropylene according to its tacticity in addition to separating it from polyethylene based on chemical composition [32]. Making use of the unique properties of a Hypercarb column and employing an adsorption-desorption method this technique swiftly and efficiently

separated polyolefins and olefin copolymers according to the chemical composition [28]. High Temperature High Performance Liquid Chromatography allows for the estimation of the chemical composition (CCD) in complex materials within a very short period of time.

The specific method used to analyse the propylene-ethylene heterophasic copolymers prepared is described in detail in Chapter 3 (Section 3.3.6). Initially it was attempted to analyse the bulk polymer samples. However, due to the extremely low concentration of phases other than the isotactic polypropylene, proper separation by chemical composition was not achieved. It was found that the bulk polymer samples elute in two regions. The first elutes in the 1-decanol phase while the second elutes at the start of the gradient. By using iPP standards it was found that all standards (except for very low molecular weight standards) elute in these two regions. It can therefore be concluded that the PP chains are partially retained by the column in the 1-decanol phase and are then desorbed during the gradient from 1-decanol to TCB [28]. Low molar mass components of the iPP elutes at approximately 1.1 mL – 1.4 mL in the 100% 1-decanol phase whereas the rest of the retained iPP elutes at approximately 3.1 mL – 3.5 mL when the gradient from 1-decanol to TCB has been started. This indicates that although the chemical composition is the primary parameter that governs the separation, the molar mass of the polymer also plays a role [28].

To try and achieve better separation using HT-HPLC the various TREF fractions of the corresponding bulk polymer samples were analysed. The results of the separation can be found in Table 4.16 (page 111). It can be seen that the more concentrated samples that resulted from the TREF analysis lead to very good separation of the various phases present in a typical propylene-ethylene heterophasic copolymer. Peaks were identified by using the work done by Cheruthazhekatt et al. [28] as a reference. Due to the very selective nature of the Hypercarb column with respect to chemical composition of polymers it can be seen that separation occurred differentiating even according to the polymer microstructure. The ethylene-propylene copolymer (also sometimes referred to as the "rubbery" part of the HECO polymer), as well as the polyethylene homopolymer fractions are fully retained due to selective adsorption on the column packing and only elute during the gradient section.

Using high temperature-2D-liquid chromatography (HT-2D-LC) to study the effects of molar mass of the components on the elution volume Cheruthazhekatt et al. [28] found that iPP has a lower molar mass component eluting in pure 1-decanol and a second higher molar mass component eluting in the gradient. While EPC with different ethylene and propylene sequences

as well as the pure PE homopolymer eluted according to the interaction with the Hypercarb column. A clear separation was seen between iPP and EPC copolymers and it was found that EPC dominated by longer propylene sequences eluted closer to the iPP while those dominated by longer ethylene sequences eluted closer to the PE homopolymer. In addition to finding similar results as described by Cheruthazhekatt et al. [28] some interesting phenomena were also observed when looking at the influence of the organic peroxide on the chemical composition of the heterophasic copolymers. When looking at Table 4.16 It can be seen that whilst the non visbroken and slightly visbroken (MS001 and MS002) samples mainly consist out of iPP, EPC and PE homopolymer in the 30 °C and 60 °C fractions, the highly visbroken sample (MS005) also shows the presence of amorphous HECO polymer fractions. For the 90 °C and 100 °C mid temperature fractions it can also be seen that the intensity of the iPP peaks at both low molar mass and high molar mass fractions tend to increase with increasing the visbreaking step. This is illustrated by Figure 4.36 and Figure 4.37 below. It is also shown that the high temperature fractions (i.e. 110 °C, 120 °C and 130 °C) consist purely of iPP. It is interesting to note however that for the highly visbroken sample the high temperature 120 °C fraction there is also a low molar mass component. This is not seen for the non visbroken and slightly visbroken cases.

This observations for MS005 correspond well with the observed particle size distribution data collected with SEM, that show a higher amount of small particle inclusions when compared to the non- and slightly visbroken samples.

The ethylene-propylene blocky/segmented copolymers, that constitute the bulk of the mid temperature fractions (i.e 60 °C – 100 °C) are crucial elements that improve the adhesion of the EPR phases (including amorphous and PE homopolymer) with that of the iPP matrix by acting as a compatibilizers between these phases. These fractions are thus crucial elements in the HECO polymer that affects the overall properties of the copolymers. This part of the investigation thus proved that HT-HPLC is able to provide crucial information on the chemical composition of different HECO polymers by not only being able to separate via chemical composition but also differentiating according to the polymer microstructure.

More results obtained during the HT-HPLC investigation, including the results obtained from the bulk HECO samples can be found in Addendum C.5.
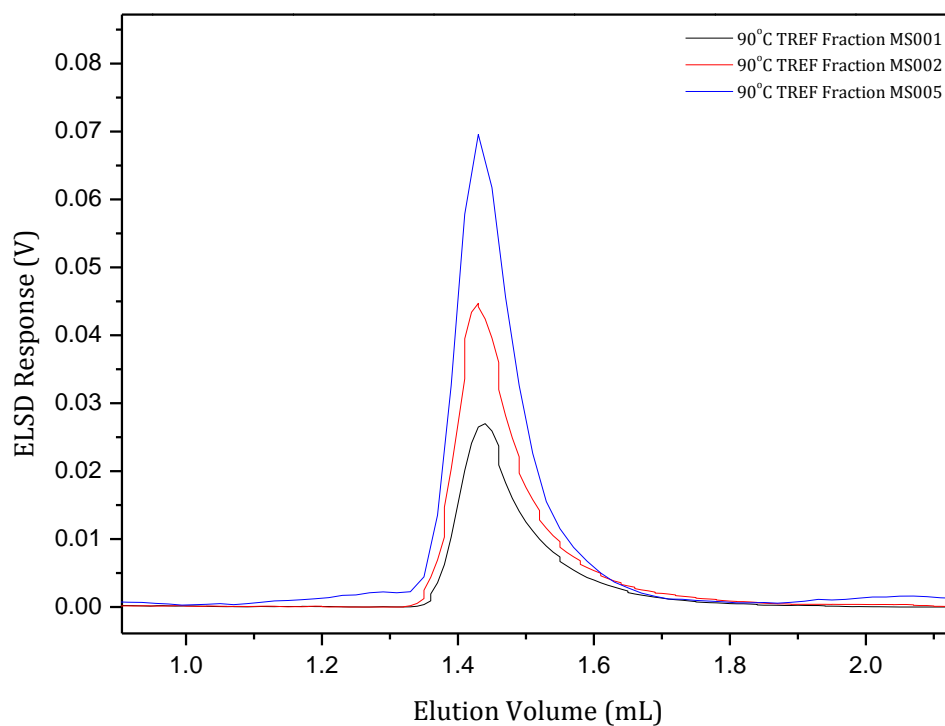
Figure 4.36   *HT-HPLC chromatograms illustrating differences in the isotactic polypropylene fraction (90 °C TREF Fraction) for samples prepared with Trigonox® 301*
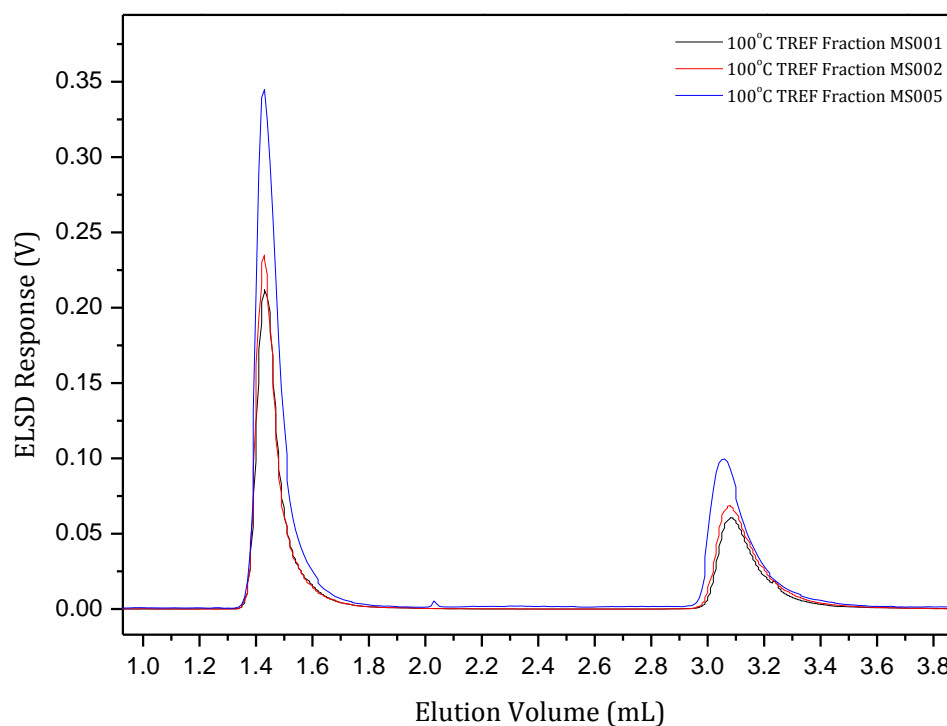
Figure 4.37   *HT-HPLC chromatograms illustrating differences in the isotactic polypropylene fraction (100 °C TREF Fraction) for samples prepared with Trigonox® 301*

Table 4.16 *Summary of Peak Elution Volumes, relative intensities and fraction identification for samples prepared with Trigonox® 301*

Temperature Fraction (°C)	Peak Elution Volume (mL)			ELSD Response (V)			Fraction Identification
	MS001	MS002	MS005	MS001	MS002	MS005	
30	-	1.0	1.2	-	0.01	0.01	amorphous HECO
	4.5	4.1	4.1	0.50	0.17	0.17	ethylene-propylene copolymer
60	1.1	1.1	1.4	0.01	0.01	0.02	isotactic polypropylene
	3.5	3.5	3.2	0.00	0.004	0.02	isotactic polypropylene
	-	-	3.5	-	-	0.02	ethylene-propylene copolymer
	-	-	4.2	-	-	0.02	amorphous HECO
	5.7	5.6	5.6	0.01	0.01	0.08	polyethylene homopolymer
80	1.4	1.4	1.4	0.05	0.01	0.06	isotactic polypropylene
	3.2	3.2	3.3	0.01	0.004	0.03	isotactic polypropylene
	-	-	3.7	-	-	0.02	ethylene-propylene copolymer
	-	-	4.3	-	-	0.02	amorphous HECO
	5.9	5.9	5.8	0.01	0.01	0.07	polyethylene homopolymer
90	1.4	1.4	1.4	0.03	0.04	0.07	isotactic polypropylene
	3.1	3.2	3.1	0.01	0.01	0.01	isotactic polypropylene
	6.1	-	6.1	0.00	-	0.01	polyethylene homopolymer
100	1.4	1.4	1.4	0.20	0.23	0.34	isotactic polypropylene
	3.1	3.1	3.1	0.06	0.07	0.10	isotactic polypropylene
110	1.4	1.4	1.4	0.06	0.17	0.13	isotactic polypropylene
	3.1	3.1	3.0	0.69	0.56	0.45	isotactic polypropylene
120	-	-	1.4	-	-	0.04	isotactic polypropylene
	3.1	3.1	3.0	0.57	0.44	0.63	isotactic polypropylene
130	3.1	3.1	3.1	0.36	0.64	0.55	isotactic polypropylene

4.4   Conclusions

It is clearly evident that the already complex structure and characteristics of propylene-ethylene heterophasic copolymers are further influenced by the use of an organic peroxide to induce visbreaking. Increasing the amount of peroxide added not only increased the MFR but also dramatically affects the physical properties of the polymer. With an increase in peroxide

concentration, there is a marked decrease in tensile modulus, stress at yield, as well as impact strength. It was also found that the decrease in stiffness seems to be more pronounced for samples prepared with Trigonox® 101 than for those prepared by Trigonox® 301. Samples prepared with Trigonox® 101 also show slightly lower impact resistance when compared to the Trigonox® 301 series. Both parallel plate and capillary rheology showed that there are clear differences in the polymer's molecular structure when visbroken with different organic peroxides. Samples prepared with Trigonox® 101 tend to show lower zero shear viscosity than those prepared with Trigonox® 301 with similar melt flow rates. SEM analysis showed that the "rubber" or "blocky" fractions of the HECO polymer (i.e. ethylene-propylene copolymer) are predominantly smaller than 1200nm. There is also a definite decrease in the average particle (or "rubber") sizes with an increase in the amount of visbreaking. For the highly visbroken grades the average "rubber" size shifted from 400 – 800 nm to, in some cases, more than 60% less than 400nm. Again a difference was seen in the particle size distribution when comparing samples prepared with Trigonox® 301 vs. Trigonox® 101. Whereas samples prepared with Trigonox® 301 still show some particles larger than 1200nm, highly visbroken samples prepared with Trigonox® 101 show none of these larger particles.

Analytical TREF, CRYSTAF and Preparative TREF all show that there is a definite difference in the polymer molecular structure with varying visbreaking steps as well as with the use of different peroxides.

Preparative-TREF analyses showed that to a large extent the high-temperature elution fractions are influenced, with the highly visbroken sample (MS005) showing a more even distribution by weight % eluted at 110 °C and 120 °C when compared to the non-visbroken (MS001) and slightly visbroken (MS002) samples. Differences can also be seen at the 30 °C elution fraction. As TREF fractionates according to crystallisability, this indicates that the visbreaking process has an effect on crystalline, semi-crystalline and amorphous parts of the polymer. NMR results indicate that fractionation is governed by a general decrease in co-monomer content as well as a general increase in isotacticity. NMR analyses further indicate differences in the long ethylene and propylene sequences (EEE and PPP) for the mid-temperature fractions (i.e. 60, 80, 90, 100 °C), with the two visbroken samples showing less long ethylene and propylene sequences and more EP junctions. It is well documented that segmented ethylene-propylene copolymers with long sequences act as compatibilizers that will enhance interfacial adhesion between random copolymer regions and propylene homopolymer regions and thereby leading to the enhanced impact strengths at low temperatures normally associated with PP/EPR copolymers [6, 7, 24]. It

can therefore be concluded that the addition of peroxide to induce visbreaking leads to the breakdown of these long sequences thus resulting in a decrease in impact strength. HT-SEC indicated that there is a general narrowing of the polydispersity with increasing peroxide concentration. HT-SEC further showed that the 80 °C and 90 °C fractions are dramatically altered with the low molecular weight portion of the 80 °C fractions decreasing with increasing peroxide concentration, whereas the same portion of the 90 °C is seen to increase with increasing peroxide concentration. As these two fractions have bi-modal distributions and therefore show compositional heterogeneity, further investigation is needed to determine the exact nature of effect of the peroxide concentration on these regions.

SEC-FTIR analyses showed that that the lower molecular weight component of the bi-modal distributions in these fractions consists mainly out of propylene homopolymer, whereas the higher molecular weight components of these fractions consist out of ethylene-propylene copolymer. It can thus be concluded that the peroxide mainly affects the propylene homopolymer in these fractions. DSC analysis indicated that both the visbroken samples exhibit crystallisation temperatures that are lower than those observed in the non-visbroken sample. An increase in peak temperatures associated with increasing TREF temperature-elutions indicates an increase in lamellar thickness. The difference in the crystallisation temperatures between the visbroken and non-visbroken samples can therefore be ascribed to the fact that the visbroken samples have slightly lower overall lamellar thicknesses. The detailed analysis of the heterophasic copolymer indicates that the organic peroxide acts across all compositions of the multiphase copolymer, influencing each phase in a unique way and thereby contributing to the overall molecular structure and properties observed.

By making use of HT-HPLC, using Hypercarb column and employing an adsorption-desorption method this technique swiftly and efficiently separated polyolefins and olefin copolymers according to the chemical composition. It was found that due to the extremely low concentration of phases other than the isotactic polypropylene, proper separation by chemical composition of the bulk HECO polymer samples could not be achieved. However, by making use of preparative TREF to separate the HECO polymer into various fractions according to their crystallinity and then subsequently running the more concentrated fractions of the HECO polymer, good separation according to chemical composition and even polymer microstructure was achieved. It was thus proven that HT-HPLC is able to provide crucial information on the chemical composition of different HECO polymers by not only being able to separate via chemical composition but also differentiating according to the polymer microstructure.

4.5   References

1.   D'Orazio L, Cecchin G. Isotactic polypropylene/ethylene-co-propylene blends: effects of composition on rheology, morphology and properties of injection moulded samples. Polymer 2001:42(6):2675-2684.

2.   Fu Z, Fan Z, Zhang Y, Feng L. Structure and morphology of polypropylene/poly(ethylene-co-propylene) in situ blends synthesized by spherical Ziegler–Natta catalyst. European Polymer Journal 2003:39:795-804.

3.   Hongjun C, Xiaolie L, Xiangxu C, Dezhu M, Jianmin W, Hongsheng T. Structure and properties of impact copolymer polypropylene. II. Phase structure and crystalline morphology. Journal of Applied Polymer Science 1999:71(1):103-113.

4.   Hongjun C, Xiaolie L, Dezhu M, Jianmin W, Hongsheng T. Structure and properties of impact copolymer polypropylene. I. Chain structure. Journal of Applied Polymer Science 1999:71(1):93-101.

5.   Lieberman R, Stewart C. Encyclopedia of Polymer Science and Technology: Propylene Polymers. John Wiley & Sons, Inc., 2002.

6.   Tan H, Li L, Chen Z, Song Y, Zheng Q. Phase morphology and impact toughness of impact polypropylene copolymer. Polymer 2005:46(10):3522-3527.

7.   Feng Y, Hay JN. The measurement of compositional heterogeneity in a propylene-ethylene block copolymer. Polymer 1998:39(26):6723-6731.

8.   Silvestre C, Cimmino S, Triolo R. Structure, morphology and crystallization of a random ethylene-propylene copolymer. Journal of Applied Polymer Science: Part B: Polymer Physics 2002:41:493-500.

9.   Lamberti G, Peters GWM, Titomanlio G. Crystallinity and the Linear Rheologal Properties of Polymers. Internal Polymer Processing 2007:3.

10.   Wang S, Yang D. Effect of copolymerized ethylene unit on the crystallization behaviour of poly(propylene-co-ethylene)s. Polymer 2004:45.

11.   Harding G. The Fractionation and Characterization of propylene-ethylene random copolymers. Stellenbosch: University of Stellenbosch, 2005.

12.   Ray GJ, Johnson PE, Knox JR. Carbon-13 Nuclear Magnetic Resonance Determination of Monomer Composition and Sequence Distribution in Ethylene-Propylene Copolymers Prepared with a Stereoregular Catalyst System. Macromolecules 1977:10(4):773-778.

13.   Randall JC. A 13C NMR Determination of the Comonomer Sequence Distributions in Propylene-Butene-1 Copolymers. Macromolecules 1978:11(3):592-597.

14.   Viville P, Daoust D, Jonas AM, Nysten B, Legras R, Dupire M, Michel J, Debras G. Characterization of the molecular structure of two highly isotactic polypropylenes. Polymer 2001:42(5):1953-1967.

15.   Randall JC. Methylene Sequence Distributions and Number Average Sequence Lengths in Ethylene-Propylene Copolymers. Macromolecules 1978:11(1):33-36.

16.   Liu Y, Bo S, Zhu Y, Zhang W. Studies on the intermolecular structural heterogeneity of a propylene-ethylene random copolymer using preparative temperature rising elution fractionation. Journal of Applied Polymer Science 2005:97(1):232-239.

17.   Phillips RA, Wolkowicz MD. Structure and Morphology, Polypropylene Handbook. Munich: Hanser, 2002.

18.   Huang TW, Alamo RG, Mandelkern L. Fusion of isotactic poly(propylene). Macrmolecules 1999:32.

19.   Alamo RG, Brown GM, Mandelkern L, Lehtinen A, Paukkeri R. A morphological studyt of a highly structurally regular isotactic poly(propylene) fraction. Polymer 1999:40.

20.   Paukkeri R, Lehtinen A. Thermal behaviour of polypropylene fractions: 2. The multiple melting peaks. Polymer 1993:34(19).

21.   Bartczak Z, Chiono V, Pracella M. Blends of propylene-ethylene and propylene-1-butene random copolymers: I Morphology and structure. Polymer 2004:45.

22.   Zhang M, Gong Y, He T. Multiple melting behaviour of isotactic polypropylene and poly(propylene-co-ethylene) after stepwise isothermal crystallization. European Polymer Journal 2003:39.

23.   Fan Z, Zhang Y, Xu J, Wang H, Feng L. Structure and properties of polypropylene/poly(ethylene-co-propylene) in-situ blends synthesized by spherical Ziegler-Natta catalyst. Polymer 2001:42(13):5559-5566.

24.   Xue Y, Fan Y, Bo S, Ji X. Characterization of the microstructure of impact polypropylene alloys by preparative temperature rising elution fractionation. Eur Polym J 2011:47(8):1646-1653.

25.   De Goede E, Mallon P, Pasch H. Fractionation and Analysis of an Impact Poly(propylene) Copolymer by TREF and SEC-FTIR. Macromol Mater Eng 2010:295(4):366-373.

26.   Zacur R, Goizueta G, Capiati N. Dispersed phase morphology of impact PP copolymers. Effects of blend composition as determined by TREF. Polymer Engineering & Science 2000:40(8):1921-1930.

27.   Zacur R, Goizueta G, Capiati N. Polypropylene reactor blends: composition evaluation by analytical TREF. Polymer Engineering and Science 1999:39(5):921-929.

28.   Cheruthazhekatt S, Pijpers TFJ, Harding GW, Mathot VBF, Pasch H. Multidimensional Analysis of the Complex Composition of Impact Polypropylene Copolymers: Combination of TREF, SEC-FTIR-HPer DSC, and High Temperature 2D-LC. Macromolecules 2012.

29.   Pasch H, Brüll A, Cabrera K. Fast HPLC analysis of poly(ethylene oxide)s for high-throughput experimentation. e-Polymers 2005:20.

30.   Macko T, Pasch H, Kazakevich YV, Fadeev AY. Elution behavior of polyethylene in polar mobile phases on a non-polar sorbent. Journal of Chromatography A 2003:988(1):69-76.

31.   Macko T, Pasch H, Brull R. Selective removal of polyethylene or polypropylene from their blends based on difference in their adsorption behaviour. A Journal of Chromatography 2006:1115:81-87.

32.   Macko T, Pasch H, Wang Y. Liquid Chromatographic Separation of Olefin Oligomers and its Relation to Separation of Polyolefins – an Overview. Macromolecular Symposia 2009:282(1):93-100.

Chapter 5

Synopsis and Conclusions

In this chapter the overall conclusions are articulated and discussed. Together with this discussion certain recommendations for future work in this field of study are also proposed.

5.1   Synopsis, conclusions and recommendations for future work

As stated in Chapter 1 (Section 1.2) the main objective of this study was to determine if there were any differences in the molecular structure and physical properties of controlled rheology grades of propylene-ethylene heterophasic copolymers and if differences did exist, what they were and how did they influence the overall properties of these types of polymers. A secondary objective of this study was also to determine if there are any differences in the molecular structure of HECO polymers based on the type of organic peroxide used to facilitate the controlled rheology process.

The investigation into the mechanical and physical properties of the prepared samples indicated several interesting phenomena. It was seen that the stiffness of almost all samples decreased with increasing visbreaking. The decrease in stiffness was found to be more pronounced for samples prepared with Trigonox® 101 than from those prepared with Trigonox® 301. This observation immediately indicated that Trigonox® 101 interacts more with the crystalline region of the HECO polymer than Trigonox® 301. Data collected from impact resistance studies further also indicated that samples prepared with Trigonox® 101 showed lower impact resistance than samples prepared with Trigonox® 301. Rheology studies also showed that samples prepared with Trigonox® 101 have lower zero shear viscosities.

Scanning Electron Microscopy on cryo-fractured sample specimens showed that there is a general decrease in the average particle size of the EPC or "rubbery" phases with increased visbreaking. It was determined that more than 50% of the particles for highly visbroken samples were smaller than 400 nm. This phenomenon corresponded well with data collected regarding the impact resistance of the samples, as smaller EPC or "rubber" particles will tend to absorb less energy than larger particles. It was also determined that samples prepared with Trigonox® 101 showed notably smaller average particle sizes than samples prepared with Trigonox® 301 and that samples prepared with Trigonox® 101 also showed a larger decrease in the average particle size with increased visbreaking. The results obtained from the SEM investigation therefore showed that the organic peroxide not only interacts with the crystalline regions of the HECO polymer (as was established earlier) but that it also interacts with the EPC region/phase.

Analytical TREF showed that with an increase in the visbreaking step there is a corresponding decrease in the peak elution temperature in the higher temperature region. Polymer eluting in the higher temperature region consists mainly out of isotactic polypropylene. Again the shift in

the peak elution temperature towards lower temperatures was more pronounced for samples prepared with Trigonox® 101 than for samples prepared with Trigonox® 301. This further reinforces the results seen earlier regarding that Trigonox® 101 interacts more with the crystalline parts of the HECO polymer than Trigonox® 301 does. Early on in the study it was therefore evident that the visbreaking process plays a significant role in the molecular structure of the HECO polymer and that the size of the visbreaking step also leads to molecular restructuring of the polymer.

CRYSTAF results indicated that for both types of peroxide there was a considerably narrower crystallisation peak commencing at a significantly lower temperature as the extent of visbreaking increases. The changes seen in the main crystallisable fraction was accompanied with subtle changes in the soluble fraction.

Preparative TREF showed similar trends than those observed during the analytical TREF investigation. In addition to the changes already highlighted above it was also noted that the MS005 polymer had a broadening of the "crystalline peak" and a shift to a lower temperature. For the Trigonox® 101 samples this shift resulted in a narrower fraction, thus indicating a significant attack on the more crystalline areas of the polymer. Several other conclusions can be made from the NMR analysis of the collected TREF fractions:

i.   There is an initial increase followed by a decrease in the ethylene content with increasing temperature. The decrease for samples prepared with Trigonox® 301 can be seen as early as at 60 °C whereas samples prepared with Trigonox® 101 only show decreases after approximately 80 °C.

ii. Samples prepared with Trigonox® 301 show long ethylene sequences at high temperatures whereas these sequences are absent at high temperatures for samples prepared with Trigonox® 101. Together with the above observation it is also noted that the propylene content and isotacticity is seen to increase with increase elution temperatures. This indicates that the fractionation is governed mainly by decreasing co-monomer content and increasing isotacticity.

iii. The main elution peak (established as isotactic polypropylene) elutes at approximately 120 °C for samples prepared with Trigonox® 301 and at approximately 110 °C for samples prepared with Trigonox® 101.

iv.   PE + EP junction sequences are seen up to fractions that eluted at 100 °C for samples prepared with Trigonox® 301 but only up to 80 °C for samples prepared with Trigonox® 101.

v.   In all samples the length of both ethylene and propylene increases with increasing elution temperature. However, for the samples prepared with Trigonox® 101 the sequence lengths of polypropylene approach infinity earlier than the corresponding samples produced with Trigonox® 301. The ethylene sequence lengths also approach zero at lower elution temperatures. These sections are indicative of the long ethylene and propylene sections that are linked and due to the nature of the in-situ gas phase polymerization process are classified as "blocky" copolymers. The long ethylene and propylene sequences with fair amounts of PE and EP junctions are crucial for good impact properties

At this stage of the study it was well established that not only does the amount of organic peroxide used during the visbreaking step influence the polymers physical and molecular characteristics, but also the specific type of peroxide plays a key role in establishing these characteristics.

Further investigation into the molecular weights of the TREF fractions for samples prepared with Trigonox® 301 also yielded interesting observations. It was found that the 30 °C fractions of the two visbroken samples have not only narrower molecular weight distributions but that the molecular weight distribution has also shifted to lower molecular weights with increasing the visbreaking step. This clearly indicated that the organic peroxide had a dramatic effect on the EPR and atactic components of the heterophasic copolymer. It was also found that the lower molecular weight portions of the 80 °C and 90 °C fractions were significantly altered. The low molecular weight component of the 80 °C fraction decreases with increasing the visbreaking step, whereas an increase with increasing the visbreaking step for the 90 °C fraction was seen. TREF-SEC does not supply any information on the chemical heterogeneity of these TREF fractions and to try and explain these anomalies TREF-SEC was coupled via a LC transform interface to FTIR.

Coupling SEC to FTIR provided information on the propylene and ethylene content as well as their respective crystallinity distributions as a function of molecular weight. The following observations were made:

    i.   Both 80 °C and 90 °C fractions for non-visbroken and visbroken samples show a steady increase in the CH_3/CH_2 ratio with increasing time and thus elution volumes (decreasing molecular weight).

    ii.   It is found that at high molecular weights (low elution volumes) the 80 °C and 90 °C are rich in ethylene content, which steadily decreases to zero with decreasing molecular weight. It can therefore be concluded that the lower molecular weight component of the bi-modal distribution in these fractions consist mainly of propylene homopolymer, whereas the higher molecular weight component of these fractions consist of ethylene-propylene copolymer.

It can therefore be concluded that the altered molecular weight distributions seen for the 80 °C and 90 °C fractions during the SEC investigation is due to the fact that with increased visbreaking the amount of isotactic polypropylene decreases in the 80 °C fraction but increases in the 90 °C fraction.

HT-HPLC was successfully used to characterize the prepared HECO polymers according to their tacticity in addition to separating it from polyethylene based on chemical composition. Due to the very selective nature of the Hypercarb column with respect to chemical composition of polymers it found that separation occurred differentiating even according to the polymer microstructure. The ethylene-propylene copolymer (also sometimes referred to as the "rubbery" part of the HECO polymer), as well as the polyethylene homopolymer fractions were fully retained due to selective adsorption on the column packing and only eluted during the gradient section. A clear separation was seen between iPP (isotactic polypropylene) and EPC copolymers and it was found that EPC dominated by longer propylene sequences eluted closer to the iPP while those dominated by longer ethylene sequences eluted closer to the PE homopolymer.

HT-HPLC enabled the observation of some interesting phenomena when looking at the influence of the organic peroxide on the chemical composition of the heterophasic copolymers. It was found that whilst the non visbroken and slightly visbroken (MS001 and MS002) samples mainly consist out of iPP, EPC and PE homopolymer in the 30 °C and 60 °C fractions, the highly visbroken sample (MS005) also shows the presence of amorphous HECO polymer fractions. For the 90 °C and 100 °C mid temperature fractions it was found that the intensity of the iPP peaks at both low molar mass and high molar mass fractions tend to increase with increasing the

visbreaking step. It was also shown that the high temperature fractions (i.e. 110 °C, 120 °C and 130 °C) consist purely of iPP.

The ethylene-propylene blocky/segmented copolymers, that constitute the bulk of the mid temperature fractions (i.e 60 °C – 100 °C) are crucial elements that improve the adhesion of the EPR phases (including amorphous and PE homopolymer) with that of the iPP matrix by acting as a compatibilizers between these phases. These fractions are thus crucial elements in the HECO polymer that affects the overall properties of the copolymers. This part of the investigation thus proved that HT-HPLC is able to provide crucial information on the chemical composition of different HECO polymers by not only being able to separate via chemical composition but also differentiating according to the polymer microstructure.

It can finally then be concluded that the amount of visbreaking notably alters the molecular structure of the HECO polymers and subsequently also the physical properties and characteristics of these polymers. It can further also be concluded that the specific type of organic peroxide used to facilitate the controlled rheology has a definite effect on the specific molecular structure of the HECO polymer and that all things being equal, using different organic peroxides may not always lead to the same physical properties and characteristics. It is therefore recommended that more work is required to understand why specific organic peroxides influence or interact differently with the various phases of HECO polymers and how the characteristics of the type of peroxide can be utilized to obtain a HECO polymer with optimal and desired properties.

Addendum A
Scanning Electron Microscopy

This addendum contains graphs and other data collected during the physical investigation of the bulk propylene-ethylene heterophasic copolymer samples. Data for the Scanning Electron Microscopy investigation is presented.

Addendum A.1: Scanning electron microscopy
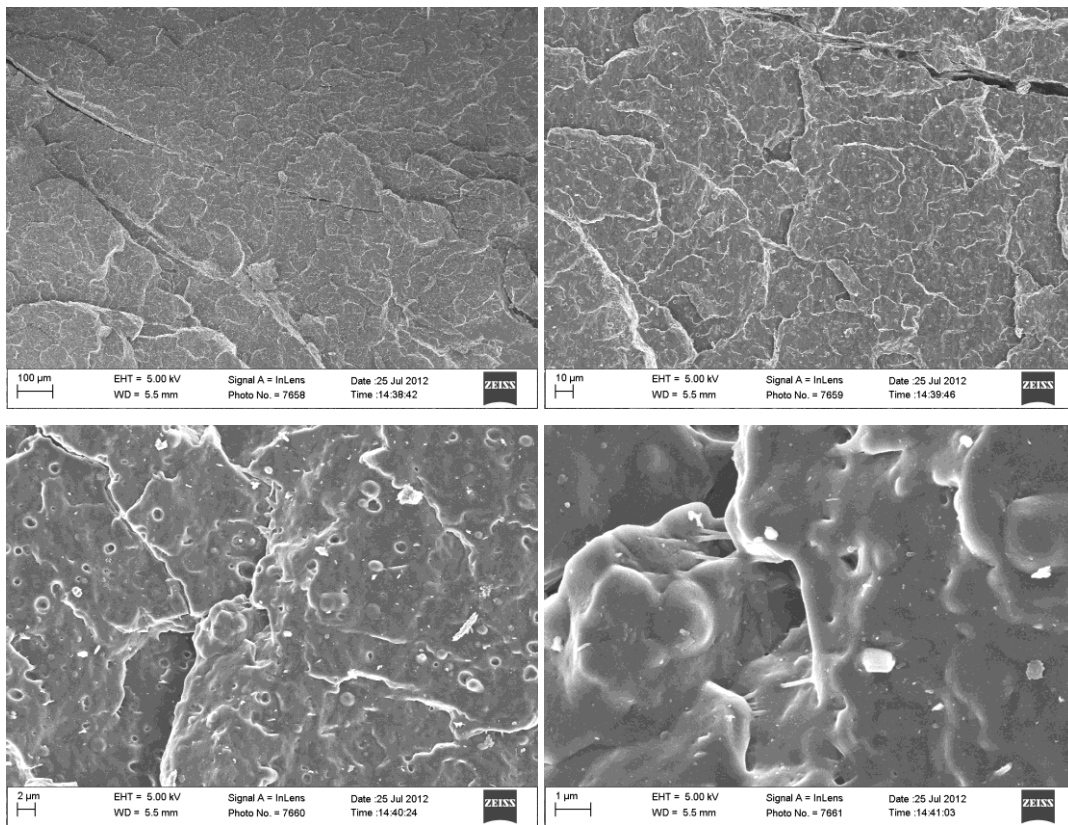
Figure A.1   *SEM micrograms at different magnifications of MS001*
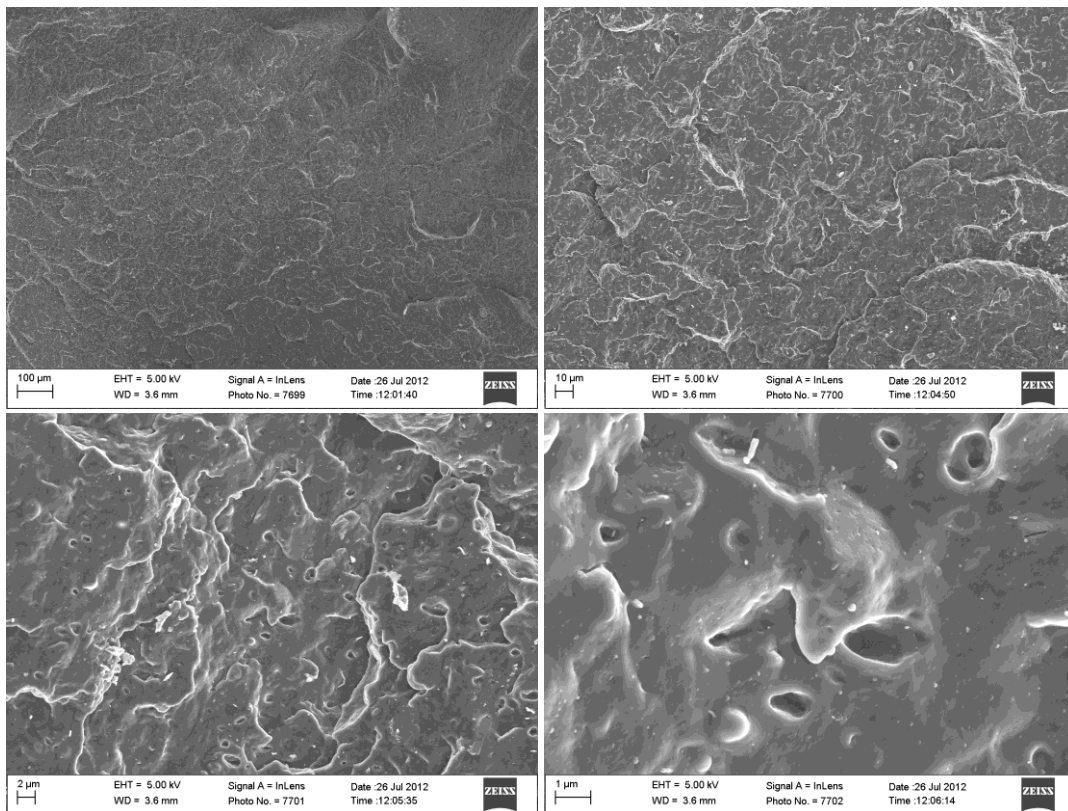
Figure A.2   *SEM micrograms at different magnifications of MS002*
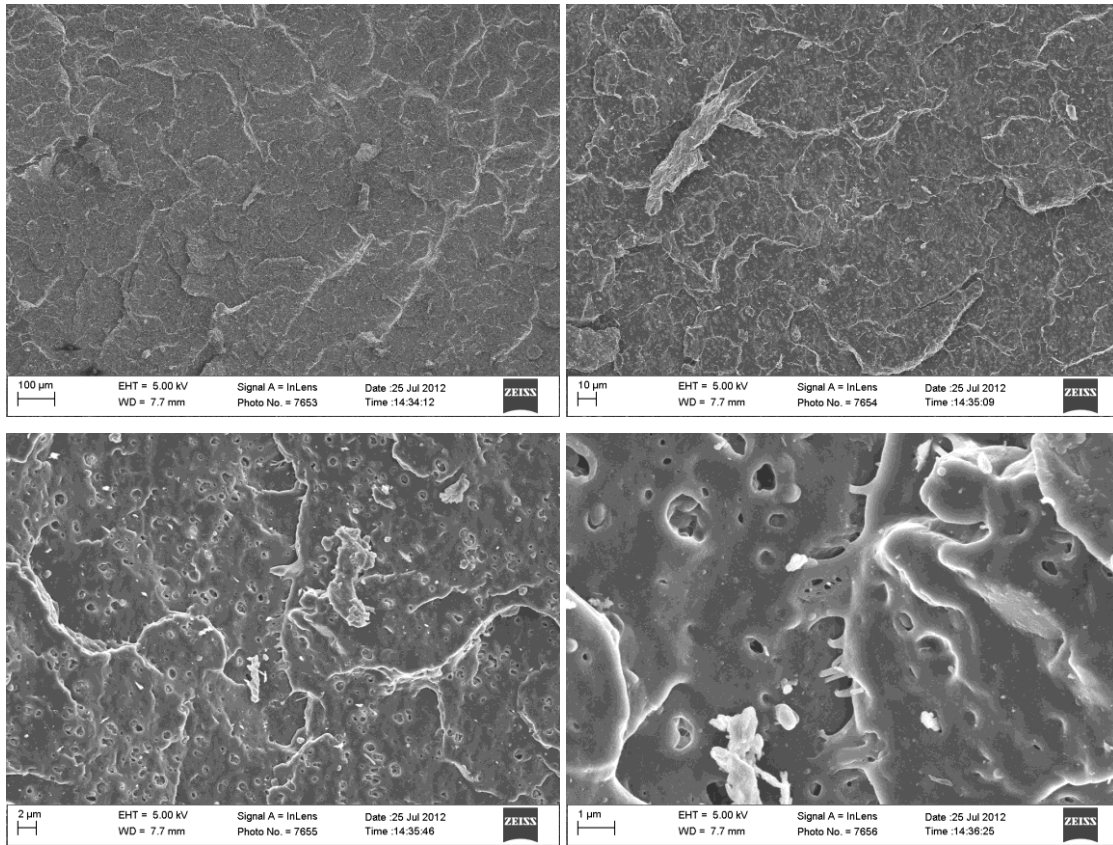
Figure A.3   *SEM micrograms at different magnifications of MS003*
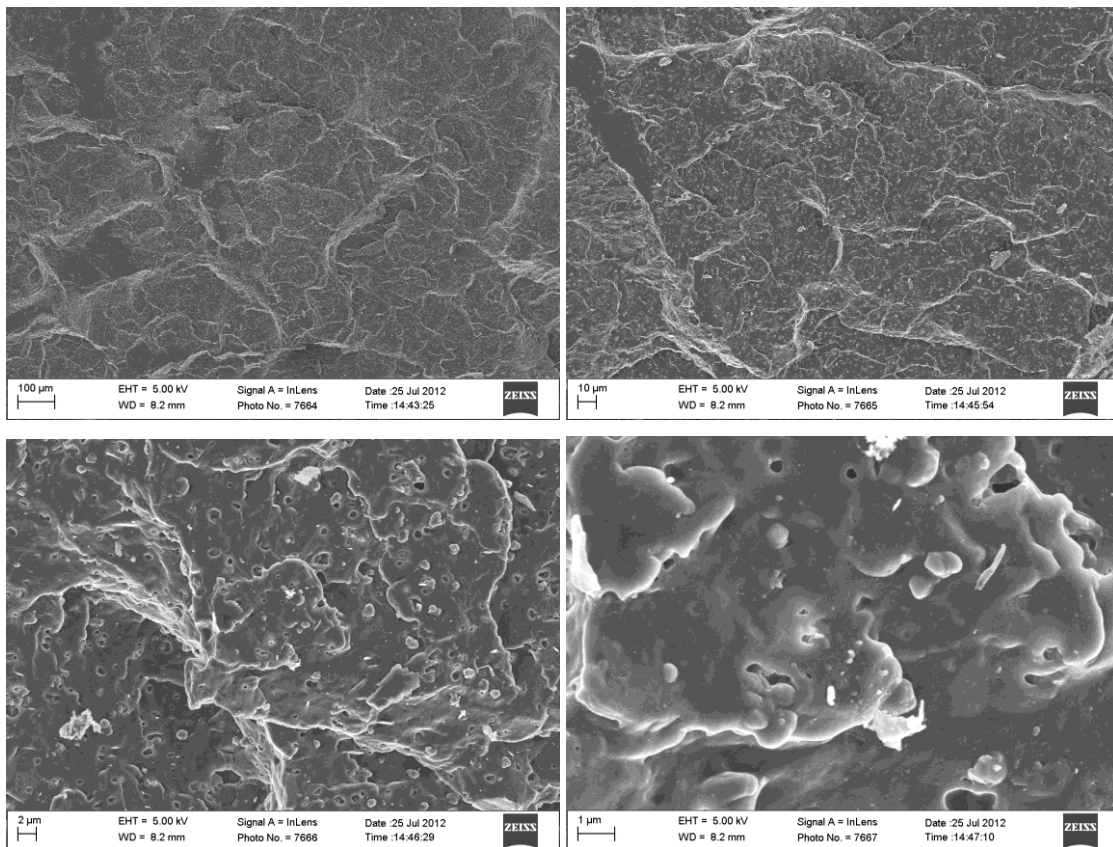
Figure A.4   *SEM micrograms at different magnifications of MS004*
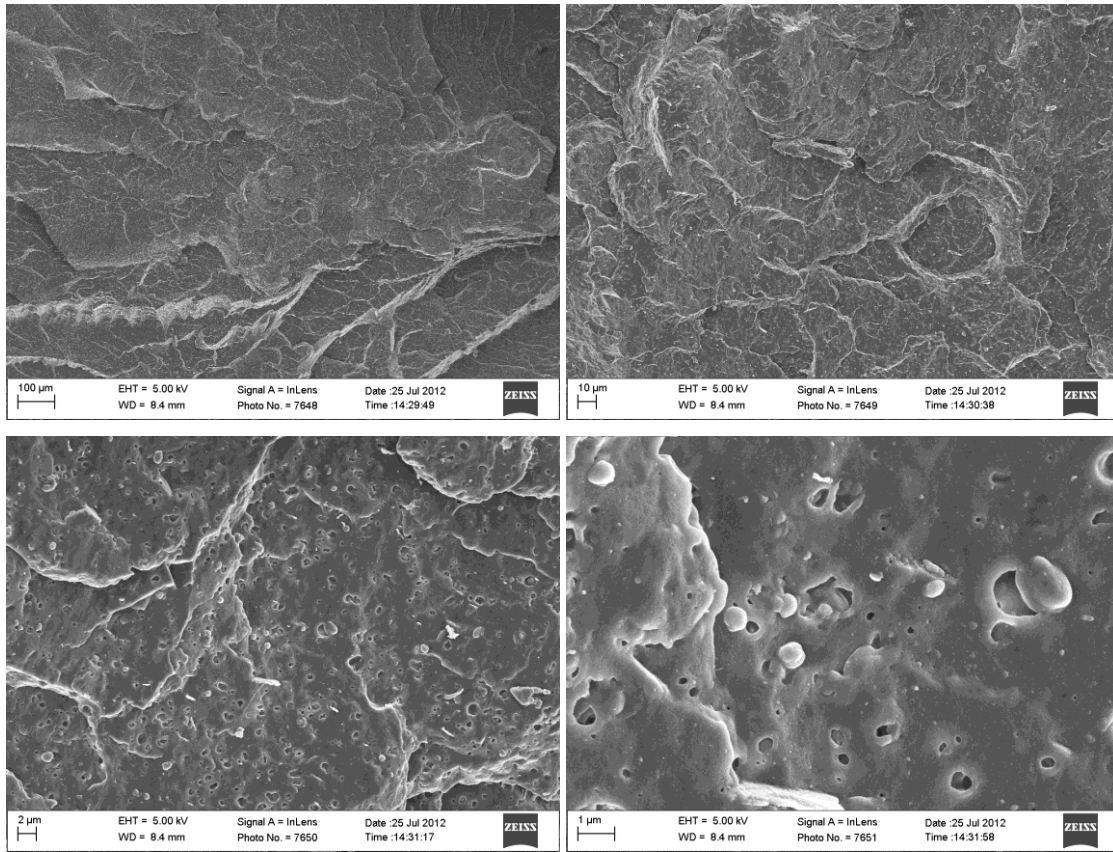
Figure A.5   *SEM micrograms at different magnifications of MS005*
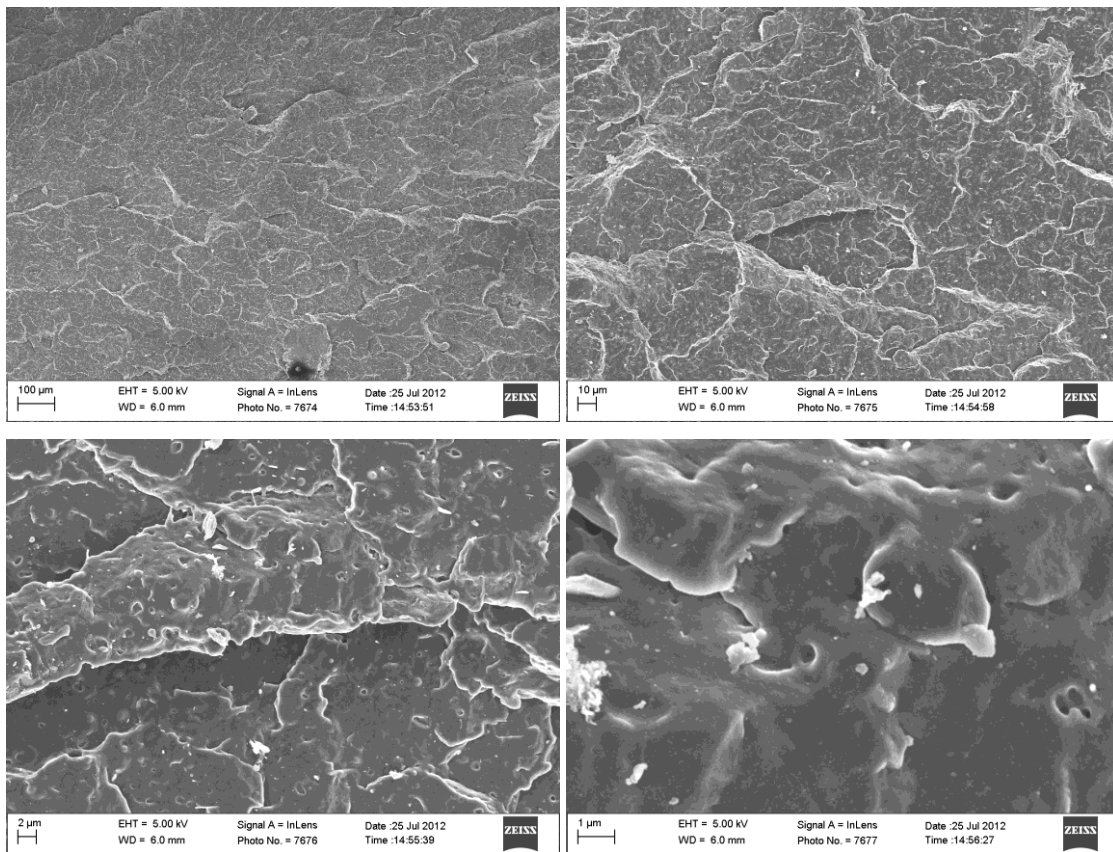
Figure A.6   *SEM micrograms at different magnifications of MS006*
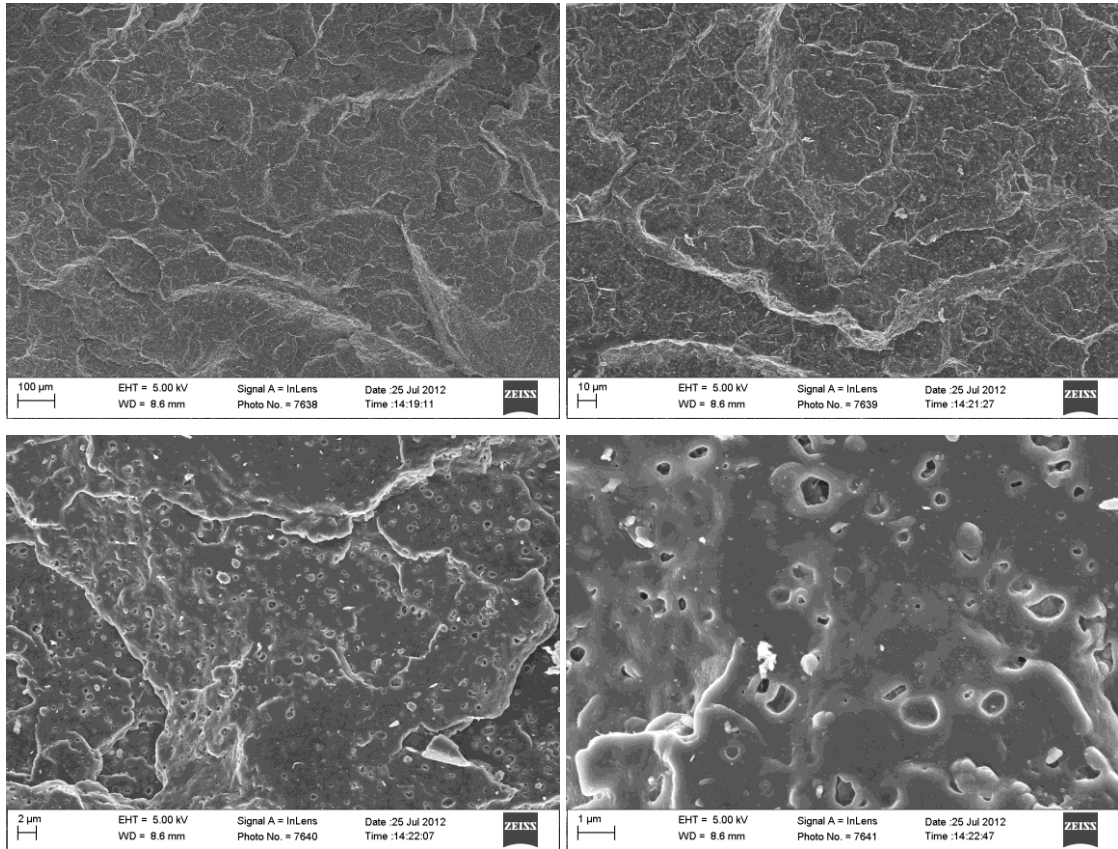
Figure A.7   *SEM micrograms at different magnifications of MS007*
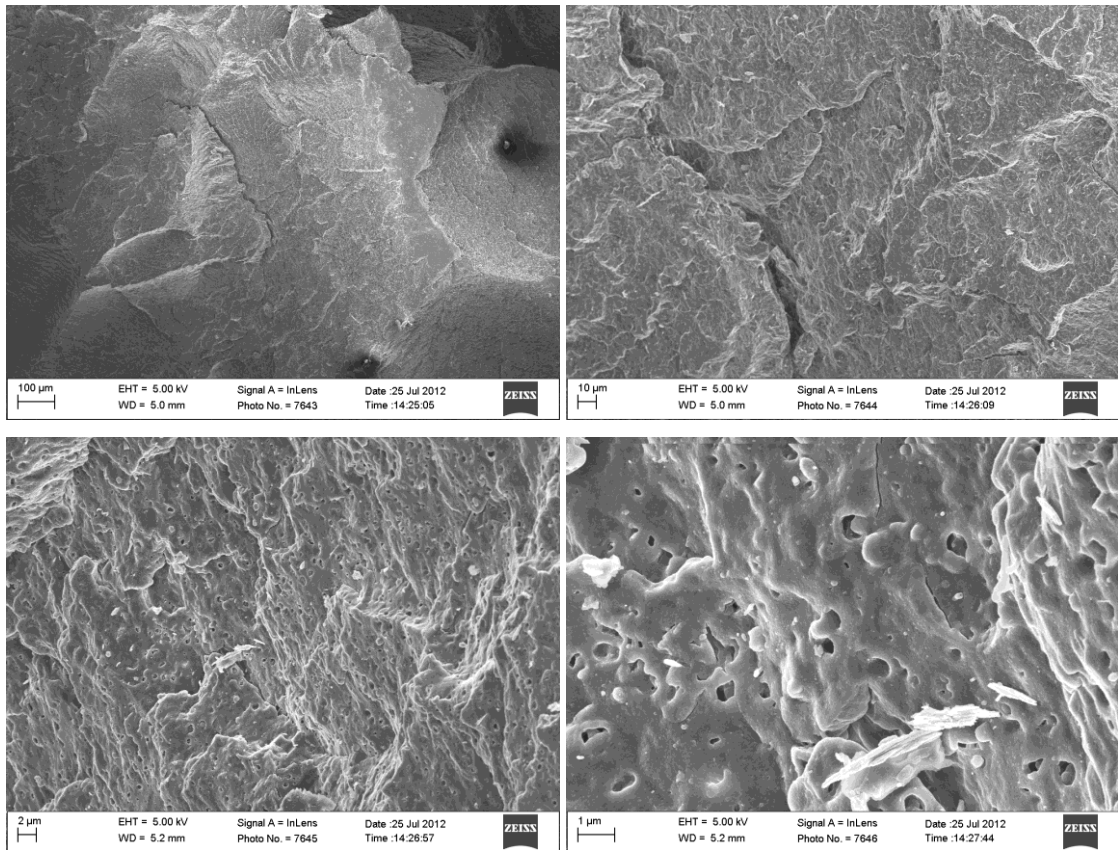
Figure A.8   *SEM micrograms at different magnifications of MS008*
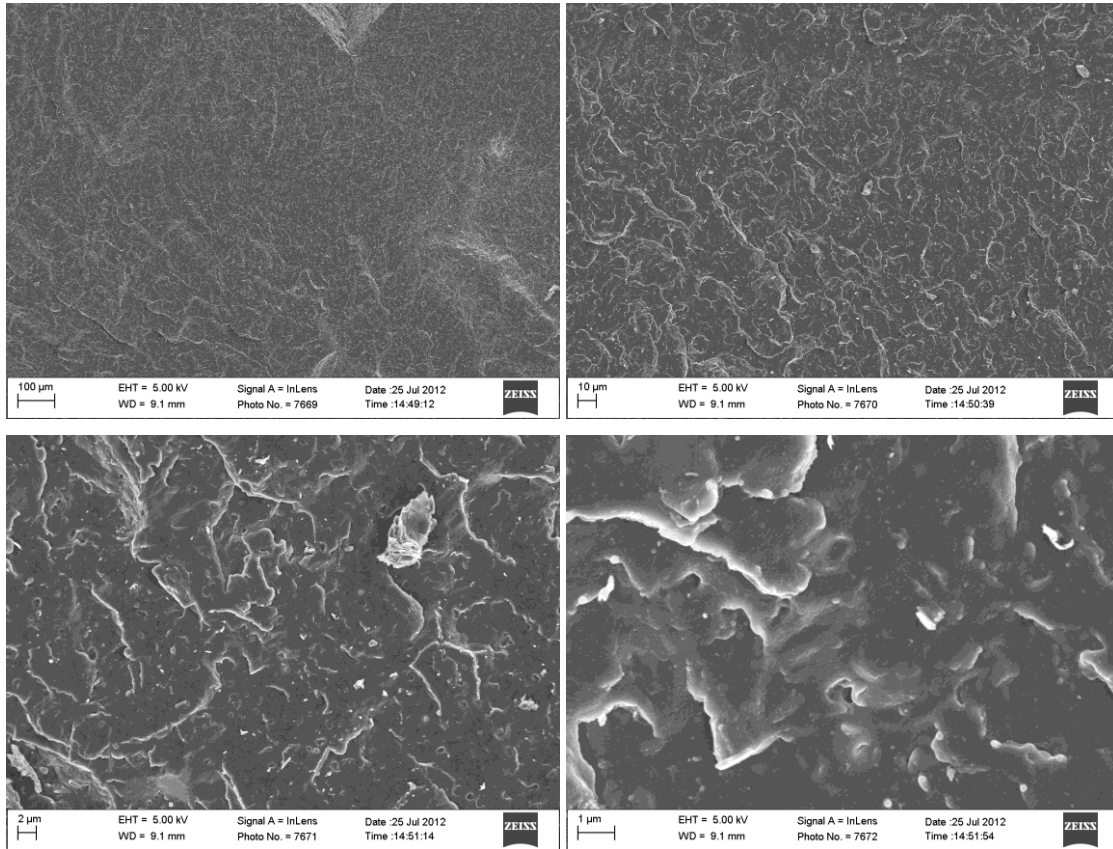
Figure A.9   *SEM micrograms at different magnifications of MS009*

Addendum B
Fractionation

This addendum contains graphs and other data collected during the fractionation investigation of the bulk propylene-ethylene heterophasic copolymer samples. Data is presented for analytical Temperature Rising Elution Fractionation, Crystallisation Analysis Fractionation and preparative Temperature Rising Elution Fractionation.

Addendum B.1: Analytical temperature rising elution fractionation
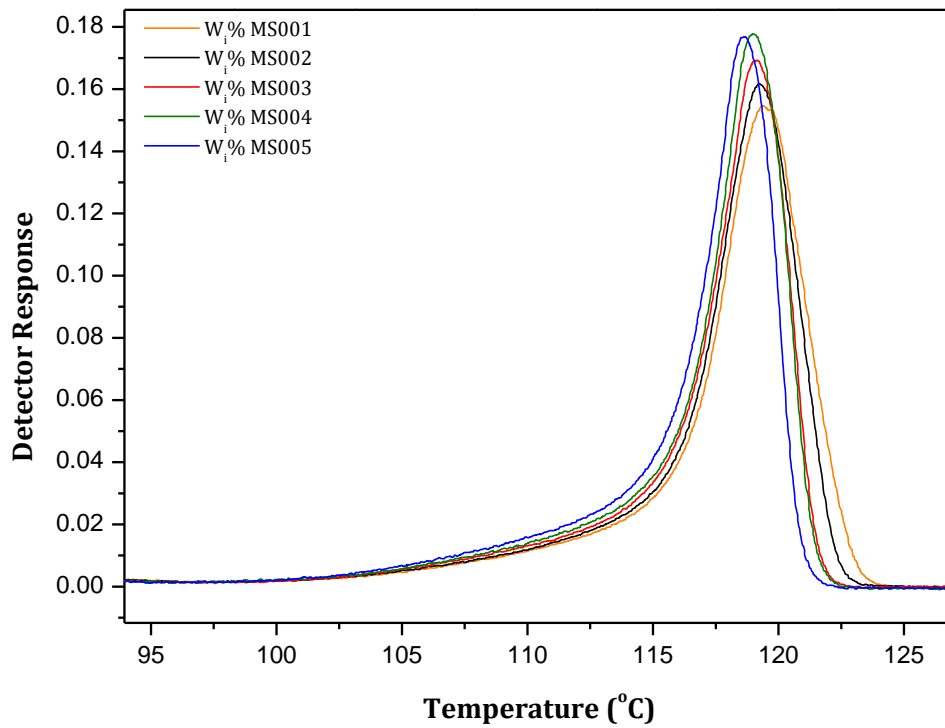
Figure B.1   A-*TREF elution data for Trigonox® 301 samples (high temperature range)*
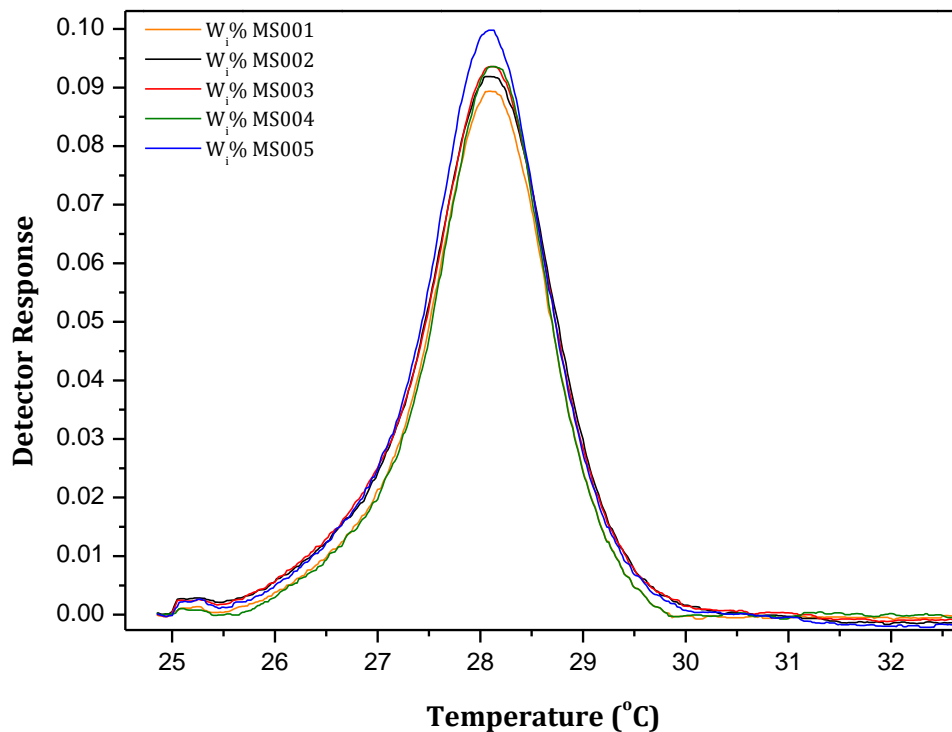
Figure B.2   A-*TREF elution data for Trigonox® 301 samples (low temperature range)*
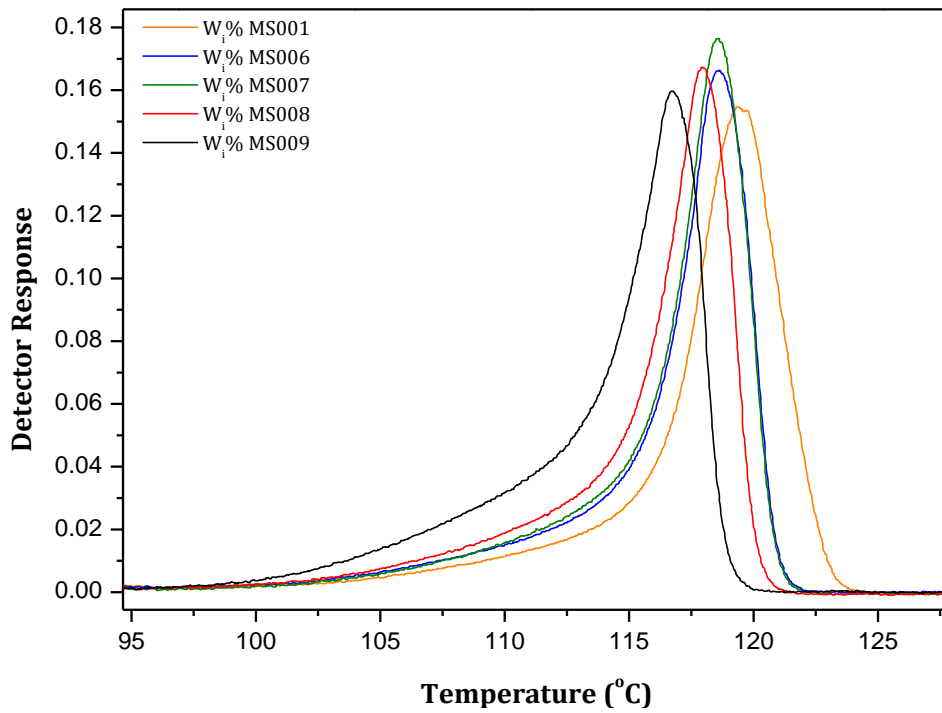
Figure B.3   A-*TREF elution data for Trigonox® 101 samples (high temperature range)*
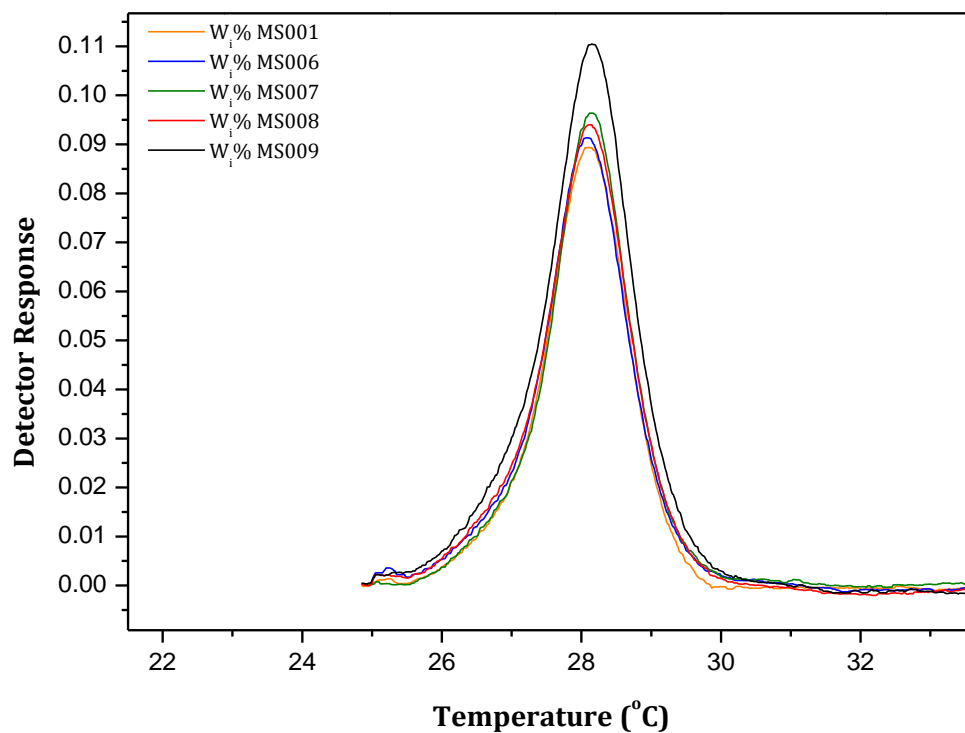
Figure B.4   A-*TREF elution data for Trigonox® 101 samples (low temperature range)*

Table B.1 *Peak elution temperatures for high temperature range*

Trigonox® 301 Sampels	Peak Elution Temperature (°C)	Trigonox® 101 Sampels	Peak Elution Temperature (°C)
MS001	119.42	MS001	119.42
MS002	119.23	MS006	118.57
MS003	119.05	MS007	118.50
MS004	118.92	MS008	117.88
MS005	118.60	MS009	116.74

Addendum B.2: Crystallisation analysis fractionation
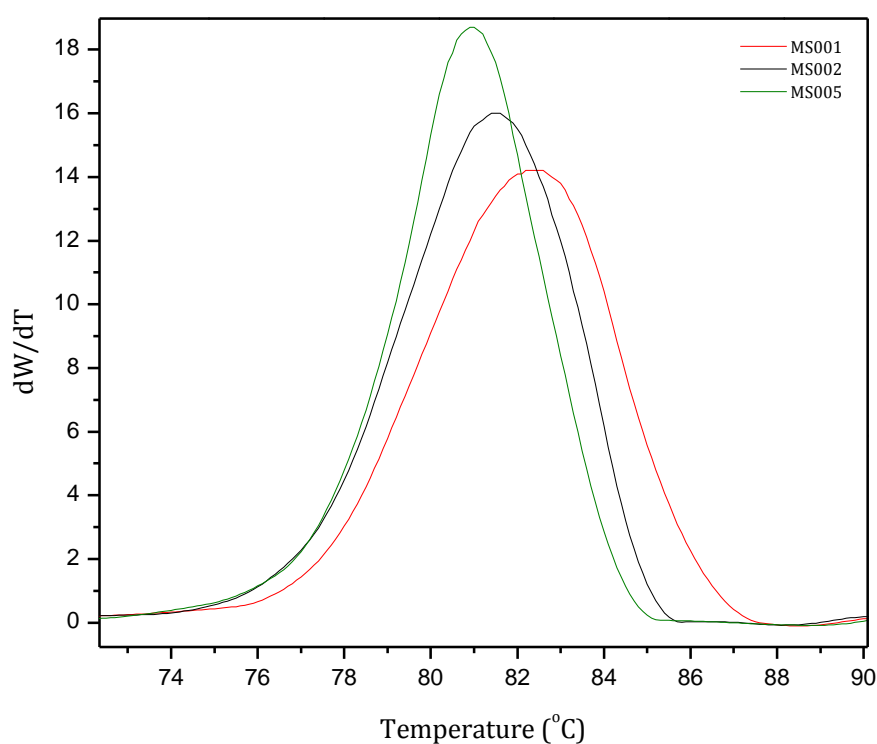
Figure B.5   CRYSTAF *elution data for Trigonox® 301 samples (high temperature range)*
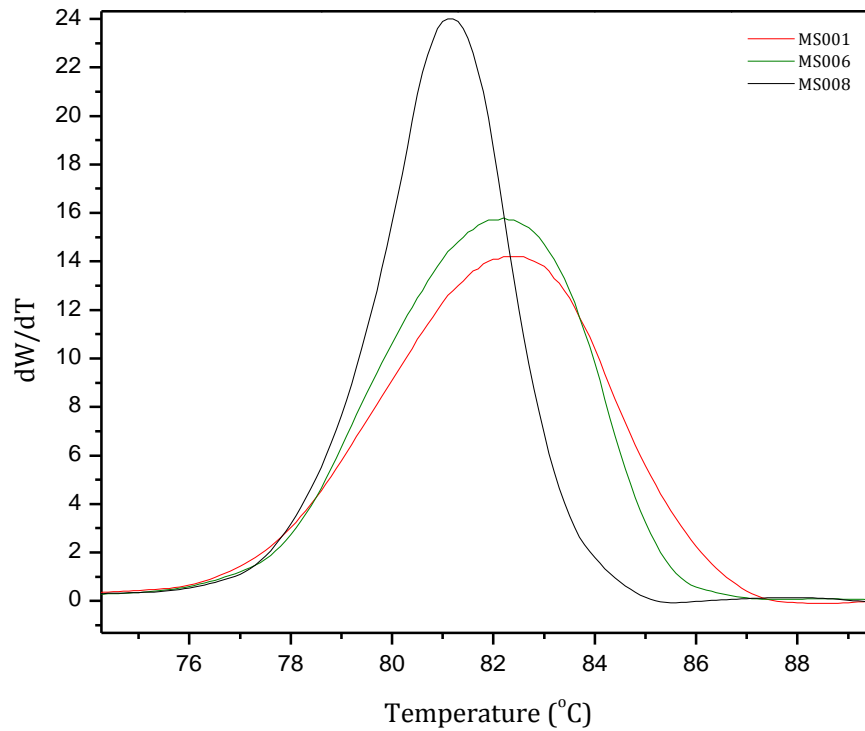
Figure B.6   CRYSTAF *elution data for Trigonox® 101 samples (high temperature range)*

Addendum B.3: Preparative temperature rising elution fractionation
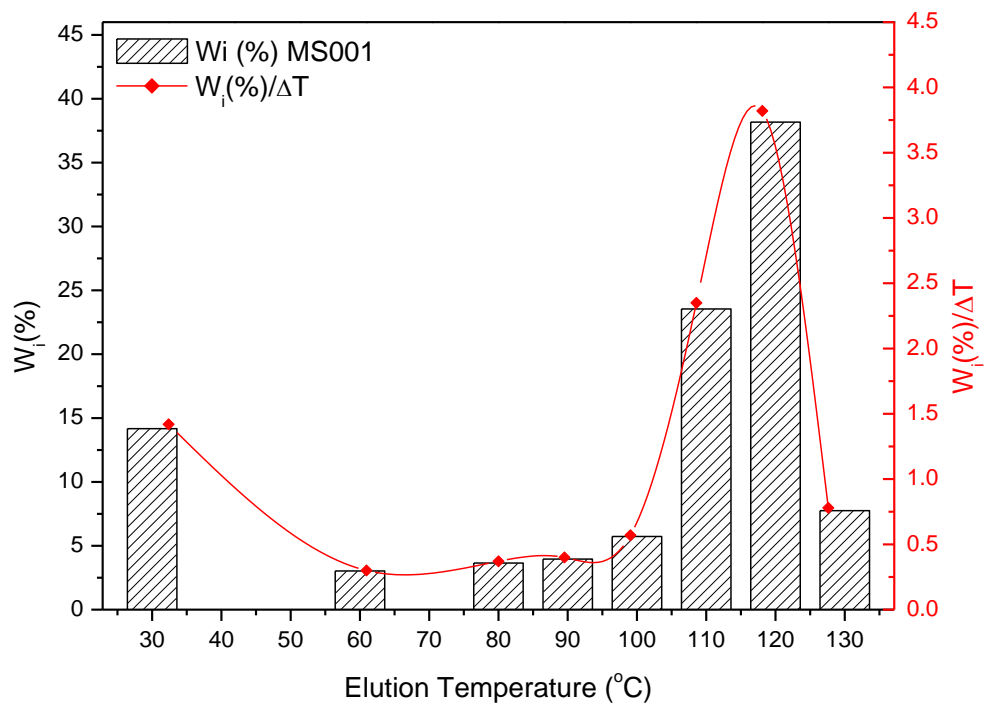
Figure B.7   *TREF Elution data illustrating the weight percentage per temperature increment and the weight percentage eluted for Sample MS001*
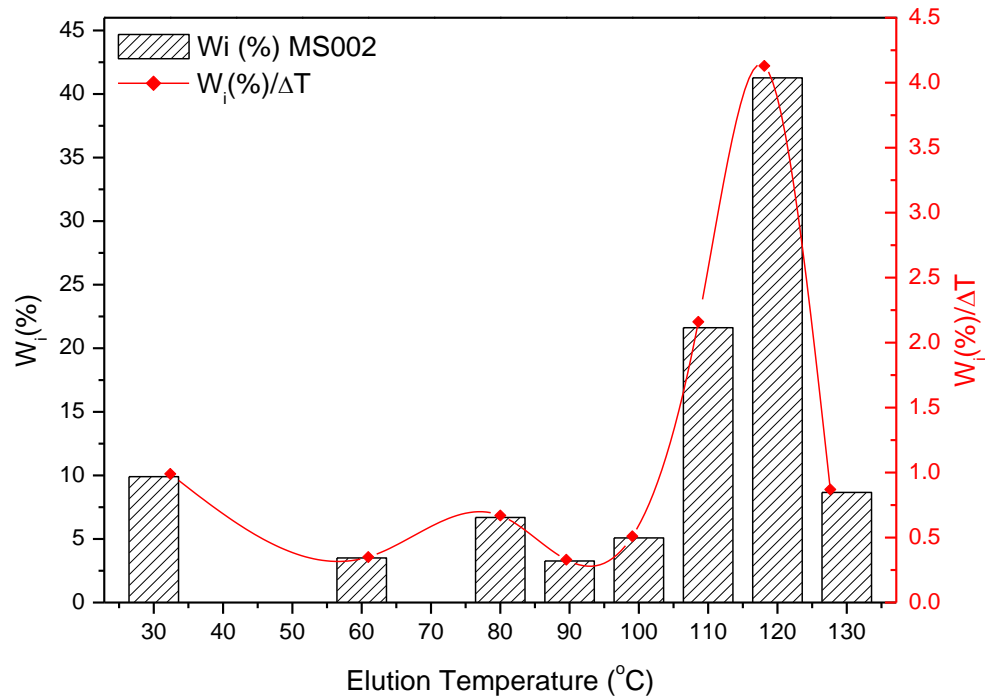
Figure B.8   *TREF Elution data illustrating the weight percentage per temperature increment and the weight percentage eluted for Sample MS002*
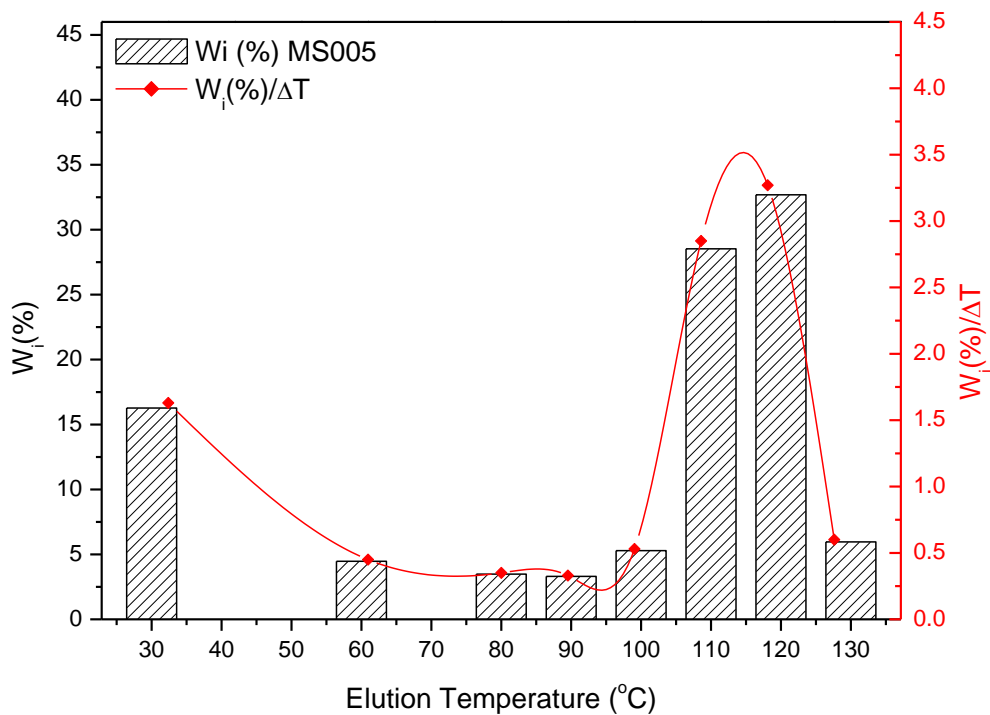
Figure B.9   *TREF Elution data illustrating the weight percentage per temperature increment and the weight percentage eluted for Sample MS005*
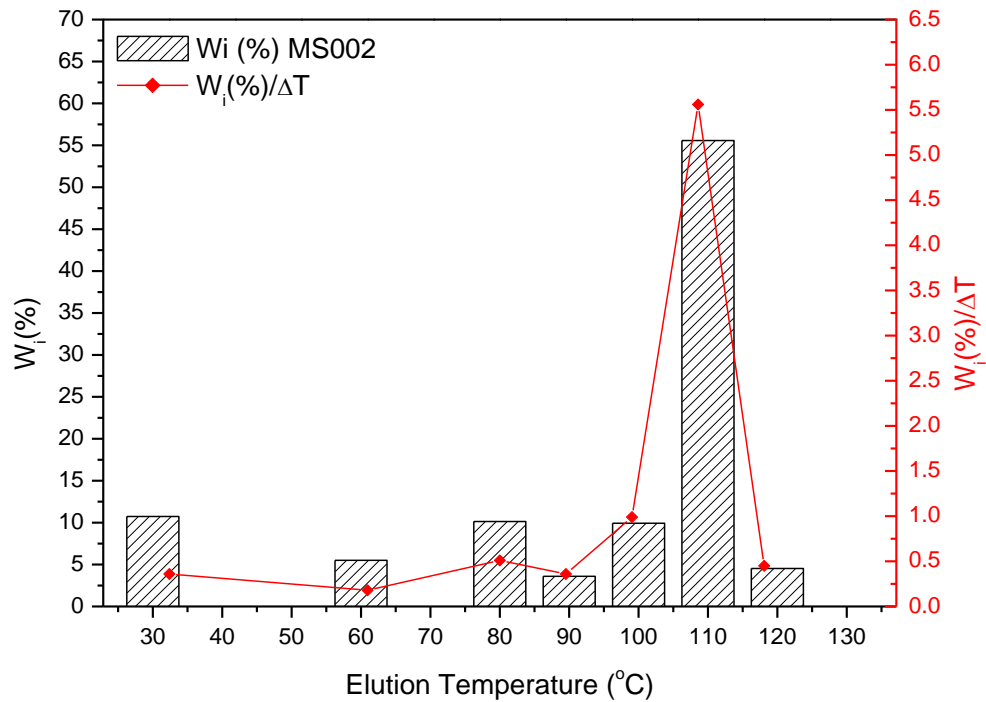
Figure B.10   *TREF Elution data illustrating the weight percentage per temperature increment and the weight percentage eluted for Sample MS006*
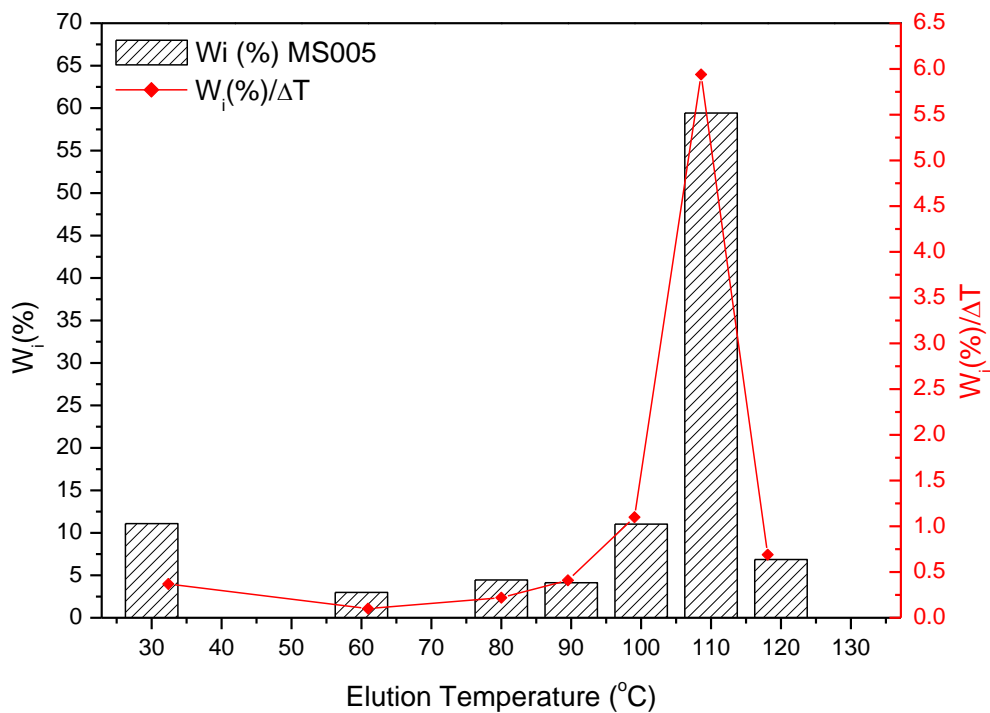
Figure B.11   *TREF Elution data illustrating the weight percentage per temperature increment and the weight percentage eluted for Sample MS008*

Addendum C
Characterization of TREF Samples

This addendum contains graphs and other data collected during the characterization phase of the investigation on bulk as well as TREF fractions. Data is presented for nuclear magnetic resonance spectroscopy (NMR), high temperature size exclusion chromatography (HT-SEC), Fourier transform infrared spectroscopy (FTIR), size exclusion chromatography coupled to Fourier transform infrared spectroscopy via the LC transform interface (SEC-FTIR) and gradient high temperature high performance liquid chromatography (HT-HPLC).

Addendum C.1: Nuclear magnetic resonance spectroscopy
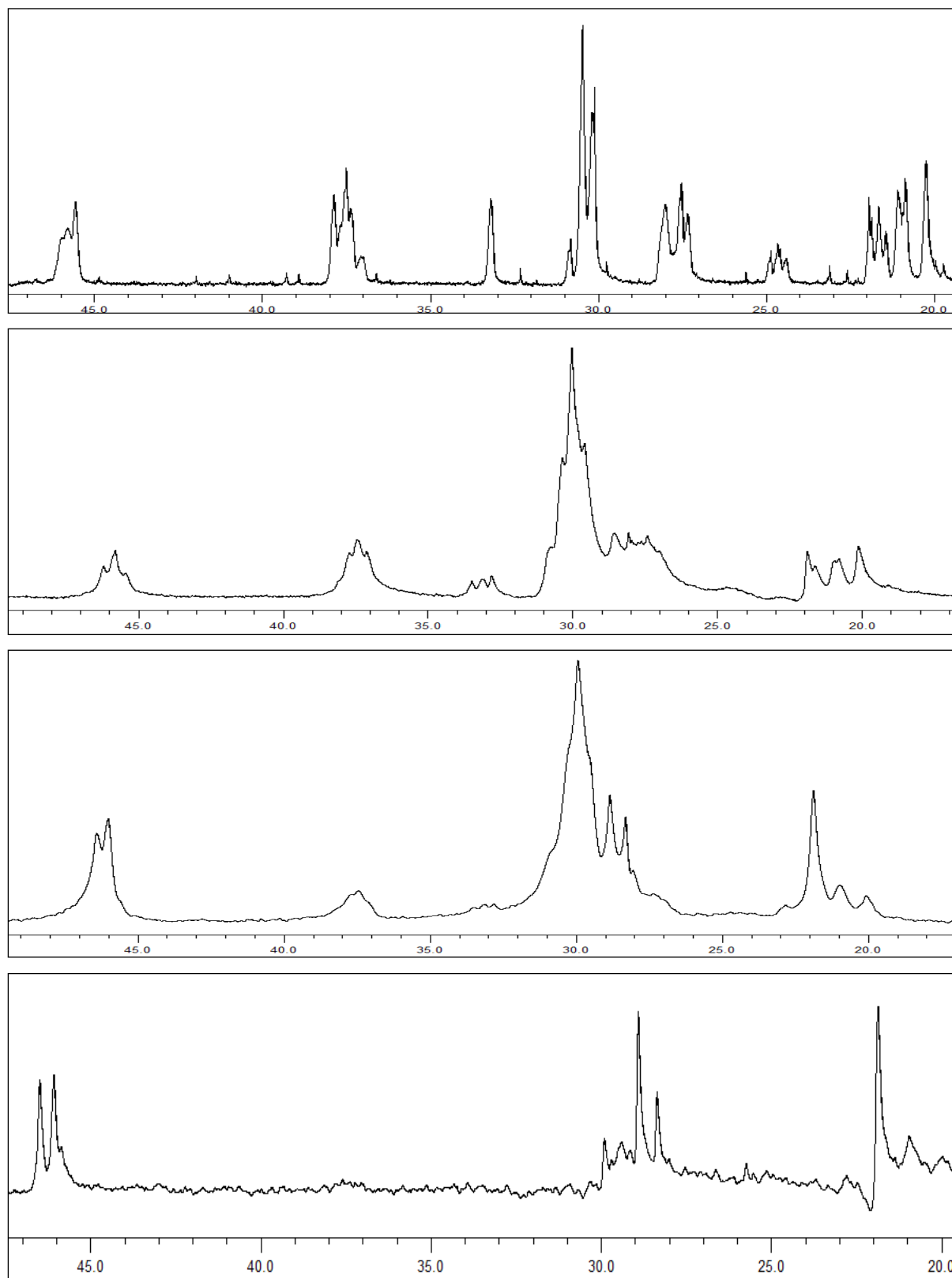
Figure C.1 ^{13}C *NMR analysis of the MS001 TREF samples (30 °C, 60 °C, 80 °C and 90 °C)*
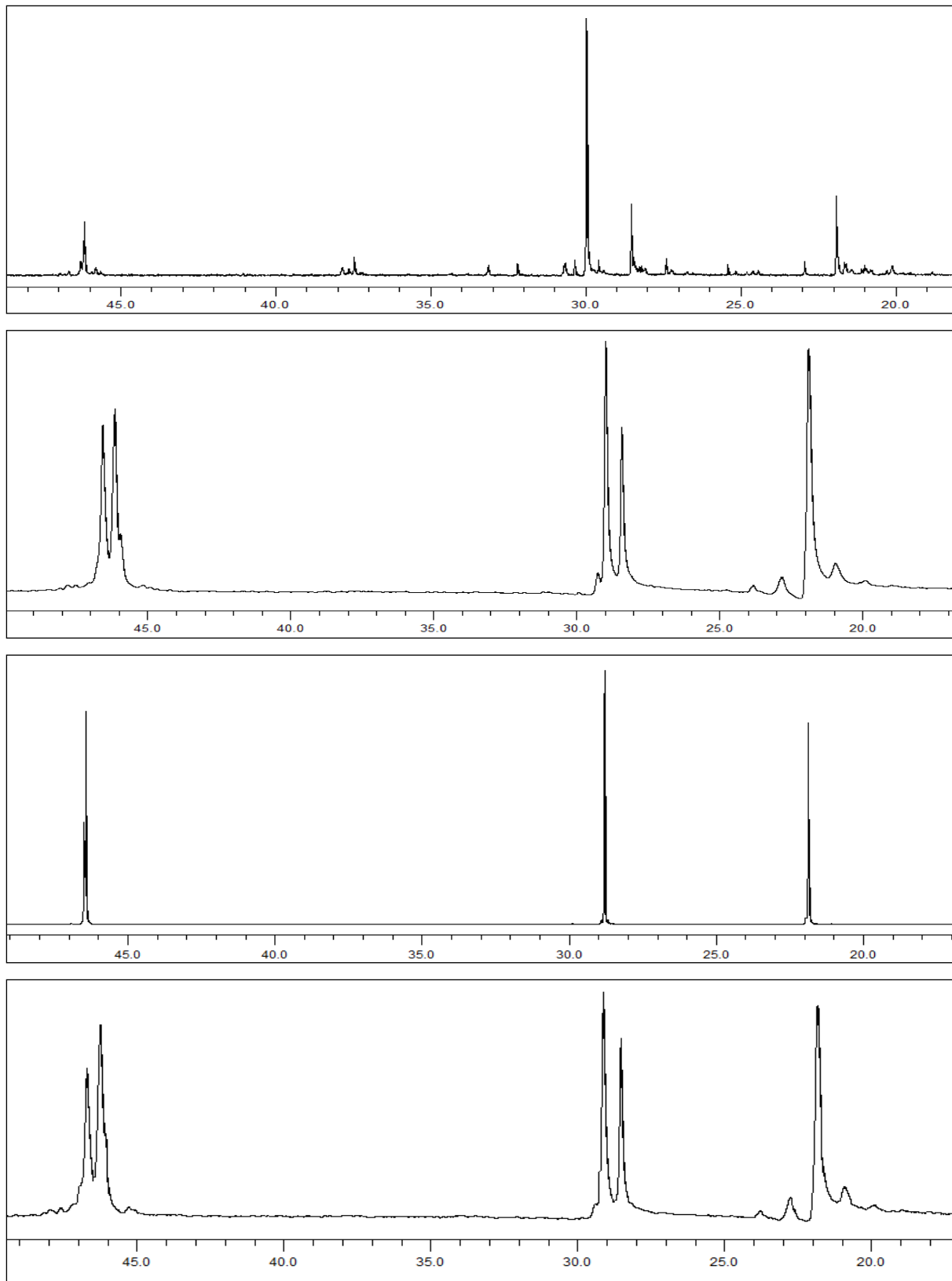
Figure C.2 ^{13}C *NMR analysis of the MS001 TREF samples (100 °C, 110 °C, 120 °C and 130 °C)*
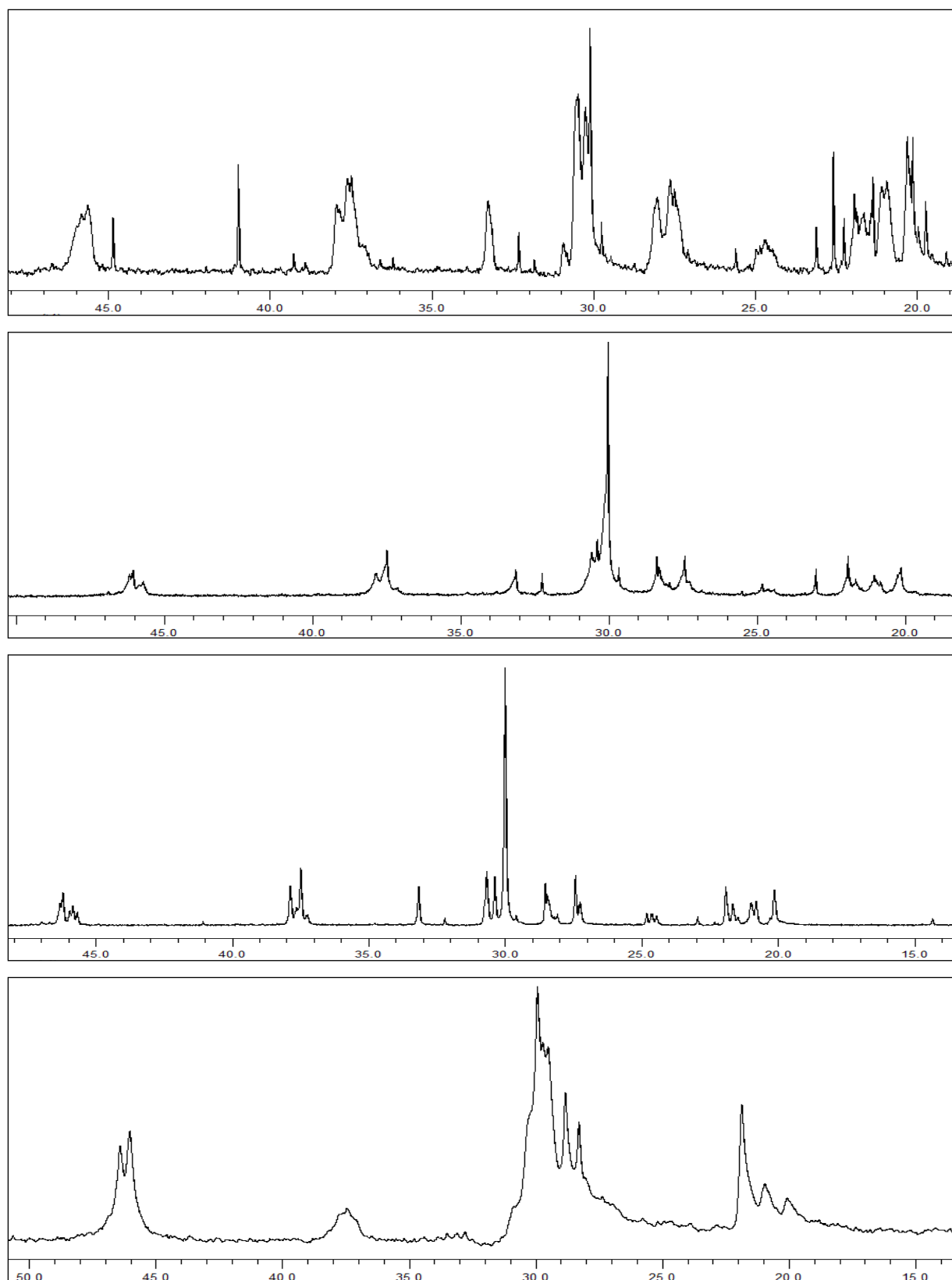
Figure C.3   ¹³C *NMR analysis of the MS002 TREF samples (30 °C, 60 °C, 80 °C and 90 °C)*
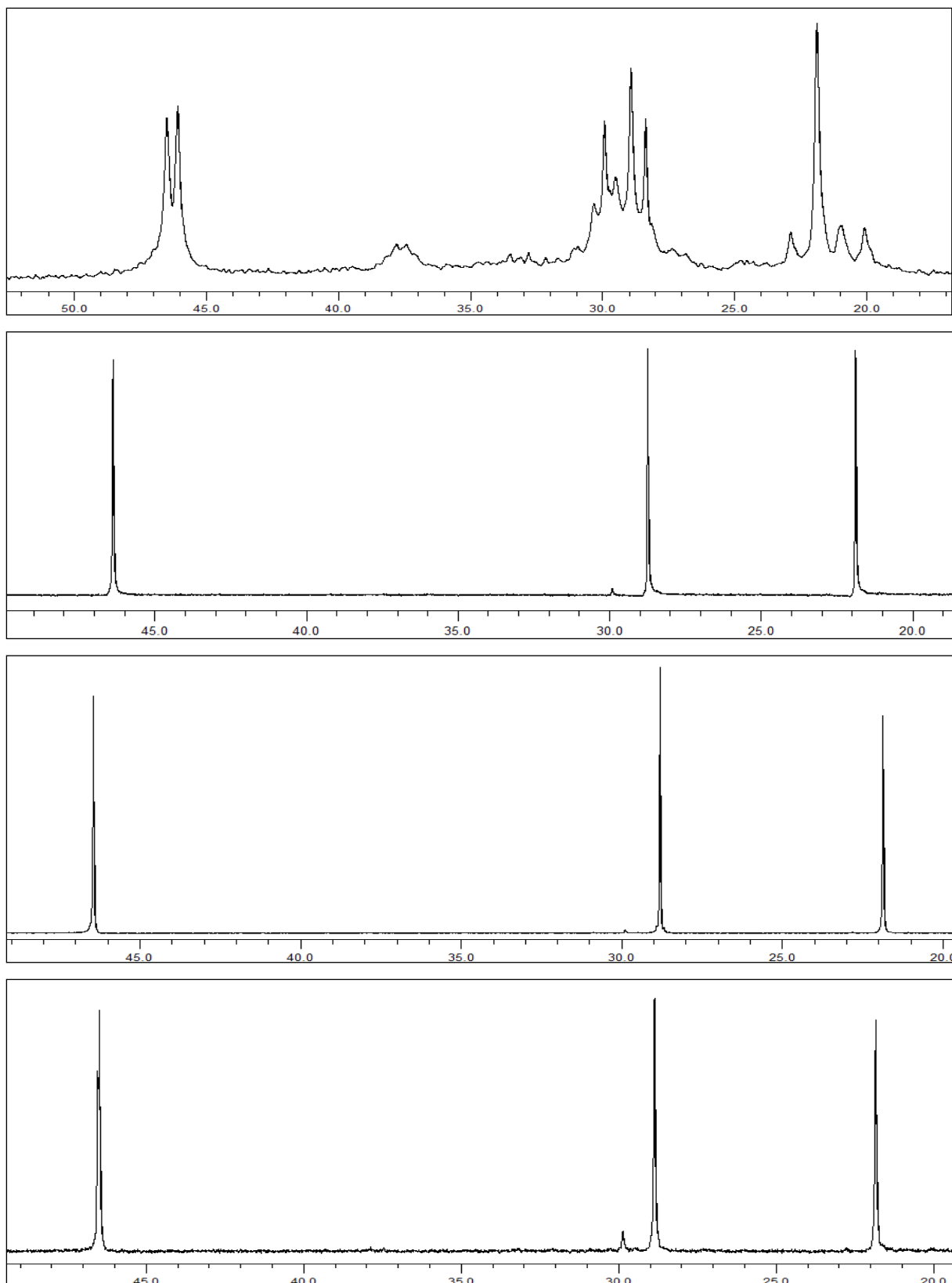
Figure C.4   ¹³C *NMR analysis of the MS002 TREF samples (100 °C, 110 °C, 120 °C and 130 °C)*
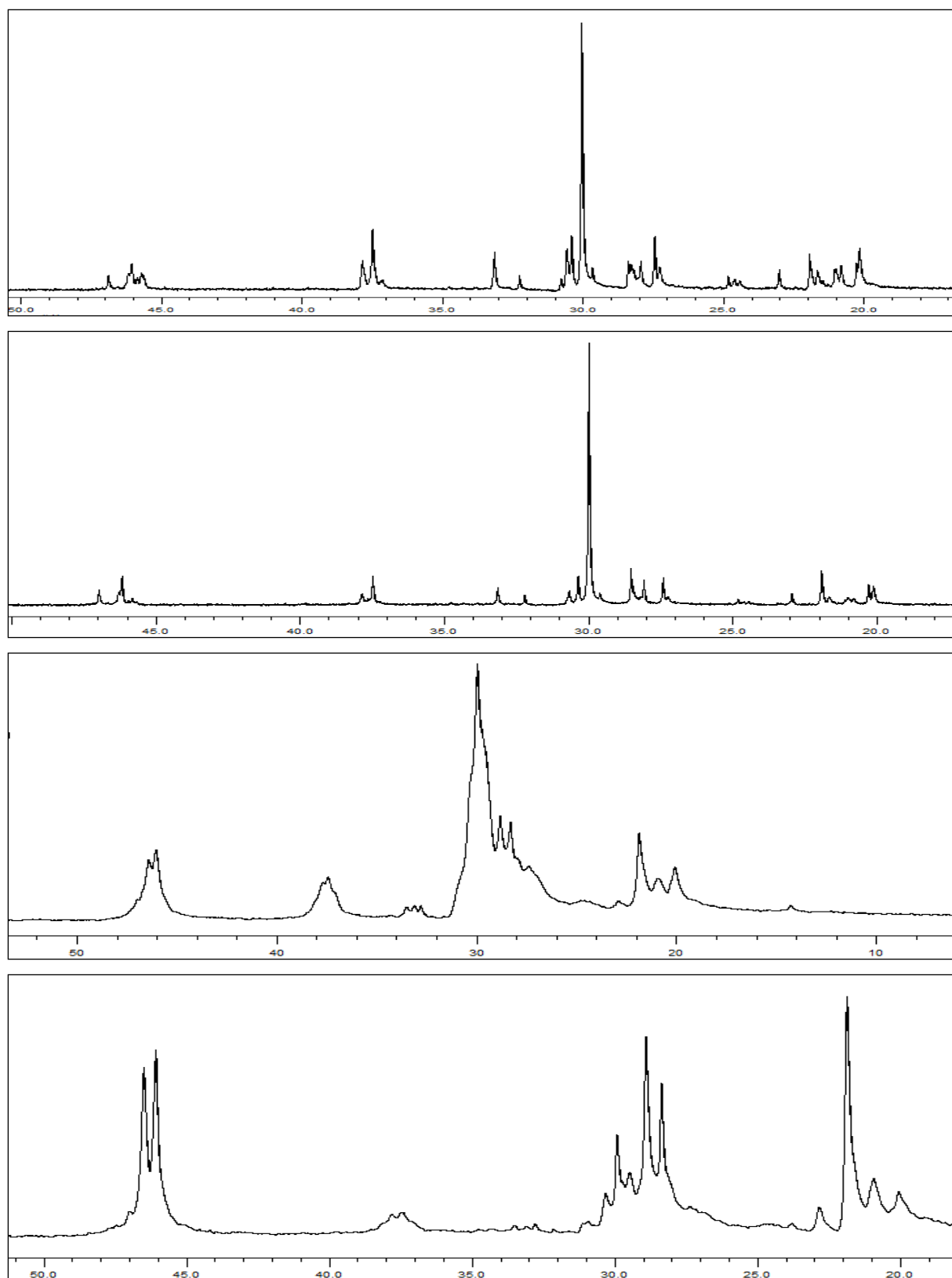
Figure C.5   ¹³C *NMR analysis of the MS005 TREF samples (60 °C, 80 °C, 90 °C and 100 °C)*
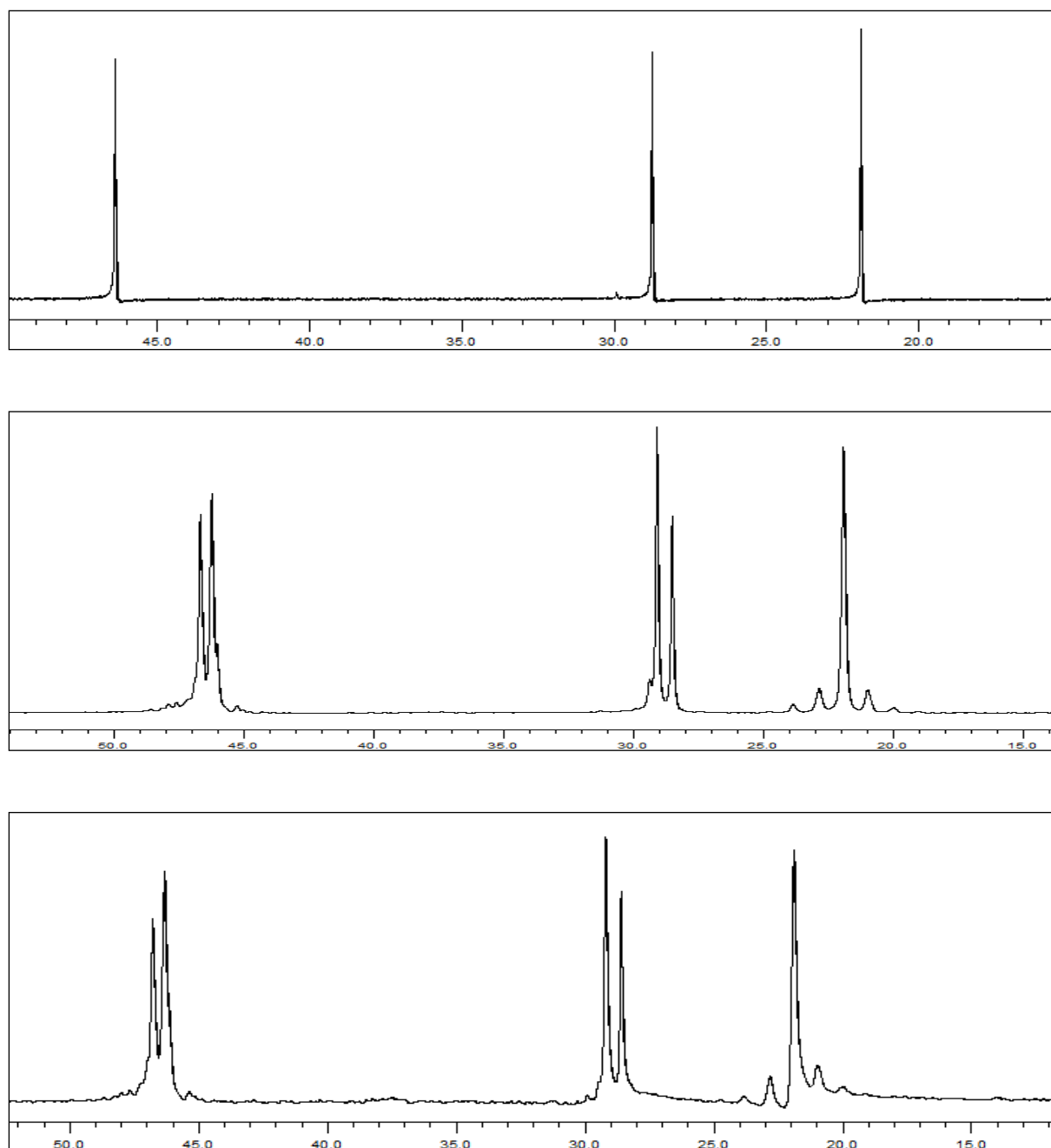
Figure C.6   ¹³C *NMR analysis of the MS005 TREF samples (60 °C, 80 °C, 90 °C and 100 °C)*
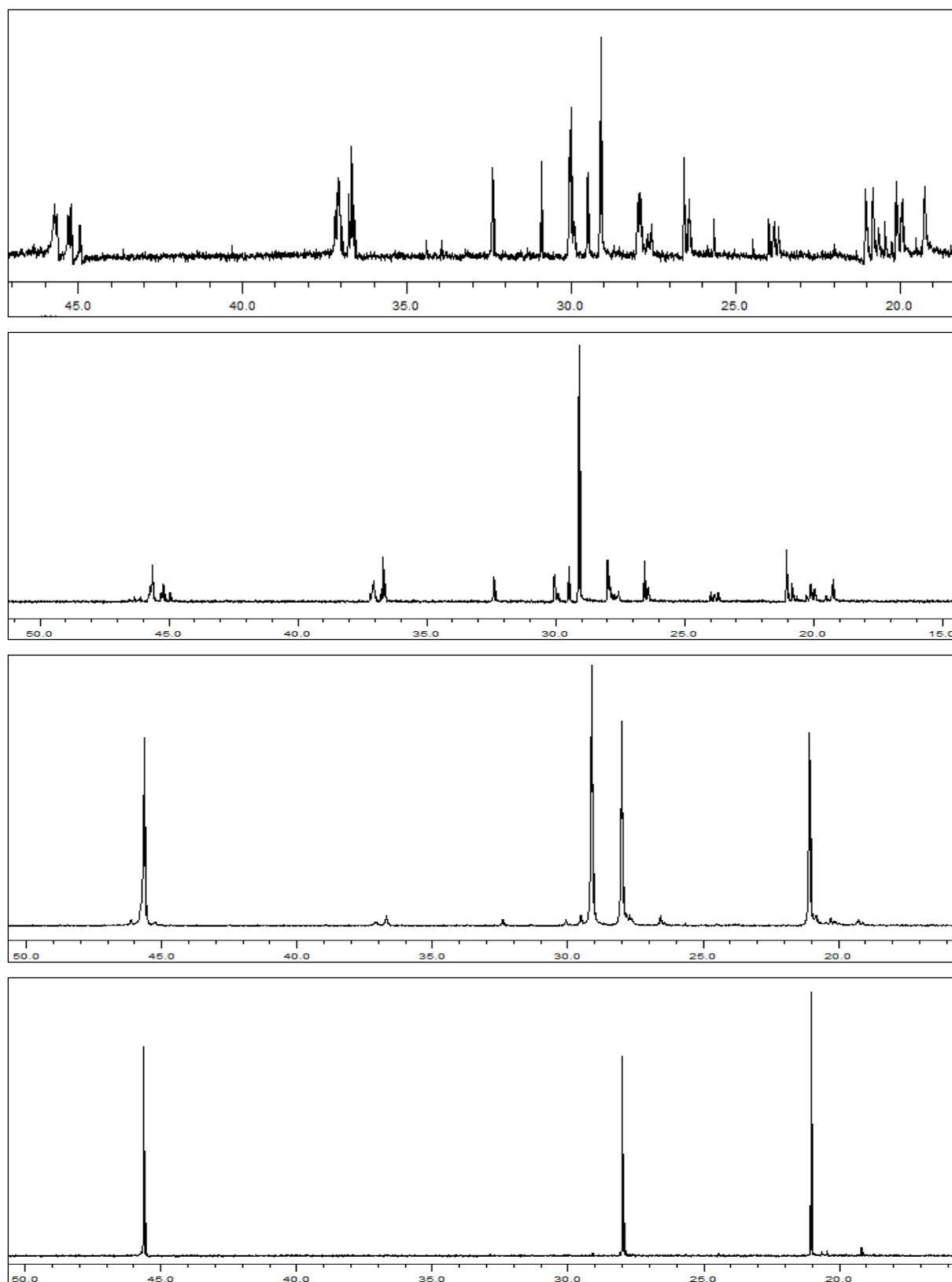
Figure C.7   ¹³C *NMR analysis of the MS006 TREF samples (30 ℃, 60 ℃, 80 ℃ and 90 ℃)*
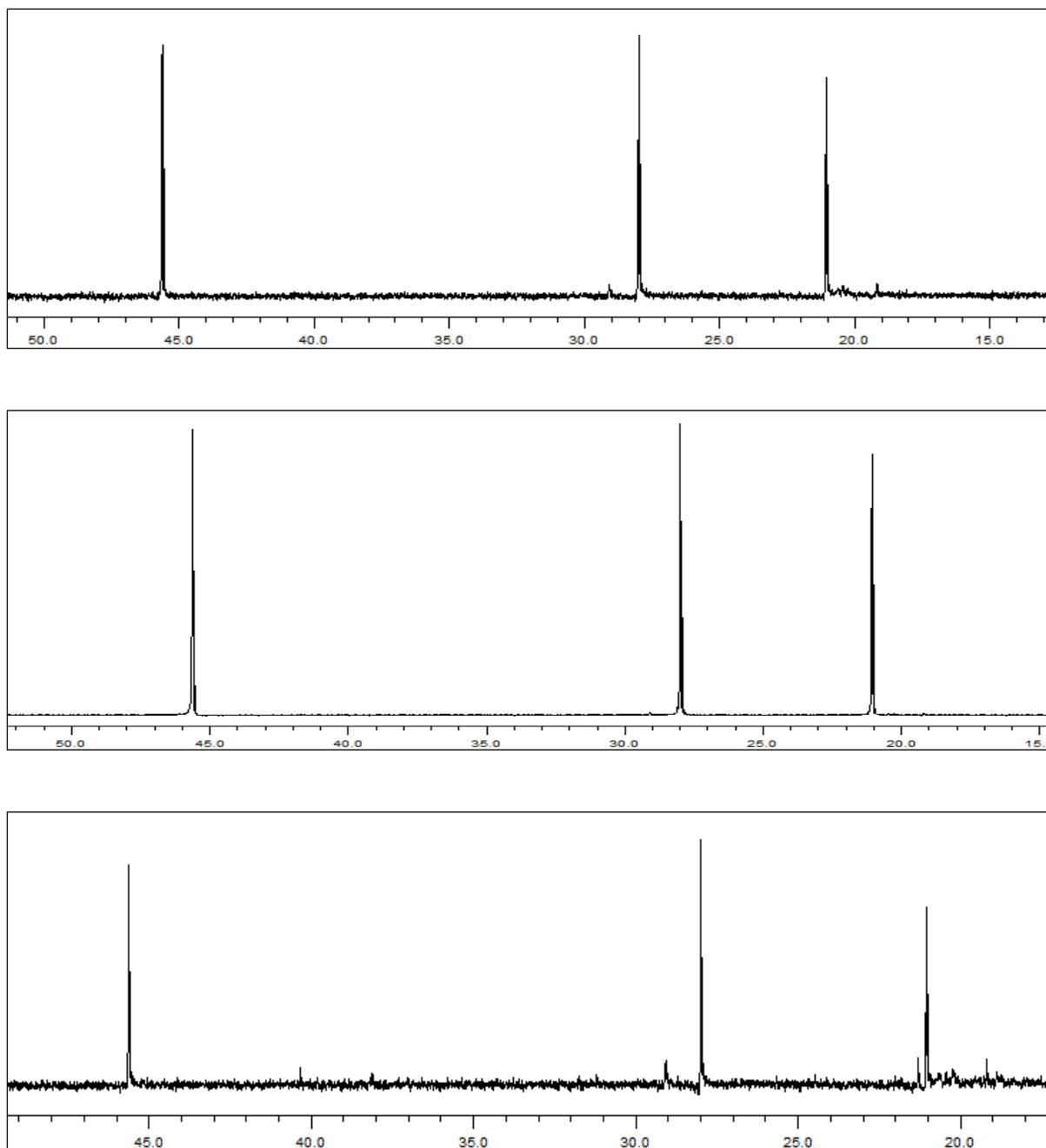
Figure C.8   ¹³C *NMR analysis of the MS006 TREF samples (100 °C, 110 °C and 120 °C)*
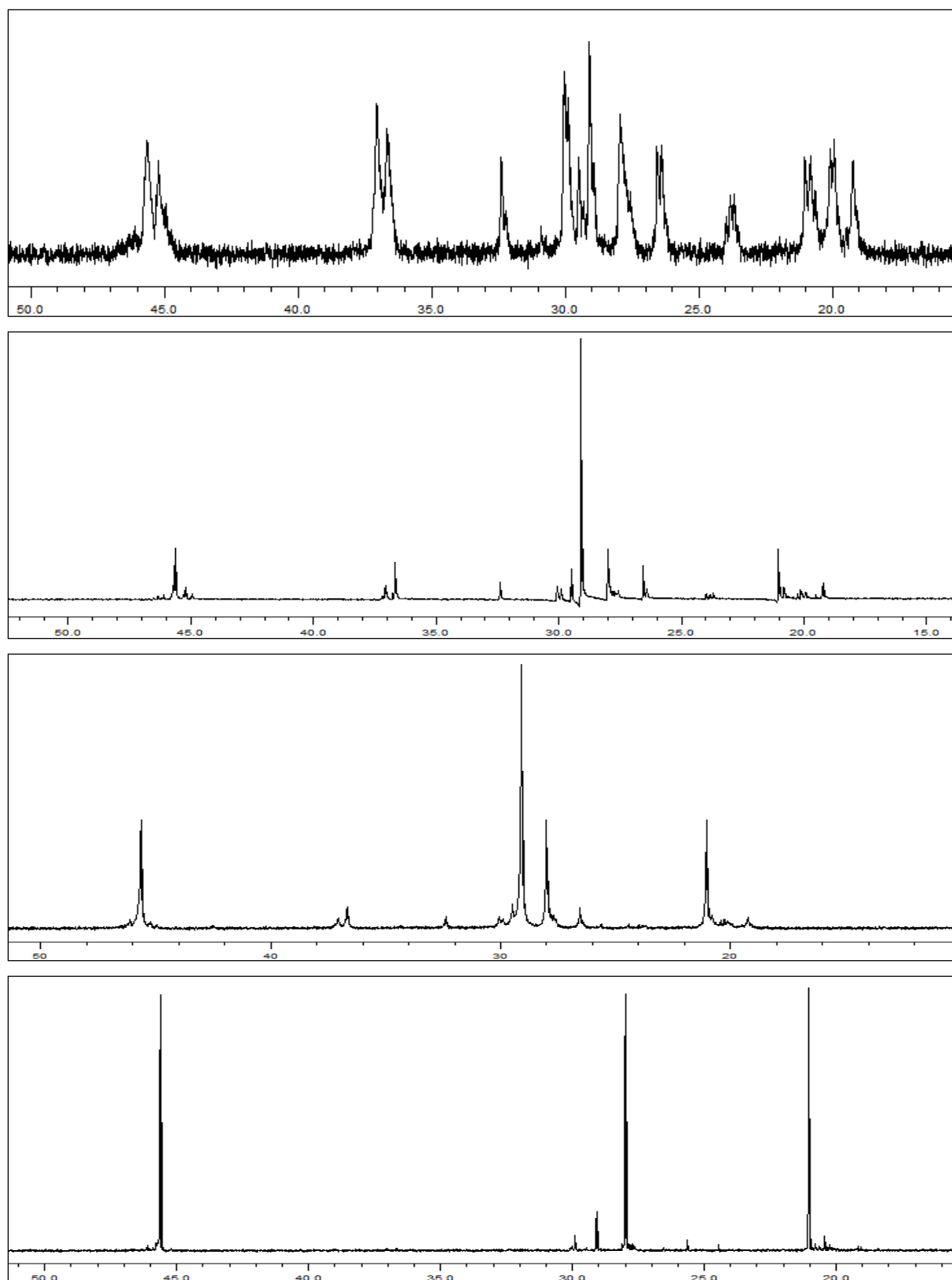
Figure C.9   ¹³C *NMR analysis of the MS008 TREF samples (30 °C, 60 °C, 80 °C and 90 °C)*
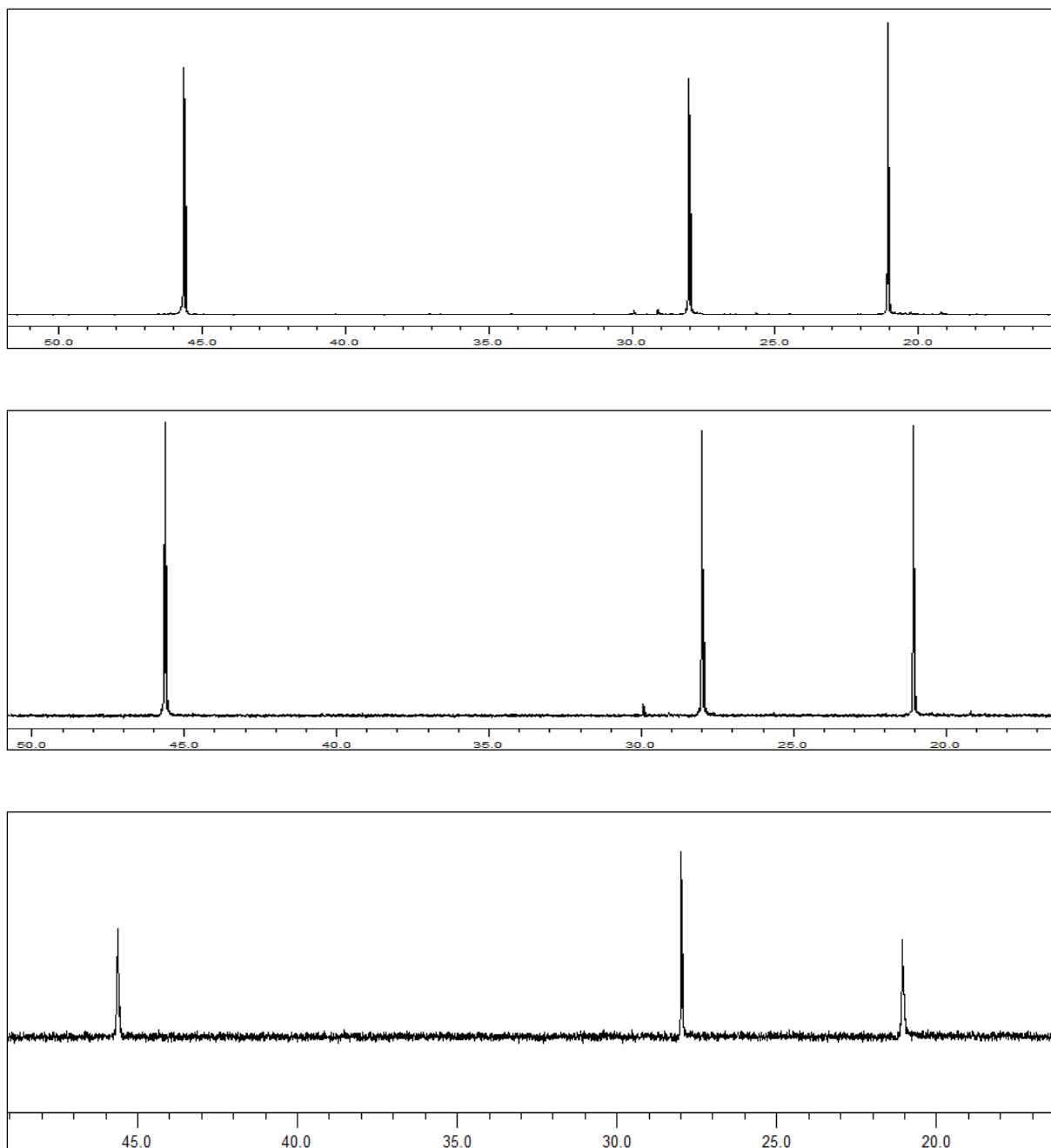
Figure C.10   ¹³C *NMR analysis of the MS008 TREF samples (100 °C, 110 °C and 120 °C)*

Addendum C.2: High temperature size exclusion chromatography
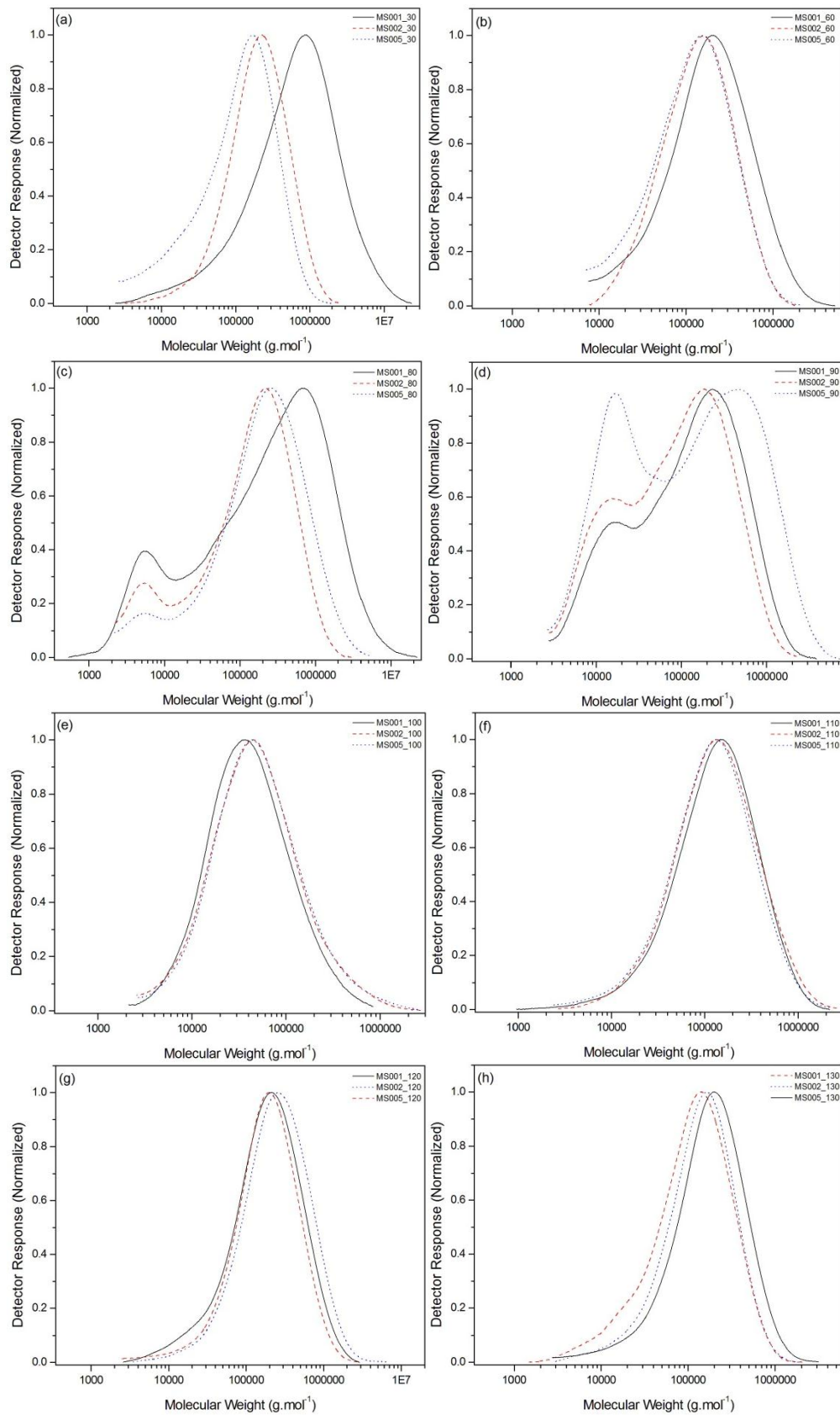
Figure C.11   *High Temperature Size Exclusion Chromatography results for the TREF fractions of samples prepared with Trigonox® 301.*

Addendum C.3: Fourier transform infrared spectroscopy
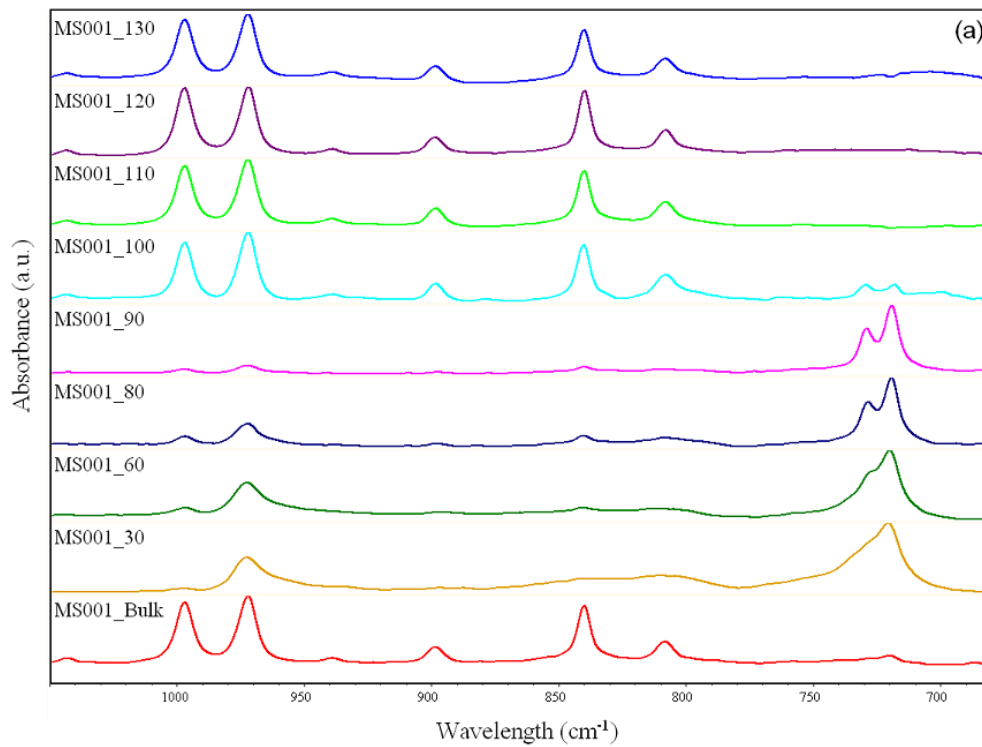
Figure C.12   *FTIR results for the TREF fractions of sample MS001*
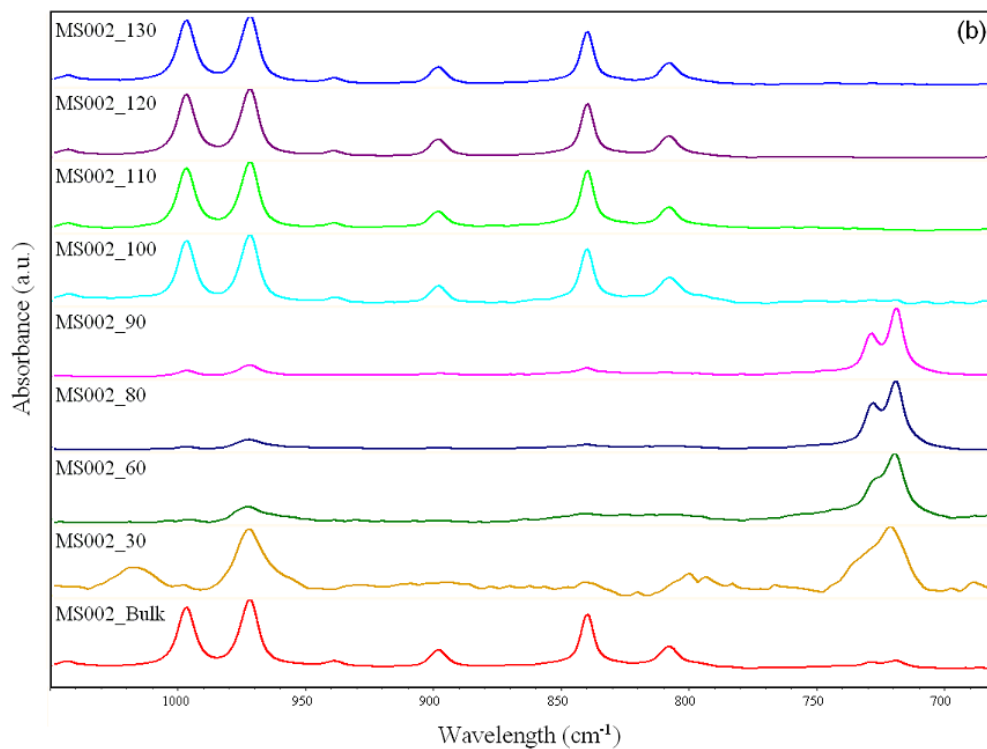
Figure C.13   *FTIR results for the TREF fractions of sample MS002*
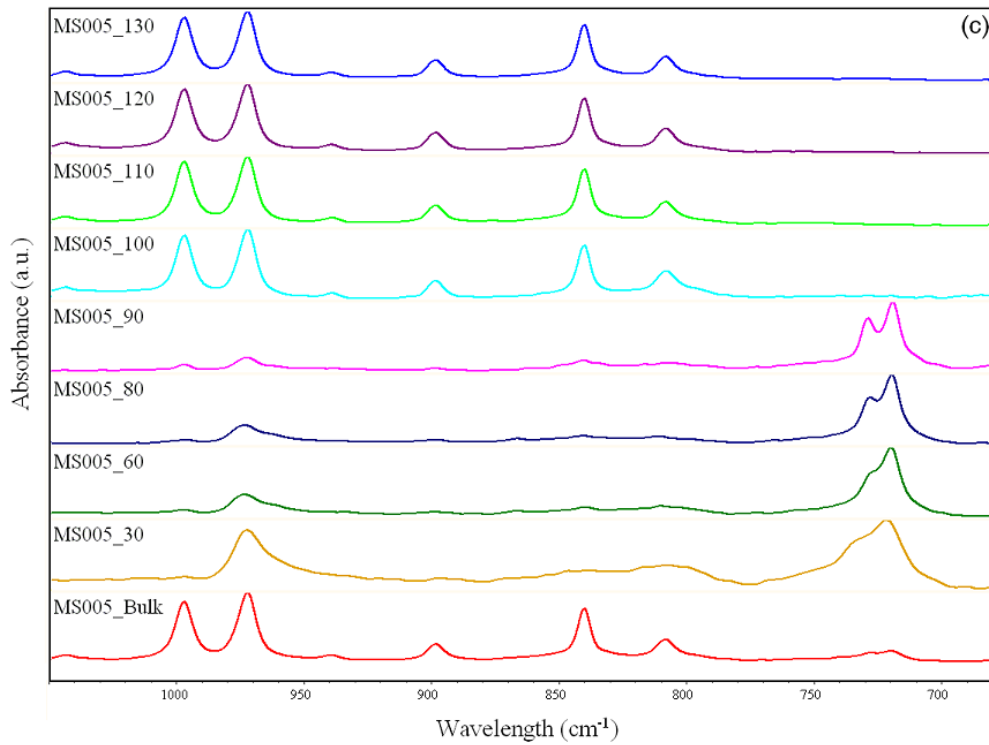
Figure C.14   *FTIR results for the TREF fractions of sample MS005*

Addendum C.4: SEC coupled to FTIR via the LC transform interface
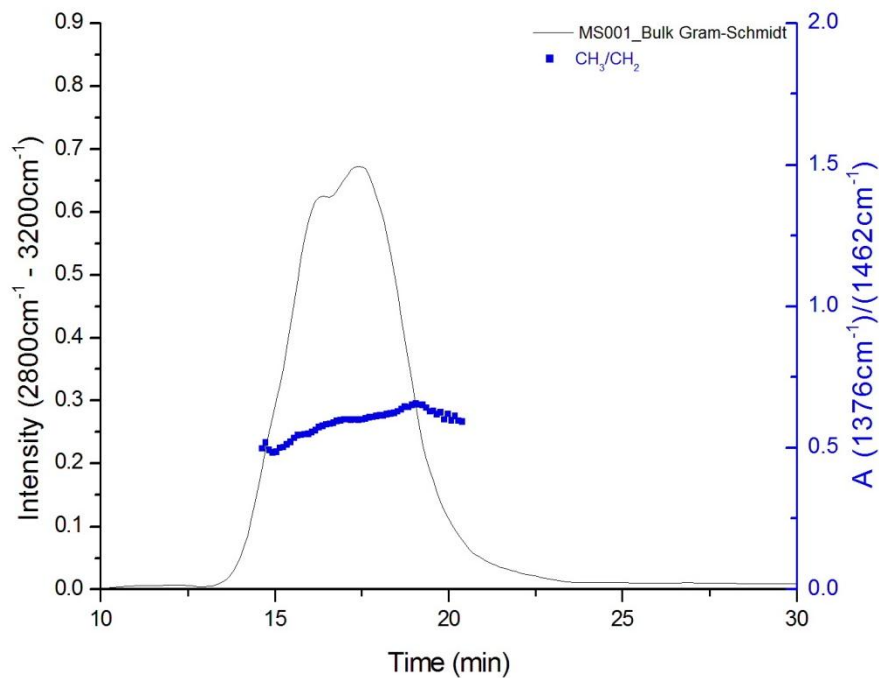
Figure C.15   *SEC-FTIR analysis of the MS001bulk sample illustrating the Gram-Schmidt plot with corresponding propylene content analysis*
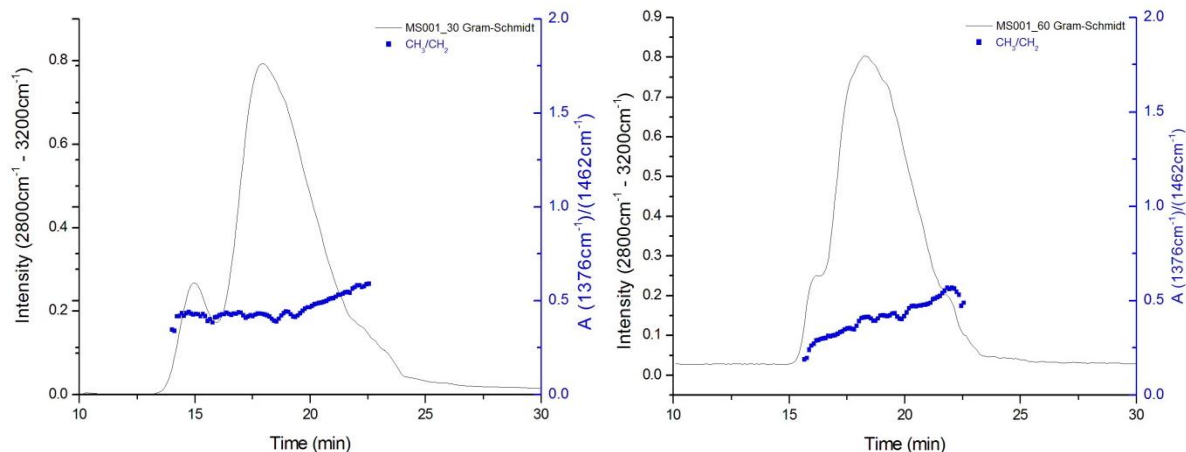
Figure C.16   *SEC-FTIR analysis of the 30 °C and 60 °C TREF fraction for MS001 illustrating the Gram-Schmidt plot with corresponding propylene content analysis*
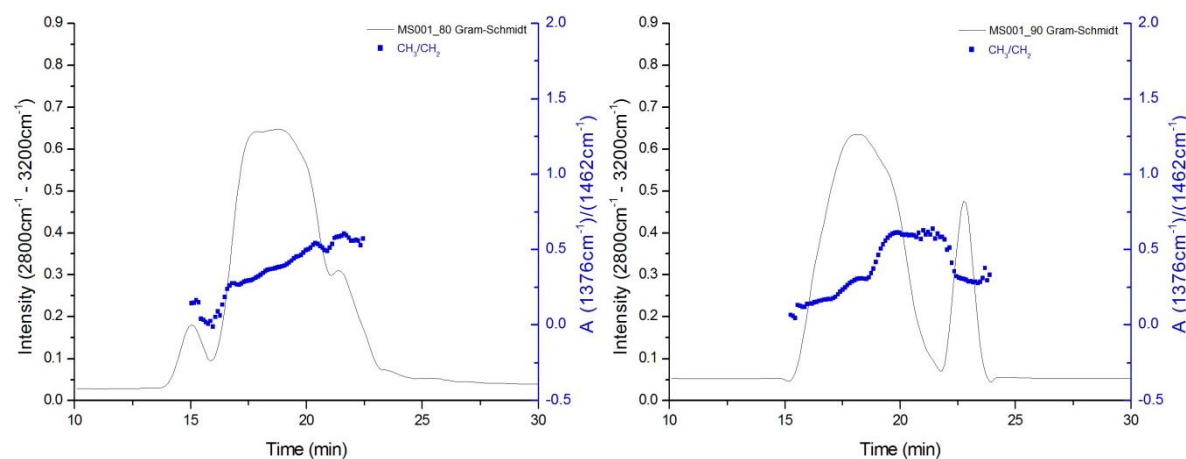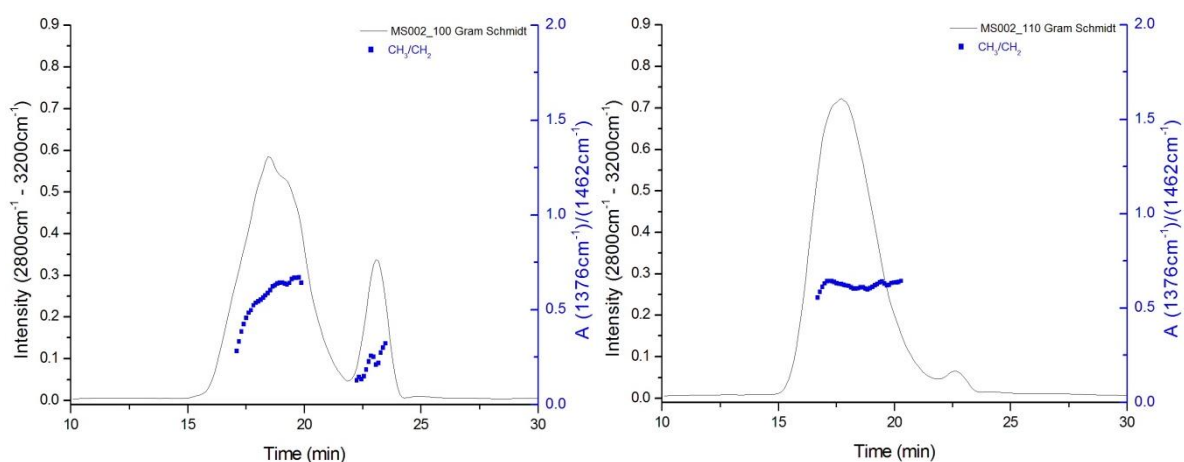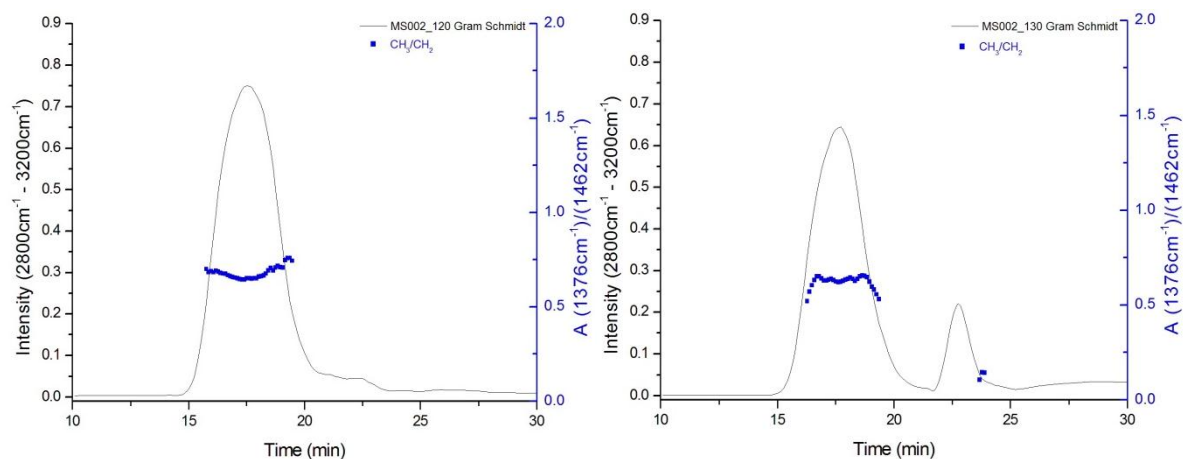

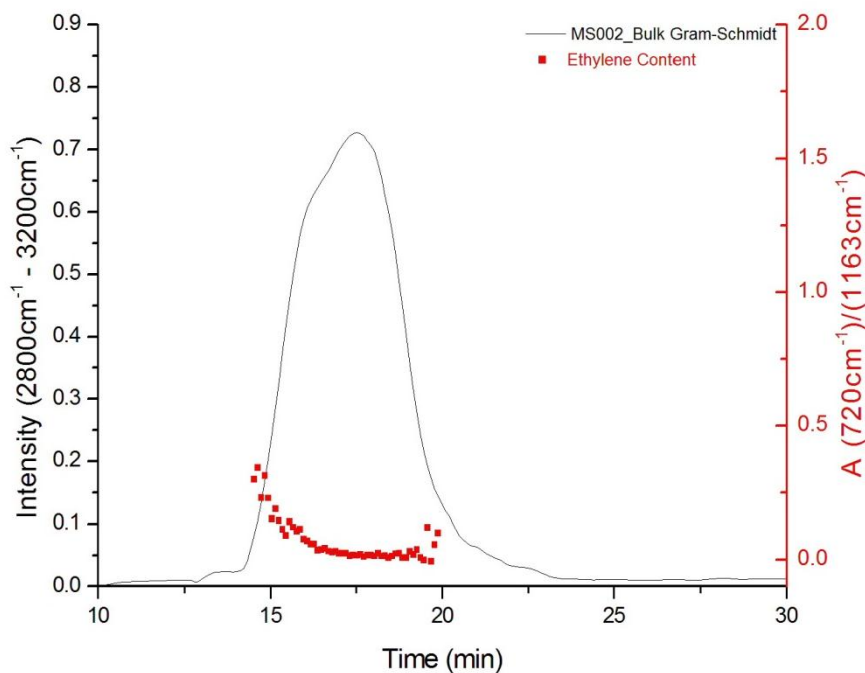**Figure C.17**   *SEC-FTIR analysis of the 80 °C and 90 °C TREF fraction for MS001 illustrating the Gram-Schmidt plot with corresponding propylene content analysis*
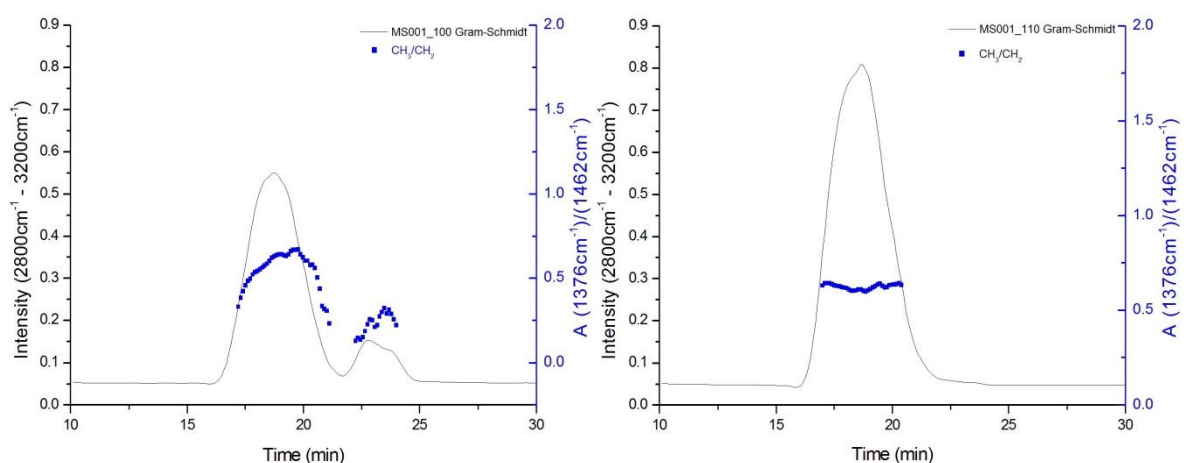
Figure C.18   *SEC-FTIR analysis of the 100 °C and 110 °C TREF fraction for MS001 illustrating the Gram-Schmidt plot with corresponding propylene content analysis*
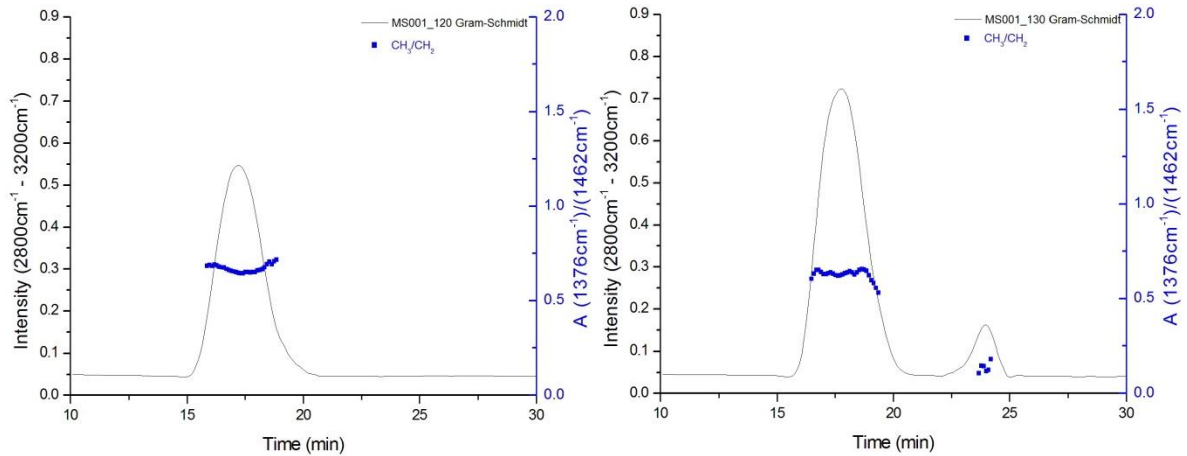
Figure C.19   *SEC-FTIR analysis of the 120 °C and 130 °C TREF fraction for MS001 illustrating the Gram-Schmidt plot with corresponding propylene content analysis*
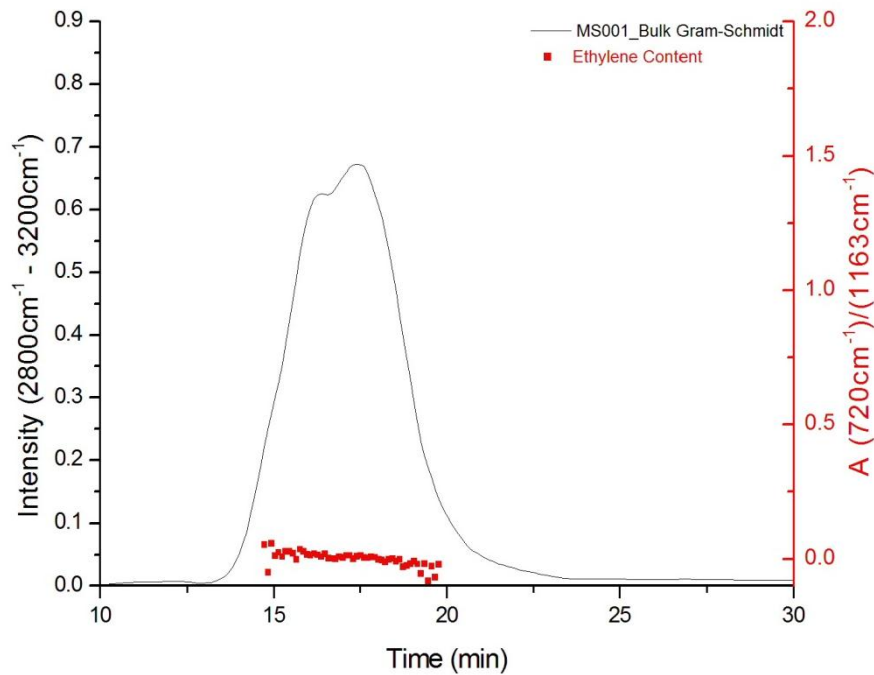
Figure C.20   *SEC-FTIR analysis of the MS001bulk sample illustrating the Gram-Schmidt plot with corresponding ethylene content analysis*
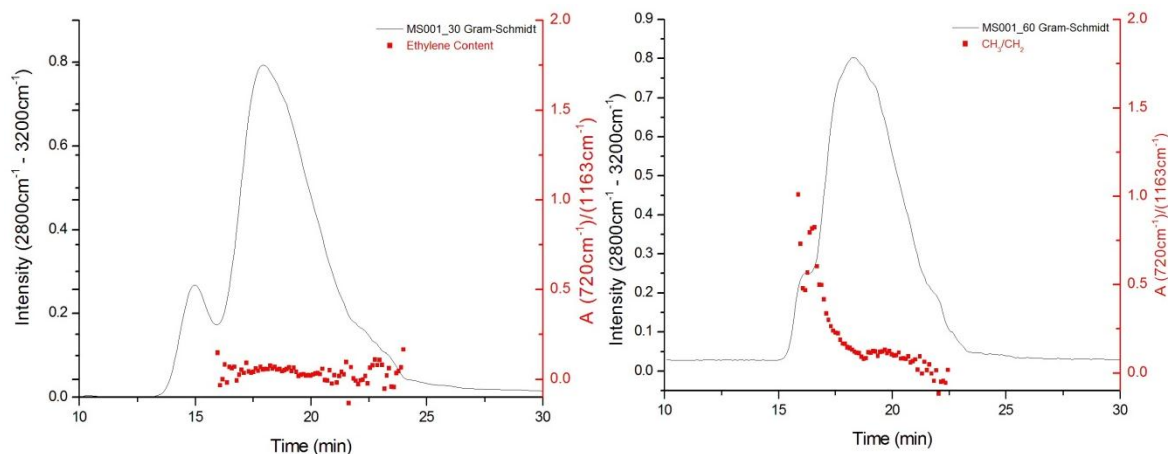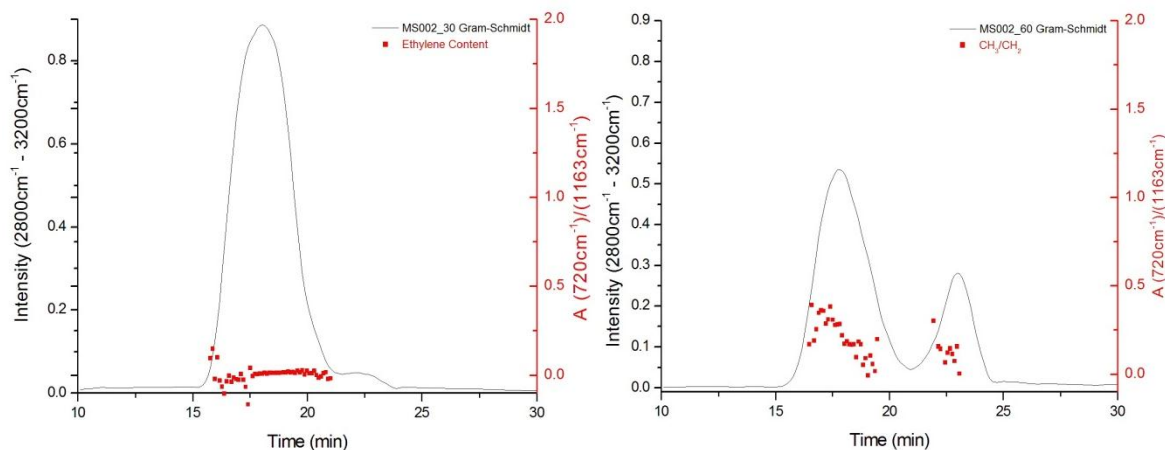
Figure C.21   *SEC-FTIR analysis of the 30 °C and 60 °C TREF fraction for MS001 illustrating the Gram-Schmidt plot with corresponding ethylene content analysis*
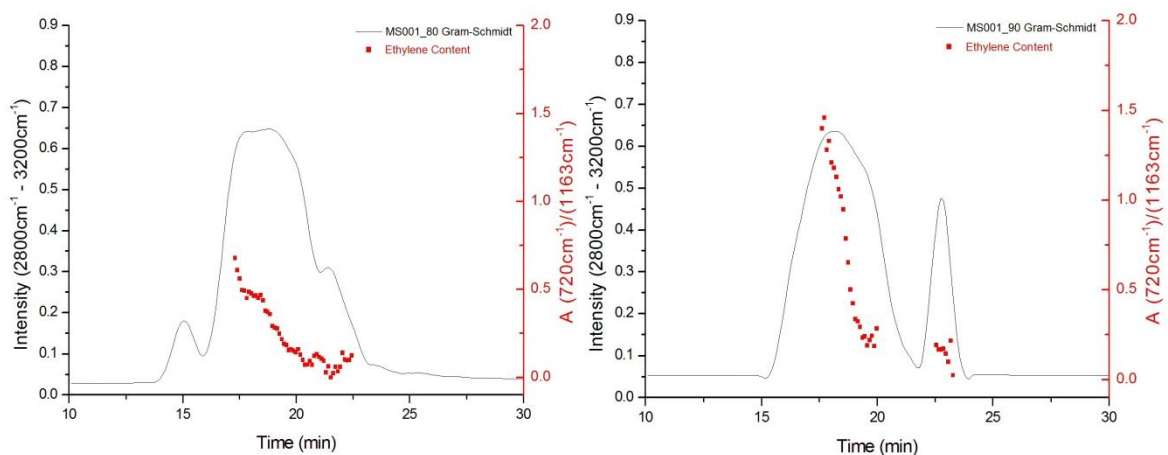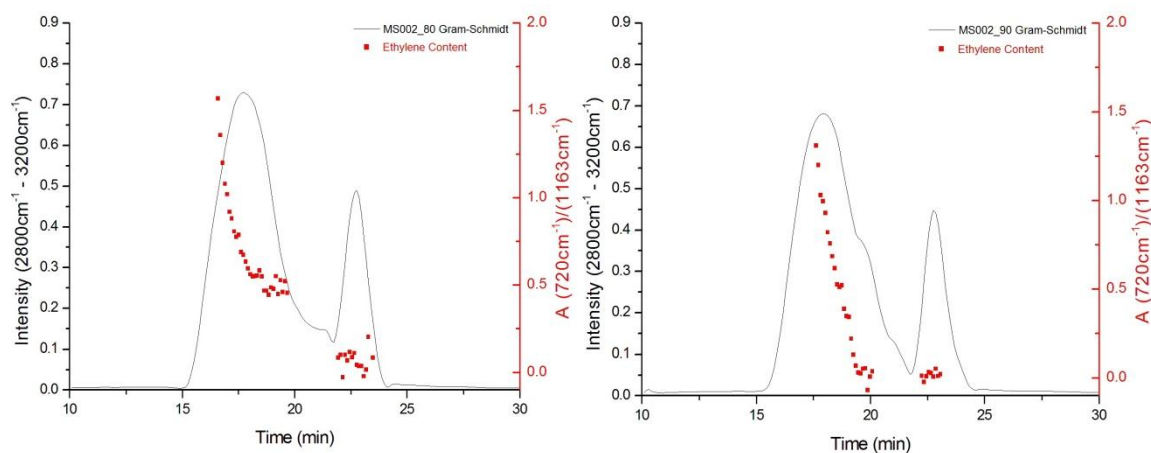

Figure C.22   *SEC-FTIR analysis of the 80 °C and 90 °C TREF fraction for MS001 illustrating the Gram-Schmidt plot with corresponding ethylene content analysis*
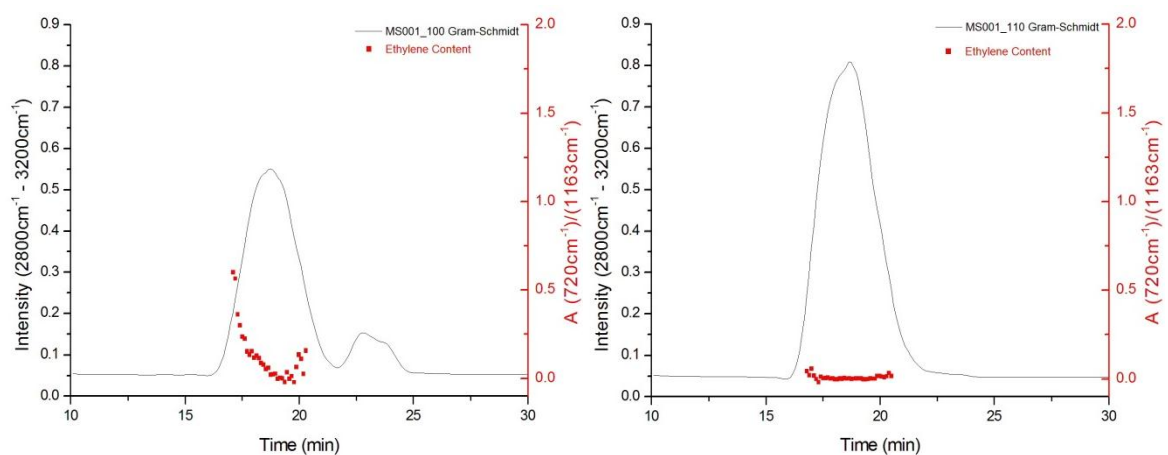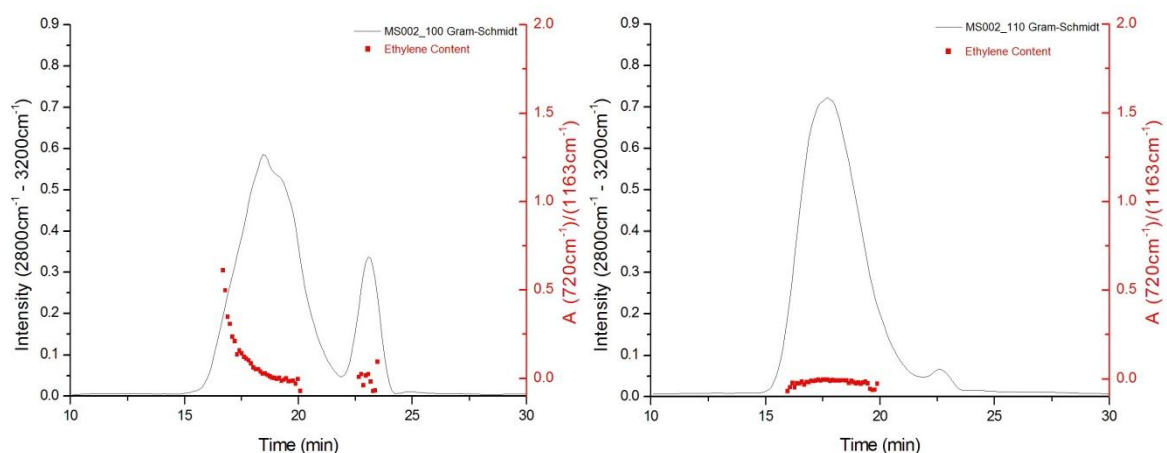

Figure C.23   *SEC-FTIR analysis of the 100 °C and 110 °C TREF fraction for MS001 illustrating the Gram-Schmidt plot with corresponding ethylene content analysis*
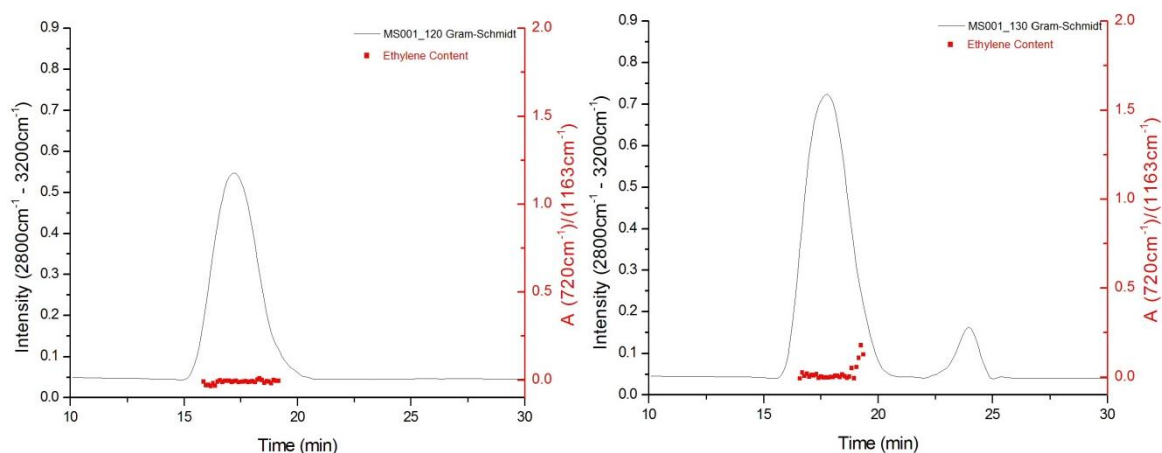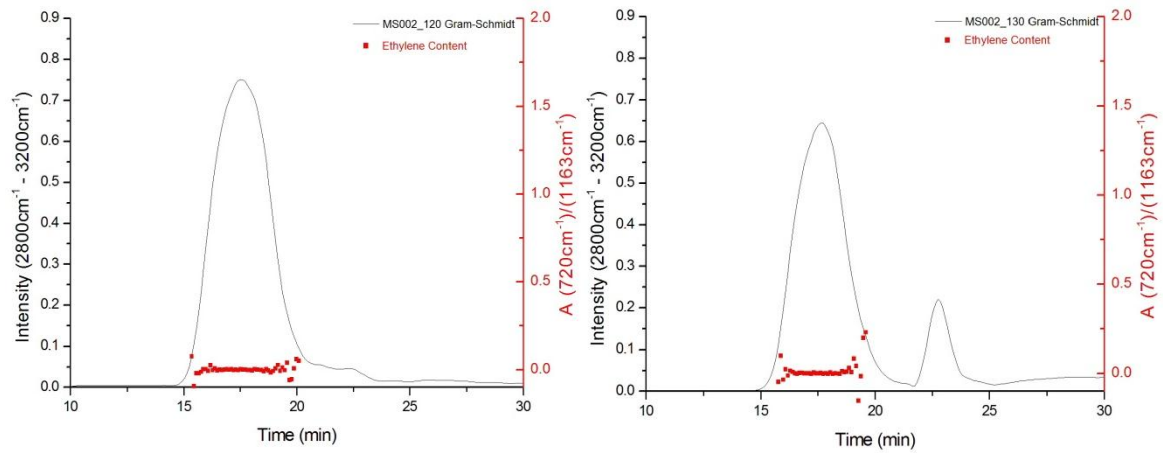
Figure C.24   *SEC-FTIR analysis of the 120 °C and 130 °C TREF fraction for MS001 illustrating the Gram-Schmidt plot with corresponding ethylene content analysis*
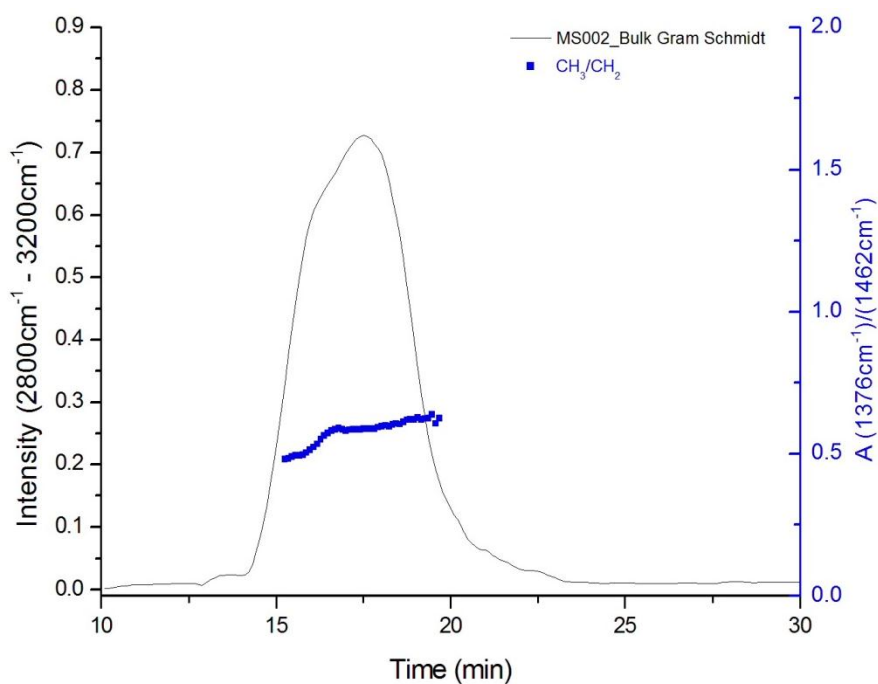
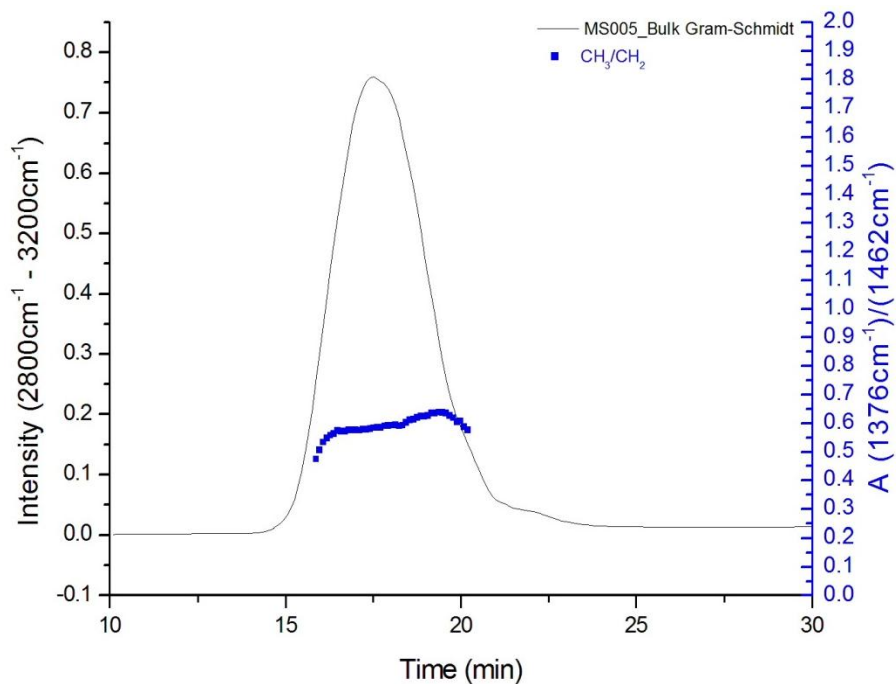**Figure C.25**   *SEC-FTIR analysis of the MS002 bulk sample illustrating the Gram-Schmidt plot with corresponding propylene content analysis*
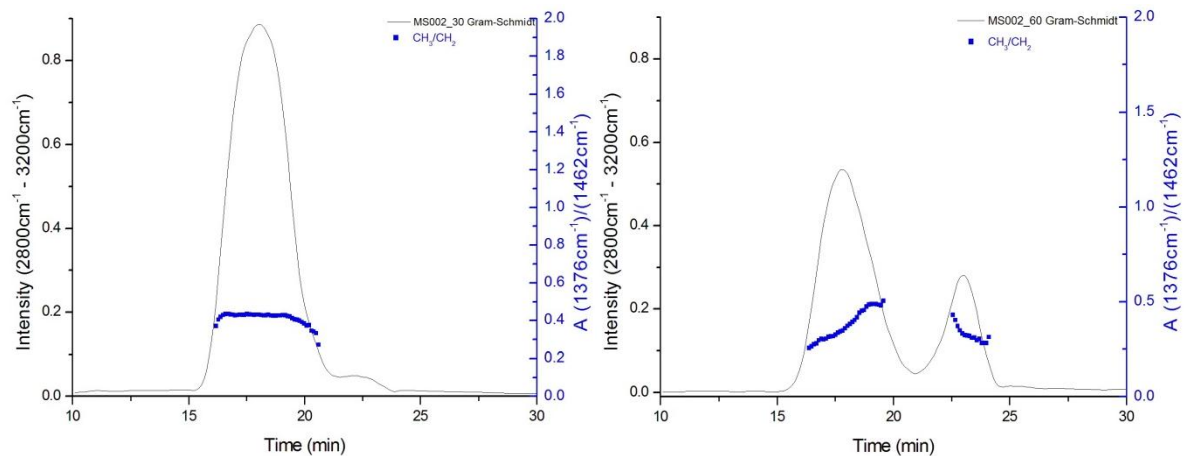
Figure C.26   *SEC-FTIR analysis of the 30 °C and 60 °C TREF fraction for MS002 illustrating the Gram-Schmidt plot with corresponding propylene content analysis*
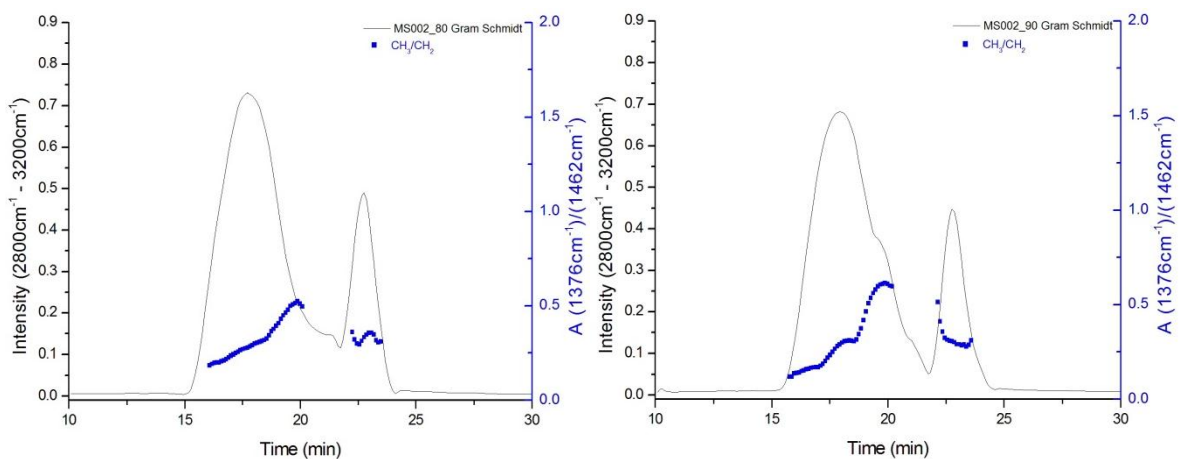
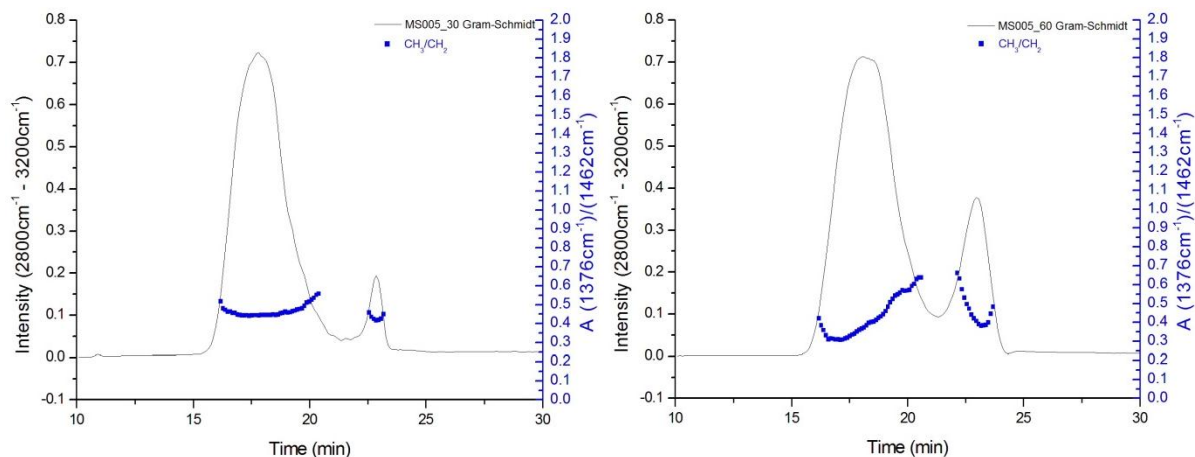**Figure C.27**   *SEC-FTIR analysis of the 80 °C and 90 °C TREF fraction for MS002 illustrating the Gram-Schmidt plot with corresponding propylene content analysis*

Figure C.28   *SEC-FTIR analysis of the 100 °C and 110 °C TREF fraction for MS002 illustrating the Gram-Schmidt plot with corresponding propylene content analysis*

Figure C.29 *SEC-FTIR analysis of the 120 °C and 130 °C TREF fraction for MS002 illustrating the Gram-Schmidt plot with corresponding propylene content analysis*

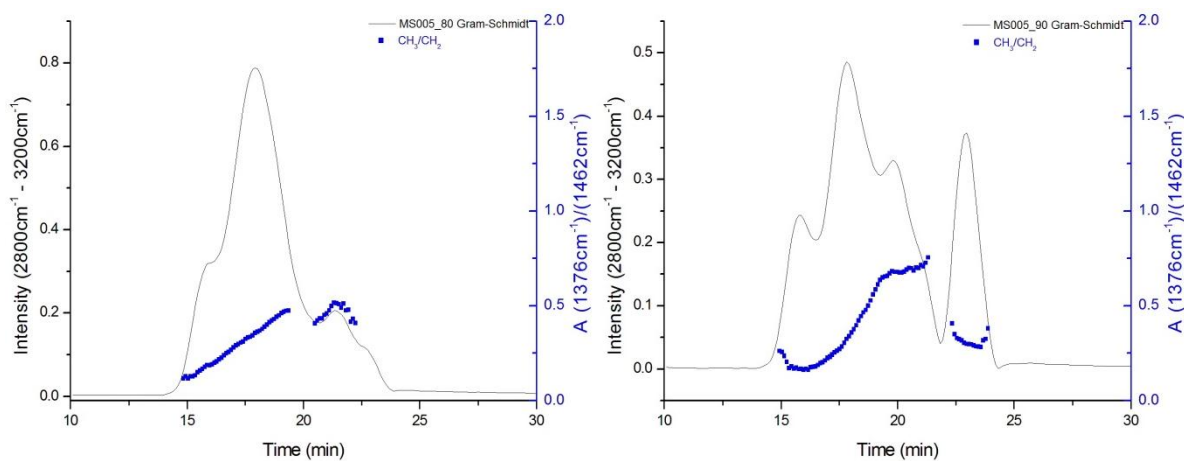
Figure C.30 *SEC-FTIR analysis of the MS002 bulk sample illustrating the Gram-Schmidt plot with corresponding ethylene content analysis*

Figure C.31   *SEC-FTIR analysis of the 30 °C and 60 °C TREF fraction for MS002 illustrating the Gram-Schmidt plot with corresponding ethylene content analysis*

Figure C.32   *SEC-FTIR analysis of the 80 °C and 90 °C TREF fraction for MS002 illustrating the Gram-Schmidt plot with corresponding ethylene content analysis*
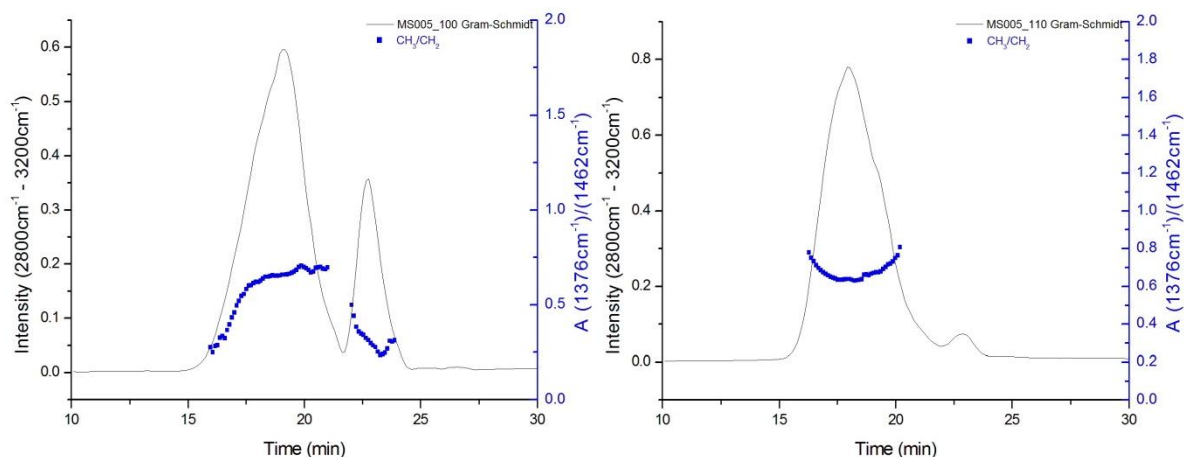

Figure C.33   *SEC-FTIR analysis of the 100 °C and 110 °C TREF fraction for MS002 illustrating the Gram-Schmidt plot with corresponding ethylene content analysis*
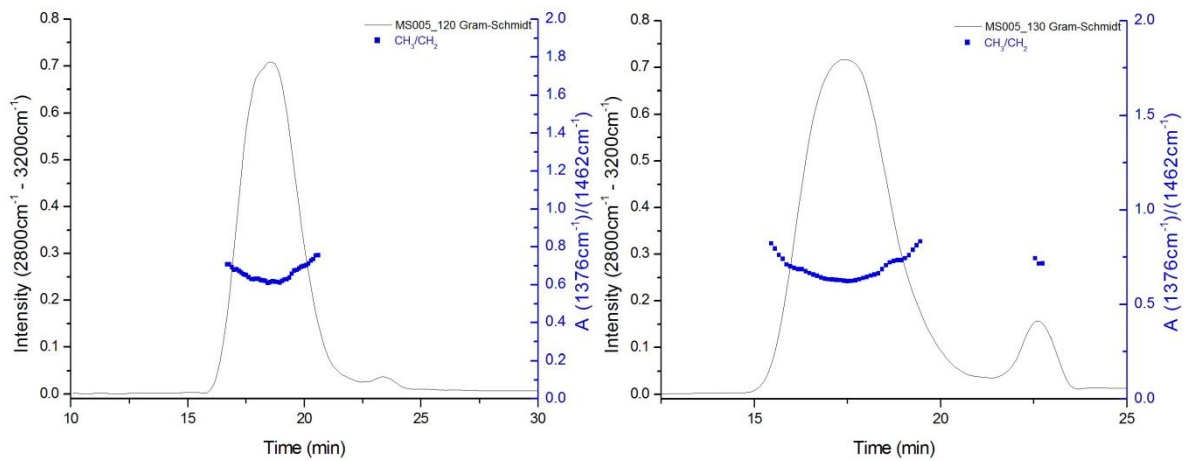
Figure C.34   *SEC-FTIR analysis of the 120 °C and 130 °C TREF fraction for MS002 illustrating the Gram-Schmidt plot with corresponding ethylene content analysis*

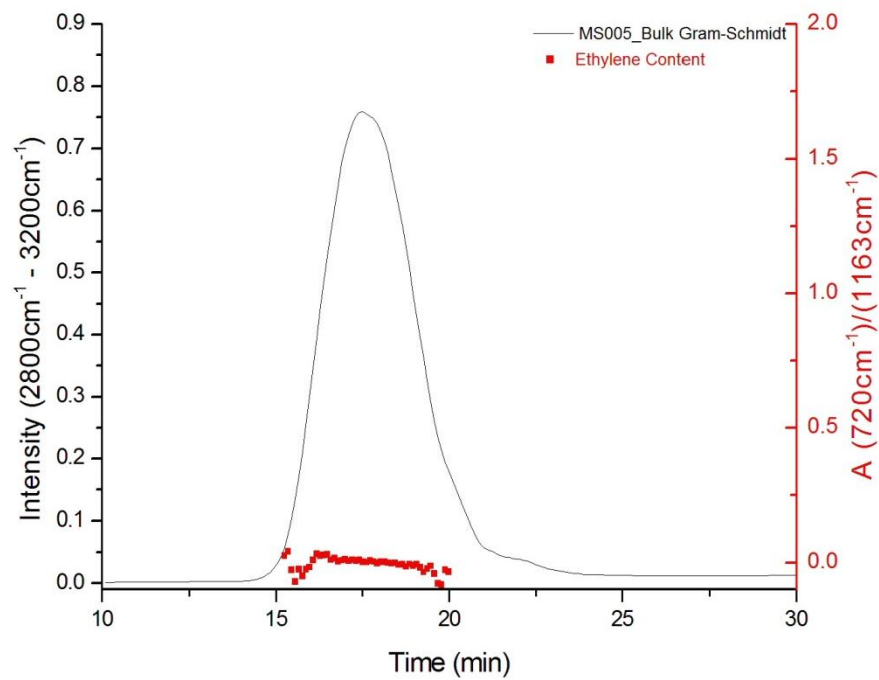**Figure C.35**   *SEC-FTIR analysis of the MS005 bulk sample illustrating the Gram-Schmidt plot with corresponding propylene content analysis*
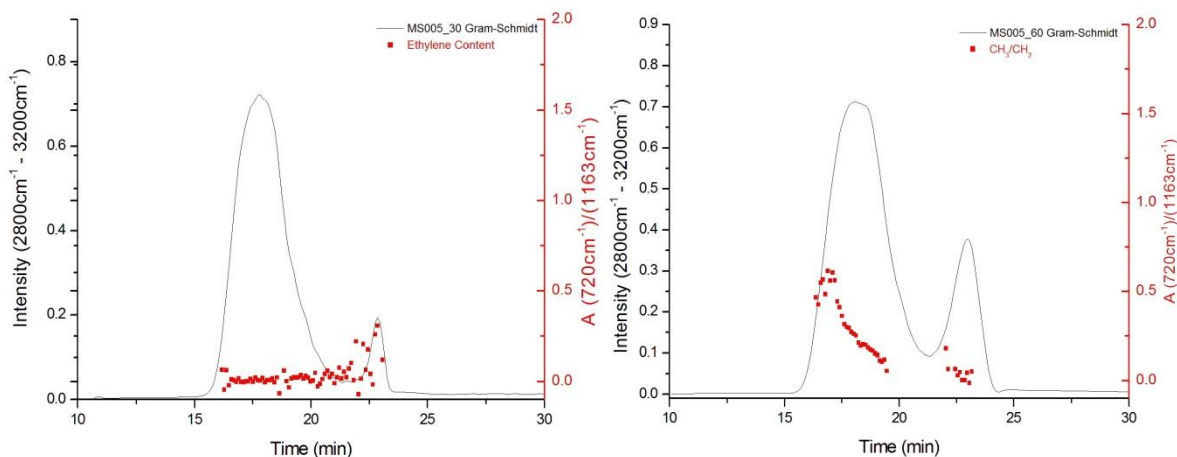
Figure C.36   *SEC-FTIR analysis of the 30 °C and 60 °C TREF fraction for MS005 illustrating the Gram-Schmidt plot with corresponding propylene content analysis*
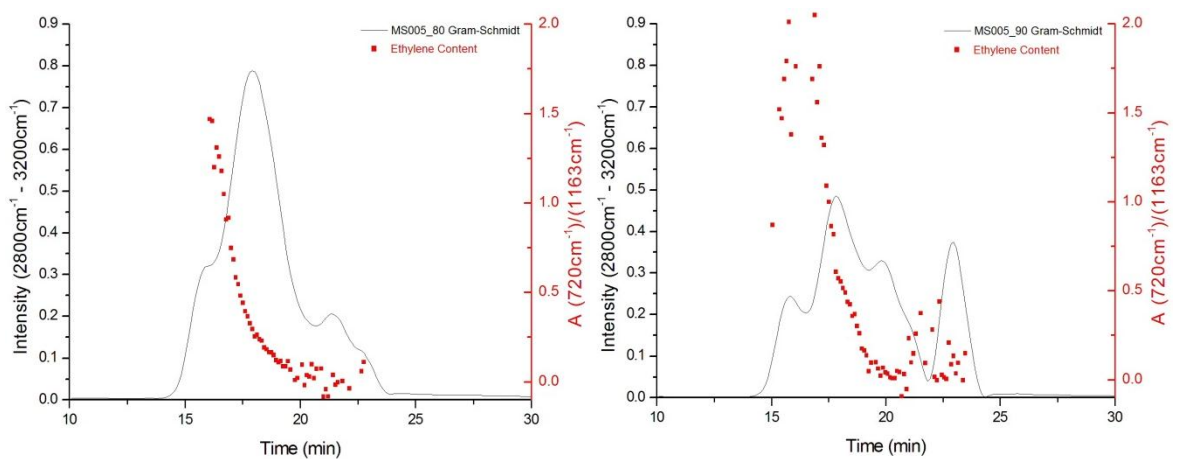

Figure C.37   *SEC-FTIR analysis of the 80 °C and 90 °C TREF fraction for MS005 illustrating the Gram-Schmidt plot with corresponding propylene content analysis*

Figure C.38   *SEC-FTIR analysis of the 100 °C and 110 °C TREF fraction for MS005 illustrating the Gram-Schmidt plot with corresponding propylene content analysis*

Figure C.39   *SEC-FTIR analysis of the 120 °C and 130 °C TREF fraction for MS005 illustrating the Gram-Schmidt plot with corresponding propylene content analysis*

Figure C.40   *SEC-FTIR analysis of the MS005 bulk sample illustrating the Gram-Schmidt plot with corresponding ethylene content analysis*

Figure C.41   *SEC-FTIR analysis of the 30 °C and 60 °C TREF fraction for MS005 illustrating the Gram-Schmidt plot with corresponding ethylene content analysis*

Figure C.42   *SEC-FTIR analysis of the 80 °C and 90 °C TREF fraction for MS005 illustrating the Gram-Schmidt plot with corresponding ethylene content analysis*
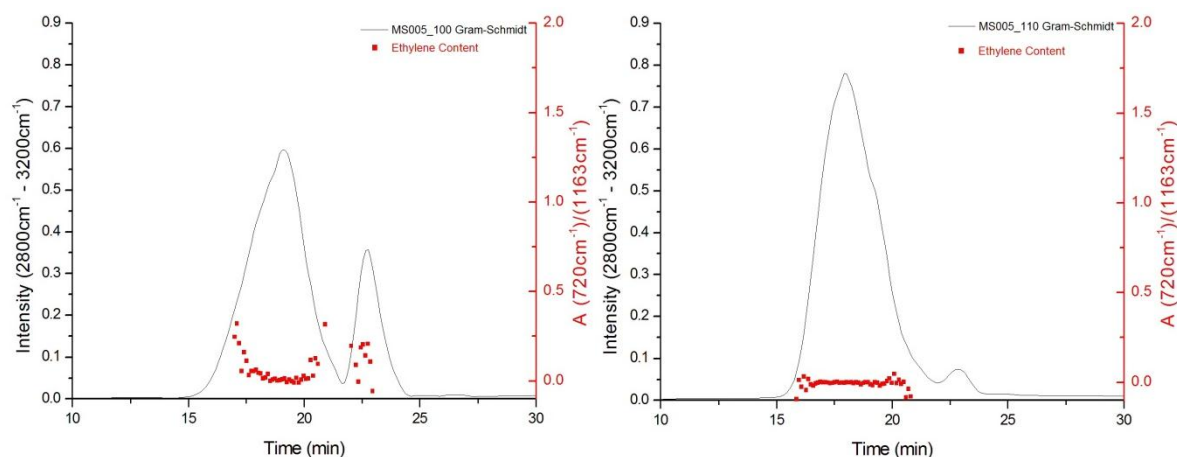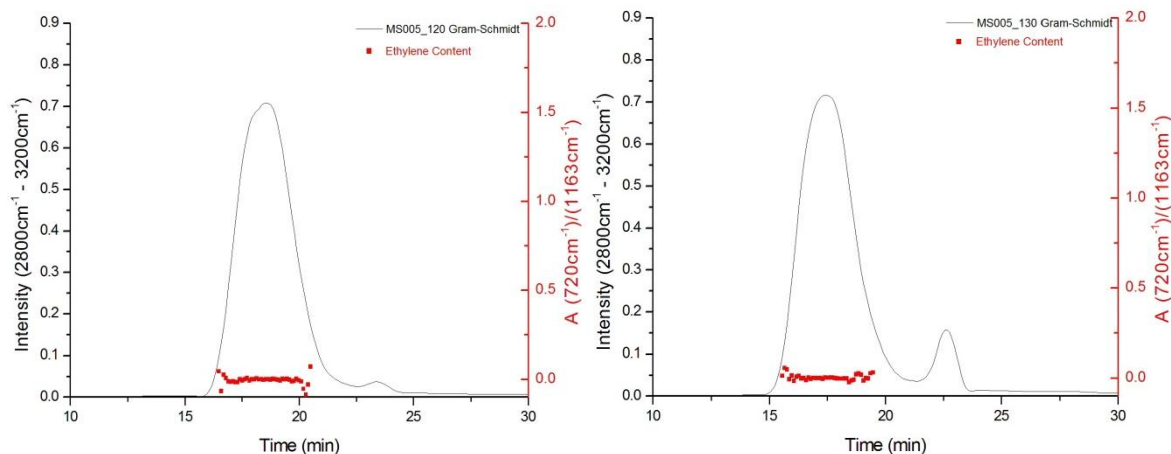

Figure C.43   *SEC-FTIR analysis of the 100 °C and 110 °C TREF fraction for MS005 illustrating the Gram-Schmidt plot with corresponding ethylene content analysis*

Figure C.44   *SEC-FTIR analysis of the 120 °C and 130 °C TREF fraction for MS005 illustrating the Gram-Schmidt plot with corresponding ethylene content analysis*

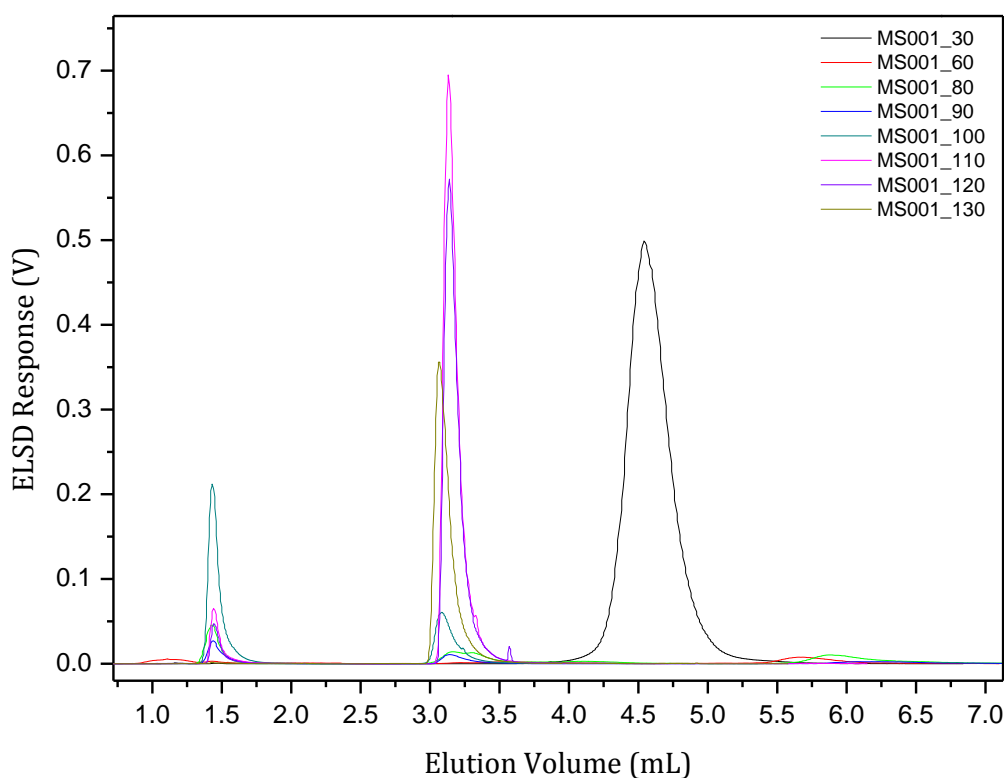## Addendum C.5: Gradient high temperature high performance liquid chromatography

Figure C.45   *HT-HPLC of TREF fractions for MS₀01 illustrating the differences in chemical composition of the various fractions*
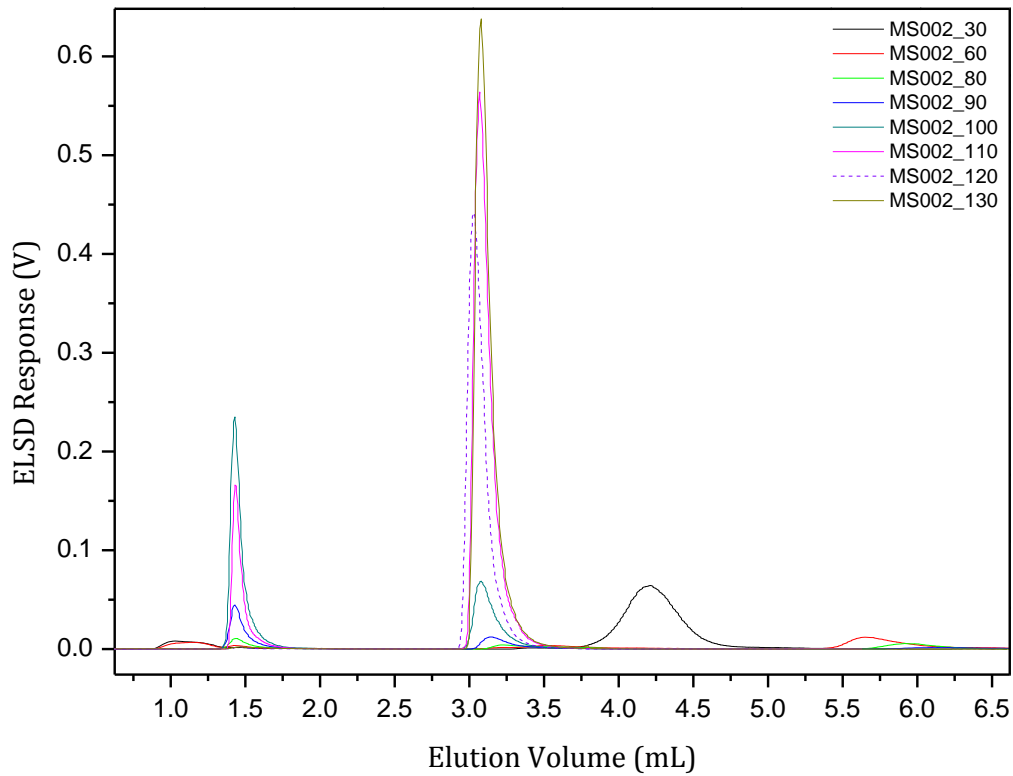
Figure C.46   *HT-HPLC of TREF fractions for MS002 illustrating the differences in chemical composition of the various fractions*
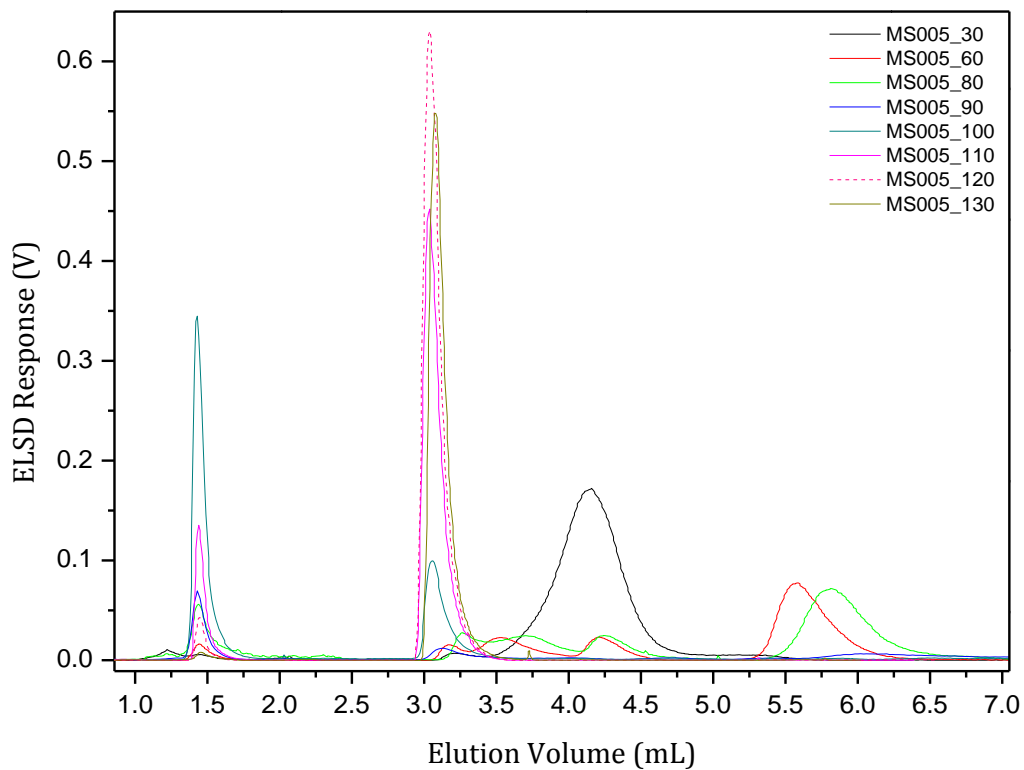

Figure C.47   *HT-HPLC of TREF fractions for MS005 illustrating the differences in chemical composition of the various fractions*